

# Understanding Upper Airway Dynamic Characteristics in OSA Patients under Invasive and non-Invasive Treatment

**Sherif Ashaat**

A thesis submitted to Auckland University of Technology

in full fulfilment of the degree of

Doctor of Philosophy



Auckland, New Zealand

Primary Supervisor: Professor Ahmed Al-Jumaily

© Sherif Ashaat

March, 2016

## **Declarations**

I hereby declare that I am the sole author of this thesis.

I authorise Auckland University of Technology to lend this thesis to other institutions for individuals for the sole purpose of scholarly research.

---

Sherif Ashaat

I further authorise Auckland University of Technology to reproduce this thesis by photocopying or by other means, in total or in part, at the request of other institutions or individuals for the sole purpose of scholarly research.

---

Sherif Ashaat

## **Borrowers Page**

The Auckland University of Technology requires the signatures of all the people using or photocopying this thesis. Accordingly all borrowers are required to fill out this page.

Date

Name

Address

Signature

---

## ACKNOWLEDGEMENTS

First and foremost, thanks are all to **God** for blessing this work until it reached its end as a little part of his generous help throughout life.

Secondly, I would like to acknowledge my deepest and sincere gratitude to **Professor Ahmed Al-Jumaily**, Professor of Biomechanical Engineering at Auckland University of Technology for his kind supervision, suggestion to the problems, constructive guidance, pointing out the mistakes, critical reading, illuminating points which were of greatest help to me while preparing the thesis, looking out for me over these years, valuable suggestions and comments, and for his continuous support.

I would also like to express my cordial thanks and deep appreciation to **Associate Professor Loulin Huang**, Lecturer of Engineering Mechanics, School of Engineering at Auckland University of Technology, for his kind supervision and continuous support.

Thanks to the Institute of Biomedical Technology (IBTec) for providing all facilities to help me bring the best performance and outcome. Thanks as well to everyone at IBTec, especially **Hassan Raslan**, my research mate, for his great efforts and support.

Thanks to the Ministry of Science and Innovation (MSI) and F&P Healthcare Limited for supporting me financially over 3 years (contract number FAPX1109). Many thanks to **Dr Andrew Somervell** for his kind help, continuous support and mentoring the project from the beginning till completion. Thanks as well to OSA team at F&P for helping me recruiting the patients. Special thanks to **Rachel Vicars** and **Hanie Yee** for their valuable suggestions and support.

Many thanks to **Dr Jim Bartley** for giving his time and efforts to examine the patients and for his valuable suggestions and ideas.

At last but not the least, I would like to convey special thanks to my lovely wife for her continuous support and patience, and my family for being there until this work has reached completion.

*To*

*My Dear Late Mother*

*My Lovely Wife, Daaa*

*My Adorable Son, Abdo*

*And My Beautiful Girl, Nooran*

## **ABSTRACT**

Obstructive sleep apnea (OSA), a common upper airway (UA) respiratory sleep disorder, is considered one of the most threatening diseases to quality of life worldwide. OSA occurs due to obstruction in the UA region, and is characterized by repeated collapse and/or obstruction of the pharyngeal airway during sleep. UA collapse occurs when the airway muscle forces are less than those generated from the airway negative pressures during respiration. The collapse may occur at the nasopharynx, oropharynx, or hypopharynx; but it is more likely to occur at the rear of the uvula (during expiration) and rear of the tongue (during inspiration).

OSA can lead to hypertension, cardiovascular disease, stroke, low sexual drive in males, atherosclerosis, and increased rate of sudden death. Treatment of this ailment can be achieved invasively and non-invasively.

Bariatric surgery is one of the invasive treatment modalities that has been used for many years for weight reduction and consequently alleviate OSA symptoms in morbid obese patients, but no biomechanical assessment for the UA characteristics and OSA symptoms before and after the surgery has been yet conducted.

For many years, continuous positive airway pressure (CPAP) has been proven to be the golden and the first line non-invasive treatment for patients with moderate to severe OSA, mainly due to its non-invasive nature. There are many side effects of CPAP including dry nose, nasal congestion (itching or rhinorrhea), and it has been reported that due to its high operating pressure, stroke symptoms were recorded for cardiovascular disease patients.

Respiratory devices that use pressure oscillations (PO) have been proven to have better respiratory outcomes in both animal and human models. PO have resulted in increasing both the activity and the stiffness of the UA muscles in both anesthetized and tracheotomised sleeping dogs, which in turn increased the UA patency and reduced its collapsibility. It has been reported that in sleeping humans, muscles in the UA increase their activity in response to high-frequency-low-amplitude pressure oscillations applied through the nasal airway. This electromyographic response was observed in both normal subjects and patients with OSA. From these results, it is clear that the PO can change the activity of the UA muscles, and consequently affect the surface tension, the airway compliance, and the airway collapsibility. Our hypothesis is that the PO superimposed on

CPAP will reduce the required mean pressure to keep the airway open during sleep, and will reduce the risk of high pressure using the conventional CPAP.

Therefore, this research aims to investigate the biomechanical changes and/or improvements in the UA characteristics before and after the invasive bariatric surgery in morbid obese OSA patients; and with the non-invasive CPAP superimposed with the PO, specifically we attempt to improve understanding of the effects of the PO on the UA respiratory system, which will lead to a more controlled method of delivering the PO in respiratory devices by determining the frequencies and amplitudes that optimise the breathing variables. Moreover, it will keep the airway open in OSA patients at a much lower CPAP than currently used, which will in turn increase the patient's comfort.

Bariatric surgery resulted in completely resolving OSA symptoms in morbid obese middle aged patients diagnosed with moderate to severe OSA. Also the use of the PO succeeded in keeping the airway open with no sign of collapse at much lower pressure distributions than the obtained values when using the conventional CPAP alone to prevent the occurrence of the apneic events.

## TABLE OF CONTENTS

<b>Declarations</b>	ii
<b>Borrowers Page</b>	iii
<b>Acknowledgements</b>	v
<b>Abstract</b>	vi
<b>Table of Contents</b>	viii-xi
<b>List of Figures</b>	xii-xiii
<b>List of Tables</b>	xiv
<b>List of Terms and Abbreviations</b>	xv
<b>Greek Letters (Symbols)</b>	xviii
 <b>Chapter 1: Background</b>	 <b>1-24</b>
1.1 Introduction	1
1.2 Background	1
1.2.1 UA Anatomic Obstructions	2
1.2.2 UA Collapse	2
1.3 Sleep Apnea Terminology	3
1.4 Apneic Event	6
1.5 Historical Notes	7
1.6 Symptoms of OSA	8
1.6.1 Day time Symptoms	8
1.6.2 Night time Symptoms	8
1.6.3 Psychological Symptoms	9
1.6.4 Physiological Symptoms	9
1.7 Risk Factors for OSA	9
1.8 Consequences of OSA	10
1.9 Age and Gender in OSA	11
1.10 Obesity and OSA	12
1.11 Race (Ethnicity) and OSA	14
1.12 OSA in New Zealand	15
1.13 Treatment Modalities for OSA	16
1.13.1 Life Style Changing	17
1.13.2 Drug Therapy	17
1.13.3 Surgical Treatment	18
1.13.4 Non-Surgical (non-invasive) Treatment	20



1.14	CPAP	21
1.14.1	CPAP Titration	23
1.14.2	Disadvantages of the CPAP	23
1.15	Closure	24
<b>CHAPTER 2: Literature Survey on UA Characteristics and Modelling</b>		<b>25-51</b>
2.1	Introduction	25
2.2	Relationship between Bariatric Surgery and OSA	25
2.3	UA Muscles Activity	32
2.4	Effects of Pressure Oscillations on the UA Muscle Activity	34
2.5	UA Modelling Techniques	36
2.5.1	Computational Fluid Dynamics (CFD)	37
2.5.2	Fluid-Structure Interaction (FSI)	46
2.6	Research Objectives	49
2.7	Closure	50
<b>CHAPTER 3: Models Formulation</b>		<b>52-66</b>
3.1	Introduction	52
3.2	3D-DOCTOR Imaging Software	52
3.3	Biomechanical Assessment before and after Bariatric Surgery	56
3.4	UA Dynamic Characteristics using the Finite Element (FE) Methods	56
3.5	CFD Modelling using Fluid-Flow (CFX) Modeller	59
3.5.1	Basic Modelling Principles	59
3.5.2	CFD Modelling Procedure using CFX Modeller	62
3.6	Fluid-Structure Interaction (FSI)	63
3.7	Meshing	64
3.7.1	Meshing on Abaqus	64
3.7.2	Meshing on ANSYS	64
3.8	Model Validation	65
3.9	Closure	66
<b>CHAPTER 4: OSA in Morbid Obese Patients Promoted for Bariatric Surgery</b>		<b>67-77</b>
4.1	Introduction	67
4.2	Clinical Protocol	67
4.2.1	Subjects	68
4.2.2	Anthropometrics	68

4.2.3	Polysomnogram	68
4.2.4	Computed Tomography	70
4.3	Airway Modelling	70
4.4	Upper Airway Parameters	71
4.5	Statistical Analyses	72
4.6	Results	72
4.7	Effects of Bariatric Surgery on OSA	75
4.8	Closure	76
<b>CHAPTER 5: Dynamic Characteristics of Healthy Upper Airways</b>		<b>78-103</b>
5.1	Introduction	78
5.2	MRI Data Collection	78
5.2.1	Recruiting Subjects	78
5.2.2	Anthropometrics	79
5.2.3	Data Collection	79
5.3	Dynamic Characteristics of Healthy Upper Airways	79
5.3.1	Healthy UA Models	79
5.3.2	Dynamic Characteristics of Healthy Isolated Uvula Models	81
5.3.3	Dynamic Characteristics of Healthy Isolated Tongue Models	92
5.4	Summary for Healthy Airway Models	98
5.4.1	Summary for Healthy UA Volumes	98
5.4.2	Comparison between Healthy Uvula and Tongue Models	100
5.4.3	Results for All Healthy Uvula Models	101
5.4.4	Results for All Healthy Tongue Models	102
5.5	Closure	102
<b>CHAPTER 6: Dynamic Characteristics of Unhealthy Upper Airways</b>		<b>104-150</b>
6.1	Introduction	104
6.2	MRI Data Collection	104
6.2.1	Recruiting Subjects	104
6.2.2	Anthropometrics	105
6.2.3	Data Collection	105
6.3	Dynamic Characteristics of Unhealthy Upper Airways	106
6.3.1	Unhealthy UA Models	106
6.3.2	Dynamic Characteristics of Unhealthy Uvula Models	107
6.3.3	Dynamic Characteristics of Unhealthy Isolated Tongue Models	114

6.4	Summary for Unhealthy Airway Models	120
6.4.1	Summary for Unhealthy UA Volumes	120
6.4.2	Comparison between Unhealthy Uvula and Tongue Models	122
6.4.3	Results for All Unhealthy Uvula Models	123
6.4.4	Results for All Unhealthy Tongue Models	123
6.5	One Way Fluid-Structure Interaction (FSI)	124
6.5.1	Results from RANS k- $\epsilon$ Turbulence Model	130
6.5.2	Results from RANS SST Turbulence Model	139
6.5.3	Conclusions	150
6.6	Closure	150
<b>CHAPTER 7: Experimental Setup and Validation</b>		<b>151-182</b>
7.1	Introduction	151
7.2	Experimental Setup	151
7.2.1	Computer	152
7.2.2	Lung Simulator	154
7.2.3	UA Simulator	158
7.3	UA Experimental Modelling	163
7.3.1	Silicon Rubber Models	164
7.3.2	Gelatine Models	168
7.4	Closure	182
<b>CHAPTER 8: Discussion and Future Work</b>		<b>183-194</b>
8.1	Introduction	183
8.2	Bariatric Surgery	184
8.2.1	Recommendations and Future Work bariatric surgery	186
8.3	Dynamic Characteristics of Healthy and Unhealthy Upper Airways	186
8.3.1	Air Volume	187
8.3.2	Tongue Volume	188
8.3.3	Uvula Volume	188
8.3.4	Entire UA Volume	188
8.3.5	Air Gaps at the Rear of the Mouth	188
8.3.6	Natural Frequency	188
8.3.7	BMI	189
8.3.8	VBMI	189
8.4	Collapse and the Effects of PO on the UA	191

8.5	Experimental Results	192
8.6	Conclusions	192
8.7	Future Work	193
	References	195-226
	Appendix A: Mathematical Modelling	227-238
	Appendix B: Combined figures for healthy uvula and tongue models	239-241
	Appendix C: Ethical approval letter, templates for the participant information sheet (PIS) and consent form	242-250
	Appendix D: Summaries of the ENT specialist reports for OSA patients	251-256
	Appendix E: Conferences and publications	257

## List of Figures

Figure 1.1: UA Anatomy and sites of obstruction	3
Figure 1.2: (a) Normal UA; (b) obstructed UA	4
Figure 3.1: Collapsible region	53
Figure 3.2: Identifying the region of interest on 3D-DOCTOR	54
Figure 3.3: Automatic boundary generation inside the ROI	54
Figure 3.4: The model boundary after: (a) removing the ROI and (b) trimming	55
Figure 3.5: Smooth boundary	55
Figure 3.6: FE modelling procedure using the Abaqus/CAE software	58
Figure 3.7: Geometry of the uvula	59
Figure 3.8: Schematic diagram showing the conservation of mass	59
Figure 3.9: Fluid element	61
Figure 3.10: CFD modelling procedure using CFX Modeller	62
Figure 3.11: Flow chart showing the FSI modelling procedure	63
Figure 4.1: Polysomnography	69
Figure 4.2: A sample of the collected CT data	70
Figure 4.3: Isolated UA models at (a) baseline, (b) 6-months and (c) 1 year after surgical intervention	70
Figure 4.4: Cross section area (A) and wetted perimeter (P) of the air gap	71
Figure 5.1: Healthy UA model isolated from the rest of the airway	79
Figure 5.2: Geometry of uniform beam (all dimensions are in mm)	80
Figure 5.3: Uniform beam (a) geometry, (b) first natural frequency from Abaqus	81
Figure 5.4: Beam geometry	81
Figure 5.5: Solution of equation (5.4) using MATLAB	83

Figure 5.6: Isolated uvula model (a) before and (b) after cutting the root	85
Figure 5.7: Summary of the FE modelling procedure	87
Figure 5.8: Approximate dimensions of a healthy uvula model (in mm)	87
Figure 5.9: Geometry of a healthy uvula model isolated from the airway	87
Figure 5.10: Mode shapes for an isolated healthy uvula model; $E = 25$ kPa	87, 88
Figure 5.11: Relationship between $E$ (Pa) and $f_n$ (Hz) for a healthy uvula model	89
Figure 5.12: Isolated tongue model (a) before and (b) after cutting the root	91
Figure 5.13: MRI images of the MSP for subjects 2 and 5	93
Figure 5.14: Geometry of a healthy tongue model isolated from the airway	93
Figure 5.15: Mode shapes of a healthy tongue model; $E = 15$ kPa	93, 94
Figure 5.16: Relationship between $E$ (Pa) and $f_n$ (Hz) for a healthy tongue model	95
Figure 5.17: Combined results for healthy uvula and tongue models; subject 1	99
Figure 5.18: Results for all healthy uvula models	100
Figure 5.19: Results for all healthy tongue models	101
Figure 6.1: Unhealthy UA model isolated from the rest of the airway	106
Figure 6.2: Geometry of an unhealthy uvula model isolated from the airway	107
Figure 6.3: Mode shapes for an unhealthy uvula model; $E = 25$ kPa	108, 109
Figure 6.4: Relationship between $E$ (Pa) and $f_n$ (Hz) for an unhealthy uvula model	110
Figure 6.5: MRI image of the MSP for patient 3	113
Figure 6.6: Geometry of an unhealthy tongue model isolated from the airway	114
Figure 6.7: Mode shapes on an unhealthy tongue model; $E = 15$ kPa	114, 115
Figure 6.8: Relationship between $E$ and $f_n$ for an unhealthy tongue model	116
Figure 6.9: Combined figure for unhealthy uvula and tongue models; patient 1	121
Figure 6.10: Results for all unhealthy uvula models	122

Figure 6.11: Results for all unhealthy tongue models	123
Figure 6.12: (a) Complete UA, (b) Tongue, (c) Uvula, (d) & (e) Air	124, 125
Figure 6.13: 1 mm thickness rubber enclosure	127
Figure 6.14: Meshing for the UA model	127
Figure 6.15: Skewness of the UA Meshing	128
Figure 6.16: Rubber duct meshing	128
Figure 6.17: Skewness of the Rubber Duct Meshing	129
Figure 6.18: UA pressure distribution during inspiration	130
Figure 6.19: Deformations and collapse of the rubber enclosure during inspiration (a) front, (b) top and (c) bottom views	130,131
Figure 6.20: UA pressure distribution during inspiration under PO	132
Figure 6.21: Deformations of the rubber enclosure during inspiration (a) front and (b) bottom views under PO	132,133
Figure 6.22: UA pressure distribution during expiration	134
Figure 6.23: Deformations and collapse of the rubber enclosure during expiration (a) front, (b) rear and (c) top views	134, 135
Figure 6.24: Pressure distribution during expiration with CPAP	135
Figure 6.25: Deformations of the rubber enclosure during expiration (a) front view and (b) top view, with CPAP	136
Figure 6.26: Pressure distribution during expiration under PO	137
Figure 6.27: Deformations of the rubber enclosure during expiration (a) front and (b) top views, under PO	137, 138
Figure 6.28: UA pressure distribution during inspiration, SST	139
Figure 6.29: Deformations of the rubber enclosure during inspiration, SST	139
Figure 6.30: UA pressure distribution during inspiration, SST	140

Figure 6.31: Deformations and collapse of the rubber enclosure during inspiration (a) front, (b) rear and (c) bottom views, SST	140, 141
Figure 6.32: UA pressure distribution during inspiration under PO, SST	142
Figure 6.33: Deformations of the rubber enclosure during inspiration (a) front and (b) bottom views, SST under PO	142, 143
Figure 6.34: UA pressure distribution during expiration, SST	144
Figure 6.35: Deformations and collapse of the rubber enclosure during expiration (a) front, (b) rear and (c) top views, SST	144, 145
Figure 6.36: Pressure distribution during expiration, SST with CPAP	146
Figure 6.37: Deformations of the rubber enclosure during expiration (a) front and (b) top views, SST with CPAP	146, 147
Figure 6.38: UA pressure distribution during expiration under PO, SST	148
Figure 6.39: Deformations of the rubber enclosure during expiration (a) front view and (b) top view, SST under PO	148
Figure 7.1: Experimental setup; (A) Lung and (B) UA Respiration simulators	150
Figure 7.2: Diagram showing how the setup works	151
Figure 7.3: Diagram showing the sequence of the connected items	151
Figure 7.4: Block diagram	152
Figure 7.5: Front panel	152
Figure 7.6: Data acquisition board	153
Figure 7.7: Servo amplifier	153
Figure 7.8: Power supply	154
Figure 7.9: Electro-mechanical relay	154
Figure 7.10: Servo motor	154
Figure 7.11: Stop switches and screw follower	155



Figure 7.12: Piston/Cylinder compartment	155
Figure 7.13: Chamber	156
Figure 7.14: Pressure transducer	156
Figure 7.15: Flow controller	157
Figure 7.16: Temperature sensor	157
Figure 7.17: Heater	158
Figure 7.18: Laminearisation probe	158
Figure 7.19: Power supply units	159
Figure 7.20: Data acquisition board	160
Figure 7.21: Microprocessor	160
Figure 7.22: DC motor driver	160
Figure 7.23: Accurate UA model	161
Figure 7.24: Simplified UA model	161
Figure 7.25: Transparent rig using vacuum forming	162
Figure 7.26: Silicon models for (a) Tongue and (b) Uvula	162, 163
Figure 7.27: Stress-Strain relationship of silicon rubber	163
Figure 7.28: Curve fitting for silicon model	164
Figure 7.29: Complete UA with silicon rubber models	164
Figure 7.30: Deformations of silicon models, upright position	165
Figure 7.31: Deformations of silicon models, supine position	165
Figure 7.32: Stress-strain relationship for gelatine material	166
Figure 7.33: Curve fitting for gelatine model	167
Figure 7.34: Gelatine (a) Tongue and (b) Uvula models	168
Figure 7.35: Complete UA with gelatine models	168

Figure 7.36: Air gap at the rear of the uvula, upright position	169
Figure 7.37: Air gap at the rear of the uvula, supine position	169
Figure 7.38: Deformations of the gelatine models, upright position	170
Figure 7.39: Deformations of the gelatine models, supine position	171
Figure 7.40: Lateral deformations of the rig, supine position	171
Figure 7.41: Deformations of the gelatine models, upright position (a) zero and (b) maximum deformation	172
Figure 7.42: Deformations of the gelatine models, supine position (a) zero and (b) maximum deformation	172
Figure 7.43: Deformations of the gelatine models, supine position (a) zero and (b) maximum deformation	173
Figure 7.44: Lateral deformations of the rig in the upright position (a) zero and (b) maximum deformation; 5 Cm H <sub>2</sub> O	174
Figure 7.45: Lateral deformations of the rig in supine position (a) zero and (b) maximum deformation; 5 Cm H <sub>2</sub> O	174
Figure 7.46: Deformations of the uvula, supine position (a) zero and (b) maximum deformation; 5 Cm H <sub>2</sub> O	175
Figure 7.47: Modal Shop SmartShaker	176
Figure 7.48: Tektronix signal generator	176
Figure 7.49: Y-Shaped connection	177
Figure 7.50: Lateral deformations of the rig in the upright position (a) zero and (b) maximum deformation; 4 Cm H <sub>2</sub> O + 1 Cm H <sub>2</sub> O with PO, f = 30 Hz	177
Figure 7.51: Lateral deformations of the rig in the upright position (a) zero and (b) maximum deformation; 4 Cm H <sub>2</sub> O + 1 Cm H <sub>2</sub> O with PO, f = 40 Hz	178
Figure 7.52: Lateral deformations of the rig in supine position (a) zero and (b) maximum deformations; 4 Cm H <sub>2</sub> O + 1 Cm H <sub>2</sub> O with PO, f = 30 Hz	178

Figure 7.53: Lateral deformations of the rig in supine position (a) zero and (b) maximum deformations; 4 Cm H<sub>2</sub>O + 1 Cm H<sub>2</sub>O with PO,  $f = 40$  Hz 179

Figure 7.54: Deformations of the uvula, supine position (a) zero and (b) maximum deformation; 4 Cm H<sub>2</sub>O + 1 Cm H<sub>2</sub>O with PO,  $f = 40$  Hz 179

## **List of Tables**

Table 1.1: Relationship between AHI and OSA severity	5
Table 1.2: Relationship between RDI and OSA severity	5
Table 1.3: Relationship between BMI and obesity	6
Table 4.1: Statistical data before surgical intervention	68
Table 4.2: Statistical data after surgical intervention	69
Table 4.3: UA volume before and after surgery	73
Table 4.4: VBMI before and after surgery	74
Table 4.5: Min. and Max. HD before and after surgery	74
Table 5.1: Demographic data from participating volunteers	79
Table 5.2: UA volume and air gaps for all healthy subjects	80
Table 5.3: Theoretical values for the natural frequencies ( $f_n$ )	84
Table 5.4: Volumes of the healthy uvula models	86
Table 5.5: Natural frequencies for a healthy uvula model for different values of E	89
Table 5.6: Values of the first natural frequencies for healthy uvula models	90
Table 5.7: Values of the second natural frequencies for healthy uvula models	90
Table 5.8: Values of the third natural frequencies for healthy uvula models	91
Table 5.9: Volumes of healthy tongue models	92
Table 5.10: Natural frequencies for a healthy tongue model for different values of E	95
Table 5.11: Values of the first natural frequencies for healthy tongue models	96
Table 5.12: Values of the second natural frequencies for healthy tongue models	96
Table 5.13: Values of the third natural frequencies for healthy tongue models	97
Table 5.14: Volumes and percentages to the total UA volume	98

Table 6.1: Demographic data for OSA patients	105
Table 6.2: UA volume and air gaps for all OSA patients	106
Table 6.3: Volumes of the unhealthy uvula models	107
Table 6.4: Natural frequencies for an unhealthy uvula for different values of E	109
Table 6.5: Values of the first natural frequencies for all unhealthy uvula models	111
Table 6.6: Values of the second natural frequencies for all unhealthy uvula models	111
Table 6.7: Values of the third natural frequencies for all unhealthy uvula models	112
Table 6.8: Volumes of unhealthy tongue models	113
Table 6.9: Natural frequencies of an unhealthy tongue for different values of E	115
Table 6.10: Values of the first natural frequencies for all unhealthy tongue models	117
Table 6.11: Values of the second natural frequencies for all unhealthy tongue models	117
Table 6.12: Values of the third natural frequencies for all unhealthy tongue models	118
Table 6.13: Volumes and percentages to the total UA volume, OSA patients	120
Table 7.1: Natural frequencies for the used gelatine models	167
Table 7.2: Summary of the obtained deformations with and without the CPAP	175
Table 7.3: Summary of the obtained deformations	180
Table 8.1: Summary of the obtained data and results for bariatric surgery	183
Table 8.2: Summary of the obtained results for healthy and unhealthy subjects	185
Table 8.3: VBMI of healthy and unhealthy subjects	187

### **Statement of Originality**

‘I hereby declare that this submission is my own work and that, to the best of my knowledge and belief, it contains no material previously published or written by another person nor material which to a substantial extent has been accepted for the qualification of any other degree or diploma of a university or other institution of higher learning, except where due acknowledgment is made in the acknowledgments.’

..... (signed)

..... (date)

## **List of Terms and Abbreviations**

A: Cross Section Area ( $\text{m}^2$ )

AHI: Apnea-Hypopnoea Index

APAP: Automatic (Adjustable) Positive Airway Pressure

B: Baseline

BMI: Body Mass Index ( $\text{kg}/\text{m}^2$ )

CFD: Computational Fluid Dynamics

CFX: Fluid Flow Modeller on ANSYS Workbench

CNS: Central Nervous System

CPAP: Continuous Positive Airway Pressure

CSA: Cross Sectional Area ( $\text{m}^2$ )

CT: Computer Tomography

$D_{\text{eq}}$ : The Equivalent Diameter of the Airway Cross Section (m)

DM: ANSYS Design Modeller

DNS: Direct Numerical Simulation Models

E: Young's Modulus of Elasticity (Pa)

EDS: Excessive Daytime Sleepiness

EMG: Electromyelograms

ENT: Ear, Nose and Throat Specialist

f: Frequency (Hz)

F: Female

FE: Finite Element

$f_n$ : Natural Frequency (Hz)

FSI: Fluid-Structure Interaction

GA: Genioglossus Advancement

HA: Hyoid Advancement

HD: Hydraulic Diameter

HFPO: High Frequency Pressure Oscillations

I: Second Moment of Area ( $m^4$ )

( $\underline{i}$ ,  $\underline{j}$ ,  $\underline{k}$ ): Unit Vectors in x, y and z directions, respectively

LAUP: Laser Assisted Uvulopalatoplasty

LES: Large Eddy Simulation Models

M: Male

MAS: Mandibular Advancement Splint

MMA: Maxilla-Mandibular Advancement

MRI: Magnetic Resonance Imaging

MSP: Mid-Sagittal Plane

OSA: Obstructive Sleep Apnea

OSAHS: Obstructive Sleep Apnea-Hypopnea Syndrome

OSAS: Obstructive Sleep Apnea Syndrome

P: Wetted Perimeter

$P_{crit}$ : Critical Closing Pressure (Pa)

$P_{in}$ : Inlet Pressure

PIS: Participant Information Sheet



$P_{\min}$ : Minimum Wall Static Pressure (Pa)

PO: Pressure Oscillations

$P_{\text{out}}$ : Outlet Pressure

PSG: Polysomnographic

$\Delta P$ : Pressure Drop or Pressure Difference (Pa)

Q: Volume Flow Rate (L/min.)

R: Airway Resistance ( $\frac{\Delta P}{Q}$ )

RANS: Reynolds-Averaged-Navier-Stokes Models

RDI: Respiratory Disturbance Index

$Re$ : Reynolds Number ( $\frac{U D_{eq.}}{\nu}$ )

ROI: Region of Interest

SA: Sleep Apnea

SA: Spalart-Allmaras

SAS: Sleep Apnea Syndrome

SD: Standard Deviation

SST: Shear Stress Transport

t: Time

TCRF: Temperature-Controlled Radio Frequency

U: Axial mean velocity (m/s)

UA: Upper Airway

UPF: Uvulopalatal Flap

UPPP or UP3: Uvulo-pharyngeal-palato-plasty or uvulo-palato-pharyngo-plasty

(u,v,w): Velocity components in x, y and z directions, respectively (m/s)

V: Volume [ $\text{m}^3$ ]

$V_{\text{max}}$ : Maximum Velocity (m/s)

$\vec{V}$ : Velocity Vector (m/s)

VBMI: Volume Body Mass Index [ $\text{m}^3/(\text{kg}/\text{m}^2)$ ]

WSS: Wall Shear Stress,  $\tau_w$  (Pa)

(x,y,z): Cartesian Coordinates

## Greek Letters (Symbols)

$\rho$ : Volumetric Density (kg/m<sup>3</sup>)

$\Delta$ : Difference

$\vec{\nabla}$ : Differential Operator =  $\left( \frac{\partial}{\partial x} \underline{i} + \frac{\partial}{\partial y} \underline{j} + \frac{\partial}{\partial z} \underline{k} \right)$

$\mu$ : Dynamic Viscosity (kg/m.s or Pa.s)

$\nu$ : Poisson's ratio

$\nu$ : Kinematic Viscosity (m<sup>2</sup>/s.)

$\tau_w$ : Wall Shear Stress (Pa)

$\omega_n$ : Natural Frequency (rad/sec.)

# **CHAPTER 1**

## **Background**

### **1.1 Introduction**

This chapter provides the available background information describing obstructive sleep apnea (OSA), section 1.2. The definitions of the used OSA terminology are given in section 1.3, followed by a detailed description of the apneic event in section 1.4. Historical notes on OSA are given in section 1.5. Sections 1.6 to section 1.8 give detailed information about OSA symptoms, risk factors and consequences; respectively. The prevalence of OSA in different ages and genders is fully explained in section 1.9. The relationship between obesity and OSA is described in section 1.10, and the prevalence of OSA in different ethnicities is explained in section 1.11. The different treatment modalities for OSA are explained in section 1.12, and the CPAP is fully described in section 1.13.

### **1.2 Background**

Obstructive sleep apnea (OSA) was firstly reported in 1985 by Flenely [1]. It is considered one of the most threatening diseases to the quality of life [2-17].

OSA is considered the most worldwide common upper respiratory system ailment, and it is one of the main sleep disordered breathing (SDB) diseases [18-23]. OSA may be referred to by the following terms:

- Sleep Apnea (SA)
- Sleep Apnea Syndrome (SAS)
- Sleep Apnea-Hypopnea Syndrome (SAHS)
- Obstructive Sleep Apnea Syndrome (OSAS)
- Obstructive Sleep Apnea-Hypopnea Syndrome (OSAHS)

OSA occurs due to obstruction (narrowing) in the upper airway (UA) region [24-27] (it is characterised by repeated obstruction and/or collapse of the pharyngeal airway during sleep [17, 20, 28-41]), although the breathing effort still exists [38, 42-45]. This in turn results in many recurrent and consecutive episodes of:

- Airflow cessation [26, 37],
- Blood oxygen de-saturation (known as Hypoxia or Hypoxemia) [26, 34, 37, 46, 47],

- Blood carbon dioxide saturation increase (known as Hypercapnia or Hypercarbia), and
- Arousal (sleep disruption) to restore the airway potency [19, 26, 28, 34, 48-52].

Upper airway (UA) obstruction may occur partially (known as hypopnea) or completely (known as apnea), and it occurs due to anatomic obstructions and/or collapse [53, 54], which will be explained in detail next.

### **1.2.1 UA Anatomic Obstructions**

The following conditions are classified as anatomic obstructions:

- Large tonsils size and/or adenoids (Hypertrophy) [27, 34, 55-57].
- Large tongue size (known as macroglossia) [27, 34, 55, 57, 58].
- Large size of soft palate tip (uvula) [27, 34, 55, 57, 59-61].
- Lowered soft palate [34].
- Deviation in nasal septum [55, 59, 60].
- Retrognathia [33, 34, 62, 63].
- Micrognathia.

These anatomic obstructions can reduce the cross sectional area (CSA) of the pharyngeal airway which in turn increases the tendency of the UA to collapse [27, 57].

### **1.2.2 UA Collapse**

UA collapse occurs when the forces of the airway wall muscles are less than the forces generated from the airway negative pressures during the respiration process [52, 64-68]. It may occur at one or more of the following pharyngeal sites [69-71]:

- Nasopharynx, sometimes known as Velopharynx or even Retropalatal pharynx: extending from rear of nose to the rear of the soft palate tip.
- Oropharynx, sometimes known as Retroglossal pharynx: extending from rear of the soft palate tip to rear of epiglottis tip.
- Hypopharynx, sometimes known as Laryngopharynx or Retro-epiglottic pharynx: extending from rear of epiglottis tip to the beginning of the Larynx.

These are the most collapsible sites due to the absence of bone support [69] and illustrated are in Figure 1.1.

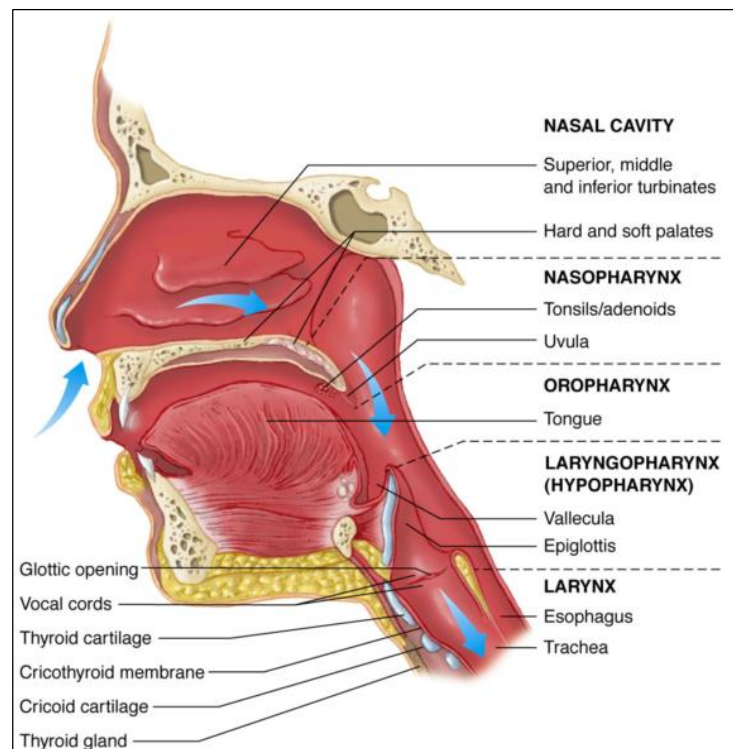


**Figure 1.1: UA Anatomy and sites of obstruction [72]**

It is reported that the obstruction in adults occurs at the level of the uvula/soft palate or tongue [55, 70, 71, 73, 74].

The tendency for UA obstruction increases when the patient sleeps in supine position. At this position, the gravitational force may pull the soft palate tip (uvula) and tongue towards the airway wall, reducing the air gap between the soft tissues and the airway wall, which in turn increases the chance for airway obstruction and collapse [75].

### 1.3 Sleep Apnea Terminology

This section summarizes the definitions of the terms that will be used in the proceeding chapters of this thesis.

#### **Apnea (complete obstruction)**

Apnea is a Greek word, which means "no breath" [19, 43]. It occurs during sleep when there is an airflow cessation (no airflow or more than 90% airflow reduction) for an interval of 10 seconds or more [17, 27], associated with 4% or more of blood oxygen de-saturation [76]. An apnea is considered obstructive if the airflow cessation is associated with continued breathing effort [17, 42, 76]. A patient is diagnosed with OSA when 30 apneic events or more are detected during seven hours of sleep [77-83].

### **Hypopnea (partial obstruction)**

It is defined as a reduction in the nasal pressure (or airflow) by 30% or more for an interval of 10 seconds or more, associated with 4% or more blood oxygen de-saturation [17, 27, 33, 69, 84, 85], however the flow of air still exists (but with lower airflow rate) [19, 42, 43]. It is sometimes defined when the airflow is reduced by 50-90% [27, 76, 86, 87]. Also, it occurs when the air gap between the uvula and the airway walls reduces by 75% accompanied by minimum wall static pressure [24]. It is usually associated with chest and abdominal movements [88] and snoring [76].

### **Collapse**

Airway collapse occurs when the forces of the airway wall muscles (known as dilating forces) are less than the forces generated from the airway negative (pharyngeal) pressures (known as collapse forces) during the respiration process [38, 52, 64-66, 89-91]. It also occurs when the airflow reduces by 90% or more, or the air gap between the soft palate tip and the airway wall reduces by 75% (partial obstruction) [24], or a reduction in blood oxygen saturation by 4%. Collapse results in reducing the diameter of the pharyngeal airway, which in turn increases the resistance of the airway to airflow [36, 92]. Collapse increases during sleeping in supine position due to the gravitational force which pulls the tongue and the soft palate tip towards the airway walls [75, 93-95], as shown in Figure 1.2.

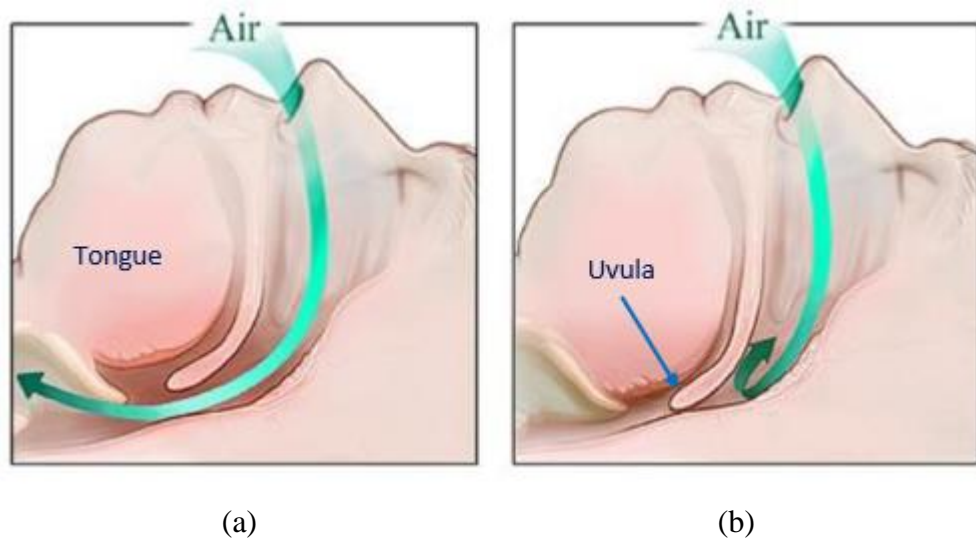


**Figure 1.2: (a) Normal UA and (b) obstructed UA [96]**

### **Closing (Critical) Pressure ( $P_{crit.}$ )**

It is defined as the pharyngeal pressure at which the area of the pharyngeal airway is zero [36, 70].

## OSA Severity Diagnosis

There are two different approaches to determine the severity of OSA:

### (i) Apnea-Hypopnea Index (AHI)

It is defined as “the total number of partial and complete obstructions occurring per hour of sleep” [34, 43, 87]. AHI is calculated by dividing the total number of apnea and hypopnea events by the number of sleeping hours per night [52, 85]. The diagnosis and severity of OSA is determined according to the value of the AHI [59], as shown in Table 1.1.

**Table 1.1: Relationship between AHI and OSA severity [17, 18, 97-99]**

OSA Severity	Apnea-Hypopnea Index
Normal (Undiagnosed)	$AHI \leq 5$
Mild	$5 < AHI \leq 15$
Moderate	$15 < AHI \leq 30$
Severe	$AHI > 30$

From the above table, it can be concluded that the patients are diagnosed with OSA when the value of the AHI is more than 5.

The apneic events are measured using a device known as the Polysomnogram [18, 38, 52, 100, 101] which was firstly introduced in 1970 and is considered as the golden scale to measure the apneic events [47, 102, 103], although it is relatively expensive and time consuming [104].

When the number of arousals is considered into calculation, the AHI can be replaced by the Respiratory Disturbance Index (RDI) [59, 60, 69, 98, 105, 106] described next.

### (ii) Respiratory Disturbance Index (RDI)

It is defined as the total number of apneas, hypopneas and arousals per hour of sleep [27, 69]. OSA severity can be determined by RDI according to the values given in Table 1.2.

**Table 1.2: Relationship between RDI and OSA severity [107]**

OSA Severity	RDI
Normal (Undiagnosed)	$RDI \leq 5$
Mild	$5 < RDI \leq 20$
Moderate	$20 < RDI \leq 40$
Severe	$RDI > 40$



### Body Mass Index (BMI)

The body mass index (BMI) is defined as the mass of the body (kg) divided by the squared height of the body (m<sup>2</sup>), which can be noted as:

$$\text{BMI} = \frac{\text{Mass}}{(\text{height})^2} = \text{kg/m}^2 \quad (1.1)$$

BMI is the measuring scale of obesity, as shown in Table 1.3 [108].

**Table 1.3: Relationship between BMI and obesity**

Weight Categories	Body Mass Index (BMI)
Underweight	< 18.5
Normal	18.5 - 24.9
Overweight	25 - 29.9
Obese	30 - 34.9
Morbid Obese	≥ 35

### Hypoxia (Hypoxmia)

It is defined as a reduction in blood oxygen saturation by 4% or more during sleep [76].

### Hypercapnia (Hypercarbia)

It is defined as an increase in carbon dioxide saturation in blood during sleep [38].

## 1.4 Apneic Event

When a person starts sleeping, the muscles of the pharyngeal airway relax causing the airway lumen to narrow, which increases the resistance to airflow causing airway obstruction [90, 95, 109]. Also due to gravity, the soft tissues move towards the airway walls narrowing the airway further. The event differs during inspiration and expiration as explained next:

1. **During Inspiration:** The diaphragm contracts causing a drop in the negative pharyngeal pressure, which pulls the airway walls (suction) interiorly increasing the airway obstruction [34, 36]. It is to be noted that during sleeping in supine position the inhaled air pushes the uvula backwards and away from the airway wall, it is therefore expected that the obstruction will not occur rear of it during inspiration. In the same time the tongue moves towards the airway wall due to pressure difference resulting from the contraction of the diaphragm, muscle relaxation and its own weight; which narrows the airway rear of the tongue; therefore the obstruction would commonly occur rear of the tongue during inspiration.

2. **During Expiration:** The diaphragm expands causing a positive pharyngeal pressure [36], which pushes the airway walls anteriorly opening the airway, however the outgoing airflow (exhaled air) pushes the uvula forward towards the airway walls (when sleeping in supine position) causing obstruction, therefore the obstruction will commonly occur rear of the uvula during expiration.

A gasp or a snort (loud snoring) may occur as the termination of the apneic event for both cases described above [34]. The obstruction may occur partially which is known as hypopnea, or completely which is known as apnea; which were both explained in detail in section 1.3.

When the obstruction occurs, the breathing effort increases to overcome the obstruction, the blood oxygen saturation ( $\text{PaO}_2$ ) decreases (known as Hypoxia or Hypoxemia) and the blood carbon dioxide ( $\text{PaCO}_2$ ) increases (known as Hypercapnia or Hypercarbia) [38], which in turn activates the central nervous system (CNS) to arouse the person [59, 102, 109] in order to allow airway wall muscles to restore their potency again [90, 91] accompanied by a snort or a gasp. The airflow is then resumed allowing the person to fall asleep again, and then the obstruction occurs again followed by an arousal, followed by an obstruction and so on, which causes sleep fragmentation [38, 55, 89, 110] and consequently restless sleep [43, 59, 89].

A patient with OSA may have hundreds of apneic events per night, ranging from 200 to 500 events [111-113], and is observed to have consecutive silence and snoring events, where silent events mean there is no airflow (apnea), and snoring events mean that the airflow obstruction is relieved [16, 41, 55, 114-117].

## **1.5 Historical Notes**

The term obstructive sleep apnea syndrome (OSAS) was firstly introduced in 1976 by Guilleminault, C., et al [28].

In 1993, Young, T., et al [20] reported that almost 4% of the American population (about 20 million) were affected by OSA. Their study was conducted on 602 middle aged subjects (352 males and 250 females) with age range of 30-60 years. They have reported that the prevalence of OSA in males was much higher than their counterparts with an approximate percentage of 24% while the prevalence in females was only 9%. These results were demonstrated recently in 2008 by Jordan, A.S. and White, D.P. [118].

Caballero et al [119] in 1998 reported that the pharyngeal airways of patients diagnosed with OSA are narrower than those of normal control persons.

In 2000, Kryger M.H. [120] reported that the prevalence of OSA is ranging from 2-26%.

In 2002, Young, T., et al [16] reported that about 20% of adults have mild OSA, from which 7% have moderate OSA.

In 2002, Namen et al [121] reported that the number of patients diagnosed with OSA was increased 12 times between 1990 and 1998.

Ayappa , I., and Rapoport, D.M. [22] in 2003 reported that OSA is responsible for the reduction of the quality of life. Also, OSA can lead to/worsen cardiovascular diseases. Moreover, OSA increases the number of driving accidents and sadly it results in increased numbers of deaths.

## **1.6 Symptoms of OSA**

OSA symptoms can be classified into four types:

### **1.6.1 Day time Symptoms**

1. Day time tiredness (fatigue) [20, 33, 34, 38, 43, 122-130].
2. Sleep attacks while driving, eating, or even talking [28, 33, 48-51, 55, 131].
3. Headache (cephalgia), especially at morning [19, 28, 33, 34, 38, 43, 55, 99, 110, 132, 133].
4. Excessive daytime sleepiness (EDS) (sometimes called hyper somnolence) [19, 20, 28, 31, 33, 34, 37, 38, 43, 48-51, 55, 59, 60, 62, 99, 118, 122, 124, 127-140].

### **1.6.2 Night time Symptoms**

1. Loud snoring and gasps [17, 19, 34, 38, 43, 47, 55, 59, 60, 62, 110, 112, 122, 123, 128-130, 141, 142]. (snoring alone does not mean that the individual has OSA, but it should be associated with other symptoms [62, 143]).
2. Nocturnal choking (angina) and pauses in breathing [17, 34, 38, 52, 55, 110].
3. Body moves excessively during sleeping [38, 110].
4. Somnambulism (walking asleep) [28, 55].
5. Long sleep duration without rest [34, 38, 43, 59, 89, 123].

6. Fragmented sleep [17, 34, 36, 37, 39, 55, 89, 110, 136].
7. Nocturia and enuresis (bed wetting) [28, 34, 38, 55, 110, 144, 145].
8. Gastro-esophageal reflux [17, 34, 38, 43].
9. Excessive night sweating (diaphoresis) [38, 110].
10. Sore throat [38, 43].
11. Insomnia [17, 55, 99].

### **1.6.3 Psychological Symptoms**

1. Less concentration [33, 38].
2. Rapid changes in mood [33, 38, 43].
3. Depression [33, 38, 55], especially in women.
4. Distress [110].
5. Memory loss [33, 38, 55].
6. Irritability [33, 38, 55].

### **1.6.4 Physiological Symptoms**

1. Excessive unexplained weight gain [33, 110].
2. Hypertension (increased blood pressure) [17, 33, 34, 99, 110, 146].
3. Arrhythmias or heart rate instability (bradycardia and tachycardia) [17, 110, 147].
4. Erythrocytosis [99].
5. Low sexual drive (libido) and erectile ability [33, 38, 43, 110].

## **1.7 Risk Factors for OSA**

The risk factors are the factors that can lead to OSA, which are:

1. Obesity ( $\text{BMI} > 28 \text{ kg/m}^2$ ) [17, 19, 34, 38, 49-51, 59, 60, 63, 110, 128-130, 141, 148-154].
2. Aging [16, 155-160].
3. Acromegaly: It was reported that 13-39% of individuals diagnosed with OSA have acromegaly [17, 55, 161, 162].
4. Retrognathia [33, 34, 62, 63].
5. Smoking: which causes airway inflammation [37].
6. Alcohols drinking [77, 163-169].
7. Sedatives [166-169].
8. Nasal obstructions [17, 34, 59, 60, 63, 170-173].

9. Neck circumference > 17 inches in males (or larger than 40 Cm), and > 16 inches in females [20, 34, 38, 43, 59, 60, 63, 128-130, 174-178].
10. Cardiovascular diseases [41, 110, 132, 179-182].
11. Hypertension [33, 49-51, 63, 110, 146].
12. Large size of uvula (hypertrophy) [33, 34, 55, 59-62].
13. Large size of tonsils and/or adenoids (hypertrophy) [17, 33, 34, 55, 56, 62, 63, 183].
14. Large tongue size (macroglossia) [33, 34, 38, 55, 58, 184-186].
15. Lowered soft palate [33, 34, 38, 62].
16. Tumours in the airway [38, 187].
17. Micrognathia.

## **1.8 Consequences of OSA**

OSA can lead to many health implications, including:

1. Blood oxygen (haemoglobin) de-saturation during sleep (hypoxia or hypoxemia) [28, 34, 39, 46, 47, 52, 55, 188-196].
2. Carbon dioxide (CO<sub>2</sub>) increase in blood during sleep [39, 47, 188-190] (hypercapnia [197], or hypercarbia [52]).
3. Excessive daytime sleepiness (EDS) [19, 20, 28, 31, 33, 34, 39, 43, 48-51, 55, 59, 62, 99, 118, 122, 124, 131-139].
4. Arrhythmias (bradycardia and tachycardia) [38, 43, 52, 59, 102, 147, 180, 198-208].
5. High ability to driving accidents [16, 118, 137-139].
6. Resistance to insulin (diabetes) [34, 43, 209-213].
7. Hypertension [33, 39, 159, 160, 180, 181, 198-201, 207-210, 214-220]. (It was reported that approximately 50% of OSA patients have hypertension [59]).
8. Stroke [16, 33, 41, 115, 160, 180, 181, 198-201, 207, 208, 214, 215, 221-224].
9. Cardiac stroke [191-193].
10. Depression [33, 55], especially in women.
11. Increased rate of sudden death [2, 16, 41, 115, 202-206, 225, 226].
12. Cardiovascular disease [33, 38, 39, 41, 102, 110, 160, 179-181, 198-201, 210, 214, 215, 220, 227-234].
13. Nocturnal enuresis [28, 55, 110, 144, 145].
14. Atherosclerosis (atherogenesis) [102, 179, 209, 235].
15. Cerebrovascular diseases [20, 136, 236, 237].

16. High rate of driving accidents [4-9, 34, 38, 40, 238-243].
17. Low sexual drive and erectile ability [33, 43, 110, 159, 160].
18. Memory loss [33, 38, 39, 43, 55].

## **1.9 Age and Gender in OSA**

OSA existence is directly proportional to age, which means that older people are more prone to OSA than young individuals due to weak airway muscles in the elderly (age physiologic feature) [8, 60, 122, 155, 244-249]. In other words, the chance of having OSA increases with age [8, 60, 122, 155, 244-248, 250, 251]. It is noted that although the prevalence of OSA increases with age, however the severity of the disease decreases with age [155].

In 1999, kapur, V., et al [252] reported that 9-24% of males and 4-9% of females for the age group of 30-60 years were diagnosed with OSA.

It was reported that the prevalence of OSA is highly increased in old persons with ages over 65 years (the rate was about 65% [248]), and the prevalence in those old persons may be double or triple the prevalence in younger persons aging between 30-64 years [20, 74, 110, 115, 123, 155, 244].

OSA can affect all ages, however it is noted that obese men, especially middle-aged, are more prone to OSA than the corresponding women [110, 253]. In other words, OSA is more likely to affect obese men before the age of 50 years rather than women with the same age range [122].

In general, it has been reported that OSA affects men more than women [20, 42, 253-259], with percentages reaching about 2% of women and 4% of men [19, 20, 116, 117, 132, 175]. It has been also reported that men have more AHI than women [46, 260, 261]. The prevalence of OSA in men is more than women due to [259]:

1. The dilator muscles in the UA are more active in women than men.
2. The upper body fat distribution is higher in men compared with women, while women tend to have more fat distribution in their lower body.
3. The soft tissue structures in the UA are larger in men than women.

O'Connor et al [260] reported that the prevalence of mild OSA in men is double than that for women, and that severe OSA in men is eight fold than women.

Young et al [262] and Jennum et al [263] reported that the prevalence of OSA was increased to 2-5% and 3-7% in middle-aged women and men, respectively.

Stierer, T., and Punjabi, N.M. [264] reported that the prevalence of OSA in middle aged adults is ranging between 5-15%.

When both men and women have the same BMI, men will then have more severe OSA [111, 265-268].

Before menopause, women with OSA are more obese than their counterparts when having the same OSA severity [46, 260, 261, 266, 269].

The prevalence of OSA has been reported to increase in women post menopause when compared to women before menopause [33, 146, 217, 250, 251, 256, 258, 270-273], reaching a percentage of 47% for women after the age of 60 years [274].

In 2001, Duran et al [274] reported that OSA affects approximately 35% of people aging between 50 and 60 years.

Another study was conducted in 2002 by Fisher, D., et al [275] showed that men have more collapsible upper airways than women during sleep.

In 2003, Tishler P.V., et al [276] reported that OSA has an equal opportunity to affect both genders over the age of 50 years. This study reported that OSA predominance is directly proportional to the value of the BMI for the age range of 50-60 years, while the effect of the BMI on OSA diminishes above the age of 60 years.

In 2004, Young et al [115] reported that the prevalence of mild to severe OSA in adults is approximately 7% and increases to 20% of adults diagnosed with mild OSA.

In 2008, Lopez -Jiminez, F., et al [277] reported that about 20% of middle-aged people have mild OSA (AHI > 5) and 7% of those having moderate-to-severe OSA (AHI > 15).

It was also reported that OSA can affect children [278-283], especially obese children who have higher ability to get affected [284].

## **1.10 Obesity and OSA**

Individuals with more weight than normal have higher risk for OSA [60, 285] as well as higher OSA prevalence [286-288].

No doubt both obesity and OSA have independent contribution to cardiovascular diseases, general morbidity and increased mortality [25].

It has been reported that obesity is responsible for the reduction of the chest wall compliance, which may increase the airway resistance to airflow [289, 290].

In 1983, Sampson et al [291] reported that the carbon dioxide saturation (Hypercapnia) during sleep apnea is higher in obese patients when compared to non-obese patients.

Fleetham, J.A. [292] reported that obese subjects have narrower pharyngeal airway than non-obese subjects.

It has been reported that the prevalence of obesity in patients with OSA is ranging between 60-90% on a basis of considering a patient as obese when the BMI is larger than 29 kg/m<sup>2</sup> [28, 153].

The predominance of OSA in morbid obese middle age subjects was reported to be as high as 42-48% in males and 8-38% in females as reported by Young, T., et al [20] and Kyzer, S. and Charuzi, I. [293].

Obesity is reported to be one of the major risk factors for OSA in obese children [294-297]. Also, it has been reported that obese children are more prone to OSA when compared to non-obese children [284].

In 2000, Valencia et al [298] reported that approximately 26% of moderate OSA patients have BMI > 30, and 33% of which have BMI > 40.

Also, in 2000, Peppard et al [299] reported that an increase in weight by 10% increases the AHI by approximately 32% which increases the risk of developing OSA by 6 times, while a reduction in weight by 10% reduces the AHI by 26%.

In 2001, Resta, O., et al [300] reported that approximately 50% of obese individuals were diagnosed with moderate to severe OSA.

In more recent studies, it has been reported that approximately 70% of OSA patients are obese; and that OSA affects about 40% of obese men and women [16, 26].

OSA associated with obesity has been proven to cause depression in adults [301-304].

In 2003, Frey W. C. and Pilcher, J. [286] reported that approximately 90% of OSA patients are morbidly obese. They have also reported that OSA affects more than 70% of morbid



obese subjects, which was demonstrated by the studies conducted by Dixon, J. B., et al [305] in 2003 and O'Keeffe, T. and Patterson, E. J. [306] in 2004.

In the same year, Dixon, J. B., et al [305] investigated the relationship between obesity and OSA. The study was conducted on a group of 99 morbid obese patients consisting of 24 men and 75 women, with age range of 20-60 years. They have reported that around 70% of the group were diagnosed with OSA.

In 2007, Fritscher, L. G., et al [307] reported that obesity is one of the major risk factors for OSA. They have also reported that OSA may aggravate obesity due to excessive daytime sleepiness which results in less exercise and consequently increases obesity.

Also, in 2007 Verhulst, S. L., et al [308] reported that OSA prevalence in obese children is approximately 20%.

In 2009, Maclel Santos, M. E. S., et al [309] reported that obese subjects are more prone to OSA than non-obese subjects due to the excessive fat tissue in their neck which tends to narrow the UA and consequently reduces the volume of the air cavity, resulting in obstructed and/or collapsed airways.

### **1.11 Race (Ethnicity) and OSA**

It has been reported that 3-30% of Caucasian people were affected by OSA [64].

In a comparison between African Americans and Caucasians, it was reported that African Americans have higher risk and severity of OSA when compared to Caucasians [73, 156, 278, 310-312].

In 1997, Redline et al [313] reported that OSA affects the African Americans at younger ages when compared with the white persons.

In another study, it was reported that OSA is widely common in [34]:

- Black skinned people,
- Pacific Islanders, and
- Latins (Hispanics).

In Asia, it has been reported that OSA affects middle age men by a percentage of 4.1-7.5%, and middle age women by a percentage of 2.1-3.2% [314].

Although obesity is not common in Asians when compared to Caucasians, however obesity still a major risk factor for OSA among them [116, 315].

Also, retrognathia is considered as a major risk factor for Asians when compared to Caucasians [73, 116].

### **1.12 OSA in New Zealand**

OSA prevalence in New Zealand is estimated to be approximately 12% in Maori men, 8% in non-Maori men, 8.5% in Maori women and 2.3% in non-Maori women [316]; which is much higher than the worldwide estimated percentages (which are 4% for men and 2% for women [19, 20]).

Maori population represents around 15% of the entire New Zealand population. They have higher prevalence of OSA when compared to non-Maori counterparts and consequently have higher risk factors for stroke, hypertension, cardiovascular diseases and diabetes [317-320]. It has been also reported that Maori and Pacific Islanders have more severe OSA than other New Zealanders [318, 319, 321].

In 1991, Tipene-Leach et al [322] and Shaw, R.A., et al [323] reported that the prevalence of asthma, diabetes, hypertension and cardiovascular mortality is higher in Maori and Pacific Islanders than their counterparts.

In 1992, Dryson, E., et al [324] reported that Maori and Pacific Islanders have most of the risk factors for OSA such as larger tongue size, shorter neck, larger neck circumference and longer soft palate when compared with other New Zealanders.

In 1998, Baldwin D. R., et al [319] investigated OSA prevalence in 233 patients (48 Maori, 33 Pacific Islanders and 152 Europeans). They have reported that OSA prevalence was found in 85% of Maori, 94% of Pacific Islanders and 49% of Europeans.

In 2009, Mihaere, K. M. et al [316] conducted a study on Maori and non-Maori subjects in Wellington region. The participants' ages range was 30-59 years. The non-Maori were considered obese if were determined to have a BMI of more than 30 kg/m<sup>2</sup>; while the Maori were considered obese if their BMI was > 32 kg/m<sup>2</sup>. Their research included a national survey that was conducted on 6928 participants (1463 Maori men, 1732 Maori women, 1714 non-Maori men and 2019 non-Maori women); followed by a regional monitoring study that was conducted on 358 participants (166 Maori and 192 non-Maori).

They have concluded that the Maori, when compared to their counterparts, smoke heavier and have:

1. Larger neck circumference,
2. Larger BMI,
3. More severe OSA, and
4. Higher OSA prevalence.

Based on their monitoring study and on the criterion of  $RDI > 5$ , they have concluded that OSA prevalence in Maori males was 22.0% while it was only 11.4% in non-Maori males; and 6.3% in Maori females while it was only 3.0% in non-Maori females. They have also reported that the general estimated OSA prevalence was approximately 12% in Maori men, 8% in non-Maori men, 8.5% in Maori women and 2.3% in non-Maori women. This indicates that the prevalence of OSA in Maori is much higher than that in non-Maori for both men and women and is much greater than the worldwide estimated percentages which are 4% for men and 2% for women [19, 20].

In the same year, Firestone, R. T. et al [321] investigated the prevalence of OSA in professional taxi drivers in New Zealand. They have reported that Maori and Pacific Islanders have larger neck size and daytime sleepiness than other counterparts. They have also reported that Maori and Pacific Islanders have more risk factors for OSA than other New Zealanders and consequently have higher risk of vehicle motor accidents. These findings were in excellent agreement with the previously conducted studies nationwide.

In 2011, Paine, S. J. et al [323] reported that Maori have poorer sleep profile than non-Maori and consequently poorer quality of life, thus Maori are of more risk to develop sleep problems and therefore Maori health care should be of main priority.

### **1.13 Treatment Modalities for OSA**

The treatment of OSA depends on the severity of the disease, which is determined according to either the AHI or RDI as described previously in section 1.3.

The purposes of any treatment method remain the same, to prevent the apneic events [19] and to improve (reduce) the flow parameters in order to keep the airway open during sleep to prevent airway collapse. These parameters are listed below [53]:

1.  $\tau_w$ : Wall shear stress (WSS).
2. Airway resistance ( $R = \frac{\Delta P}{Q}$ ).
3. Maximum velocity ( $V_{max.}$ ).
4. Minimum wall static pressure ( $P_{min.}$ ).

The treatment modalities can be divided into four main types:

1. Life style changing,
2. Drug therapy,
3. Surgical treatment, and
4. Non-Surgical (non-invasive) treatment.

#### **1.13.1 Life Style Changing**

Changing the life style is considered as one of the treatment modalities for patients diagnosed with OSA; of main concern is weight loss which is an easy method for treating obese patients diagnosed with only mild OSA [34, 38, 150, 325, 326]. This results in: (i) reduced hyper somnolence, (ii) less apneic time during sleep and (iii) decreases blood oxygen de-saturation [327]. If a patient is diagnosed with moderate to severe OSA, then losing weight is not an effective treatment method. Also, not all patients have the ability to lose weight [110].

Changing life style may also be done by stopping drinking alcohols, stopping taking sedatives (which relaxes muscles) and quit smoking [34, 38, 110]. Also the patient must avoid sleeping in supine position to reduce the tendency for apneic events [34, 328, 329]. The patient is advised to sleep at an incline of 30-60 degrees (to the horizontal) [38] to minimize the apneic events that occur during sleeping in supine position due to the gravitational force which pulls the tongue and the uvula towards the airway walls [94].

#### **1.13.2 Drug Therapy**

Over many decades of time, no drug was proved to be an effective treatment for patients diagnosed with OSA. This is because drug therapy was:

- restricted only for patients with mild to severe OSA [330], and
- associated with bad side effects such as urine retention, sore throat, constipation and low erectile ability [330].

### 1.13.3 Surgical Treatment

The surgical treatment (also known as invasive treatment) is considered to be effective for patients diagnosed with mild OSA. It can be also used for more severe OSA but with less success rates. Surgical treatment can also be used effectively when the patient has large size of anatomic obstructions such as tonsils, adenoids and uvula [331, 332].

There are several surgical (invasive) procedures for the treatment of OSA, which are listed below:

1. Nasal septoplasty and reducing turbinate: This procedure aims to reduce the nasal obstruction, however the results are so poor [333, 334].
2. Adenotonsillectomy [25, 335-337]: It is considered as the most common treatment for obese children diagnosed with OSA, however the success rate is approximately 50% only [25].
3. Uvulo-pharyngeal-palato-plasty (or uvulo-palato-pharyngo-plasty) [335-338]: It is sometimes known as UPPP or UP3 [43, 339]. Through this surgery, a part of the soft tissues of the pharynx, tonsils, adenoids, soft palate and uvula [43, 339-342] is removed. The success rate is only about 40% because this procedure does not reduce the obstruction in the laryngopharynx [343]. It was reported that this surgical procedure is not as efficient as the CPAP device [344] mainly due to the resulting irresistible pain. It was also reported that this procedure results in swallowing difficulties as well as narrowing the velopharynx [343].
4. Uvulopalatal Flap (UPF): This procedure results in less pain when compared to UPPP procedure, however the patients still have pain [345].
5. Laser Assisted Uvulopalatoplasty (LAUP): This procedure was firstly introduced in 1990 by Kamami Y.V. [346, 347]. It aims to excise the uvula and part of the soft palate using carbon dioxide laser [342]. Sadly, this procedure results in awful pain and swallowing difficulties [348, 349]. In 2000, Littner et al [350] reported that this procedure is not recommended as a treatment for OSA.
6. Hyoid Advancement (HA): The aim of this procedure is to expand the airway by moving the hyoid bone forward [342, 351, 352]. This procedure cannot be used alone, it may be used with UPPP [353] or Genioglossus Advancement (GA) [354-356]. This procedure needs “an external incision on the neck” [338]

which is really hard to convince the patients to accept. Also this procedure may result in difficulties in swallowing and serum formation [351, 354-356].

7. Genioglossus Advancement (GA): This procedure cannot be used alone as a treatment for OSA, it may be used together with UPPP or Hyoid Advancement (HA). Also, the success rate of this procedure is not guaranteed [326, 342, 352, 354, 355, 357].
8. Maxilla-Mandibular Advancement (MMA) [53, 335-337, 358-363]: At which both mandible and maxilla are pulled forward, which enlarges the retropalatal region [338, 342, 364], which in turn improves the flow characteristics (as the airway cross sectional area increases, the static pressure decreases) [53]. It was reported that this surgical procedure is the best for OSA patients [354, 357, 363, 365-368] with success rate as high as 75-100% [369], especially for patients with severe OSA which was demonstrated by Fan et al [19]. Also, it was reported that MMA may cause airway bleeding and infections [370].
9. Mandible advancement [371-373]: The aim of this procedure is to reposition the tongue anteriorly in order to enlarge the retropalatal airway [342].
10. Maxilla-Mandibular Expansion: Although this procedure is less invasive when compared to MMA, however after this operation, mouth distractors are used for long time to help stabilizing the expansion in both the mandible and maxilla. After that the patient will need orthodontic therapy which is really hard to be accepted by the patient [338].
11. Temperature-Controlled Radio Frequency (TCRF) Tongue Base Reduction [374, 375]: This procedure results in difficulties and pain in swallowing, as well as abscess in the tongue that needs to be drained [338]. It also results in weight gain, higher RDI and higher oxygen de-saturation [376]. In addition to the previous noted disadvantages, this procedure cannot be used alone as a treatment for OSA [338].
12. Tracheostomy: It is commonly used for morbid obese ( $BMI > 35$ ) and cardiovascular disease patients [342, 370]. It has been reported that the symptoms of the hyper somnolence and arousals have disappeared within a period of time of only 48 hours [377]. Also the symptoms of arrhythmia were remarkably decreased after the tracheostomy [378]. Sadly, there are many disadvantages for tracheostomy, such as [338, 379]:
  - Secretions,
  - Partial obstruction and dyspnoea may occur due to head movement,

- Some tissues can granulate at the site of tracheostomy (not so good to be seen), and
- Depression due to bad overall configuration.

13. **Bariatric surgery:** It is a commonly used treatment to reduce the body weight and consequently attenuate OSA in morbid obese patients [380-385] diagnosed with moderate-to-severe OSA [386-388]. More information about bariatric surgery will be explained in details in section 2.2.

In general, the main disadvantages of the surgical treatment are its invasive nature and complexity [335-337]. It has been also reported that the success rates for the surgical interventions are relatively low, especially for morbid obese patients as well as patients diagnosed with severe OSA [110].

#### **1.13.4 Non-Surgical (non-invasive) Treatment**

The non-surgical treatment is preferred than the surgical treatment due to the non-invasive nature. Also the non-surgical treatment is so easy to be used (user friendly) by the patient. The non-surgical modalities are listed below:

1. **Continuous Positive Airway Pressure (CPAP):** It is considered the most effective non-invasive OSA treatment [16, 34, 38, 104, 110, 115, 146, 326, 328, 331, 335-337, 389-395]. It is mainly used for patients diagnosed with moderate to severe OSA [34, 285, 328, 396]. The CPAP device provides a continuous pressurized and humidified air in order to prevent airway collapse [19, 38, 332, 339, 365, 393, 397]. The main problem of using the CPAP device is that it needs to be accurately calibrated to suit every patient (patient specific) although it is so efficient [335-337]. CPAP is explained in detail in section 1.14.
2. **Automatic (Adjustable) Positive Airway Pressure (APAP):** Sometimes it is known as Auto-adjustable or Auto-Titrating Continuous Positive Airway Pressure (A-CPAP) [104, 398]. It is considered the most recent non-invasive treatment for OSA as it adjusts the pressure instantaneously and continuously to achieve the best patient's comfort [350, 398-402]. It was reported that the APAP resulted in reducing both sleep fragmentation [403-417] and hyper somnolence [404, 411-414, 418-420]. The main problem for using the APAP device is its relatively high cost when compared with the conventional CPAP device. Also Rodenstein [421] reported that the maximum operating pressure for the APAP is higher than that for the conventional CPAP devices, which is

considered as another disadvantage. The APAP can be used to specify the optimum operating pressure (pressure titration) for the patient and then the conventional CPAP device can be used effectively, which will of course reduce the cost of the continuous use of the APAP [398].

3. **Mandibular Advancement Splint (MAS):** It is a device that attaches to the mouth during sleep in order to push the lower jaw forward and down (when compared to the normal relaxed position), which prevents the tongue from moving to the back towards the airway walls which in turn tends to increase the pharyngeal airway; thus preventing the apneic events that may occur at the rear of the tongue in the normal relaxed position [38, 331, 422]. This device can be used effectively and successfully for non-obese patients with mild to moderate OSA only [38, 325, 382, 423], however it was reported to be very uncomfortable to be used [382]. In 2002, Randerath et al [424] and Engleman et al [425] reported that the treatment with the CPAP is better than using mouth devices for apneic patients diagnosed with mild to moderate OSA. In general this device is not as efficient as the CPAP [331], because the obstruction may occur in other sites rather than rear of the tongue such as rear of uvula (during expiration), or somewhere in the pharyngeal airway (during inspiration) [344]; although it is considered more user friendly than the CPAP device.

#### **1.14 CPAP**

The use of the CPAP device was firstly introduced in 1981 by Sullivan et al [426]. Since then, it became the main treatment for patients diagnosed with OSA [16, 34, 38, 104, 110, 115, 146, 326, 328, 331, 335-337, 390-395, 423, 427].

The concept of the CPAP device is to deliver a continuous supply of humidified air which is tolerated to a certain pressure that is suitable and comfortable to the patient in order to prevent the airway collapse [94, 104, 332, 389, 390, 393, 397, 428], which means that the operating pressure must for sure be above the closing (critical) pressure [429].

Sullivan et al [426] and Iber et al [430] reported that the use of the CPAP device resulted in a remarkable reduction in blood oxygen de-saturation during sleep.

Also, Rapoport et al [423] and Berry et al [431] reported that from the first night of using the CPAP device it resulted in reducing the blood oxygen de-saturation during sleep;



followed by a remarkable improvement in the excessive daytime sleepiness (EDS) through the first week of usage.

The improvement in hyper somnolence as a result of using the CPAP device was also reported by McArdle, N., and Douglas, N.J. [432], Lamphere et al [433], Jenkinson et al [328], Marti et al [337], Pichel et al [434], Teran et al [40] and Montserrat et al [329].

Also, it was reported that snoring was drastically decreased after using the CPAP device [55].

Ingbar et al [55] and Marti et al [337] reported that the use of the CPAP device for patients with OSA resulted in remarkable reduction in both OSA morbidity and mortality.

Findley et al [243, 435] and George, C.F. [436] reported that the use of the CPAP device resulted in improving the motor driving performance and consequently reduced the risk for driving accidents. This in turn will reduce the mortality that may occur due to OSA [40, 225, 337, 434].

Hypertension was also reported to improve after using CPAP device [219, 437], as well as arrhythmia [206].

It was reported that the health care utilization was reduced when OSA patients were treated with CPAP device [438].

In 2000, Oliver et al [439] reported that the CPAP operating pressures changed only by  $\pm 0.2$  kPa for most of the participating patients, which facilitates the titration of the CPAP device to a very small range of change in order to obtain the suitable pressure for each patient.

Pichel et al [434] reported that the treatment of OSA using the CPAP improves the quality of life.

In 2005, Marin et al [179] reported that when patients with OSA used the CPAP device, it resulted in remarkable reduction in both OSA morbidity and mortality. They have also reported that the hyper somnolence symptoms were reduced from the first time of using the CPAP.

Also, it has been reported that the best results can be obtained when the CPAP is used every day for more than 4 hours of sleep [440, 441].

Lam et al [442], Noda et al [443] and Bayram et al [444] reported that the use of the CPAP as a treatment for OSA may reduce the risk of cardiovascular diseases.

#### **1.14.1 CPAP Titration**

In order to use the CPAP as a treatment for a patient diagnosed with OSA, the operating pressure should be specified to achieve the best patient's comfort, this is known as "CPAP titration" and is currently done by using overnight polysomnogram in sleep centres and adjust the CPAP manually until the optimum operating pressure is obtained [445], or using the APAP for one week at home [446]; which are considered to be time consuming and relatively expensive.

#### **1.14.2 Disadvantages of the CPAP**

Although the CPAP is considered the most effective non-invasive OSA treatment method for OSA patients, however it was reported to have the following disadvantages:

1. Nasal occlusion (itching or rhinorrhea) [447-451],
2. Dry nose [447-451],
3. The CPAP facial mask is not comfortable during sleep [38, 452-454],
4. The CPAP facial mask may cause facial abrasions (skin marks) [38, 452-454],
5. Air leaking may occur during sleep [38, 452-454],
6. The exhaling process may not be as comfort as required [38, 452-454], and
7. Ear pressure.

In addition to the above noted disadvantages, it has been reported that the optimum operating pressure may change (reduce) after a period of time (for long term CPAP therapy), another titration may therefore be required to specify the new suitable operating pressure [455]. The same result as well as the cost were documented by Collard, P., et al [456].

Also, due to the high operating pressures there has been lots of patients' rejection [457], reaching a percentage of more than 30% as reported by Berthon-Jones, M., et al. [458] or even as high percentage as 50-80% according to Meurice, J. C., et al [459] and Zozula, R., et al [460]; especially for patients with cardiovascular disease (it has been reported that CPAP may introduce stroke symptoms in those patients).

It was also reported that OSA patients who are using CPAP still have poor quality of life and sleep and daytime somnolence; according to the results of Vgontzas, A. N., et al [461] and Barnes, M., et al [462].

### **1.15 Closure**

This chapter presented background information on OSA and showed the currently used treatment modalities including the CPAP which is the main treatment for OSA, basically due to its non-invasive nature. This chapter also showed the disadvantages of the CPAP device due to the high operating pressures. In order to investigate the conditions of collapse and try to reduce the operating pressures and consequently reduce patients' rejection, it is necessary to understand the available modelling techniques and identify their weakness points to be avoided in our study; which is discussed in detail in the next chapter.

## CHAPTER 2

### Literature Survey on UA Characteristics and Modelling

#### 2.1 Introduction

This chapter presents a literature survey covering the relationship between bariatric surgery and OSA, which is given in section 2.2. It also summarizes the reported differences in the UA muscle activity between healthy subjects and OSA patients, section 2.3. Section 2.4 covers the effects of the PO on the UA muscle activity. The techniques used in modelling the UA are explained in section 2.5, including the different computational fluid dynamics (CFD) methods as well as the interaction between the airflow through the UA and the deformations of the soft tissues by investigating the Fluid-Structure Interaction (FSI). Finally, the research objectives are presented in section 2.6.

#### 2.2 Relationship between Bariatric Surgery and OSA

The available information relating bariatric surgery and OSA does not include large number of participating patients and the results were evaluated subjectively (subject specific) not objectively [307, 383, 386, 387, 463-470]. Nevertheless, the available information for the relationship between bariatric surgery and OSA are listed below.

In 1978, Remmers, J. E., et al [91] reported that the upper airways in obese OSA patients are more collapsible than those of normal weight counterparts.

In 1984, Peiser, J., et al [471] studied the relationship between OSA and weight reduction using bariatric surgery as a treatment for morbid obese OSA patients. The study was conducted on 15 OSA patients consisting of 14 males and 1 female. The participants' ages were 24-59 and 53 years for the males and the female, respectively. Before surgical intervention, the BMI for the participating males ranged from 34.75 to 68.17 kg/m<sup>2</sup> and for the female was 44.29 kg/m<sup>2</sup>. Another evaluation was conducted 2-4 months after the surgery for all patients, followed by another evaluation that was conducted for six patients after 4-8 months from the first evaluation. These evaluations showed that the BMI for the males was reduced to 25.95-40.76 kg/m<sup>2</sup>, and for the female it was reduced to 38.26 kg/m<sup>2</sup>. Also, OSA was completely resolved in 12 of the participants as a result of weight loss due to surgical intervention. They have concluded that bariatric surgery is a successful treatment for morbid obese OSA patients. Unfortunately, their study did not report the effectiveness of bariatric surgery for severe OSA.

One year later, Charuzi, I., et al [468] reported that bariatric surgery is the right treatment choice for morbid obese patients diagnosed with severe OSA. They have also reported that the AHI dropped from 88.8 to 11.8 event/h after only 6 months from surgical intervention.

Another research by Charuzi, I., et al [387] was conducted in 1987 on 46 OSA patients (39 men and 7 women) who were morbidly obese and promoted for bariatric surgery. They have reported that the work of breath decreases due to weight loss. They have also reported that bariatric surgery resulted in remarkable improvement in OSA symptoms through the follow ups conducted 1 year and 7 years after the surgery. Their results showed that the AHI was dropped from 58.8 to 36.1 events/hr. Also, they have reported that bariatric surgery is a suitable treatment choice for morbid obese OSA patients.

In 1988, Rubinstein, I., et al [472] reported that weight loss resulted in improving the performance of the UA and OSA.

In 1990, Summers, C. L., et al [473] reported that bariatric surgery resulted in remarkable improvements in OSA.

In 1991, Schwartz, A. R., et al [474] reported that OSA was almost completely resolved as a result of weight loss. They have reported that this is true for patients with UA closing pressure less than 4 Cm H<sub>2</sub>O (mild-to-moderate OSA).

In 1992, Smith, D. K., et al [475] reported that more than 95% of obese patients will regain their weights if they are using dieting only to lose weight. This means that dieting is not an effective weight loss treatment for OSA due to recidivism.

In the same year, Sugerman, H. J., et al [466] conducted a large study on 57 morbid obese OSA patients. A follow-up was conducted  $4.5 \pm 2.3$  years after surgical intervention showed substantial improvements in both BMI and OSA symptoms. They have reported that the mean AHI was reduced from 64 to 26 events/hr, the mean BMI was reduced from 58 to 39 kg/m<sup>2</sup> just 1 year after the surgery; and that 38 subjects were completely cured from OSA after 2 years from surgical intervention.

A much bigger study was conducted in 1992 by Charuzi, I., et al [476] on 798 morbid obese OSA patients consisting of 199 men and 599 women evaluated for bariatric surgery. The study was conducted over 8 years. They have reported that bariatric surgery resulted in a complete cure from OSA in 319 subjects and that the AHI was remarkably reduced

in 575 subjects. They have also reported that bariatric surgery is effective in losing weight and improving OSA symptoms if the patients were committed to a diet after surgical intervention to prevent any recidivism and consequently regain weight and OSA.

Bariatric surgery resulted in improving OSA symptoms in 11 patients out of 12 morbid obese OSA patients, as reported in 2000 by Dhabuwala, A., et al [477].

In 2001 Dixon, J. B., et al [478] reported that bariatric surgery resulted in reducing the symptoms of OSA from 33% preoperatively to only 2% postoperatively.

In 2001, Scheuller, M. and Weider, D. [479] studied the relationship between bariatric surgery and OSA in 15 morbid obese patients (10 males with age range of 25-48 years and 5 females with age range of 20-43 years). All patients were diagnosed with severe OSA. Before surgery, the weight of participating males ranged from 122.5 to 190 kg, and for the participating females it was 119-184.6 kg. After surgery, the weight range was reduced to 81.6-137 kg and 72.5-131.5 kg for males and females, respectively. They have reported that bariatric surgery resulted in resolving OSA symptoms in all patients and it is the suitable treatment choice for morbid obese OSA patients. The same result was reported by Guardiano, S. A., et al [470] in 2003.

In 2003, Frey, W. C. and Pilcher, J. [286] studied the predominance of OSA in patients promoted for bariatric surgery. This study was conducted on 41 morbid obese patients (34 women and 7 men) evaluated for bariatric surgery. OSA was found in 29 subjects (23 females and 6 males) with a percentage of 71%. The age group for females was 25-60 years and for males it was 19-58 years. The BMI range for the females and males was 37-58 and 41-58 kg/m<sup>2</sup>, respectively. OSA severity ranged from mild to severe. They have reported the high prevalence of OSA in patients evaluated for bariatric surgery.

OSA severity was reported to decrease as a result of bariatric surgery in morbid obese adults as reported by Rasheid, S., et al [381] in 2003. They have reported that the mean AHI was reduced from 56 to 23 events/hr at a follow up conducted postoperatively.

Sugerman, H. J., et al [480] conducted a study in 2003 on 33 morbid obese adolescents consisting of 19 females and 14 males promoted for bariatric surgery. The mean BMI was reduced from  $53 \pm 11$  kg/m<sup>2</sup> preoperatively to  $36 \pm 10$  kg/m<sup>2</sup> only 1 year postoperatively. Another follow up was conducted 5 years after surgery showed that the mean BMI was further reduced to  $33 \pm 11$  kg/m<sup>2</sup>. They have reported that 6 participants were diagnosed

with OSA preoperatively and that bariatric surgery resulted in resolving OSA symptoms in all subjects.

In the late of 2003, Guardiano, S. A., et al [470] studied the relationship between bariatric surgery and OSA on 34 morbid obese OSA patients. Unfortunately, only 8 subjects (7 women and 1 man) have completed the study by participating in a follow up conducted 9-60 months after surgical intervention. The age group was 35-55 years. They have reported that bariatric surgery resulted in remarkable improvement in the BMI which was reduced from 32-73 kg/m<sup>2</sup> before surgery to 25-63 kg/m<sup>2</sup> after surgery; as well as the RDI that was reduced from 7-94 to 2-44 events/hr. Also, OSA symptoms were completely resolved in 5 subjects.

In 2004, Valencia-Flores, M., et al [481] studied the effects of bariatric surgery on OSA. The study was conducted on 16 females and 13 males before and after surgical intervention. The participants' ages ranged from 20 to 56 years. The BMI and the AHI before surgery were 39.6–88.9 kg/m<sup>2</sup> and  $51.9 \pm 47.2$  events/hr, respectively. Another evaluation was conducted approximately one year after the surgery where the participants were divided into two groups, a group with OSA and the other group without OSA. They have reported that the BMI, the AHI and the neck circumference were remarkably decreased after the surgery in both groups, and that 13 subjects were completely cured from OSA with a success rate of approximately 46%. They have concluded that bariatric surgery can resolve moderate OSA in morbid obese patients.

In the same year, O'Keeffe, T. and Patterson, E. J. [306] studied the predominance of OSA in patients evaluated for bariatric surgery. This study was conducted on 170 morbid obese patients promoted for bariatric surgery, consisting of 21 men and 149 women. The participants' age range was 20-64 and 24-72 years for women and men, respectively. They have reported that 131 patients were diagnosed with OSA which means that the prevalence of OSA was approximately 77%.

Another study was conducted in the same year by Frigg, A., et al [463]. They have monitored the participating patients over a period of 4 years postoperatively. They have reported that OSA symptoms completely resolved in 75% of the participants and improved in the remaining 25% of the participants.

A systematic review was also conducted in 2004 by Buchwald, H., et al [482] showed that bariatric surgery was a very successful procedure for morbid obese OSA patients, as OSA symptoms were disappeared in 85.7% of the participating patients.

Also, in 2004 Dolan, K., M. et al [483] and Simard, B., et al [464] reported that some bariatric surgery procedures may result in resolving around 98% of OSA symptoms in morbid obese subjects.

In 2005, Kalra, M., et al [382] studied the relationship between bariatric surgery and OSA in morbid obese adolescents. This study was conducted on 35 morbid obese adolescents (23 females and 12 males) from which 19 were diagnosed with OSA. The BMI range was 48-87 kg/m<sup>2</sup> and the weight was 170 ± 31.38 kg. After the surgery, 10 subjects returned for a follow up after 5.1 ± 1.2 months at which a remarkable reduction in OSA severity was detected. They have also concluded that OSA severity increases as the BMI increases; and that bariatric surgery is a suitable treatment choice for morbid obese OSA adolescents.

In the same year, Dixon, J. B., et al [383] studied the relationship between bariatric surgery and OSA in 49 morbid obese moderate-to severe OSA patients. Only 25 subjects returned for a follow up 12-42 months postoperatively. The data collected through the follow up showed that bariatric surgery resulted in reducing the BMI (weight loss was 18-103 kg), and the mean AHI was reduced from 61.6 ± 31.9 to 13.4 ± 13 events/hr. Also, the follow up data showed that only 4 subjects still have moderate-to-severe OSA and that is why they continued using the CPAP but with lower operating pressures to keep their airways open during sleep. They have also reported that the quality of both life and sleep was remarkably improved; and that bariatric surgery was a successful treatment choice for morbid obese OSA patients in both losing weight and improving their OSA symptoms.

In 2007, Fritscher, L. G., et al [388] studied the relationship between bariatric surgical intervention in excessive overweight OSA patients. This study was conducted on 12 morbid obese OSA patients (9 men and 3 women) who were promoted for bariatric surgery. A follow-up was conducted 24.2 ± 6.4 months after surgery showed that OSA was completely resolved in 3 subjects, and OSA severity was improved in another 6 subjects. Also, the obtained results showed that bariatric surgery is a suitable treatment choice for excessively overweight subjects diagnosed with severe OSA.

Another research was conducted by Fritscher, L. G., et al [307] in the same year. They have reported that bariatric surgery is a suitable weight loss treatment choice for morbid



obese patients. They have also reported that on long term basis, OSA may return with less severity which might be related to age that is inversely related to muscle tone activity.

In the same year, a much bigger study was conducted over 7 years by Haines, K. L., et al [107] on 349 morbid obese patients promoted for bariatric surgery. Before the surgery, PSG data showed that 289 patients had OSA (approximately 83%), from which 116 had severe OSA, 63 had moderate OSA and 110 had mild OSA. A follow up was conducted 6-12 months after surgical intervention on 101 patients showed remarkable improvements in BMI which was reduced from  $56 \pm 1$  to  $38 \pm 1$  kg/ m<sup>2</sup> as well as the RDI which was reduced from  $51 \pm 4$  to  $15 \pm 2$  events/hr. They have reported that the BMI and the RDI were dramatically improved in patients with severe OSA, less improved for patients diagnosed with moderate OSA and further less improved for patients diagnosed with mild OSA. Their findings confirmed that bariatric surgery is the best treatment choice for morbid obese patients with severe OSA. The only limitation to their study is that only 101 of 289 patients returned for the follow up which is approximately 35% of the participants which may affect the strength of their findings.

Also, in 2007 Flancbaum, L. and Belsley, S. [484] investigated the risk factors for patients undergoing bariatric surgery. This study was conducted on 1000 morbid obese patients (146 males and 854 females) promoted for bariatric surgery with age range of 15-73 years. They have reported that perioperative mortality incidence was increased three times in OSA patients undergoing bariatric surgery.

Another case study was conducted in 2008 by Kuzniar, T. J. and Morgenthaler, T. I. [485] on a 27 years old morbid obese male who was diagnosed with severe OSA (AHI=44 events/hr) and was evaluated for bariatric surgery. A follow up was conducted 7 months postoperatively showed that the participant lost 47.6 kg which resulted in reducing the BMI from 44.5 to 29.4 kg/m<sup>2</sup>, as well as remarkable improvements in OSA symptoms.

In the early 2009, Nguyen, N. T., et al [486] studied the relationship between bariatric surgery and OSA in 104 morbidly obese subjects consisting of 80 women and 24 men, with mean age of  $41 \pm 11$  years. Before surgery, the mean BMI was  $48 \pm 6$  kg/m<sup>2</sup>. They have reported that 30 subjects (29%) were diagnosed with OSA. Many follow ups were conducted after surgical intervention starting from 1 month and then every 3 months. They have also reported that the patients lost  $54 \pm 23\%$  of their excess weight only 1 year after the surgery, and that OSA symptoms were remarkably improved after the surgery.

In 2010, Sharkey, K. M., et al [487] investigated the prevalence of OSA in 296 morbid obese women (mean BMI was 50.1 kg/m<sup>2</sup>) promoted for bariatric surgery. The age range was 19-61 years. They have reported that 255 women were diagnosed with OSA giving a prevalence percentage of 86.15% which demonstrates the high prevalence of OSA in the morbid obese subjects evaluated for bariatric surgery.

In 2011, Sareli, A. E., et al [488] studied the prevalence of OSA in morbid obese patients promoted for bariatric surgery. This study was conducted over two years from late 2005 to early 2007 on 342 morbid obese patients promoted for bariatric surgery, consisting of 279 women and 63 men. Preoperatively, the mean age and BMI were 43.8 ± 10.9 years and 49.5 ± 10 kg/m<sup>2</sup>; respectively. They have reported that 264 subjects were diagnosed with OSA (77.2%) consisting of 205 women (73.5%) and 59 men (93.6%) and that OSA severity was much higher in males than females. The mean AHI for the males and the females was 48.6 and 26.3 events/hr; respectively. These results show that obesity and the male gender are considered as major risk factors for OSA, which agrees with the reported studies in the background (Chapter 1).

In 2012, Ravesloot, M. J. L., et al [489] investigated the prevalence of OSA in 279 obese patients (214 women and 65 men) evaluated for bariatric surgery in their clinic. The patients' age range was 18-65 years. They have reported that OSA severity increases as the BMI increases and that men have higher OSA severity than their counterparts. Their results showed that approximately 70% of the patients evaluated for bariatric surgery were diagnosed with OSA. One year later, a follow up was conducted by the same group [490] to investigate OSA prevalence after undergoing bariatric surgery and reported remarkable reductions in both the BMI and the AHI.

In 2013, Bakker, J. P. et al [384] studied the effects of bariatric surgery on obese patients diagnosed with OSA. This study was conducted on twelve patients (10 women and 2 men) with BMI range of 42-51.4 kg/m<sup>2</sup> (morbid obese), neck circumference range of 39.6-47.97 Cm and AHI range of 16.3-67.5 events/hr (moderate to severe OSA). After six months of the surgery, the BMI range was reduced to 30.1-38.7 kg/m<sup>2</sup>, which indicates that the maximum BMI after the surgery is less than the minimum BMI before surgery. The neck circumference was also reduced to 35.1-41.1 Cm. The AHI range was also reduced after the surgery to 5-20.8 events/hr which is considered as mild-to-moderate OSA. They have reported that the surgery resulted in substantial reductions in the AHI and the BMI as well as the neck circumference.

## **2.3 UA Muscles Activity**

During sleep, both the activity of the UA muscles and UA compliance decrease, which increases the ability of the airway to be obstructed and/or collapsed. These symptoms were reported for OSA patients. This indicates that OSA patients have less chest compliance and UA muscle activity during sleep especially for obese subjects. These findings are explained in detail through the following section.

In 1978, Remmers et al [91] reported that when the person falls asleep, the activity of the UA muscles reduces, which increases the ability of the airway to be obstructed or collapsed and may develop OSA.

In 1982, Onal and Lopata [195] reported that during wakefulness, the activity of the genioglossus muscle in patients with OSA is less than that of the normal subjects.

In 1992, Mezzanotte et al [491] reported that during sleep, the activity of the genioglossus muscle was remarkably reduced in patients with OSA compared to normal subjects, which is clearly in excellent agreement to the results of Remmers et al [91].

In 1994, Van Der Touw et al [492] reported that the negative pressure in the UA during the inspiratory breathing phase can recruit the activity of the UA muscles. The same results were reported for humans in 1995 by Mortimore et al [493].

Later on, in 1998 Henke et al [494] reported that the phasic activity of the UA muscles is not the main factor for the UA potency during sleep.

In 2005, Fogel et al [495] experimentally studied the changes in the activity of the UA muscles during both cases of wakefulness and sleeping, with and without the use of nasal CPAP. The study was conducted on 35 subjects divided into three groups as described below:

1. Twelve healthy young males,
2. Eleven healthy old males, and
3. Twelve patients with OSA.

They studied the UA muscles activity with and without (basal breathing) the use of the CPAP, during both cases of wakefulness and sleeping. Throughout this study, the patients were sleeping in supine position (which is the worst sleeping position for OSA patients).

The CPAP range was 5-10 Cm H<sub>2</sub>O. They have concluded the following results during both cases of wakefulness and sleeping:

1. **Without the use of CPAP (basal breathing):** The activity of the genioglossus muscles was found to be higher in patients with OSA than the healthy subjects.
2. **Using the CPAP:** The use of CPAP resulted in reducing the activity of the genioglossus muscles in the three groups, with considerably more reduction in patients with OSA than the healthy subjects.
3. OSA patients have narrower and more collapsible upper airways when compared to the healthy subjects, which is similar to the upper airways of the older healthy subjects when compared to the middle aged subjects.
4. Obese subjects have both less compliance of the chest wall and UA muscles activity; which increases the required work of breath in order to provide the appropriate ventilation.

The main limitation to their study is that the participants had different values of BMI, which means that the comparison between the obtained results from the different individuals is not powerful, because of the fact that obesity (and consequently BMI) has a direct effect in worsening the severity of OSA due to the narrowing the UA because of the large size of the soft tissues, as well as reducing the activity of the UA muscles.

In 2007, Lo et al [496] conducted an experimental study on 10 healthy subjects to study the changes in the UA muscles activity during both cases of wakefulness and sleeping. The participating subjects were:

1. Healthy,
2. Normal weight, and
3. The age range was 19-52 years.

All subjects had nasal breathing using positive pressure ventilator while lying in supine position during both cases of wakefulness and sleeping. The pressure ventilator operating pressure ranged between 4 and 8 Cm H<sub>2</sub>O. They have reported that the activity of the genioglossus muscles was higher during wakefulness when compared to the sleeping case.

The main limitations to their study are:

1. All the participating subjects were healthy, so they dropped the study of the changes in the activity of the UA muscles in patients with OSA.

2. All the participants had normal weights, so they dropped the more critical case of obese subjects.

It has been reported that the activity of the UA muscles can be altered by the pressure oscillations (PO), therefore the next section presents a literature survey on the effects of the PO on the UA muscle activity.

## **2.4 Effects of Pressure Oscillations on the UA Muscle Activity**

Pressure oscillations (PO) have been proven to increase the activity of the UA muscles in both sleeping animals and humans. This will be explained in detail later on.

In 1968, Robin [497] reported that the pressure waves resulting during human snoring have high frequencies ranging between 30 to 50 Hz.

In 1990, Plowman et al [498] had an experimental study on three sleeping tracheotomised dogs (weight range was 20-30 kg). They used PO waves similar to those occurring during human snoring (30 Hz) as previously described by Robin [497], combined with an amplitude of  $\pm 3$  Cm H<sub>2</sub>O. They have reported that the activity of the genioglossus muscle was increased by the effect of the PO.

In 1992, Zhang et al [499] had an experimental study on 10 anesthetized supine dogs. They studied the effects of the PO at 10, 20 and 30 Hz, combined with an amplitude of  $\pm 2.5$  Cm H<sub>2</sub>O. They have concluded that the PO increased the activity of the pharyngeal receptors.

In 1993, Henke et al [500] experimentally studied the effects of the PO on the UA muscles during the inspiratory breathing phase on 6 normal subjects and 10 patients with OSA. The PO were delivered to the UA via a nasal mask using a pressure wave ventilator. The normal subjects were allowed to sleep in any position, while OSA patients were asked to sleep in supine position if they did not have apneic events while sleeping on their sides. They have reported the following:

1. The activity of the UA muscles was increased as a result of the effect of the PO in both normal and OSA subjects, and
2. In some patients with OSA, the PO succeeded in keeping the airway open and prevented obstruction.

Their study had the following limitations:

1. The study was conducted during the inspiratory breathing phase only, while some of the respiratory problems and apneic events occur during the expiratory breathing phase.
2. The patients were allowed to sleep in different sleeping positions, which means that the reported sleeping data were not equivalent to one another as the compliance of the airway muscles depends not only on whether the subject is awake or asleep, but also on the sleeping position itself.

In 1996, Brancatisano et al [501] reported that the PO resulted in increasing both the activity and stiffness of the UA muscles in anesthetized dogs, which in turn increased the UA potency and reduced its collapsibility.

In 1999, Eastwood et al [502] experimentally studied the effect of high-frequency-pressure oscillations (HFPO) on the genioglossus muscles in three tracheotomised sleeping dogs. They used PO waves of 30 Hz, combined with amplitudes of  $\pm 2$  and  $\pm 4$  Cm H<sub>2</sub>O. They have concluded that the activity of the genioglossus muscles was increased due to the effect of HFPO during both expiratory and inspiratory breathing phases, but with more activity during the expiratory breathing phase.

In 2001, Badia et al [503] experimentally studied the effect of HFPO on the UA muscles in humans (seven male patients), diagnosed with moderate-to-severe OSA. These subjects had the following characteristics:

1. Ages ranged between 43 and 65 years,
2. AHI range was 22-64 events/hr, and
3. BMI range was 28-32 kg/m<sup>2</sup>.

They used PO with an amplitude of 1 Cm H<sub>2</sub>O at a frequency of 5 Hz (which is typically used in clinical studies) and a frequency of 30 Hz (which is typically produced during snoring in humans). They have reported that the use of the PO:

1. Did not restore the airflow during the apneic events, or the length of the apneic event itself, and
2. Had no effect on the activity of the electromyogram (EMG), nor the electroencephalogram (EEG).

The limitations to their study are:

1. The study was done only for a pressure amplitude of 1 Cm H<sub>2</sub>O, while the UA muscles have been proven to be activated (in animal models) when the amplitude of the PO ranges between 2-4 Cm H<sub>2</sub>O.
2. All patients were allowed to sleep in their preferred position.
3. The patients used the CPAP for the first time during the study.
4. All patients were overweight or obese, and no normal weight subjects were considered.
5. The last two conditions have been proven to reduce both the activity and response of the UA muscles [504, 505].

In 2005 Vanderveken et al [506] used the forced oscillation technique in an experimental study to accurately specify the potency of the airway during sleeping disturbances. They used the PO with a frequency of 5 Hz which is the smallest stimulating frequency for the UA muscles. The study was conducted on 8 men diagnosed with OSA. The patients had the following characteristics:

1. Ages ranged between 42 and 58 years,
2. Weights ranged between 75 and 95 kg,
3. BMI ranged between 24 and 30 kg/m<sup>2</sup>, and
4. RDI ranged between 11 and 65 events/hr.

They have reported that the airway has an equal opportunity to get obstructed during the expiratory breathing phase as well as the inspiratory breathing phase. This result was in accordance with the result previously reported by Morrell et al [507], but at the same time contradicted most of the previous researches which reported that the UA is more likely to collapse during the inspiratory breathing phase rather than the expiratory breathing phase, such as Kuna [29].

## **2.5 UA Modelling Techniques**

This section describes the different modelling techniques that have been used for modelling the human upper airways.

### **2.5.1 Computational Fluid Dynamics (CFD)**

Computational Fluid Dynamics (CFD) have been used successfully for many years in modelling the human UA respiratory system, as well as describing the airflow parameters and characteristics [25, 220, 284, 361, 362, 372, 373, 508-521], and describing the interaction between the fluid and the structure of the airway [522-524]. This is mainly because these methods are non-invasive, which is a major success point in research that led to an undeniable confidence for the use of the CFD in biomedical researches and development. CFD modelling has become the key of knowledge for determining the changes in the flow characteristics when any variation occurs to the flow variables [525, 526].

In order to use CFD in modelling the UA system in humans, the airway models must be available which can be reconstructed either from the “magnetic resonance imaging (MRI) or computer tomography (CT) data” [284, 378, 510, 514, 527-529]. Once these data are available, a virtual model for the airway can be generated, on which CFD can work accurately to describe the characteristics (flow variables) of the airway model, such as [25, 284, 509, 510, 514, 519, 530]:

- Pressure distribution,
- Velocity distribution, and
- Wall Shear Stress distribution.

CFD can also accurately specify whether or not the subject has structural abnormalities in the airway that may cause airway obstruction and collapse during sleep [529]. Also the sites of constriction can be accurately specified, allowing the right choice of a suitable treatment method from the surgical interventions or using a non-invasive treatment (such as CPAP or APAP), or even changing the life style (such as losing weight, stop drinking alcohols, quit smoking,...etc.) as described in section 1.13.

CFD offers low cost, quick, non-invasive and impeccable accurate modelling techniques which can easily specify the airflow characteristics as well as the sites of constriction through the human airway respiratory system [24].

In 2005, Kalra et al [382] reported that when the characteristics of the airflow in the human airway are obtained using CFD, the patient can then be specified if he/she is diagnosed with OSA or not.



Through many researches [25, 509, 517, 531-533], CFD was used successfully to describe the airflow characteristics in both anatomically accurate and simplified UA models, however the airway walls were assumed rigid, which means that the compliance of the airway walls was neglected, which for sure gave inaccurate results as it is expected that the sites of constriction will change when the compliance of the airway is considered through calculations, due to the deformations of the airway walls and the soft tissues [24].

To describe the characteristics of the human UA respiratory system, the following models have been used:

1. Reynolds-Averaged-Navier-Stokes (RANS) models.
2. Direct Numerical Simulation (DNS) models.
3. Unsteady Large Eddy Simulation (LES) models.
4. Fluid-Structure Interaction (FSI) models.

#### **(I) Reynolds-Averaged-Navier-Stokes (RANS) Models**

These models are divided into 4 types [517]:

1. RANS with  $k$ - $\epsilon$  turbulence model.
2. RANS with  $k$ - $\omega$  turbulence model.
3. RANS with  $k$ - $\omega$  Shear Stress Transport (SST) turbulence model.
4. RANS with one equation Spalart-Allmaras (SA) turbulence model.

For the above mentioned RANS models, the flow is assumed to be either steady or unsteady, incompressible, and fully developed turbulent [534]. These models are considered the most common used models for modelling the respiratory system [284, 361, 510, 514], mainly because they are considered to be fast and simple models [535].

The RANS with  $k$ - $\epsilon$  turbulence models can be further subdivided into two types:

1. RANS models with Low Reynolds number  $k$ - $\epsilon$  turbulence.
2. RANS models with standard  $k$ - $\epsilon$  turbulence.

Also, the RANS with  $k$ - $\omega$  turbulence models can be subdivided into two types:

1. RANS models with Low Reynolds number  $k$ - $\omega$  turbulence.
2. RANS models with standard  $k$ - $\omega$  turbulence.

The main disadvantages of these models are [534]:

1. For steady models, the flow is assumed to be steady while in most cases it is not steady at all, which means that the results concerning the flow separation and adverse pressure gradients are not accurate.
2. The airway wall compliance is neglected (rigid walls) which is completely not real.
3. The flow is only assumed to be fully developed turbulent, while typical flows in human airways are varying from laminar to transient or turbulent.
4. Although the costs of using these models are low, however the accuracy of the obtained results is also low.

Wilcox et al [534] and Menter et al [377] reported that the steady RANS  $k-\omega$  with SST turbulence model is considered as the best RANS model, because of its high ability in describing the viscous effects near the airway walls which will in turn affect the adverse pressure gradient.

In 2003, Zhang et al [536] reported the validity of the low Reynolds number  $k-\omega$  turbulence model in accurately describing the main characteristics of laminar, transitional, and turbulent flows.

In 2007, Jeong et al [514] used the steady low Reynolds number  $k-\varepsilon$  turbulence model to describe the characteristics of the UA for a patient diagnosed with mild OSA, and compared their results with the available data obtained by using the steady RANS model with standard  $k-\varepsilon$  turbulence, and experimental data. Their study was focused on a middle aged man, who had the following characteristics:

- Age of 37 years old,
- Normal weight ( $BMI \approx 23.8 \text{ kg/m}^2$ ), and
- He was diagnosed with mild OSA ( $RDI \approx 9.4$ ).

The flow was assumed to be:

- Three dimensional,
- Steady,
- Incompressible,
- Newtonian, and
- Turbulent.

The patient was awake and positioned in supine position while collecting the CT images and the study was done for many flow rates during the inspiratory breathing phase.

They have concluded that the results obtained by the low Reynolds number  $k-\epsilon$  turbulence model were much better and closer to the experimental data than the results obtained from the steady RANS model with standard  $k-\epsilon$  turbulence. The limitations to their study are:

- The airway walls still considered rigid.
- Only the inspiratory breathing phase was considered, while most of the airway obstructions and collapses have been proven to occur during the expiratory breathing phase.
- The patient was awake during the study which differs from sleeping conditions where the airway muscles are completely relaxed.
- The flow was assumed to be steady, which is really not true.

In 2008, Suh, J. and Frankel, S.H. [379] reported that there is another RANS model that can yield better accuracy than the steady RANS models. This model is known as the unsteady RANS  $k-\omega$  SST model. This model can describe the flow unsteadiness more accurate than the steady RANS models. Unfortunately, the compliance of the airway walls is still neglected, and the accuracy is not up to the required level.

In the same year, Mihaescu et al [25] studied the effect of the surgical intervention of adenotonsillectomy on an obese female patient diagnosed with mild OSA (AHI = 12). They used three dimensional steady RANS model with standard  $k-\epsilon$  turbulence. They considered only the inspiratory phase, with only one mass flow rate of 5 L/min. The flow was assumed to be steady, three dimensional, and incompressible.

Their results showed that OSA symptoms were resolved after the surgical operation. The main limitations of their research are:

- The airway walls were assumed rigid.
- The flow was assumed steady.
- Only the inspiratory phase was considered, while most of the airway obstructions occur during the expiratory breathing phase.
- They used only one flow rate of 5L/min, which is very low compared to real human respiratory flow rates.

Also, in 2008 Mihaescu et al [509] used the steady RANS model with standard  $k-\epsilon$  turbulence to describe the flow characteristics of the human UA for an awake patient diagnosed with OSA. They considered four different cases of the inspiratory flow rates ( $Q = 3, 5, 10$ , and  $15 \text{ L/min.}$ ). The flow was assumed to be steady, three dimensional and incompressible. They have reported the following results:

1. The changes in the flow variables (velocity distribution, pressure profiles, and wall shear stress distribution) are proportional to the change in the flow rate, which means that the patterns of the flow variables remain the same for different values of the flow rate.
2. The pressure drops more with increasing the flow rate, which means that as the flow rate increases the ability of the airway to collapse increases, which commonly occurs at the sites of the minimum cross sectional area.

Unfortunately, their study had the following limitations:

1. The study focused only on the inspiratory breathing phase, while most of the airway obstructions and collapses have been proven to occur during the expiratory breathing phase.
2. The study was based only on four different values of the inspiratory volume flow rate.
3. They unconditionally assumed linear relationships between both the static pressure and the wall shear stress, with the inspiratory flow rates.
4. The patient was awake, while the main problems for OSA patients occur during sleep as a result of the relaxation of the airway muscles.
5. The airway compliance was not considered (rigid airway walls).

In the same year, Nithiarasu et al [220] used the steady RANS model with one equation Spalart-Allmaras (SA) turbulence to describe the airway characteristics during the inspiratory breathing phase for many flow rates ( $16.88 \text{ L/min.}$ ,  $33.76 \text{ L/min.}$ , and  $50.64 \text{ L/min.}$ ), for anatomically accurate human UA of a middle aged female. The flow was assumed three dimensional, incompressible and turbulent. Their results showed good agreement with the available experimental data. The limitations to their study are that the airway compliance was neglected and the expiratory breathing phase was not considered.

Also, in 2008, Mihaescu et al [516] compared the steady RANS model with standard  $k-\epsilon$  turbulence and the steady RANS model with standard  $k-\omega$  turbulence. They have reported

that the results of the steady RANS model with standard  $k-\omega$  are better than those of the steady RANS model with standard  $k-\epsilon$ .

In 2009, Mylavarapu et al [517] made a comparison between the steady RANS models, and the experimental results. They have reported that among these models, the steady RANS model with standard  $k-\omega$  turbulence resulted in the best agreement with the experimental data. Through their research, the patient was a 17 years old overweight male with a BMI of  $26 \text{ kg/m}^2$ , the flow was assumed to be incompressible ( $M \ll 0.3$ ) and turbulent; and the expiration flow rate was 200L/min. which was really too high and may minimise the value of the results of this research.

Also, in 2009 Chung et al [361] used the unsteady Low Reynolds number  $k-\epsilon$  turbulence model in describing the airway characteristics of two patients diagnosed with severe OSA ( $AHI > 50$ ), before and after the surgical intervention of maxilla-mandibular advancement (MMA). The flow was assumed unsteady, three dimensional, incompressible, and turbulent. The volume flow rate was 8 L/min. The reported results showed substantial improvements in the airway characteristics, as well as widen the UA. The limitations to their study are that the airway compliance was not considered and only one flow rate was investigated.

In 2010, Steven et al [537], used the low Reynolds number  $k-\omega$  turbulence model (which was previously approved to be used successfully in describing the UA characteristics, by Mylavarapu et al [517] and Xu et al [284]) to describe and compare the characteristics of the UA for both normal and OSA young children. The child diagnosed with OSA was 5.5 years old, and the normal one was 5.1 years old. Both children were supine and sedated during the MRI studies, the obtained MRI images were then used to construct three dimensional virtual models which were solved by using the CFD. Their study was done on different flow rates during both the inspiratory and the expiratory breathing phases. They have reported that at the site of maximum narrowing, the static pressure was extremely high (which means that the pressure drop is a maximum) combined with the lowest flow rate, these two parameters led to increase the airway resistance, and consequently increased the airway collapsibility. This can be shown clearly from the following equation:

$$R = \frac{\Delta P}{Q} \quad (2.1)$$

Where:

R: Airway resistance

$\Delta P$ : Pressure drop

Q: Volume flow rate

The limitations to their study are:

- The airway walls were assumed rigid (no compliance was considered).
- The comparison was done on two young children with different age and BMI, which means that they have different airway characteristics, which means that the comparison is practically unacceptable.
- Both children were sedated during the MRI studies, which is not equivalent to sleeping conditions, because sedatives tend to relax the airway muscles more than the normal sleeping conditions.

In 2011, Yasushi et al [538] applied the steady RANS model with standard k- $\epsilon$  turbulence to describe the flow characteristics of the human UA before and after the surgical intervention of maxilla-mandibular advancement (MMA). Their study was done over 23 patients with different ages, BMI values, genders and RDI values, which means that their calculations were done on both laminar and turbulent flow conditions (depending on the Reynolds number, which is related to the flow rate). Their calculations were done on many inspiratory flow rates, based on every patient age and weight. Also, the flow was assumed to be incompressible and three dimensional. The compliance of the airway walls was neglected. Their results showed remarkable improvements in the UA characteristics after the MMA surgical procedure.

Although they have done a huge and powerful study, however they had some limitations which are listed below:

- The airway compliance was not considered.
- No calculations were done during the expiratory breathing phase, although obstructions are more likely to occur during the expiratory breathing phase.

Also, in 2011, Mihaescu et al [529] compared between three of the RANS models (standard k- $\epsilon$ , k- $\omega$ , and k- $\omega$  SST) and experimental data. Their results agreed with the previous results of Wilcox et al [534] and Menter et al [377] that the k- $\omega$  SST model was the best RANS model to give the closest results to the experimental data.

Later on, in 2011 Powell et al [53] used the steady RANS  $k-\omega$  model with SST turbulence to specify the flow patterns in the pharyngeal airway for both normal and OSA patients during both the expiratory and inspiratory breathing phases for awake patients. They used a peak respiratory flow rate of 30 L/min and assumed that the flow was three dimensional and incompressible. They have demonstrated the previous results of Mihaescu et al [509] that the changes in the flow variables are proportional to the change in the flow rate, which means that the patterns of the flow variables remain the same for different values of the flow rate. The limitations to their study are:

- The flow was assumed steady.
- The compliance of the airway was neglected.
- The study was restricted on one flow rate only.
- The study was conducted on patients during wakefulness, which is considered as the best condition, because the problems of obstruction and collapse occur during sleeping due to muscles relaxation.

Recently, in the late of 2011, Fan et al [19] used the CFD to describe the characteristics of the UA before and after mandibular advancement for a 45 years old Chinese man. The patient was classified to have normal weight ( $BMI = 21 \text{ kg/m}^2$ ) and was diagnosed with severe OSA. Also the lower jaw of the patient was observed to be so small (micrognathia), which might have contributed to increasing the severity of the disease. They used low Reynolds number  $k-\epsilon$  turbulence model with the following assumptions and conditions:

1. The flow was assumed to be three dimensional, incompressible and turbulent.
2. The study was done on an inspiratory flow rate of 18 L/min.
3. The patient was awake, supine and the mouth was closed (normal nasal breathing).
4. The airway walls were assumed rigid (no compliance).

After six years of the surgical intervention and based on the patient's CT data, they have reported that the airway characteristics were improved after the surgery. The following are the limitations to their study:

1. The patient was awake, which is considered the best calculating conditions that completely differ from the conditions during sleep, mainly due to muscles relaxation which in turn increases the ability of the airway to collapse.
2. Only one inspiratory flow rate was considered.

3. The airway compliance was not considered which in fact affects the sites of obstruction as well as the ability of the airway to collapse.
4. They compared the available data before the surgery with data obtained six years after surgical intervention, which means that the BMI might have been changed (logically). Also, as noted before, the muscle structure changes with age, therefore the two cases before and after the surgical intervention are not equivalent to one another, which means that the comparison is unreasonable.

## **(II) Direct Numerical Simulation (DNS) Models**

Although this approach is considered as a high level CFD technique that can accurately describe the flow characteristics; however it is not commonly used because it is relatively expensive and time consuming [514, 517].

## **(III) Unsteady Large Eddy Simulation (LES) Models**

For many years, the unsteady large eddy simulation (LES) technique has been considered the main CFD technique in describing the turbulent unsteady flows. This technique was developed to avoid all the disadvantages of both the RANS models (lack of accuracy) and the DNS models (which are so expensive and time consuming) [535]. The accuracy of the unsteady LES models is directly proportional to the used grid size; in other words, the smaller the used grid size, the higher is the obtained accuracy [514]. The main disadvantages of this computational technique are:

1. This method is still expensive when compared to other RANS models.
2. The compliance of the airway walls is still neglected (rigid airway walls are considered).

In 2008, Mihaescu et al [516] compared between the unsteady LES computational technique and two of the steady RANS models ( $k-\epsilon$  and  $k-\omega$ ) by using the data obtained from a morbid obese female adolescent ( $BMI \approx 54 \text{ kg/m}^2$ ), who was 18 years old of age and diagnosed with OSA. The flow was assumed to be three dimensional and incompressible. The results were obtained during the inspiratory breathing phase for a volume flow rate of 10 L/min. They have reported that the unsteady LES is better and more accurate than the used two steady RANS models in describing the flow characteristics. They have also reported that the results of the steady RANS model with standard  $k-\omega$  turbulence are better than those obtained from the steady RANS model with standard  $k-\epsilon$  turbulence, and are in good agreement with the results of the unsteady LES technique.



The limitations to their study are:

1. The airway compliance was neglected.
2. The calculations were performed only during the inspiratory breathing phase, while most of the sleeping obstructions and/or collapses are more likely to occur during the expiratory breathing phase.

In 2011, Mihaescu et al [529] compared between three RANS models (standard k- $\epsilon$ , standard k- $\omega$ , and k- $\omega$  SST), the unsteady LES and experimental data. Their study based on a patient diagnosed with moderate OSA (AHI = 26). The patient was subjected to MMA surgical intervention as a treatment for the OSA, and they reported the airway characteristics before and after the operation. The flow was assumed to be three dimensional, unsteady and incompressible. The calculations were done on a volume flow rate of 30 L/min during the inspiratory breathing phase only. They have concluded that the airway characteristics were improved after the surgery and that the results obtained by the unsteady LES model were the closest to the available experimental data. They have also reported that among the RANS models, the k- $\omega$  SST model was the best RANS model to give the closest results to the experimental data, but still not as accurate as the unsteady LES model. From this it can be concluded that the unsteady large eddy simulation (LES) is better than the simple RANS models, because LES can describe accurately the variation of the flow dynamics with time when the flow is transient or turbulent, but still relatively more expensive than the RANS models.

### **2.5.2 Fluid-Structure Interaction (FSI)**

In this method the behaviour of the airflow through the UA respiratory system is investigated as well as the compliance of the airway walls which occurs as a result of the effect of the pressure and shear forces on the airway walls [53]. The compliance of the airway was reported to affect both the collapsibility and the characteristics of the human UA [91, 539, 540].

This method is considered the most efficient, accurate and modern method in modelling the UA respiratory system, because the compliance of the airway walls is considered, rather than the old modelling techniques where the airway walls were considered rigid and the non-slip conditions were applied directly, which does not occur in reality due to the deformations of the airway walls. The lack of the bony structure that can support the pharyngeal airway will cause the pharyngeal airway walls to deform and therefore cannot be considered rigid, which in turn will affect the sites of constriction [53, 541-543].

In 2002, Malhotra et al [544] used the FSI to specify the differences between the characteristics of the UA between normal men and women. This study was conducted on 19 men and 20 women. They assumed that the flow was two dimensional, fully developed laminar and that the posterior airway walls were rigid. They have concluded that:

1. Men have larger soft palates than women.
2. Men have larger pharyngeal airway length than women.
3. Females have lower closing pressures than men, which means that at a certain negative pressure, the airway of a male may be obstructed while for a female it still remained opened. This means that although men have larger pharyngeal airways, their airways are more collapsible than those of women.

In 2006, Chouly et al [532] applied the two dimensional FSI method to accurately describe the characteristics of the UA respiratory system in two patients diagnosed with OSA, before and after the surgical intervention of maxilla-mandibular advancement (MMA). The flow was assumed to be quasi-steady, two dimensional, incompressible and laminar. The obtained results were for many inspiratory flow rates. They compared the obtained numerical results with the available experimental data and were in excellent agreement. The main limitations to their study are that the flow was assumed steady (while it is not steady at all in reality), and that they focused only on the inspiratory breathing phase.

In 2008, Nithiarasu et al [220] recommended the use of the FSI method to accurately specify the airway collapse for patients diagnosed with OSA.

In 2010, Mylavarapu et al [24] used the two dimensional FSI method to completely describe the characteristics of the UA for both normal and narrow models. They studied the case of a supine patient during wakefulness with an open mouth. They considered the compliance of the airway wall through their calculations in order to obtain accurate results, however the posterior pharyngeal airway walls were considered rigid as they are supported by vertebral bodies. They assumed that the flow was laminar ( $Re < 2300$ ) and incompressible ( $\rho$  is constant, and  $M \approx 0.1$ ). They have concluded that:

1. The closing pressures ( $P_{crit.}$ ) increased as the soft palate stiffness increased which in turn reduced the deflection of the uvula.
2. The ability for airway obstruction and collapse increased during the expiratory breathing phase rather than the inspiratory breathing phase.
3. The closing pressures during the expiratory breathing phase are lower than those during the inspiratory breathing phase, which means that the tendency of

the airway to collapse increases during the expiratory breathing phase rather than the inspiratory breathing phase.

4. During expiration, the site of constriction was at the rear of soft palate and shifts to the rear of the tongue during inspiration.

They have also reported that their study was based on an awake patient, which is considered as a disadvantage for the power of their results due to the changes in the mechanical properties of the soft tissues during sleep rather than during wakefulness.

In 2011, Powell et al [53] reported that although the FSI method is the best to describe the flow characteristics of the UA respiratory system, however there are some difficulties that impede the use of this method such as:

1. The used mechanical properties change from one person to another. Also these properties can change for the same person depending on whether he/she is awake or asleep.
2. The available approved mechanical properties for the soft tissues that surround the airway for sleeping patients are not sufficient to provide a complete image for the effect of the used treatment method as well as the changes in the mechanical properties during sleep.
3. The quality and availability of the used MRI for sleeping patients are not sufficient to construct accurate virtual computational models, which are needed to use the CFD to accurately describe the characteristics of the airway.

These mechanical properties are [53]:

1.  $E$ : Young's modulus of elasticity
2.  $\nu$ : Poisson's ratio
3.  $\rho$ : Density

The above literature review shows that the previously conducted studies on bariatric surgery were in the form of anthropometric measurements and PSG data, but no biomechanical assessment was investigated to describe the outcomes of the surgery in terms of the changes in the dynamic characteristics of the UA before and after surgical intervention. Also there is no correlation between the dynamic characteristics of the UA and the body size before and after surgery. In addition to these, very few previous studies have investigated the interaction between the airflow and the deformations of the UA soft

tissues by using the two dimensional FSI, but none of these studies have investigated the problem using the three dimensional FSI. Also, the effects of using the PO superimposed on the CPAP on the dynamic characteristics of the human UA have not been yet investigated. Therefore these will be the main objectives of the current research project as described below.

## **2.6 Research Objectives**

This research project aims to investigate the biomechanical assessment and the effectiveness of bariatric surgery in losing weight and help alleviate the apneic symptoms in morbid obese OSA patients. It also aims to identify the effects of using the PO on the performance of the human UA, which requires a better understanding of the characteristics of the healthy and the unhealthy upper airways and identify the conditions of collapse in the unhealthy airways, investigate the effects of using the CPAP to keep the airway open as well as the effects of using the PO on the UA performance. Therefore the main objectives of the current research project are:

1. To investigate the biomechanical changes of the UA characteristics before and after bariatric surgery.
2. To investigate the UA characteristics for healthy and unhealthy subjects.
3. To determine the conditions of the UA collapse in the unhealthy airways using the FSI method.
4. To investigate the effects of using the CPAP in preventing the UA collapse and keep the airway open.
5. To investigate the effects of using the PO superimposed on the CPAP to keep the airway open at lower CPAP pressure than the currently used.

The main objective of this work is to understand the dynamic and mechanical characteristics of the UA before and after an invasive and non-invasive treatments. Specifically this thesis focuses on the bariatric surgery and pressure oscillations. This requires mathematical and physical modelling. Therefore the thesis is structured in following format:

1. Present the background theories and methods for the procedure adopted in the thesis; Chapter 1.

2. Conduct a literature survey on the relationship between bariatric surgery and OSA, UA muscle activity, effects of the PO on the UA muscle activity, and the different UA modelling techniques; Chapter 2.
3. Present the models formulation and the used imaging and modelling softwares; Chapter 3.
4. Recruit morbid obese OSA patients promoted for bariatric surgery, collect CT data for their upper airways before and after surgical intervention and perform UA modelling; Chapter 4.
5. Recruit healthy volunteers and determine the dynamic characteristics of their healthy upper airways; Chapter 5.
6. Recruit OSA patients, investigate the dynamic characteristics of their unhealthy upper airways, determine the conditions of collapse during inspiration and expiration, investigate the effect of using the CPAP to prevent the UA collapse and investigate the effects of the PO on the performance of the upper airways; Chapter 6.
7. Construct experimental setups to validate the obtained theoretical results from chapters 5 and 6, study the dynamic characteristics of the UA before and after using the CPAP; and then investigate the effects of the PO superimposed on the CPAP; Chapter 7.
8. Discuss the results of the conducted study on the relationship between bariatric surgery and OSA, compare between the obtained results from the healthy subjects and OSA patients, discuss the results of the experimental validation and identify the conclusions and proposed future work; Chapter 8.

## **2.7 Closure**

This chapter presented a literature review covering the relationship between bariatric surgery and OSA, the activity of the UA muscles in healthy and unhealthy airways, the effects of using the PO on the activity of the UA muscles, and the used techniques in modelling the human upper airways. The next chapter will identify the regions of interest in the human UA to be considered throughout this study, and discuss the basic governing equations describing the airflow and the deformations of the soft tissues. It will also present the boundary conditions and indicate the considered assumptions. Also the next chapter will explain the modelling procedure of using the finite element method (FE) in investigating the UA dynamic characteristics, and provide a detailed explanation about

the CFD modelling for the airflow and the interaction between the airflow and the deformations of the soft tissues by using the FSI modelling.

## **CHAPTER 3**

### **Models Formulation**

#### **3.1 Introduction**

This chapter gives some of the background theories used in the modelling process and also summarizes the modelling procedure used to investigate the dynamic characteristics of the upper airway (UA) under different conditions. Section 3.2 describes the 3D-DOCTOR imaging software (Version 5, Able Software Corp, MA, USA) which is used throughout this research project to construct the UA models. Section 3.3 presents the modelling procedure in investigating the dynamic characteristics of the UA in morbid obese apneic patients before and after bariatric surgery. Section 3.4 covers the modelling procedure for determining the dynamic characteristics of the healthy and the unhealthy upper airways using the finite element (FE) method by using the Abaqus/CAE software (Version 6.11, Dassault Systems Corp, RI, USA). The detection of collapse in the apneic patients is described in section 3.5, which describes the modelling procedure for the air model using the Computational Fluid Dynamics (CFD) by using the CFX Modeller on the ANSYS Workbench (Version 14, SAS IP Software Inc, PA, USA), and the interaction between the airflow and the deformations of the soft tissues using the Fluid-Structure Interaction (FSI) method by using the Static-Structural Modeller on the ANSYS Workbench. Section 3.6 describes the modelling procedure in investigating the effects of the pressure oscillations (PO) on the performance of the UA. Section 3.7 describes the used meshing methods on the Abaqus and the ANSYS softwares. Finally, section 3.8 describes the model validation.

To construct and simulate airway models for healthy and unhealthy subjects, an ethics application was prepared and approved at the beginning of the study. Subjects were recruited based on the inclusion and exclusion criteria given in the participant information sheet (PIS), consent forms were sent to the interested candidates prior to the initiation of study procedures.

#### **3.2 3D-DOCTOR Imaging Software**

It is an advanced software for image processing, three dimensional modelling and measurements of MRI and CT scans [545]. Once the CT or MRI data is collected, the stack of these data can be easily opened on the software and the model can be then constructed by specifying the region of interest (ROI), which is that part of the UA that

includes the model which is required to be constructed and then simulated. The ROI may change from one study to another depending on the type of the required investigation. For example, if it is required to detect the conditions of the UA collapse, which is reported to occur either at the rear of the uvula or rear of the tongue [55, 70, 71, 73, 74], therefore imaging data should be collected to cover the collapsible region between the very bottom of the nasopharynx (the level of the hard palate) and the level of the hypopharynx, as indicated by A and B in Figure 3.1; respectively. This region includes three main elements, the air, the tongue and the uvula.

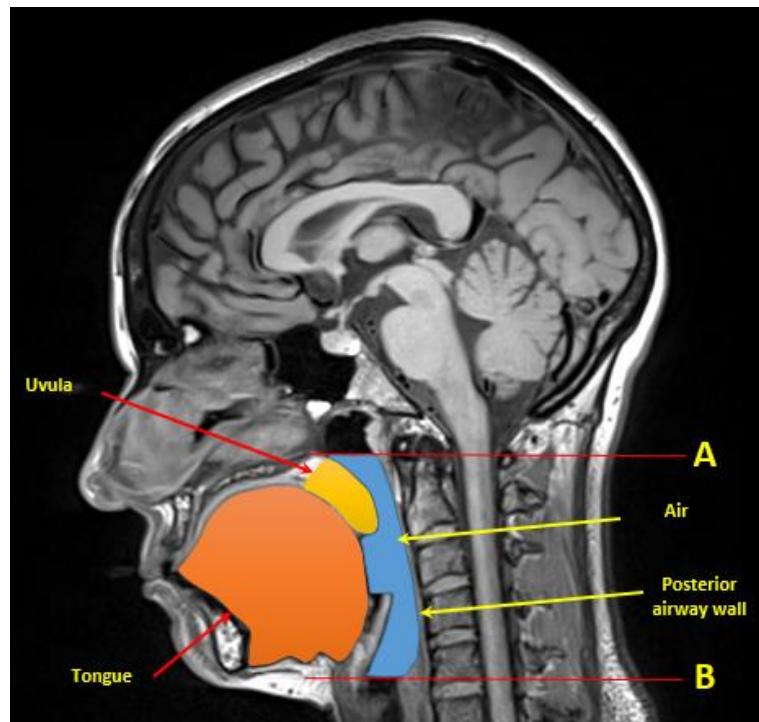


**Figure 3.1: Collapsible region**

To construct the isolated air model inside the shown collapsible region using 3D-DOCTOR software, the following procedure was used:

1. Since collapse occurs either at the rear of the uvula or the tongue [24], choose the ROI to expand from the top of the uvula to the very bottom of the tongue as shown in Figure 3.2.



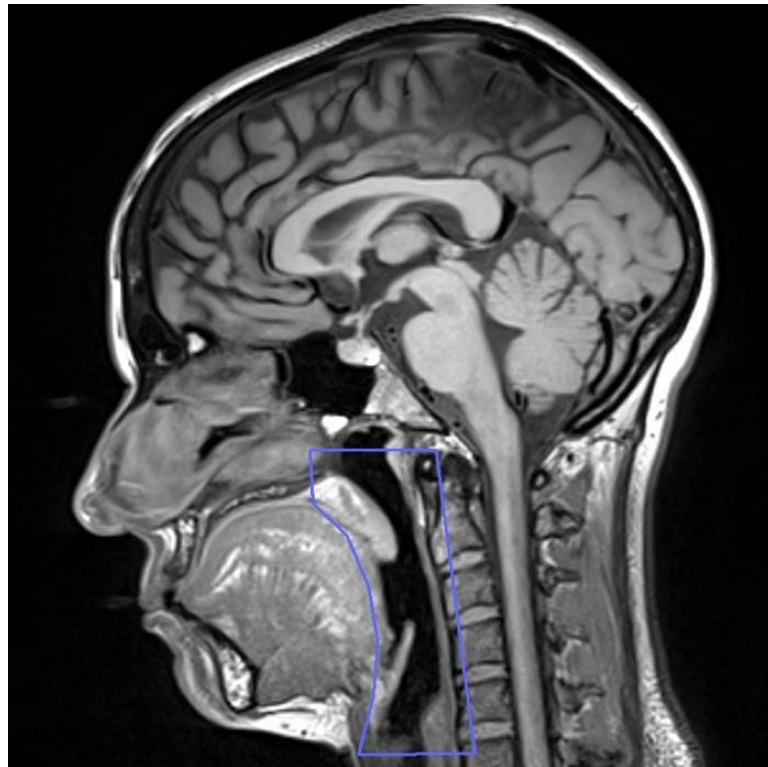


**Figure 3.2: Identifying the region of interest on 3D-DOCTOR**

2. Specify the start and end slices that contain the model.
3. The user may trace the boundary of the model inside the ROI either manually or automatically to produce accurate 3D models, Figure 3.3.

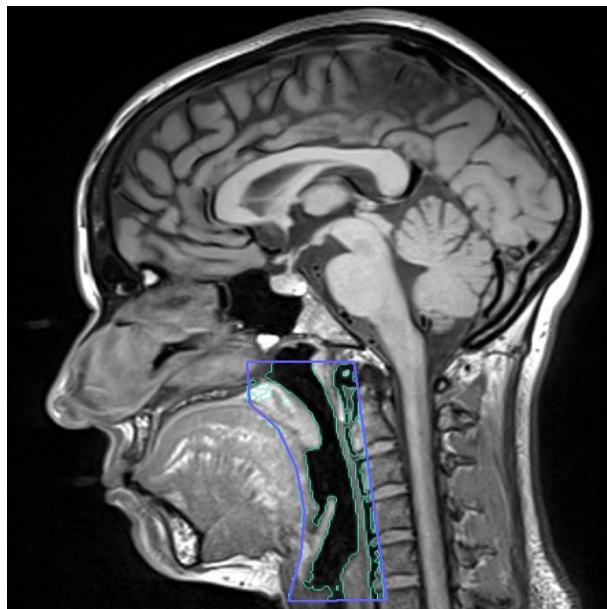


**Figure 3.3: Automatic boundary generation inside the ROI**

4. The ROI can be then removed and the boundary inside it is trimmed to include only the UA model, Figure 3.4.

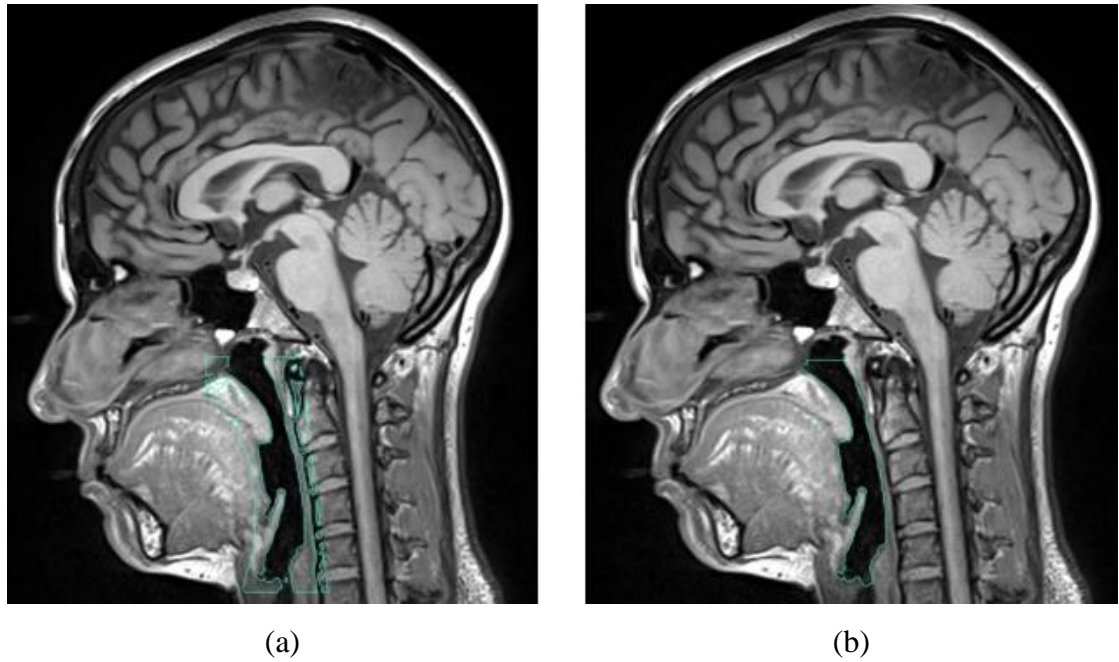


**Figure 3.4: The model boundary after: (a) removing the ROI and (b) trimming**

5. The resulting boundary can be smoothed to reduce the irregularity, Figure 3.5.

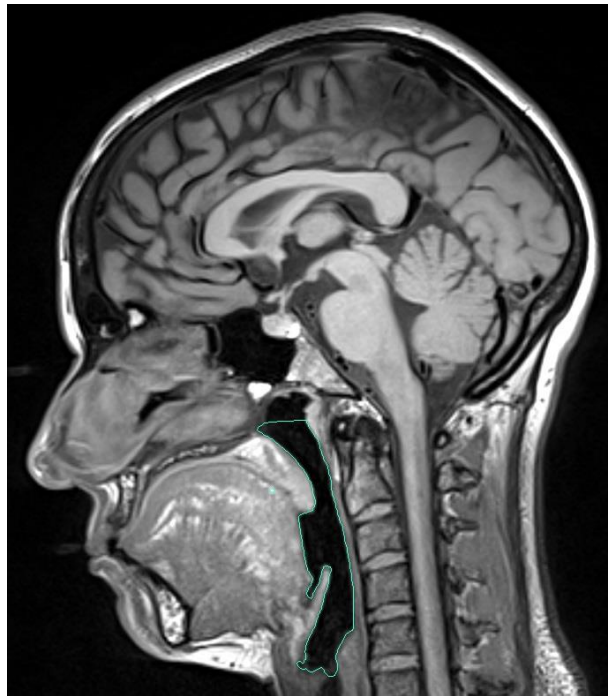


**Figure 3.5: Smooth boundary**

6. After repeating steps 4 and 5 to all slices, the three dimensional UA model can be produced using “complex surface rendering” option and the resulting model can then be saved in different file formatting to be compatible with the used simulation software.

3D-DOCTOR software was used in this research project to assess the biomechanical changes in the UA characteristics before and after bariatric surgery according to the modelling procedure described in section 3.3, as well as to construct isolated models for the airway, uvula and tongue as described in section 3.4.

### **3.3 Biomechanical Assessment before and after Bariatric Surgery**

Bariatric surgery is one of the invasive treatment methods that has been used in reducing the weight of the morbid obese apneic patients and consequently help alleviate OSA symptoms. The background (Chapter 1) shows that the success rate differs from one study to another. To assess the biomechanical changes in the UA before and after surgical intervention, the following modelling procedure was used in Chapter 4:

1. Recruit morbid obese OSA patients promoted for bariatric surgery.
2. Collect CT data for the UA expanding from the roof of the mouth till the beginning of the trachea, before and after surgical intervention.
3. Collect PSG data before and after the surgery and record the AHI score, as well as the BMI.
4. Specify the ROI and use 3D-DOCTOR software to construct three dimensional models of the UA before and after the surgery by following the procedure given in section 3.2.
5. Calculate the values for the UA volume and the min. and max. hydraulic diameter (HD) before and after the surgery by using the tools of 3D-DOCTOR software.
6. Compare between the obtained results and check their relationship to the age
7. Use the obtained data to undertake statistical analyses to check the significance of the results.
8. If possible, try to introduce new parameters to describe the success of the surgery in reducing OSA symptoms.

### **3.4 UA Dynamic Characteristics using the Finite Element (FE) Methods**

This section presents the procedure for constructing isolated healthy and unhealthy uvula and tongue models using 3D-DOCTOR software, and conduct simulations on these models using the finite element (FE) methods by using the Abaqus software. The simulations and results are explained in Chapter 5 and Chapter 6 for the healthy and the unhealthy subjects, respectively.

Isolated models for the uvula and tongue were constructed by following the first six steps described in section 3.2, however the ROI was changed to enclose the uvula or the tongue only in each case. The model was then imported into the SolidWorks software (version 12, Dassault Systemes, SolidWorks Corp., MA, USA) and was saved as an IGES file which was easily imported to the Abaqus/CAE software to determine the natural frequencies of the soft tissues.

The Abaqus software allows the user to either create their own models on its interface or to import pre-constructed models from any CAD program (such as the SolidWorks software) or image processing softwares using MRI or CT data. This software has two main model databases: (i) Standard/Explicit Model which is used in FE modelling; and (ii) CFD Model which is used in the computational fluid dynamics modelling. In this section, the procedure of using the Standard/Explicit Model in determining the natural frequencies of the soft tissues is explained in detail. The procedure steps are:

1. To design a model, choose “Part” from the “Module” menu, press “Create Part”, this is where the user needs to name the part and then start drawing the part model using the available drawing tools.
2. If the model was already constructed using an image processing software (e.g. 3D-DOCTOR) or any CAD program (e.g. SolidWorks), the first step can then be replaced by choosing “File” from the task bar, then select “Import” and choose “Part”.
3. When the part is ready, go to the “Module” menu and choose “Property”, press “Create Material”, this where the user may name the used material and specify the material properties such as density, elasticity modulus ... etc.
4. From the “module” menu, choose “Assembly”, press “Instance Part” and then choose “mesh on part”.
5. Go to the “Module” menu and choose “Step”, press “Create Step”, this is where you can specify the solution procedure type. To determine the natural frequencies, select “Linear perturbation” from the “Procedure type” option and then choose “Frequency”.
6. In the “Model” menu, choose “BCs” under the “Step” that you have created before. This allows the user to assign the boundary conditions to the part.
7. Now go to the “Module” menu and select “Mesh”, press “Seed Part Instance” and specify the mesh size. The user can change the mesh element shape by pressing on

- “Mesh” from the task bar, select “Controls” and choose the Element Shape” from Hex, Hex-dominated, Tet, or Wedge. Now press “Mesh Part” to mesh the model.
8. Choose “Job” from the “Module” menu, press “Create Job” and give a reference name to the simulation. Press the “Job Manager” and press “Submit” to start the simulation.
  9. Once the simulation is finished, the job status will indicate “Completed”. Press on “Results” and select “Plot Contours on Deformed Shape” to allow the user to visualise the results.

This procedure was repeated for different values of the Young’s Modulus of Elasticity to cover the changes that might occur in different ages, genders, races as well as different sleep stages and/or positions.

The above FE modelling procedure using the Abaqus/CAE software is summarized into the following illustrating diagram, Figure 3.6.

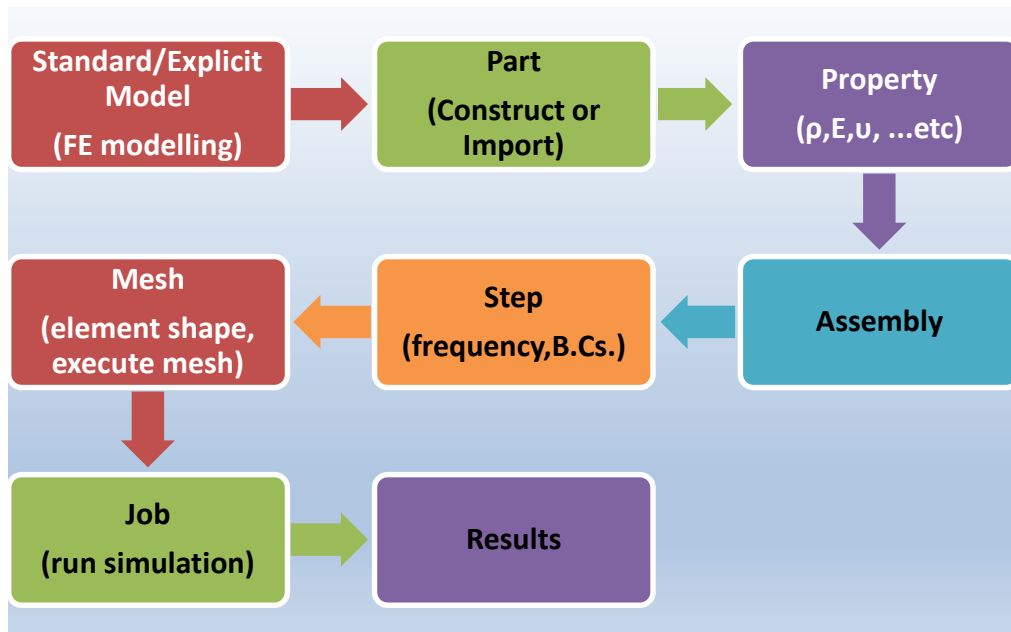


**Figure 3.6: FE modelling procedure using the Abaqus/CAE software**

Since the uvula is attached to the hard palate from one end and free to deform from the other end as shown from the MRI image given in Figure 3.7, therefore the isolated uvula model may be considered as a clamped-free beam model; which is explained in detail in Chapter 5.

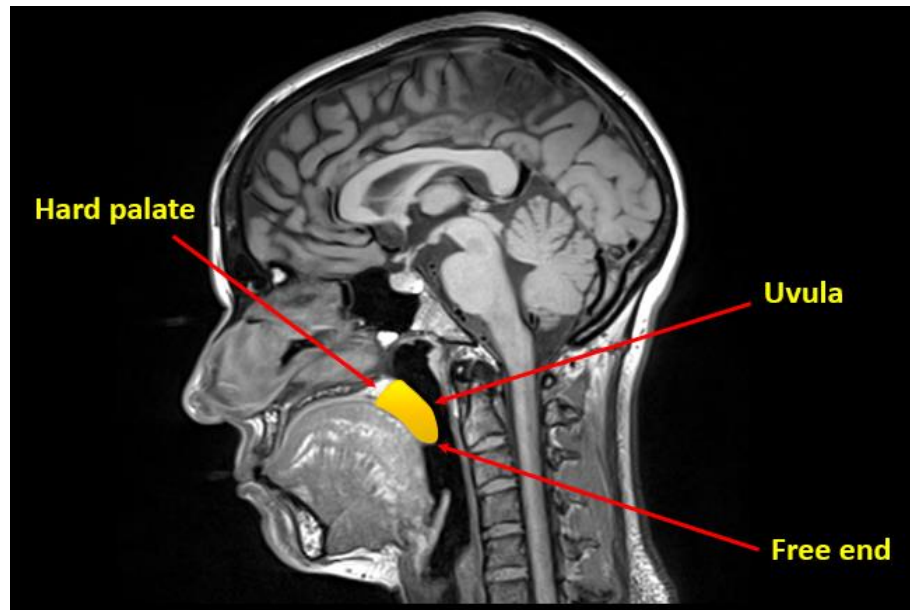


**Figure 3.7: Geometry of the uvula**

### **3.5 CFD Modelling using Fluid-Flow (CFX) Modeller**

The isolated air models were simulated by using the Fluid-Flow (CFX) Modeller on the ANSYS Workbench, which has been successfully used for more than 20 years in solving a wide range of problems involving fluid flow by using the finite volume (FV) method for mesh generation [546]. This modeller is based on the basic laws of physics as described in the next section.

#### **3.5.1 Basic Modelling Principles**

The airflow inside the UA obeys the basic laws of physics given below:

##### **(I) Continuity Equation:**

The total mass of airflow entering and leaving the UA is the same ( $m = \text{constant}$ ), Figure 3.8.

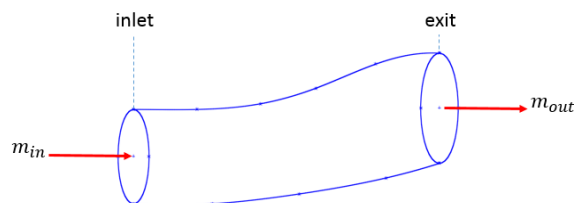


**Figure 3.8: Schematic diagram showing the conservation of mass**

Therefore the rate of change of the mass entering and leaving the UA equals to zero, thus:

$$\frac{dm}{dt} = 0 \quad (3.1)$$

And from the definition of the total derivative [547]:

$$\frac{d}{dt} = \frac{\partial}{\partial t} + (\vec{\nabla} \cdot \vec{V}) \quad (3.2)$$

Where:

$\frac{\partial}{\partial t}$ : the local derivative

$\vec{\nabla}$ : the differential/gradient operator =  $\frac{\partial}{\partial x}\vec{i} + \frac{\partial}{\partial y}\vec{j} + \frac{\partial}{\partial z}\vec{k}$

$\vec{V}$ : the velocity vector (field)

$(\vec{\nabla} \cdot \vec{V})$ : the velocity convective term, which is also referred to as the divergence of the velocity field.

Combining equations (3.1) and (3.2) and simplifying, we get:

$$\frac{\partial \rho}{\partial t} + (\vec{\nabla} \cdot \rho \vec{V}) = 0 \quad (3.3)$$

Where  $\rho$  is the fluid density

For incompressible fluid flow,  $\rho = \text{constant}$ , and equation (3.3) simplifies to:

$$\text{div } \vec{V} = 0 \quad (3.4)$$

Which can be written as:

$$\therefore \frac{\partial u}{\partial x} + \frac{\partial v}{\partial y} + \frac{\partial w}{\partial z} = 0 \quad (3.5)$$

Where  $u$ ,  $v$  and  $w$  are the velocity components in  $x$ ,  $y$  and  $z$  directions; respectively.

Equation (3.5) represents the three dimensional form of the continuity equation for incompressible fluid flow. Detailed derivation of equation (3.5) is given in Appendix A.

## (II) Momentum Equations (Navier-Stokes):

The momentum of the airflow through the UA is conserved, the Navier-Stokes equations are therefore applicable. Consider the motion of the fluid element shown in Figure 3.9:

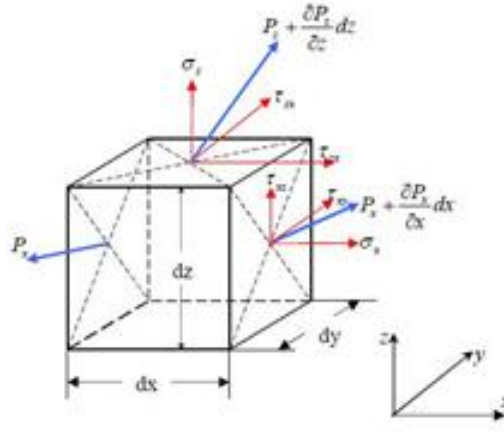


**Figure 3.9: Fluid element [548]**

Since the momentum of this fluid element is conservative, therefore the Navier-Stokes equations are applicable. Recalling that [547]:

$$\rho \frac{D\vec{V}}{Dt} = -\vec{\nabla}P + \vec{b} + \vec{\nabla} \cdot \vec{\tau} \quad (3.6)$$

Where:

P: Pressure

$\vec{V}$ : the velocity vector (field)

$\vec{b}$ : Body and external forces

$\vec{\tau}$ : Stress tensor

Neglecting the term of the body and external forces and after mathematical manipulation, equation (3.6) can be written as:

$$\underline{i} \text{ direction} \quad \frac{\partial u}{\partial t} + u \frac{\partial u}{\partial x} + v \frac{\partial u}{\partial y} + w \frac{\partial u}{\partial z} = -\frac{1}{\rho} \frac{\partial P}{\partial x} + \nu \left( \frac{\partial^2 u}{\partial x^2} + \frac{\partial^2 u}{\partial y^2} + \frac{\partial^2 u}{\partial z^2} \right) \quad (3.7)$$

$$\underline{j} \text{ direction} \quad \frac{\partial v}{\partial t} + u \frac{\partial v}{\partial x} + v \frac{\partial v}{\partial y} + w \frac{\partial v}{\partial z} = -\frac{1}{\rho} \frac{\partial P}{\partial y} + \nu \left( \frac{\partial^2 v}{\partial x^2} + \frac{\partial^2 v}{\partial y^2} + \frac{\partial^2 v}{\partial z^2} \right) \quad (3.8)$$

$$\underline{k} \text{ direction} \quad \frac{\partial w}{\partial t} + u \frac{\partial w}{\partial x} + v \frac{\partial w}{\partial y} + w \frac{\partial w}{\partial z} = -\frac{1}{\rho} \frac{\partial P}{\partial z} + \nu \left( \frac{\partial^2 w}{\partial x^2} + \frac{\partial^2 w}{\partial y^2} + \frac{\partial^2 w}{\partial z^2} \right) \quad (3.9)$$

The mathematical derivation of the above equations is given in detail in Appendix A.

The continuity and momentum equations are applied to all fluid elements. The CFD methods are used to solve these equations simultaneously using iterations until the error between two consecutive iterations becomes less than a pre-set value. These calculations are performed for each fluid element and the obtained new values are then used to apply the equations on the next adjacent fluid element and so on until the equations are applied to all the fluid elements. The iterations will continue running until the pre-set error value



is fulfilled at all the fluid elements. Therefore, meshing is required to be generated to produce the computational domain where these equations are applied to each fluid element by using the compatibility conditions. The CFX Modeller on the ANSYS Workbench was used in this research project to perform the CFD modelling and simulations for the airway models, and therefore is explained in the next section.

### 3.5.2 CFD Modelling Procedure using CFX Modeller

The CFD modelling was performed on the constructed airway models resulting from the 3D-DOCTOR software as described previously in section 3.2, followed by the steps given below:

1. Save the resulting UA model obtained from 3D-DOCTOR software as an STL file which is compatible with the SolidWorks software.
2. Import the three dimensional model into the SolidWorks and save it as an IGES file which can be easily imported into the Design Modeller (DM) on the ANSYS Workbench.
3. Use the DM to smoothen and/or simplify the surface of the model if needed.
4. Import the model into the CFX-Meshing Modeller to generate meshing, then import the model to the CFX-Pre Modeller to assign the boundary conditions that fall within the reported pharyngeal pressure values during the inspiratory and expiratory breathing phases, as described in Chapter 6; and run the simulations using the CFX-Post Modeller.

Figure 3.10 shows the CFD modelling procedure using the CFX Modeller

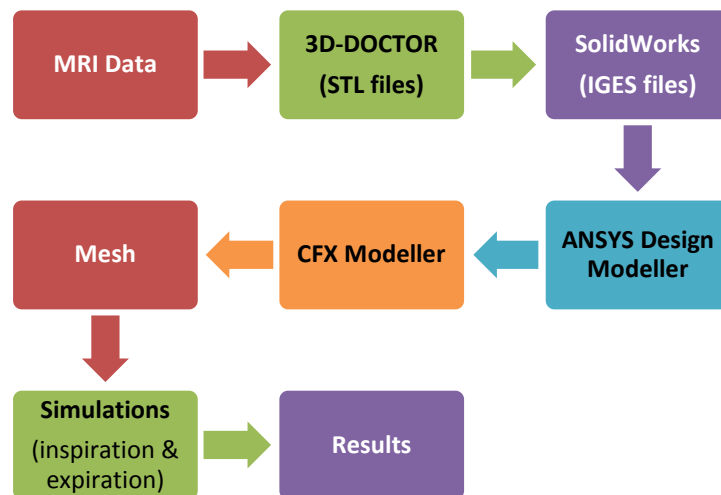


**Figure 3.10: CFD modelling procedure using the CFX Modeller**

The obtained pressure distributions were used to determine the resulting deformations of the soft tissues by using the FSI method as described in the next section.

### 3.6 Fluid-Structure Interaction (FSI)

The obtained pressure distributions from the CFX Modeller were used to determine the resulting deformations of the UA soft tissues using one-way FSI method by using the Static Structural Modeller, which is one of the analysis solvers of the ANSYS package which can be used in structural analysis (to determine the deformations, stresses ... etc.) [546]. One-way FSI was done by importing the resulting pressure distribution from the CFX Modeller into the Static Structural Modeller to determine the corresponding deformations of the soft tissues under the obtained pressure distribution. Simulations were repeated for different boundary conditions until collapse was detected during inspiration and expiration. Figure 3.11 shows a flow chart explaining the one-way FSI modelling procedure from the early stages till completion.

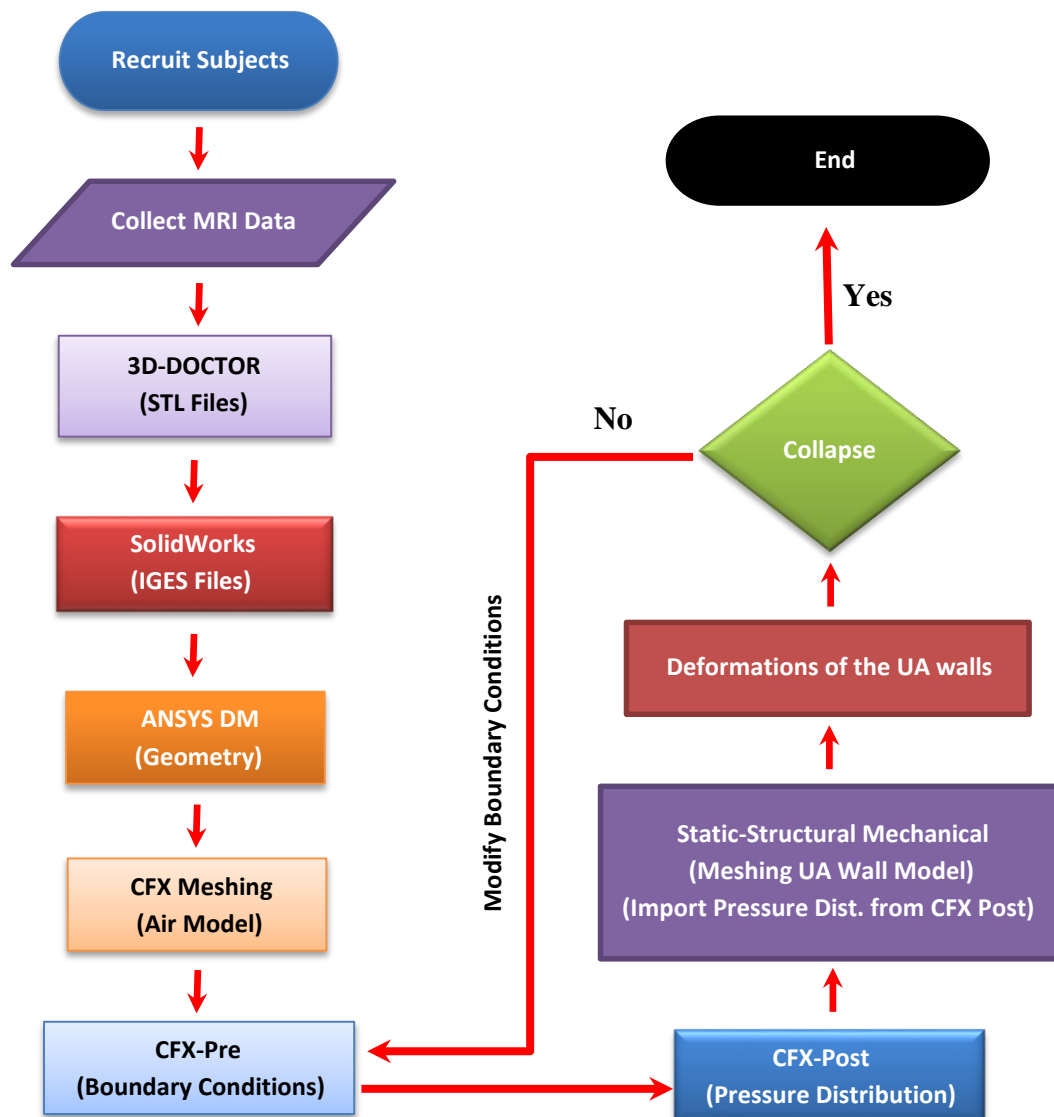


Figure 3.11: Flow chart showing the FSI modelling procedure

Simulations were then conducted to investigate the effects of using the CPAP to keep the airway open. Also an algorithm for the PO was added to investigate the effects of the PO superimposed on the CPAP on the performance of the UA and determine the associated pressure distributions and deformations and compare between these results and those obtained when using the conventional CPAP alone, as described in Chapter 6. The model validation for the obtained results is described in section 3.8.

### **3.7 Meshing**

The UA models and the soft tissues require different types of meshing methods, as the UA models need to be meshed by using the FE methods while the soft tissues should be meshed by using the CFD methods. The soft tissues were simulated by the Abaqus software to determine their natural frequencies, and by the ANSYS Workbench to determine the interaction between the airflow and the resulting deformations of the soft tissues. The UA models were simulated by using the CFX Modeller and the Static Structural Modeller on the ANSYS Workbench as described in section 3.5.2. Therefore this section describes the used meshing methods on the Abaqus software and the ANSYS Workbench.

#### **3.7.1 Meshing on Abaqus**

There are different meshing methods which could be used on the Abaqus/CAE software depending on the shape of the mesh element such as Hex, Hex-dominated, Tetrahedrons (Tet) and Wedge. A suitable meshing method is selected based on the complexity of the geometry.

Several meshes were attempted using different meshing methods and algorithms, and finally the appropriate mesh method that gave reasonable results was selected. The uvula and tongue models in this thesis were therefore meshed by using the Tet method with the default algorithm, which is a simple and robust meshing method and resulted in no meshing errors or warnings.

#### **3.7.2 Meshing on ANSYS**

The ANSYS Workbench has many meshing methods which can be used by the CFX Modeller and the Static-Structural Modeller to mesh the fluid and the structural models, respectively. For the CFX Modeller the available meshing methods are Automatic, Tetrahedrons, Sweep, Hex-Dominant and Multi-Zone [546]. In this thesis the Automatic method was used to avoid any mismatch in the resulting meshing.

For the Static-Structural Modeller the available meshing methods are Quadrilateral Dominant, Triangles, Uniform Quad/Tri and Uniform Quad [546]. In this thesis, the Quadrilateral Dominant method was used.

The mesh quality can be improved by using the tools of resizing, inflation, mapped face and refinement. It can be validated by checking the skewness of the produced mesh, which measures the distortion of an element relative to its ideal shape. The mesh quality is therefore classified according to the following ranges of the skewness [546]:

- Excellent: 0-0.25
- Very good: 0.25-0.50
- Good: 0.50-0.80
- Acceptable: 0.80-0.95
- Bad: 0.95-0.98
- Unacceptable: 0.98-1.00

### **3.8 Model Validation**

The outcomes of any research project need to be physically tested to prove the validity of the obtained results. Unfortunately there is no available equipment that can be used to capture clear images to show the deformations of the soft tissues inside the human upper airways neither during normal sleeping conditions nor when using the CPAP. Therefore, experimental setups were designed and constructed for physical validation, and fulfil the following requirements:

1. It can produce the human breath cycle with different flow rates and limitations to simulate the different breathing conditions (wakefulness, sleeping, at rest or after exercising... etc.) produced by different subjects. A Lung simulator that was designed at earlier stages at the Institute of biomedical Technologies (IBTec) was used for this purpose.
2. Another setup was designed and constructed to simulate the human UA that can be easily connected to the lung simulator, to allow the user to control and detect the flow rates and temperature, as well as monitoring the pressure inside the UA. This setup is equipped with a computer software that has a user friendly interface to control and monitor the aforementioned flow parameters.

3. The deformations of the UA soft tissues need to be visualised and analysed, therefore a transparent rig was designed and produced for easy visualisation, and models for the soft tissues were designed and produced from soft materials and were then inserted into the transparent rig to simulate the performance of the UA soft tissues.

Experiments were then conducted and the resulting deformations were captured by using a high quality camera. An image processing software was used to analyse these deformations by converting their values from pixels into millimetres. These setups will be explained in detail in Chapter 7.

### **3.9 Closure**

This chapter described the used imaging software, 3D-DOCTOR, and presented the used modelling procedure in investigating the UA dynamic characteristics in morbid obese OSA patients before and after bariatric surgery. The modelling procedure of using the Abaqus software in investigating the natural frequencies of the isolated soft tissues using FE methods was also described. This chapter also described the CFD modelling procedure for the isolated airway models using the CFX Modeller on the ANSYS Workbench, as well as the one-way FSI modelling procedure using the Static-Structural Modeller on the ANSYS Workbench. Also this chapter described the used physical simulation for model validation. The next chapter will investigate the dynamic characteristics of the upper airways in morbid obese OSA patients before and after bariatric surgery by following the modelling procedure described in section 3.3, while the dynamic characteristics of the healthy and the unhealthy UA models will be investigated in Chapters 5 and 6, respectively.

## **CHAPTER 4**

### **OSA in Morbid Obese patients promoted for Bariatric Surgery**

#### **4.1 Introduction**

This chapter presents a biomechanical assessment of OSA in morbid obese patients before and after bariatric surgery. It explains the used clinical protocols including the process of CT data collection and gives a detailed explanation on how the participants were recruited, exclusion criteria and the followed protocol in collecting these data; as given in section 4.2. Section 4.3 describes the airway modelling before and after surgical intervention. The UA parameters are described in section 4.4. Section 4.5 presents the statistical analysis used. The results are presented in section 4.6 and the effects of bariatric surgery on OSA are investigated in section 4.7.

Bariatric surgery is a commonly used treatment to reduce the body weight, and consequently attenuate OSA in morbid obese patients [380-385] diagnosed with moderate-to-severe OSA [386-388]. Data depicting the ability of bariatric surgery to completely resolve OSA symptoms varies widely, ranging from 25-100% in previous studies [386, 388, 463, 466, 469-471, 476, 480, 482]. These differential effects may be attributed age and initial severity of the disease, or may vary according to weight loss-induced changes in airway physiology of the individual patient.

It has been reported that generally the success rate of bariatric surgery is high in patients with severe OSA, low for patients with moderate OSA and further low for patients with mild OSA [107]. However the biomechanical impact of bariatric surgery on the UA is incompletely understood and requires further elucidation. Our aim is to assess the manner in which the loss in the body weight after bariatric surgery affected the biomechanical properties of the UA specifically flow characteristics, volumetric measurements and dynamic response.

#### **4.2 Clinical Protocol**

Ethics application was prepared by our collaborators in the US and was successfully approved by Summa Health System's Institutional Review Board, and informed consents were obtained prior to initiation of study procedures.

### 4.2.1 Subjects

Ten morbid obese patients (coincidentally all females) were recruited (by our collaborators in the USA) between the ages of 20 and 62, who were pending laparoscopic Roux-en-Y Gastric Bypass surgery for weight loss, and who presented with a diagnosis of OSA during routine preoperative evaluation. Patients were excluded from participation if were determined to be ineligible for bariatric surgery or did not have OSA diagnosed via PSG by a board-certified sleep medicine physician. Baseline data for the Age, BMI and AHI are depicted in Table 4.1. Despite a baseline AHI of  $< 5$ , one participant (#4) was determined to have positional OSA (supine AHI = 7) and was therefore not excluded from the study.

**Table 4.1: Statistical data before surgical intervention**

Patient ID	Age (Years)	Baseline BMI (kg/m <sup>2</sup> )	Baseline AHI (events/hr)
1	58	46.2	73
2	39	60.4	63
3	28	54.7	22
4	31	51.4	2
5	60	40.0	34
6	41	50.4	29
7	54	38.0	32
8	49	46.8	95
9	30	47.6	16
10	62	49.7	15
Mean $\pm$ SD		48.5 $\pm$ 6.5	38.1 $\pm$ 29.4

After eligibility was determined, all participants were asked to undergo measurements of anthropometric, diagnostic polysomnogram, and non-contrast CT scans of their upper airways, three times during the study (baseline/preoperatively, then at 6 months and 12 months post-operatively) as described below.

### 4.2.2 Anthropometrics

Body weight was measured to the nearest 0.01 kg using a portable electronic scale (Model 770, Seca, Columbia, MD). Height was measured to the nearest 0.1 Cm using a portable stadiometer (Model 225, Seca, Columbia, MD).

### 4.2.3 Polysomnogram

Polysomnography was administered by a registered sleep technician and took place at a sleep laboratory accredited by the American Academy of Sleep Medicine. The participants were asked to sleep (overnight) in a laboratory environment designed to mimic a traditional bedroom. Prior to sleep, subjects were connected to monitoring

equipment including finger probe pulse oximeter (SpO<sub>2</sub>) and electromyograms (EMG) (performed at the anterior tibialis muscle and chin sites and used to assess nocturnal muscle movement). Chest and abdominal movements were measured by piezoelectric belts while electroencephalogram and electrooculogram were used to measure brain wavelengths and eye movements, Figure 4.1.

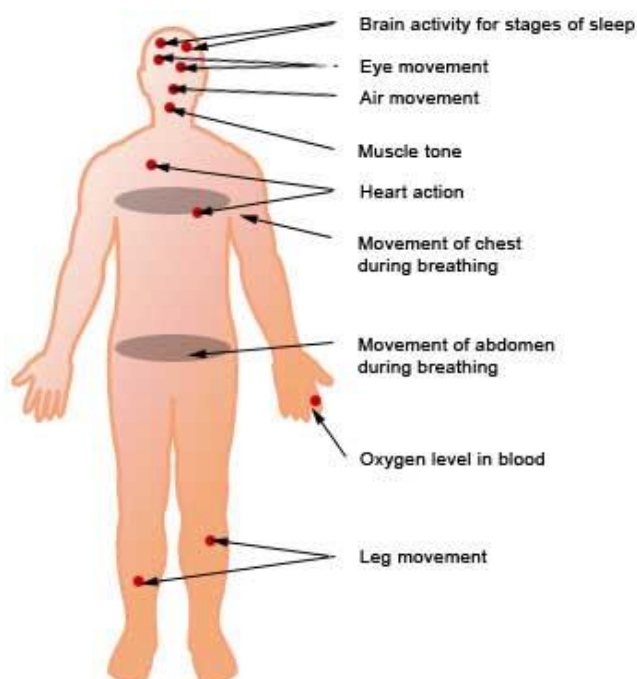


**Figure 4.1: Polysomnography [549]**

Airflow measurements were assessed by a thermistor and/or pressure transducer worn as a cannula underneath the nose during sleep. Some patients refused to undergo the third PSG (12 months after surgery) citing financial reasons (referred to as N/A in Table 4.2), therefore discussion results in these cases are given based on the 6-months data only, Table 4.2.

**Table 4.2: Statistical data after surgical intervention**

Patient ID	BMI (kg/m <sup>2</sup> )		AHI (events/hr)	
	6-Months	12-Months	6-Months	12-Months
1	36.2	33.8	37	29
2	40.7	32.8	9	1
3	35.3	28.8	0	0
4	33.5	33.3	3	4
5	29.3	26.6	44	N/A
6	34.9	30.0	12	0
7	25.5	23.2	19	N/A
8	34.7	34.6	5	N/A
9	33.3	30.8	5	0
10	33.3	28.9	23	N/A
Mean ± SD	33.7 ± 4.0	30.3 ± 3.6	15.7 ± 15.0	5.6 ± 10.2



#### 4.2.4 Computed Tomography

CT data were collected by our collaborators in the US. Transverse CT scans of the UA expanding from the roof of the mouth to the beginning of the trachea were collected by a trained radiologist according to the standard guidelines set forth by Summa's Department of Radiology. Each scan included a limited study of the neck, where the participant was placed in a supine position on the mobile scanner bed then passed through the scanner field. The resulting generated CT images were stored as part of the study record and subsequently used to determine volumetric measurements (as described below). Figure 4.2 shows a sample of the collected CT images showing the air gap.



**Figure 4.2: A sample of the collected CT data**

#### 4.3 Airway Modelling

Three dimensional airway models were constructed from baseline, 6 and 12-months data for all patients using 3D-DOCTOR software as described previously in sections 3.2 and 3.3. Figure 4.3 shows a sample of the constructed isolated three dimensional UA models.

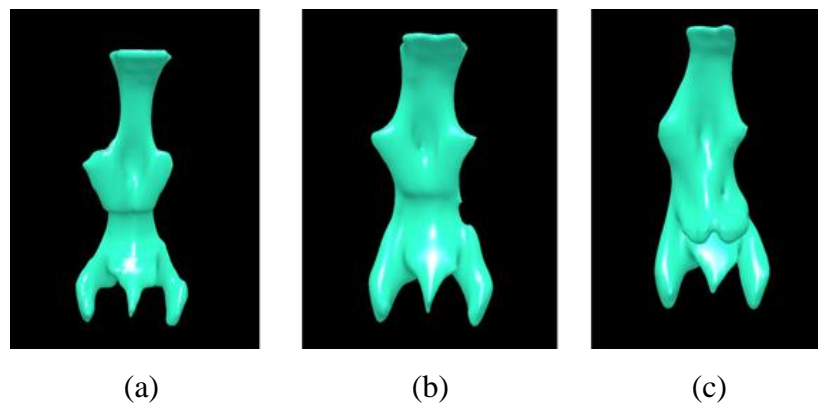


**Figure 4.3: Isolated UA models at (a) baseline, (b) 6-months and (c) 1 year after surgical intervention**

#### 4.4 Upper Airway Parameters

Measurements of the UA expanding from the beginning of the nasopharynx to the end of the hypopharynx were determined, including:

- UA volume (V),
- Cross section area (A) of the air gap,
- Wetted perimeter (P): which is the region of contact between the air and the airway walls, and
- The hydraulic diameter (HD) which was calculated at each transverse location (slice) using the obtained values for cross section area (A) and the wetted perimeter (P) as shown in Figure 4.4, where the HD is calculated by using the following formula:

$$HD = \frac{4A}{P} \text{ mm} \quad (4.1)$$

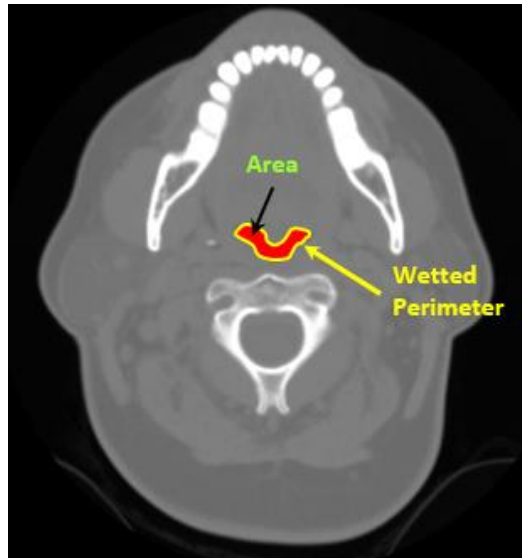


**Figure 4.4: Cross section area (A) and wetted perimeter (P) of the air gap**

When a fluid flows through a non-circular cross section the solution becomes really complicated, however it can be simplified by considering the cross section to be circular with a diameter equal to the value of the HD determined from the geometry of the non-circular cross section by using equation (4.1). The HD is considered as the characteristic length for determining some flow variables such as Reynolds Number and pressure loss.

In order to combine the effect of the changes in the upper airway volume (V) and the body mass index (BMI), a new parameter which takes into consideration the weight and the height of the body is introduced to assess the accessibility of the airflow with respect to the body size, namely Volume Body Mass Index (VBMI) which is defined as:

$$VBMI = \frac{\text{Upper Airway Volume}}{\text{Body Mass Index}} = \frac{V \text{ (m}^3\text{)}}{BMI \text{ (kg/m}^2\text{)}} \quad (4.2)$$

If the surgery is successful, it is expected that the volume of the upper airway increases and the body mass index decreases, consequently the VBMI increases and OSA symptoms (if exist) are expected to improve. Therefore in case of VBMI decreases, it is expected that OSA may deteriorate.

#### 4.5 Statistical Analyses

The surgical intervention resulted in many changes to all variables, these changes needed to be statistically analysed to check the significance of the surgery in improving those variables. This study included the HD which is determined based on the changes in the UA geometry before and after surgery, statistical analysis was needed to determine whether or not those changes were significant and check if there is a correlation between those changes and the success rate of the surgery; and consequently decide whether or not to recommend using this variable in similar future studies. Also, the changes in BMI, AHI and V needed to be statistically analysed to determine whether the surgical intervention has resulted in significant improvements or not. This study has also introduced a new parameter, VBMI, which was needed to be statistically examined to check its significance and consequently decide whether to recommend using it in future similar studies or not.

Therefore, univariate statistics were calculated for all the variables. A standard paired t-test was performed to check the significance of the results and assess the differences between means assuming equal variance of the study groups (baseline, 6-months and 12-months after surgery). All statistical analyses were considered significant when  $p \leq 0.05$ . Changes in the HD, BMI, AHI, V and VBMI were assessed by the analysis of variance (ANOVA).

#### 4.6 Results

The data recorded in Tables 4.1 and 4.2 (n=10) show that the AHI was decreased in four patients (1, 2, 3, 6 and 9). Same results have been recorded for patients 7 and 8 as the AHI

was significantly reduced after 6 months from surgery ( $p \leq 0.05$ ), but no PSG data could be collected for them after 12-months following surgical intervention as they could not afford the co-pay of the third PSG. Patient 4 had positional OSA at baseline (supine AHI = 7) and her AHI started to increase from 2 at baseline to 3 and 4 after 6 and 12 months following surgical intervention, respectively. For patients 5 and 10 (age > 60), the AHI was increased after 6 months from surgery, unfortunately no PSG data could be collected for them after 12 months following surgical intervention as they could not afford the co-pay of the third PSG. Also these data show significant changes in the mean AHI which was  $38.1 \pm 29.4$  events/hr at baseline ( $p \leq 0.05$ ), reduced by 59% to  $15.7 \pm 15$  events/hr 6 months after surgery and further reduced to  $5.6 \pm 10.2$  events/hr one year following surgical intervention (85% reduction compared with baseline).

These data also show an expected significant reduction in the BMI in all patients postoperatively ( $p \leq 0.05$ ). The mean BMI was  $48.5 \pm 6.5$  kg/m<sup>2</sup> at baseline, reduced by 31% to  $33.7 \pm 4.0$  kg/m<sup>2</sup> 6 months following surgery and further reduced to  $30.3 \pm 3.6$  kg/m<sup>2</sup> one year after surgical intervention (38% reduction compared with baseline mean value).

Values for the upper airway volume (V) were determined before and after surgical intervention and summarized in Table 4.3. These values show an increase in V for all patients except patient #4 (non-apneic at baseline) where V was dramatically reduced (n=10,  $p < 0.05$ ) after one year of surgical intervention.

**Table 4.3: UA volume before and after surgery**

Patient ID	V(mm <sup>3</sup> )		
	Baseline	6-Months	12-Months
<b>1</b>	14907.1	15202.9	16642.9
<b>2</b>	12575.8	14842.1	16442.3
<b>3</b>	12638.7	15715.2	16942.5
<b>4</b>	40441.5	23533.8	22914.2
<b>5</b>	14143.1	10813.2	16682.3
<b>6</b>	23982.1	24486.2	24059.6
<b>7</b>	22593.5	29894.5	24157.3
<b>8</b>	8715.9	10597.9	13129.5
<b>9</b>	9033.3	14967.8	12313.3
<b>10</b>	11289.4	17432.0	19338.7
Mean $\pm$ SD	17032.0 $\pm$ 9691.8	17748.6 $\pm$ 6258.5	18262.3 $\pm$ 4256.6

In order to combine the changes in V and BMI, a new parameter has been introduced, namely VBMI which represents the ratio of V to the BMI and was calculated for each patient at baseline, 6 and 12 months post surgery, Table 4.4.

**Table 4.4: VBMI before and after surgery**

Patient ID	VBMI ( $\text{m}^3/(\text{kg}/\text{m}^2)) \times 10^{-9}$		
	Baseline	6-Months	12-Months
1	322.7	420.0	492.4
2	208.2	364.7	501.3
3	231.1	445.2	588.3
4	786.8	702.5	688.1
5	353.6	369.1	627.2
6	475.8	701.6	802.0
7	594.6	1172.3	1041.3
8	186.2	305.4	379.5
9	189.8	449.5	399.8
10	227.2	523.5	669.2
Mean $\pm$ SD	357.6 $\pm$ 202.4	545.4 $\pm$ 258.0	618.9 $\pm$ 198.7

The data in Table 4.4 shows that the VBMI was increased in all patients post-surgery except patient 4 where the VBMI was decreased. Statistical calculations showed a significant increase in the VBMI one year following surgical intervention (n=10, p<0.05).

Values for the minimum and maximum HD were determined before and after surgery for all patients, Table 4.5.

**Table 4.5: Min. and Max. HD before and after surgery**

Patient ID	HD (mm)					
	Baseline		6-Months		12-Months	
	Min	Max	Min	Max	Min	Max
1	8.0	17.9	9.0	18.0	8.0	14.3
2	4.5	12.9	5.6	17.6	7.7	17.2
3	4.6	12.2	6.0	16.0	6.0	14.5
4	7.9	35.2	9.9	38.1	4.7	41.7
5	6.2	18.8	4.9	15.1	6.4	16.5
6	9.6	35.2	8.3	17.8	8.6	18.1
7	5.6	20.6	6.6	40.7	5.7	20.6
8	6.4	15.2	7.0	15.6	7.5	14.2
9	6.6	15.7	9.4	33.8	7.1	13.9
10	5.1	14.9	7.1	40.8	10.3	40.4

#### 4.7 Effects of Bariatric Surgery on OSA

Significant decrease in the BMI for all patients occurred during the first year after bariatric surgery ( $n=10$ ,  $p<0.05$ ) which is similar to the outcomes of previous studies [107, 384, 386, 388, 470]. Morbid obesity was resolved in all participants as five patients became overweight and the remaining five were classified as obese.

After surgery, the AHI was reduced in all patients except those with age  $\geq 60$  years and patient 4 where it was increased. OSA was completely resolved in all patients under 50 years diagnosed with moderate-to-severe OSA at baseline ( $n=5$ ), improved in patients with age range 50-60 years diagnosed with severe OSA at baseline ( $n=2$ ), worsened in patients  $\geq 60$  years diagnosed with mild-to-moderate OSA at baseline ( $n=2$ ) and is developing in the patient originally diagnosed with positional OSA ( $n=1$ ). These results agree with the previous outcomes where bariatric surgery either resolved or improved OSA symptoms in morbid obese patients under the age of 60 years [107, 384, 386, 469, 470]. Consequently, sleep architecture was improved in patients where OSA was either resolved or improved.

In terms of volumetric changes, V and the VBMI were increased in all subjects (compared to baseline values) one year after surgery except for patient 4 where both values were reduced and consequently the AHI was increased to double the baseline value indicating that OSA is developing.

Although there is no trend in the minimum or maximum HD variation, the data in Tables 4.1 and Table 4.2 indicate that OSA was completely resolved in patients 2, 3, 6, 8 and 9 (age  $< 50$  years) regardless to the changes in their HD values given in Table 4.5. For patients 1 and 7 ( $50 < \text{age} < 60$  years) the minimum HD was increased after 6-months from surgery and then decreased at 12 months following surgical intervention while OSA symptoms were improved (but not completely resolved). For patients 5 and 10 (age  $\geq 60$  years) OSA was worsened irrespective to the changes in their HD. Finally for patient 4 diagnosed with positional OSA at baseline, the minimum HD was increased 6 months post surgery and then decreased to a value smaller than the baseline value one year following surgical intervention associated with 2-fold the baseline AHI value. Therefore, bariatric surgery had no significant effect on the minimum HD in morbid obese middle-aged OSA patients ( $< 50$  years) although OSA was completely resolved in this age group ( $p \leq 0.05$ ).

The data in Table 4.1 and Table 4.5 shows that the increase in the VBMI was associated with reductions in the AHI for all morbid obese apneic patients under the age of 60 years (7 patients out of 10, 70%), while both the VBMI and the AHI were increased for those with age  $\geq 60$  years. This trend if widely investigated could be used to predict the outcome of the surgery for morbid obese apneic patients under the age of 60 years by only specifying their VBMI without the need for the expensive and time consuming follow up PSG. In other words, if there is an apneic patient with age less than 60 years and his/her VBMI was increased after surgical intervention, it is expected that the AHI has decreased and consequently OSA symptoms have improved and the surgery was successful in both weight reduction and improving OSA symptoms; the opposite (if occurred) would mean that the surgery was unsuccessful and OSA symptoms may have been deteriorated.

It is believed that the good response of the UA muscles for younger subjects in this study is the main contributor to resolve OSA symptoms regardless of the changes in the HD, which explains the complete resolution of OSA in the age group under 50 years. Also because the response of the UA muscles decreases with age, the surgery would only improve OSA symptoms but not completely resolve them; thus helping explain the results for the participants with age between 50 and 60 years. In patients with the age of 60 years and older, the results suggest that it is difficult to stimulate the UA muscles in this age group even with the improvements in all other parameters analysed (BMI, HD, V and VBMI).

This study has some limitations including only female patients were recruited (though recruitment was consecutive), relatively small sample size, and incomplete 12 months data for some participants. Furthermore, the image processing was performed manually which may have contributed some errors in the delineation of the beginning and end of the airway image.

#### **4.8 Closure**

This chapter investigated the effectiveness of bariatric surgery, which is used in reducing weight and improving OSA symptoms in 10 morbid obese patients. The results show that bariatric surgery may be a good treatment in losing weight and consequently alleviate OSA symptoms for morbid obese patients under 50 years of age, which is mainly due to the very good response of the UA muscles in the young age. The next chapter will describe

the MRI data collection, and investigate the dynamic characteristics of healthy UA models using FE modelling by using the Abaqus software.



## CHAPTER 5

### Dynamic Characteristics of Healthy Upper Airways

#### 5.1 Introduction

This chapter explains the recruitment process of healthy volunteers for MRI data collection, and indicates the exclusion criteria as well as the protocol of collecting the data, section 5.2. It also describes the investigation of the dynamic characteristics of healthy models for the soft tissues using the finite element (FE) methods by using the Abaqus software, section 5.3. A summary of the obtained results for the healthy subjects is given in section 5.4.

#### 5.2 MRI Data Collection

All study procedures were approved by the ethics committee at Auckland University of Technology at earlier stages (Ethics application number 10/121) and informed consents were obtained prior to initiation of study procedures.

##### 5.2.1 Recruiting Subjects

Posters were prepared and distributed inside the Auckland University of Technology inviting volunteers to participate in the study. Templates for the participant information sheet (PIS) and consent forms were prepared and sent to the interested candidates. The PIS indicated that subjects were excluded from the study if they were:

- Having metallic implants through their upper airways,
- Using pacemakers,
- Having any UA infection,
- Smokers, and
- Pregnant patients (if applicable) were also excluded.

Interested candidates sent back their signed consent forms, and mutually agreeable times were arranged for an ear, nose and throat (ENT) specialist, Dr Jim Bartley, to examine the interested participants and giving reports about their upper airways.

A screening process was then undertaken to exclude those who are unsuited for the study and to provide the desired population sample variety. The final sample consisted of eight healthy volunteers including four males and four females between the ages of 21 and 53 years. The BMI range was 23.7-27.7 kg/m<sup>2</sup>. The selected participants were notified

and mutually agreeable times were arranged to undergo measurements of anthropometric and for the MRI data to be collected, as described below.

### **5.2.2 Anthropometrics**

Body weight was measured to the nearest 0.01 kg using a portable electronic scale (Model 770, Seca, Columbia, MD). Height was measured to the nearest 0.1 Cm using a portable stadiometer (Model 225, Seca, Columbia, MD).

### **5.2.3 Data Collection**

MRI data of the UA expanding from the nasopharynx to the hypopharynx were collected and administered by a registered radiographer and took place at The Centre for Advanced Magnetic Resonance Imaging (CAMRI) at The University of Auckland which is accredited by the International Accreditation New Zealand and is an affiliated provider for Southern Cross Healthcare and a health services provider for the Accident Compensation Corporation (ACC). The data were collected according to the following steps:

- Each participant assumed the supine position (during wakefulness) within the MRI scanner and the MRI head coil was then positioned over their head.
- After a suitable settling time, the MRI scanner recorded the geometry of their UA.
- The above procedure was repeated for all participants.

Transverse MRI sequences (axial T1) of 1 mm thickness were collected using 1.5 Tesla MRI scanner covering the entire pharyngeal airway from the top of the nasal cavity to the bottom of the hypopharynx.

## **5.3 Dynamic Characteristics of Healthy Upper Airways**

This section describes the construction and simulation of real UA models including air and soft tissues (uvula and tongue) for healthy subjects. It also provides summaries of the obtained results and holds comparisons between the dynamic characteristics for the healthy subjects.

### **5.3.1 Healthy UA Models**

Eight healthy subjects were recruited for the study consisting of 4 males and 4 females. The demographic data for the eight healthy participants is summarized in Table 5.1, including age, gender, weight, height, BMI and ethnicity.

**Table 5.1: Demographic data from participating volunteers**

Subject ID	Age (Years)	Gender	Weight (Kg)	Height (m)	BMI (Kg/m <sup>2</sup> )	Ethnicity
1	21	M	65	1.65	23.9	Indian
2	22	M	66	1.67	23.7	Chinese
3	53	F	76	1.68	26.9	NZ European
4	30	M	90	1.88	25.5	Caucasian
5	29	M	82	1.72	27.7	Arab
6	35	F	64	1.55	26.4	Southeast Asian
7	33	F	68	1.67	24.4	Argentinian
8	26	F	72	1.70	24.9	NZ European
Mean $\pm$ SD	31.1 $\pm$ 10.1				25.4 $\pm$ 1.5	

Isolated airway models were constructed for all subjects from the collected MRI data using 3D-DOCTOR software following the procedure described previously in sections 3.2 and 3.4. Figure 5.1 shows a sample of the resulting UA models isolated from the rest of the airway.

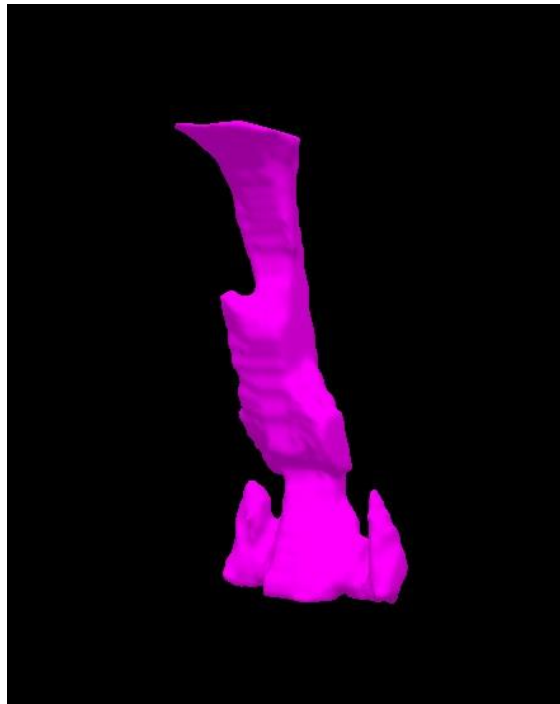


**Figure 5.1: Healthy UA model isolated from the rest of the airway**

Measurements of the UA were determined including airway volume and air gaps at the rear of the uvula and tongue at the mid-sagittal plane (MSP) using the tools of 3D-DOCTOR software; and are summarized in Table 5.2.

**Table 5.2: UA volume and air gaps for all healthy subjects**

Subject ID	Air Volume (mm <sup>3</sup> )	Min. gap rear of tongue at MSP (mm)	Min. gap rear of uvula at MSP (mm)
1	15080.7	8.8	6.7
2	18803.1	12.9	9.7
3	7824.0	7.0	3.8
4	7880.1	3.8	7.3
5	16979.5	4.7	2.6
6	11064.2	14.9	6.5
7	10337.6	5.0	2.4
8	10210.0	4.8	2.4
Mean $\pm$ SD	12272.4 $\pm$ 4161.6	7.7 $\pm$ 4.2	5.2 $\pm$ 2.8

### 5.3.2 Dynamic Characteristics of Healthy Isolated Uvula Models

The isolated uvula model may be considered as a clamped-free beam model as explained in section 3.4, with the dimensions shown in Figure 5.2 which are the approximate dimensions of a real uvula model; where the beam is clamped from the left end (where it is attached to the hard palate), and free to deform from the right end.

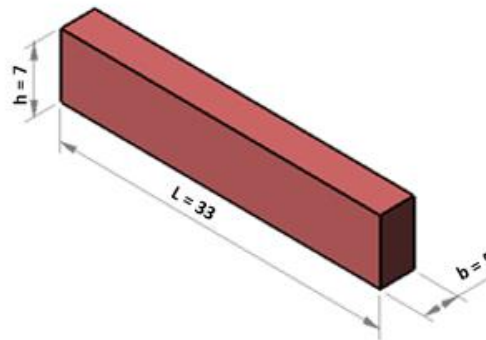


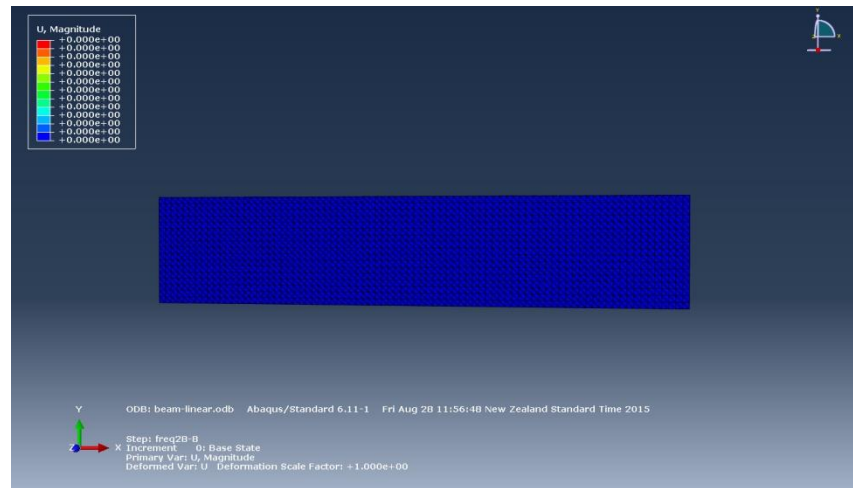
**Figure 5.2: Geometry of uniform beam (all dimensions are in mm)**

The main reason for the following calculations is to give a quick pre-assessment of the values of the natural frequencies for preliminary investigation.

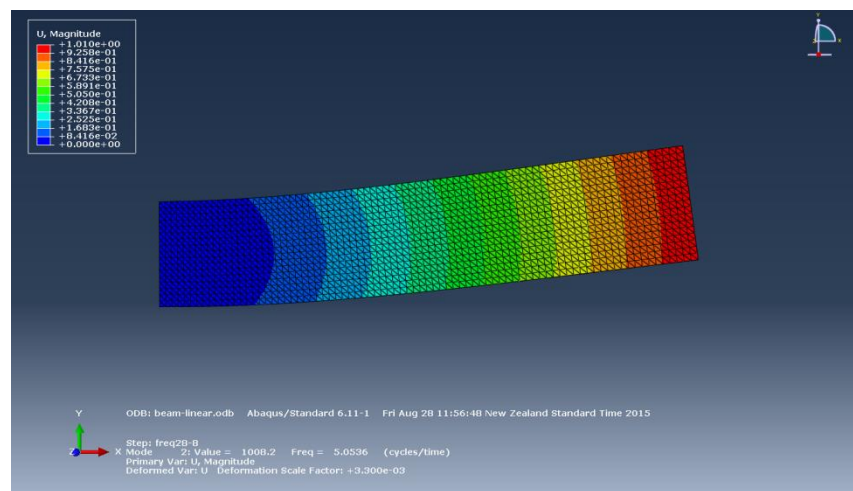
Assuming the same properties as the real uvula [24]:

- $E = 25 \text{ kPa}$
- $\rho = 1040 \text{ kg/m}^3$
- $\nu = 0.45$

Figure 5.3 shows the geometry of the clamped-free beam and the first natural frequency obtained from the Abaqus/CAE software after following the procedure described in section 3.4.



(a)



(b)

**Figure 5.3: Uniform beam (a) geometry and (b) first natural frequency from the Abaqus software**

Figure 5.3 (b) shows that the first natural frequency obtained from the Abaqus software is 5.05 Hz. To check the accuracy of the obtained results from the Abaqus, consider the theoretical analytical solution of the transverse vibration of a uniform homogeneous clamped-free beam model given in Figure 5.4.

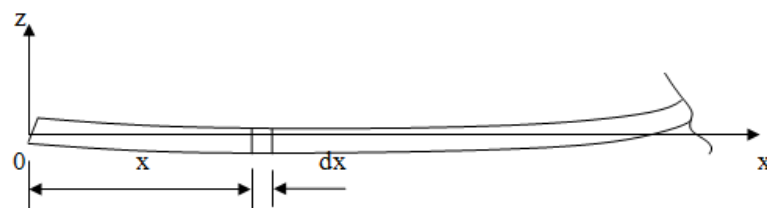


**Figure 5.4: Beam geometry**

For the case of a clamped-free beam, the boundary conditions are:

(i) At  $x = 0$

$$w = 0, \frac{dw}{dx} = 0$$

(ii) At  $x = L$

$$\frac{d^2w}{dx^2} = 0 \text{ (No bending), } \frac{d^3w}{dx^3} = 0 \text{ (No shear)}$$

Applying the conditions of equilibrium along with the boundary conditions, we get:

$$\therefore -EI \frac{d^4w}{dx^4} = \rho A \frac{d^2w}{dt^2} \quad (5.1)$$

Where

E: Young's Modulus of Elasticity

I: Moment of area of the cross section area of the beam

w: Vertical deflection of the beam

$\rho$ : Density of the beam

A: Cross sectional area of the beam

Equation (5.1) is known as “Euler-Bernoulli Beam Theory”; and the solution is given by [550]:

$$\cosh \lambda_n L \cos \lambda_n L = -1 \quad (5.2)$$

Where

$$\lambda_n = \left( \frac{\rho A}{EI} \omega_n^2 \right)^{\frac{1}{4}} \quad (5.3)$$

And  $\omega_n$  is the natural frequency.

Rearranging equation (5.2), we get:

$$\cos \lambda_n L = \frac{-1}{\cosh \lambda_n L} \quad (5.4)$$

$$\therefore \cos \lambda_n L = -\operatorname{sech} \lambda_n L$$

Now, let

$$y_1 = \cos x \text{ and } y_2 = -\operatorname{sech} x$$

Where  $x = \lambda_n L$

Therefore the solution is obtained when  $y_1 = y_2$ , which is represented by the points of intersection of the two graphs. Figure 5.5 shows the graph of the two functions using the MATLAB software (version 2012b, The MathWorks Inc., MA, USA). Full derivation of the equations and the used MATLAB code are provided in Appendix A.

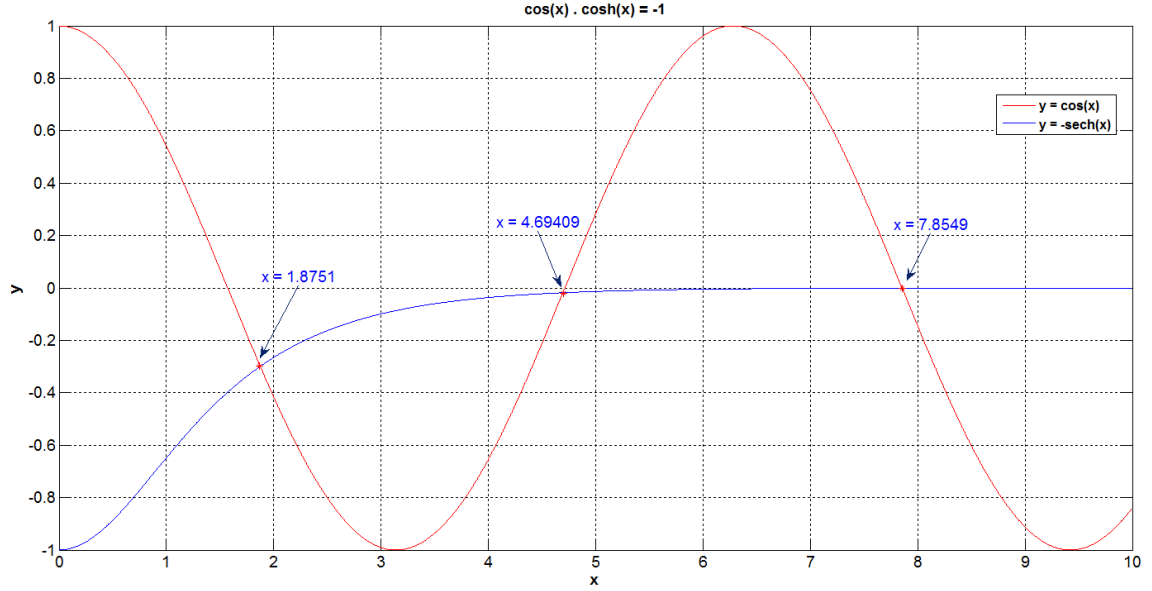


**Figure 5.5: Solution of equation (5.4) using MATLAB**

The solution is represented by the points of intersection between the two curves shown in Figure 5.5, which are found to be:

$$\begin{aligned} x_1 &= \lambda_1 L = 1.8751 \\ x_2 &= \lambda_2 L = 4.69409 \end{aligned} \quad (5.5)$$

$$x_3 = \lambda_3 L = 7.8549$$

The corresponding natural frequencies ( $\omega_n$ ) are calculated by recalling equation (5.3):

$$\lambda_n = \left( \frac{\rho A}{EI} \omega_n^2 \right)^{\frac{1}{4}} \quad (5.3)$$

$$\therefore \omega_n = \lambda_n^2 \sqrt{\frac{EI}{\rho A}} \text{ (rad/sec.)}$$

$$\omega_n = \frac{(\lambda_n L)^2}{L^2} \sqrt{\frac{EI}{\rho A}} \text{ (rad/sec.)} \quad (5.6)$$

And the natural frequencies in Hz (vibrations/second) can be calculated as follows:

$$f_n = \frac{\omega_n}{2\pi} \text{ (Hz)} \quad (5.7)$$

Now, applying the properties of the real uvula [24]:

- $E = 25 \text{ kPa}$

- $\rho = 1040 \text{ kg/m}^3$
- $\nu = 0.45$

Therefore

$$I = \frac{1}{12} bh^3 = \frac{1}{12} (0.005)(0.007)^3 = 1.43 \times 10^{-10} \text{ m}^4 \quad (5.8)$$

The cross sectional area is given by:

$$A = (0.005) \times (0.007) = 3.5 \times 10^{-5} \text{ m}^2 \quad (5.9)$$

Therefore, the theoretical natural frequencies can be obtained from equation (5.6) as follows:

$$\omega_n = \frac{(\lambda_n L)^2}{(0.033)^2} \sqrt{\frac{(25000)(1.42917 \times 10^{-10})}{(1040)(3.5 \times 10^{-5})}} \text{ (rad/sec.)} \quad (5.10)$$

From equations (5.7) and (5.10), the theoretical values for the first three natural frequencies are summarized in the Table 5.3 as well as the results from the Abaqus software.

**Table 5.3: Theoretical values for the natural frequencies ( $f_n$ )**

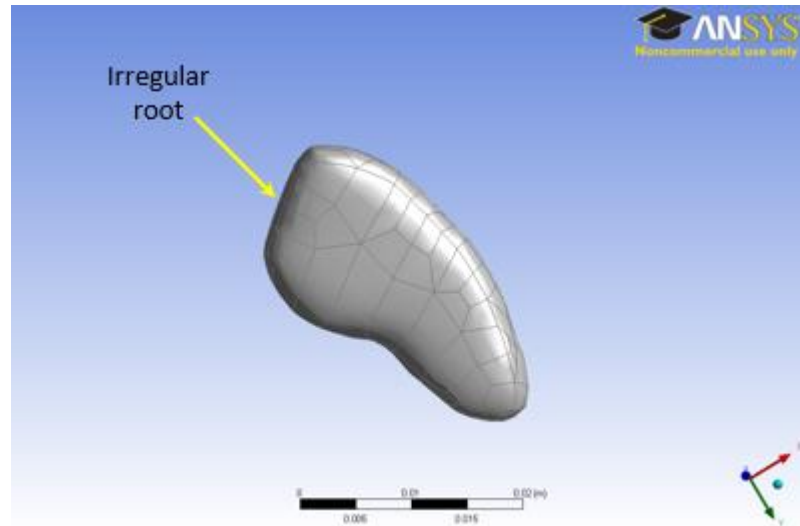
Mode (n)	$\lambda_n L$	$\omega_n$ (rad/s)	$f_n$ (Hz)	$f_n$ (Hz) Abaqus
1	1.9	32.0	5.1	5.1
2	4.7	200.5	31.9	26.4
3	7.9	561.3	89.3	61.8

The comparison between the obtained theoretical and numerical results for the first three natural frequencies given in Table 5.3 shows that the values for the first natural frequency are approximately the same, the values for the second natural frequency are still close to one another, however there is a relatively big difference between the obtained theoretical and numerical values for the third natural frequency. From these results we conclude that this FE modelling procedure using the Abaqus software can be applied accurately in determining the first two natural frequencies for the real uvula and tongue models, however it may result in relatively non-accurate values for the third natural frequency.

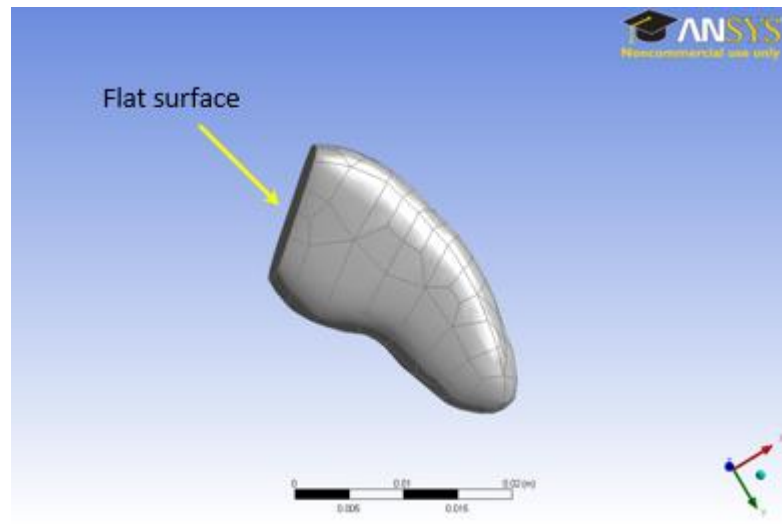
Isolated uvula models were accurately constructed from the MRI data using 3D-DOCTOR software following the same procedure described in sections 3.2 and 3.4. The resulting isolated uvula models had irregular roots from where the uvula is attached to the hard palate and these irregular roots had to be removed to produce flat surfaces that were easily



simulated on the Abaqus software as clamped-free beams as described in section 3.4. To achieve this, the models obtained from 3D-DOCTOR software were saved as STL files and then imported into the SolidWorks software to be converted to IGES files. The resulting IGES models of the uvula were then imported into the ANSYS DM to cut these irregular roots. Figure 5.6 (a) and (b) shows an uvula model before and after cutting the root; respectively.



(a)



(b)

**Figure 5.6: Isolated uvula model (a) before and (b) after cutting the root**

The resulting isolated uvula models were then imported into the Abaqus software to determine the natural frequencies for different values of the Young's Modulus of Elasticity ( $E$ ) for each subject specific, by assigning a fixed support condition at the flat

root where the uvula is attached to the hard palate as explained above. The following material properties were used based on the information reported in the background (Chapter 1) [24]:

- $\rho = 1040 \text{ kg/m}^3$
- $\nu = 0.45$
- $E = 25 \text{ kPa}$  (normal control value)

There are many parameters that may affect the stiffness of the soft tissues such as age, race, gender and different sleeping positions and/or stages. Simulations were therefore conducted on the Abaqus software for different values of  $E$  to cover the effects of all these parameters. Figure 5.7 summarizes the detailed FE modelling procedure.

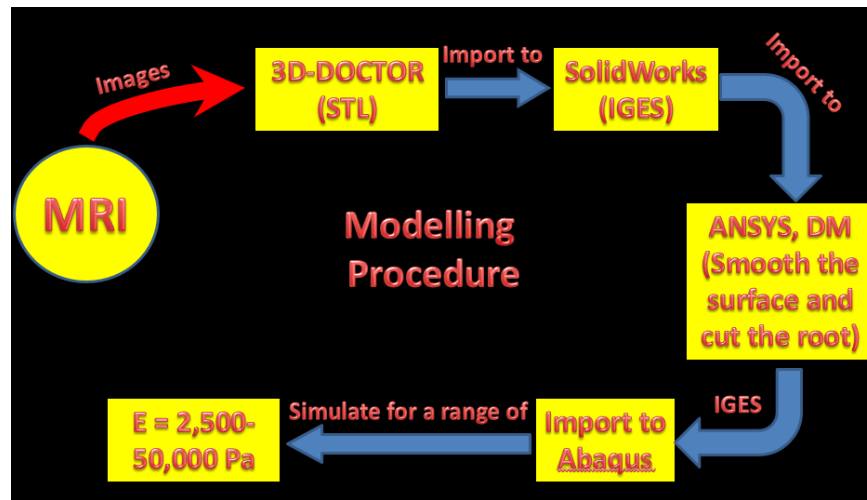


**Figure 5.7: Summary of the FE modelling procedure**

The relationship between  $E$  and  $f_n$  was then plotted for all healthy uvula models. The same analysis procedure was done for a range of the Poisson's ratio, 0.42-0.49, and it resulted in no effect on the natural frequencies. Values obtained from 3D-DOCTOR software for the volume of the healthy uvula models are summarized in Table 5.4.

**Table 5.4: Volumes of the healthy uvula models**

Subject ID	Uvula Volume (mm <sup>3</sup> )
1	1240.0
2	1039.9
3	1348.1
4	1491.8
5	1667.0
6	1245.7
7	1029.5
8	941.0
Mean $\pm$ SD	1250.4 $\pm$ 248.0

The approximate dimensions of a healthy uvula model isolated from the airway are shown in Figure 5.8 and the real geometry is shown in Figure 5.9.

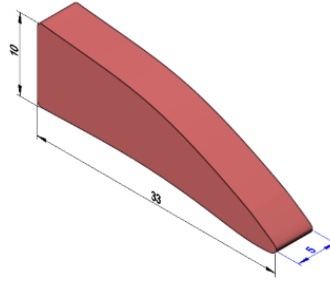


**Figure 5.8: Approximate dimensions of a healthy uvula model (in mm)**

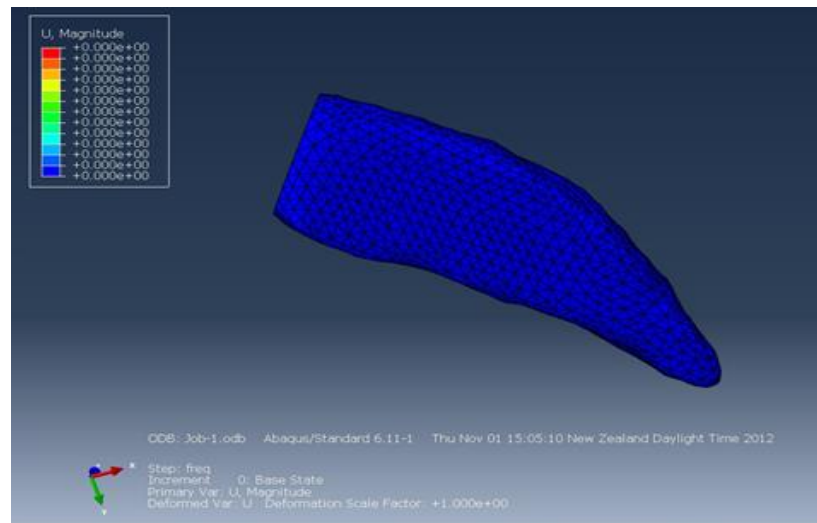
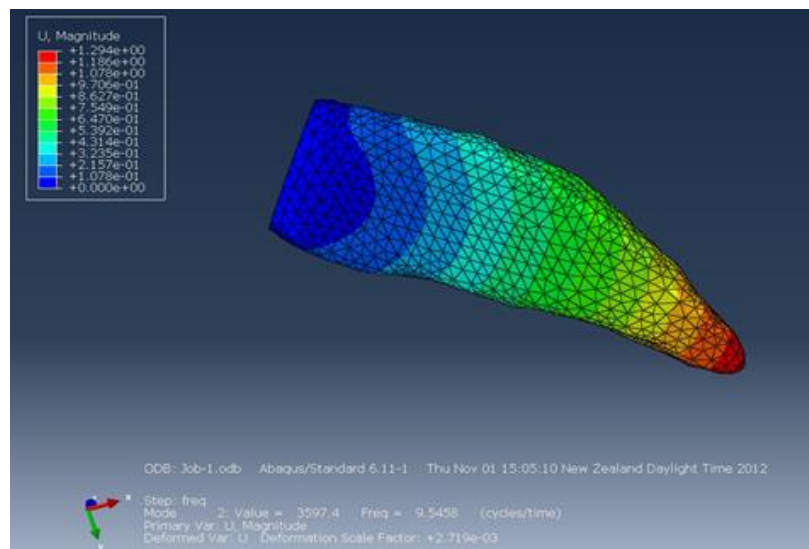
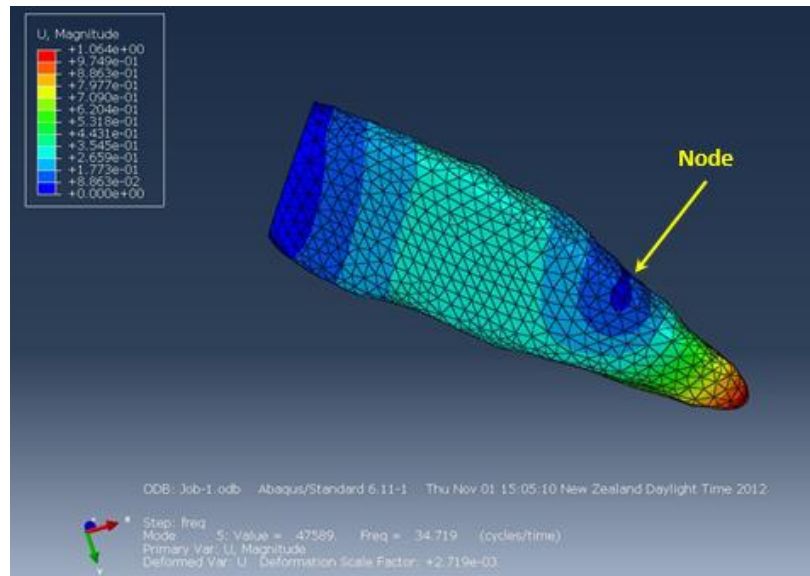


**Figure 5.9: Geometry of a healthy uvula model isolated from the airway**

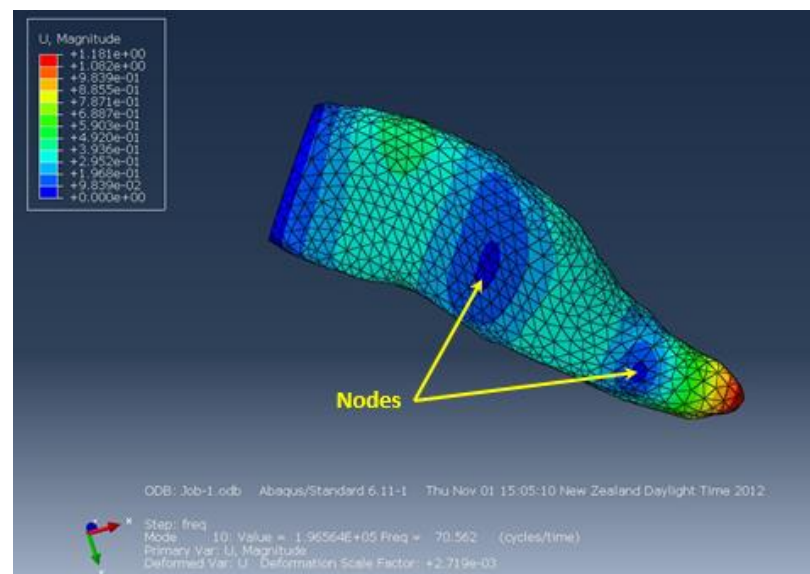
The first three mode shapes and the corresponding values of the natural frequencies are shown in Figure 5.10, a, b and c; respectively for a normal control value of  $E = 25$  kPa.



**(a) First mode shape**



(b) Second mode shape



(c) Third mode shape

**Figure 5.10: Mode shapes for an isolated healthy uvula model;  $E = 25$  kPa**

The results for the first three natural frequencies  $f_n$  for different values of  $E$  for a healthy uvula model are summarized in Table 5.5, and plotted in Figure 5.11.

**Table 5.5: Natural frequencies for a healthy uvula model for different values of E**

<b>E (Pa)</b>	<b><math>f_{n1}</math>(Hz)</b>	<b><math>f_{n2}</math>(Hz)</b>	<b><math>f_{n3}</math>(Hz)</b>
<b>0</b>	0	0	0
<b>2500</b>	3.0	11.0	22.3
<b>5000</b>	4.3	15.5	31.6
<b>10000</b>	6.0	22.0	44.6
<b>15000</b>	7.4	26.9	54.7
<b>20000</b>	8.5	31.1	63.1
<b>25000</b>	9.6	34.7	70.6
<b>30000</b>	10.5	38.0	77.3
<b>35000</b>	11.3	41.1	83.5
<b>40000</b>	12.1	43.9	89.3
<b>45000</b>	12.8	46.6	94.7
<b>50000</b>	13.5	49.1	99.8

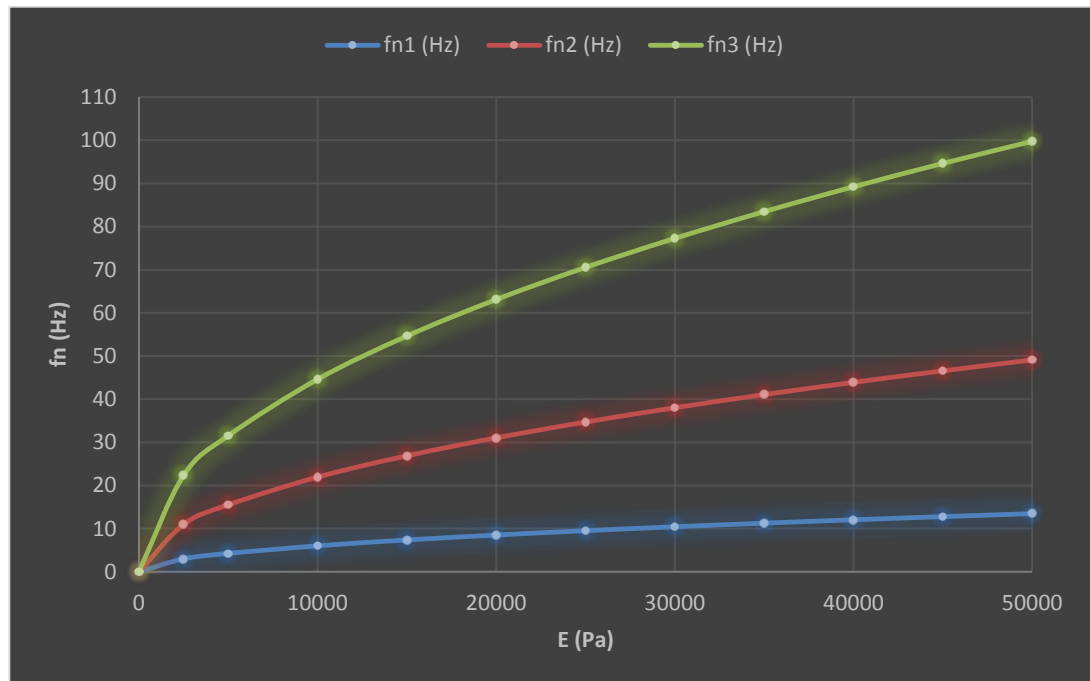


**Figure 5.11: Relationship between E (Pa) and  $f_n$  (Hz) for a healthy uvula model**

The above procedure for determining the natural frequencies for the isolated healthy uvula models using the Abaqus software was repeated for all models. Values for the first, second and third natural frequencies for all healthy uvula models are summarized in Tables 5.6, 5.7 and 5.8; respectively.

The mean values for the natural frequencies are calculated below each table for the normal control value of  $E = 25$  kPa.

**Table 5.6: Values of the first natural frequencies for healthy uvula models**

<b>E(Pa)</b>	<b>Subject 1</b>	<b>Subject 2</b>	<b>Subject 3</b>	<b>Subject 4</b>	<b>Subject 5</b>	<b>Subject 6</b>	<b>Subject 7</b>	<b>Subject 8</b>
2500	3.0	3.1	3.0	2.7	2.7	3.2	3.2	3.3
5000	4.3	4.3	4.3	3.8	3.8	4.5	4.5	4.7
10000	6.0	6.1	6.1	5.4	5.4	6.3	6.3	6.6
15000	7.4	7.5	7.4	6.6	6.6	7.7	7.7	8.1
20000	8.5	8.6	8.6	7.6	7.6	8.9	8.9	9.3
25000	9.6	9.7	9.6	8.5	8.5	10.0	10.0	10.4
30000	10.5	10.6	10.5	9.3	9.4	10.9	10.9	11.4
35000	11.3	11.4	11.4	10.1	10.1	11.8	11.8	12.3
40000	12.1	12.2	12.1	10.8	10.8	12.6	12.6	13.2
45000	12.8	12.9	12.9	11.4	11.5	13.4	13.4	13.9
50000	13.5	13.6	13.6	12.0	12.1	14.1	14.1	14.7

Mean  $\pm$  SD =  $9.5 \pm 0.7$  for  $E = 25$  kPa

**Table 5.7: Values of the second natural frequencies for healthy uvula models**

<b>E(Pa)</b>	<b>Subject 1</b>	<b>Subject 2</b>	<b>Subject 3</b>	<b>Subject 4</b>	<b>Subject 5</b>	<b>Subject 6</b>	<b>Subject 7</b>	<b>Subject 8</b>
2500	11.0	9.9	10.1	12.2	9.7	10.8	10.9	11.7
5000	15.5	14.0	14.2	17.2	13.8	15.3	15.6	16.5
10000	22.0	19.8	20.1	24.3	19.5	21.6	21.7	23.3
15000	26.9	24.2	24.6	29.8	23.9	26.4	26.6	28.6
20000	31.1	28.0	28.4	34.4	27.5	30.5	30.7	33.0
25000	34.7	31.3	31.8	38.4	30.8	34.1	34.3	36.9
30000	38.0	34.2	34.8	42.1	33.7	37.4	37.6	40.4
35000	41.1	37.0	37.6	45.5	36.4	40.4	40.6	43.6
40000	43.9	39.5	40.2	48.6	39.0	43.2	43.4	46.6
45000	46.6	41.9	42.7	51.5	41.3	45.8	46.0	49.5
50000	49.1	44.2	45.0	54.3	43.6	48.3	48.5	52.1

Mean  $\pm$  SD =  $34.0 \pm 2.7$  for  $E = 25$  kPa

**Table 5.8: Values of the third natural frequencies for healthy uvula models**

E(Pa)	Subject 1	Subject 2	Subject 3	Subject 4	Subject 5	Subject 6	Subject 7	Subject 8
2500	22.3	21.0	21.0	30.0	21.5	24.4	24.9	26.5
5000	31.6	29.7	29.7	42.4	30.3	34.6	35.1	37.4
10000	44.6	42.0	42.0	60.0	42.9	48.9	49.7	52.9
15000	54.7	51.4	51.4	73.4	52.5	59.9	60.9	64.8
20000	63.1	59.3	59.4	84.8	60.7	69.1	70.3	74.9
25000	70.6	66.3	66.4	94.8	67.8	77.3	78.6	83.7
30000	77.3	72.7	72.7	103.8	74.3	84.7	86.1	91.7
35000	83.5	78.5	78.6	112.2	80.3	91.5	93.0	99.1
40000	89.3	83.9	84.0	119.9	85.8	97.8	99.4	105.9
45000	94.7	89.0	89.1	127.2	91.0	103.7	105.4	112.3
50000	99.8	93.8	93.9	134.1	95.9	109.3	111.1	118.4

Mean  $\pm$  SD = 75.7  $\pm$  10.0 for E = 25 kPa

### 5.3.3 Dynamic Characteristics of Healthy Isolated Tongue Models

The isolated tongue models were accurately constructed from the collected MRI data by following the same procedure described previously for the uvula models in section 5.3.2, and were also imported into the ANSYS Design Modeller (DM) to cut the irregular root, Figure 5.12 (a), where the tongue is attached to the lower jaw to produce a flat surface, Figure 5.12 (b).

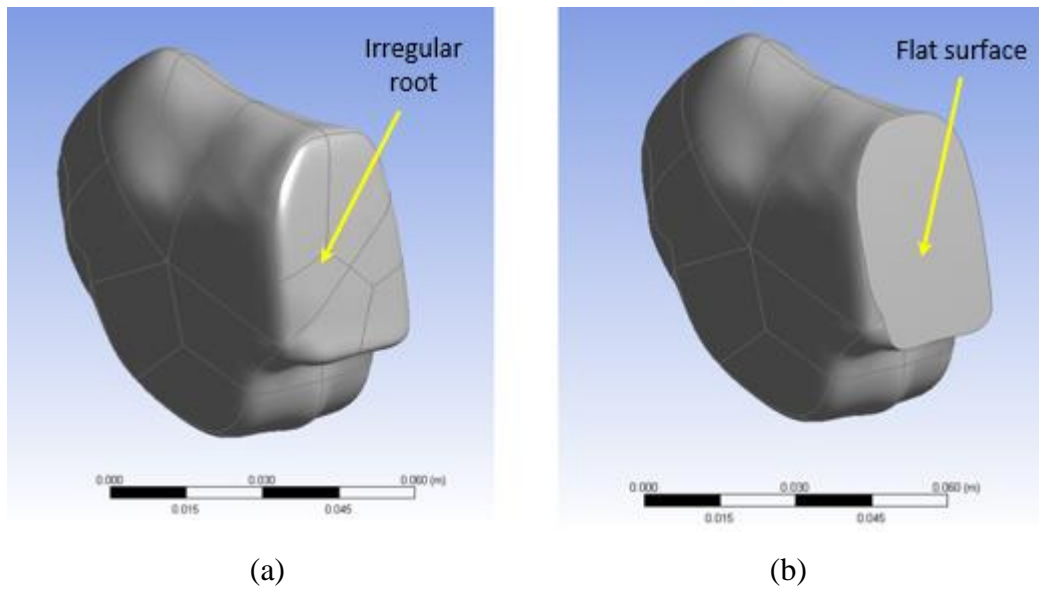


**Figure 5.12: Isolated tongue model (a) before and (b) after cutting the root**

The natural frequencies for all the isolated tongue models were determined using the Abaqus software for different values of E by assigning a fixed support condition to the flat surface where the tongue is attached to the lower jaw. The following material properties were used based on the information reported in the background (Chapter 1) [24]:

- $\rho = 1040 \text{ kg/m}^3$
- $\nu = 0.499$
- $E = 15 \text{ kPa}$  (normal control value)

There are many parameters that may affect the stiffness of the soft tissues such as age, race, gender and different sleeping positions and/or stages. Simulations were therefore conducted on the Abaqus software for different values of E to cover the effects of all these parameters. Values obtained from 3D-DOCTOR software for the volume of the healthy tongue models are summarized in Table 5.9.

**Table 5.9: Volumes of healthy tongue models**

Subject ID	Tongue Volume (mm <sup>3</sup> )
1	73427.4
2	N/A
3	81243.6
4	70709.9
5	N/A
6	56594.6
7	57131.4
8	60110.4
<b>Mean <math>\pm</math> SD</b>	<b>66536.2 <math>\pm</math> 10097.5</b>

The data in Table 5.9 indicates that the tongue volumes for subjects 2 and 5 are not available (noted as N/A) as these two participants were using mouth retainers and their tongue geometries could not be accurately detected by the MRI scanner, which can be seen by the highlights in Figure 5.13. Therefore the following results show the outcomes of six tongue models only.



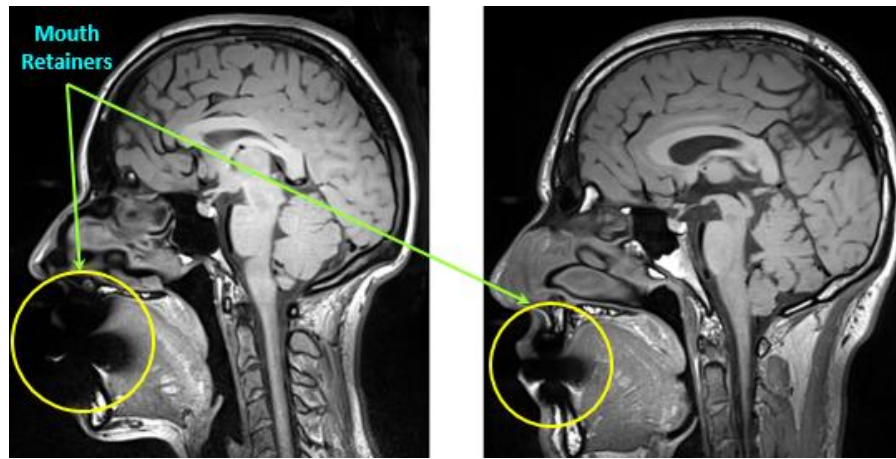


**Figure 5.13: MRI images of the MSP for subjects 2 and 5**

The geometry of a healthy tongue model isolated from the airway is shown in Figure 5.14, and the first three mode shapes are given in Figure 5.15 for the normal control value of  $E = 15$  kPa.

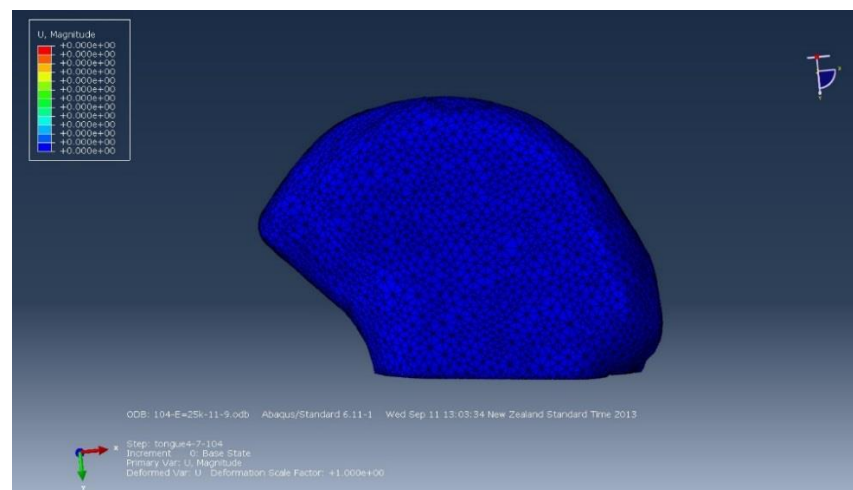
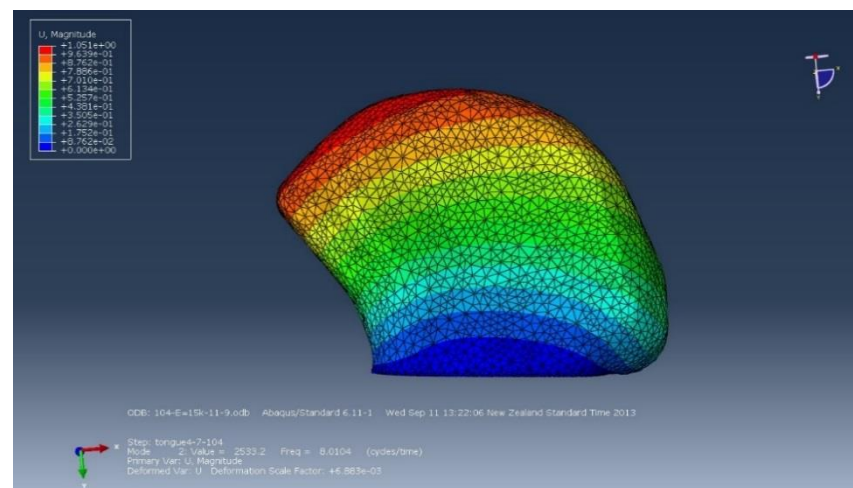


**Figure 5.14: Geometry of a healthy tongue model isolated from the airway**



**(a) First mode shape**



**Table 5.10: Natural frequencies for a healthy tongue model for different values of E**

E (Pa)	$f_{n1}$ (Hz)	$f_{n2}$ (Hz)	$f_{n3}$ (Hz)
0	0	0	0
2500	3.3	9.6	14.0
5000	4.6	13.5	19.9
10000	6.5	19.1	28.1
15000	8.0	23.4	34.4
20000	9.3	27.1	39.7
25000	10.3	30.3	44.4
30000	11.3	33.2	48.7
35000	12.2	35.8	52.6
40000	13.1	38.3	56.2
45000	13.9	40.6	59.6
50000	14.6	42.8	62.8

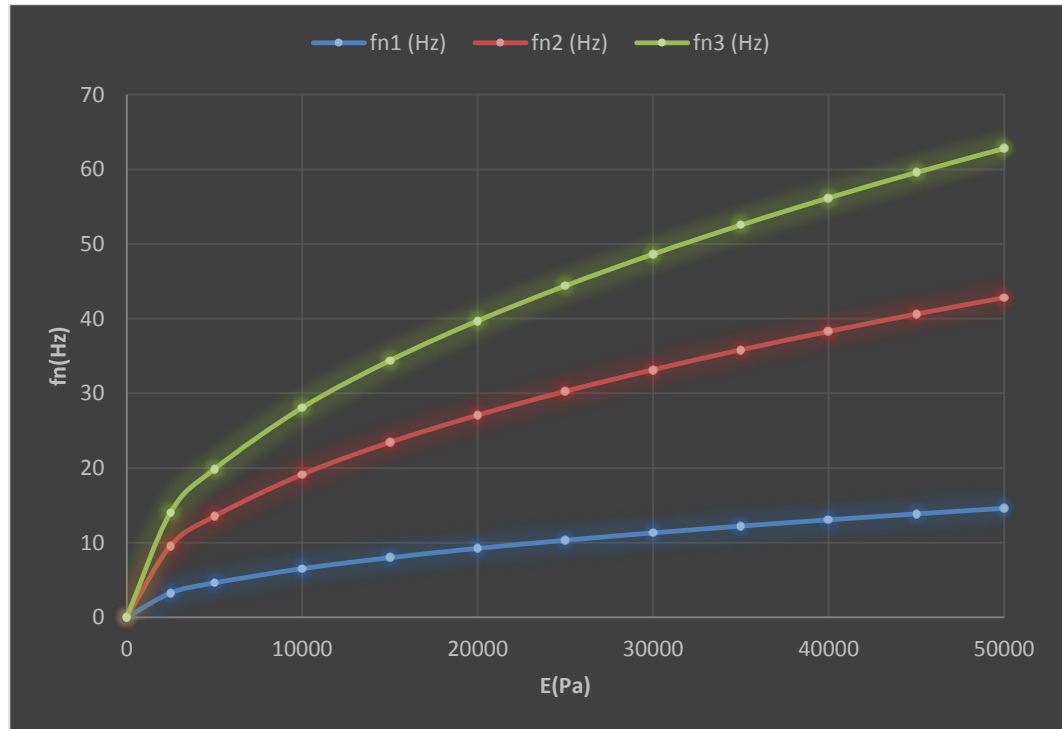


**Figure 5.16: Relationship between E (Pa) and  $f_n$  (Hz) for a healthy tongue model**

The above procedure for determining the natural frequencies for the isolated healthy tongue models using the Abaqus software was repeated for all models. Values for the first, second and third natural frequencies for all healthy tongue models are summarized in Tables 5.11, 5.12 and 5.13; respectively.

The mean values for the natural frequencies are given below each table for the normal control value of  $E = 15$  kPa, as well as for  $E = 25$  kPa for comparison purposes with the obtained results of the isolated uvula models given in section 5.3.2.

**Table 5.11: Values of the first natural frequencies for healthy tongue models**

<b>E(Pa)</b>	<b>Subject 1</b>	<b>Subject 3</b>	<b>Subject 4</b>	<b>Subject 6</b>	<b>Subject 7</b>	<b>Subject 8</b>
2500	3.3	2.8	3.0	2.0	2.7	2.7
5000	4.6	4.0	4.2	2.8	3.8	3.8
10000	6.5	5.6	5.4	4.0	5.4	5.4
15000	8.0	6.9	7.3	4.9	6.6	6.6
20000	9.3	7.9	8.5	5.7	7.7	7.6
25000	10.3	8.9	9.4	6.3	8.6	8.5
30000	11.3	9.7	10.4	6.9	9.4	9.3
35000	12.2	10.5	11.2	7.5	10.1	10.1
40000	13.1	11.2	12.0	8.0	10.8	10.8
45000	13.9	11.9	12.7	8.5	11.5	11.4
50000	14.6	12.5	13.4	9.0	12.1	12.1

Mean  $\pm$  SD =  $6.7 \pm 1.0$  for  $E = 15$  kPa (normal control value)

Mean  $\pm$  SD =  $8.7 \pm 1.3$  for  $E = 25$  kPa

**Table 5.12: Values of the second natural frequencies for healthy tongue models**

<b>E(Pa)</b>	<b>Subject 1</b>	<b>Subject 3</b>	<b>Subject 4</b>	<b>Subject 6</b>	<b>Subject 7</b>	<b>Subject 8</b>
2500	9.6	8.6	9.2	8.0	9.2	9.1
5000	13.5	12.1	12.9	11.3	13.0	12.9
10000	19.1	17.1	18.3	15.9	18.4	18.3
15000	23.4	21.0	22.4	19.5	22.5	22.4
20000	27.1	24.2	25.9	22.5	26.0	25.9
25000	30.3	27.1	28.9	25.2	29.1	28.9
30000	33.2	29.7	31.7	27.6	31.9	31.7
35000	35.8	32.1	34.3	29.8	34.4	34.2
40000	38.3	34.3	36.6	31.9	36.8	36.6
45000	40.6	36.4	38.8	33.8	39.0	38.8
50000	42.8	38.3	40.9	35.6	41.2	40.9

Mean  $\pm$  SD =  $21.9 \pm 1.4$  for  $E = 15$  kPa (normal control value)

Mean  $\pm$  SD =  $28.2 \pm 1.8$  for  $E = 25$  kPa

**Table 5.13: Values of the third natural frequencies for healthy tongue models**

<b>E(Pa)</b>	<b>Subject 1</b>	<b>Subject 3</b>	<b>Subject 4</b>	<b>Subject 6</b>	<b>Subject 7</b>	<b>Subject 8</b>
2500	14.0	13.8	13.3	13.6	14.2	14.4
5000	19.9	19.6	18.9	19.3	20.1	20.3
10000	28.1	27.7	26.7	27.3	28.4	28.8
15000	34.4	33.9	32.6	33.4	34.8	35.2
20000	39.7	39.1	37.7	38.6	40.1	40.7
25000	44.4	43.8	42.1	43.1	44.9	45.5
30000	48.7	47.9	46.2	47.2	49.2	49.8
35000	52.6	51.8	49.9	51.0	53.1	53.8
40000	56.2	55.4	53.3	54.5	56.8	57.5
45000	59.6	58.7	56.6	57.9	60.2	61.0
50000	62.8	61.9	59.6	61.0	63.5	64.3

Mean  $\pm$  SD = 34.1  $\pm$  1.0 for E = 15 kPa (normal control value)

Mean  $\pm$  SD = 44.0  $\pm$  1.2 for E = 25 kPa

## 5.4 Summary for Healthy Airway Models

This section contains the following:

1. Summary of the obtained volumes for the healthy air, uvula and tongue models.
2. Comparisons between the obtained results for the healthy tongue and uvula models; for each subject specific.
3. Comparisons between the obtained results for all healthy uvula models for different subjects.
4. Comparisons between the obtained results for all healthy tongue models for different subjects.
5. Overall conclusion.

### 5.4.1 Summary for Healthy UA Volumes

Volumes for the entire UA, tongue, uvula and air models were summarized in Table 5.14 as well as the percentage that each element occupies to the entire UA volume. The data in this table does not include the values for the tongue volumes for subjects 2 and 5 as they were using mouth retainers and therefore the MRI scanner could not detect accurate images for their tongues, which was explained previously in section 5.3.3.

**Table 5.14: Volumes and percentages to the total UA volume**

<b>Subject ID</b>	<b>Tongue V (mm<sup>3</sup>)</b>	<b>Uvula V (mm<sup>3</sup>)</b>	<b>Air V (mm<sup>3</sup>)</b>	<b>Total V (mm<sup>3</sup>)</b>	<b>%Tongue V</b>	<b>%Uvula V</b>	<b>%Air V</b>
<b>1</b>	73427.4	1240.0	15080.7	89748.1	81.8	1.4	16.8
<b>2</b>	N/A	1039.9	18803.1	N/A	N/A	N/A	N/A
<b>3</b>	81243.6	1348.1	7824.0	90415.7	89.9	1.5	8.7
<b>4</b>	70709.9	1491.8	7880.1	80081.8	88.3	1.9	9.8
<b>5</b>	N/A	1667.0	16979.5	N/A	N/A	N/A	N/A
<b>6</b>	56594.6	1245.71	11064.2	68904.5	82.1	1.8	16.1
<b>7</b>	57131.4	1029.5	10337.6	68498.5	83.4	1.5	15.1
<b>8</b>	60110.4	941.0	10210.0	71261.4	84.4	1.3	14.3
<b>Mean ± SD</b>	66536.2 ± 10097.5	1250.4 ± 248.0	12272.4 ± 4161.6	78151.7 ± 10146.7	85.0 ± 3.4	1.6 ± 0.2	13.5 ± 3.4

These results show that the UA volume ranges from 68498.5-90415.7 mm<sup>3</sup> (78151.7 ± 10146.7 mm<sup>3</sup>), from which the tongue occupies 85.0 ± 3.4%, uvula occupies 1.6 ± 0.2% and the air occupies 13.5 ± 3.4% of the total UA volume. Also, the obtained results show that the minimum air gaps at the rear of the uvula and tongue in the MSP had the range of 5.2 ± 2.8 mm and 7.7 ± 4.2 mm, respectively.

#### 5.4.2 Comparison between Healthy Uvula and Tongue Models

In order to compare between the obtained results for the healthy uvula and tongue models, the figures describing the relationship between  $f_n$  and  $E$  for each subject specific were combined together into one figure. A sample of the combined figures is given in Figure 5.17 for subject 1.

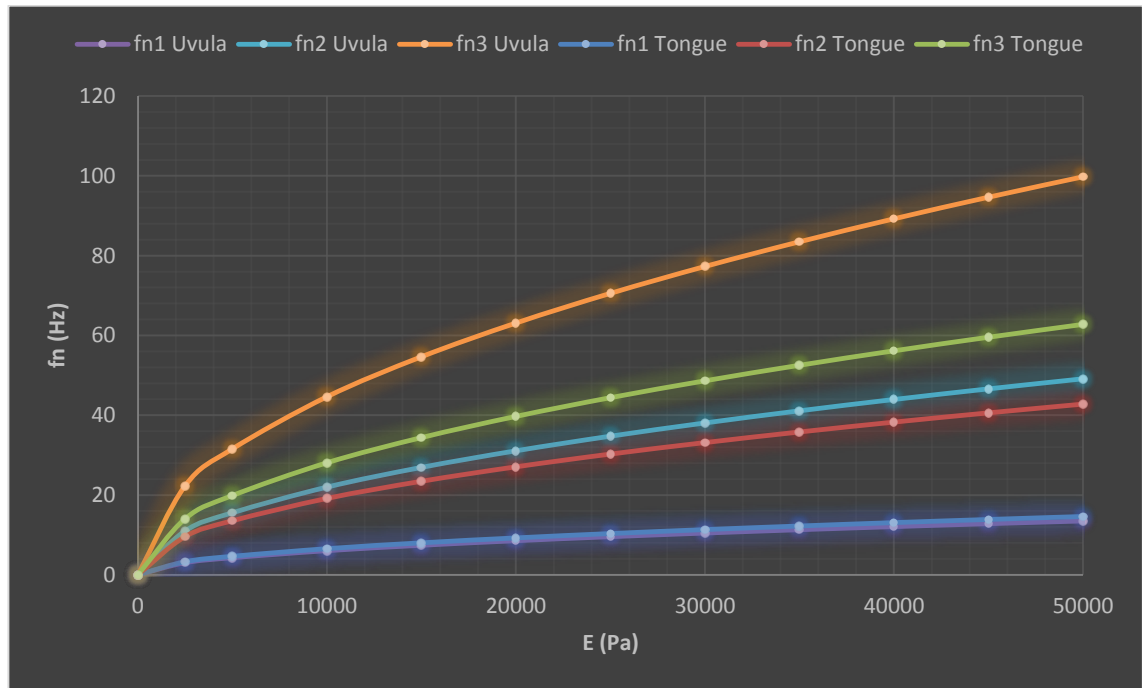


**Figure 5.17: Combined results for healthy uvula and tongue models; subject 1**

The same was done for all the subjects, except subjects 2 and 5 as they were using mouth retainers during the MRI data collection as explained in section 5.3.3. The combined figures for the rest of the subjects are given in appendix B. From these combined figures for each subject specific we conclude that:

1. The first and second natural frequencies for the uvula and tongue models are very close to one another, and fall within the previous findings [497-500, 502].

2. The third natural frequencies for the uvula and tongue are relatively different when compared to the results of the first and second natural frequencies.
3. The used simulation technique yielded excellent results for both the uvula and tongue when compared to one another, as well as when compared to the previous findings [497-500, 502].

#### 5.4.3 Results for All Healthy Uvula Models

Figure 5.18 combines the results of all the healthy uvula models that represent the relationship between  $E$  and  $f_n$ , where the bottom group of line graphs represents the first natural frequencies, the middle group represents the second natural frequencies and the top group of line graphs represents the third natural frequencies.

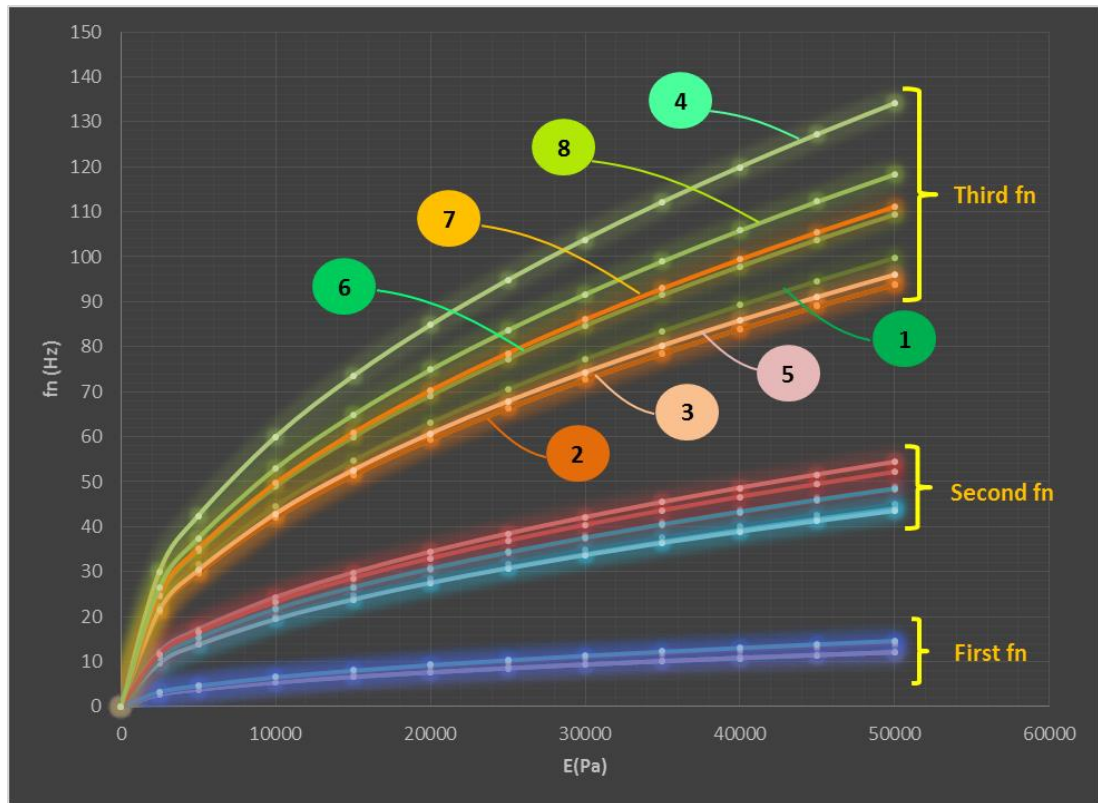


**Figure 5.18: Results for all healthy uvula models**

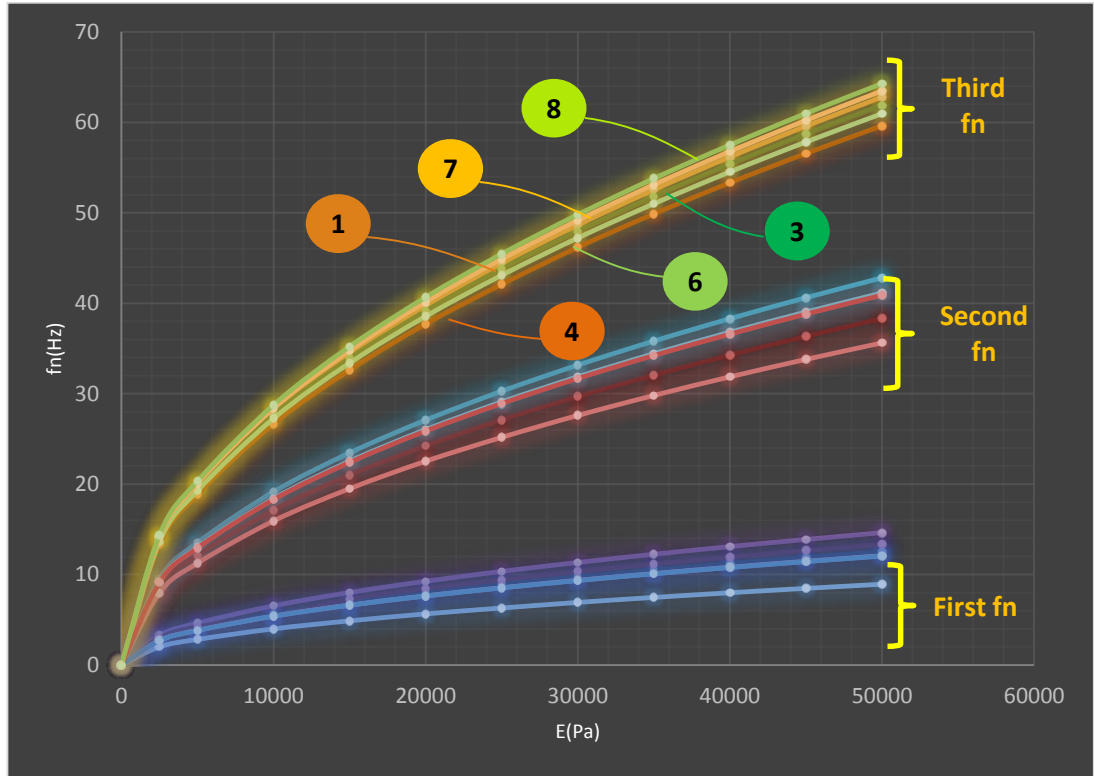
(Numbers on graph indicate subject ID)

Figure 5.18 shows that the first and second natural frequencies for all healthy uvula models are very close to one another, which indicates that the response of the healthy subjects is very close to one another. Also these frequencies fall within the values reported in previous findings [497-500, 502], while the values for the obtained third natural frequencies fall outside the reported values.



#### 5.4.4 Results for All Healthy Tongue Models

Figure 5.19 combines the results of all the healthy tongue models that represent the relationship between  $E$  and  $f_n$ , where the bottom group of line graphs represents the first natural frequencies, the middle group represents the second natural frequencies and the top group of line graphs represents the third natural frequencies.



**Figure 5.19: Results for all healthy tongue models**

(Numbers on graph indicate subject ID)

Figure 5.19 shows that the values for the first and second natural frequencies for all healthy tongue models are very close to one another and fall within the values reported in previous findings [497-500, 502]. The values for the third natural frequency are also very close to one another and fall within these reported values for  $E \leq 30$  kPa. The obtained frequencies for  $E > 30$  kPa have fallen outside the reported range.

#### 5.5 Closure

This chapter investigated the dynamic characteristics of healthy UA models, and presented the results of using the FE methods by using the Abaqus software in determining the dynamic response of the healthy soft tissues. The next chapter will investigate the dynamic response of unhealthy UA models using the Abaqus software. It will also

investigate the interaction between the airflow and the deformations of the UA soft tissues by using the Static Structural Modeller on the ANSYS Workbench to detect the conditions of collapse as well as the effects of the PO on the performance of the UA.

## **CHAPTER 6**

### **Dynamic Characteristics of Unhealthy Upper Airways**

#### **6.1 Introduction**

This chapter explains the recruitment process of the OSA patients for MRI data collection and indicates the exclusion criteria as well as the protocol of collecting the data, section 6.2. It also describes the investigation of the dynamic characteristics of unhealthy models for the soft tissues using the finite element (FE) methods by using the Abaqus software, section 6.3, followed by a summary for the obtained results for the apneic patients in section 6.4. Finally section 6.5 explains the investigation of the CFD modelling for the air models using the CFX Modeller on the ANSYS Workbench to determine the pressure distribution using different turbulence models; and also presents the investigation for airway collapse during inspiration and expiration using one-way FSI modelling by using the Static Structural Modeller on the ANSYS Workbench, as well as the investigation of the effects of using the PO superimposed on the CPAP on the dynamic characteristics of the UA.

#### **6.2 MRI Data Collection**

All study procedures were approved by the ethics committee at the Auckland University of Technology (Ethics application number 13/355) and informed consents were obtained prior to initiation of study procedures (Ethics approval letter, templates for participant information sheet, consent and demographic forms are attached in Appendix C).

##### **6.2.1 Recruiting Subjects**

Fisher & Paykel (F&P) Healthcare has a list of OSA patients on their records as they maintain a pool of volunteers for this purpose. Templates for the participant information sheet (PIS) and consent forms were prepared and sent to the OSA team at F&P who passed these forms on to all OSA patients inviting them to participate in the study. The PIS indicated that subjects were excluded from the study if they were:

- Having metallic implants through their upper airways,
- Using pacemakers,
- Having any UA infection,
- Smokers, and
- Pregnant patients (if applicable) were also excluded.

Interested candidates sent back their signed consent forms, and mutually agreeable times were arranged for an ear, nose and throat (ENT) specialist, Dr Jim Bartley, to examine the interested participants and giving reports about their upper airways.

A screening process was then undertaken to exclude those who are unsuited for the study and to provide the desired population sample variety. The final sample consisted of 10 OSA patients including 7 males and 3 females between the ages of 42 and 66 years. The BMI range for OSA patients was 28.9-61.8 kg/m<sup>2</sup>. The selected participants were notified and mutually agreeable times were arranged to undergo measurements of anthropometric and for the MRI data to be collected, as described below.

### **6.2.2 Anthropometrics**

Body weight was measured to the nearest 0.01 kg using a portable electronic scale (Model 770, Seca, Columbia, MD). Height was measured to the nearest 0.1 cm using a portable stadiometer (Model 225, Seca, Columbia, MD).

### **6.2.3 Data Collection**

MRI data of the UA expanding from the nasopharynx to the hypopharynx were collected and administered by a registered radiographer and took place at The Centre for Advanced Magnetic Resonance Imaging (CAMRI) at The University of Auckland which is accredited by the International Accreditation New Zealand and is an affiliated provider for Southern Cross Healthcare and a health services provider for the Accident Compensation Corporation (ACC). The data were collected according to the following steps:

- Each participant assumed the supine position (during wakefulness) within the MRI scanner and the MRI head coil was then positioned over their head.
- After a suitable settling time, the MRI scanner recorded the geometry of their UA.
- The above procedure was repeated for all participants.

Transverse MRI sequences (axial T1) of 1 mm thickness were collected using 3 Tesla MRI scanner covering the entire pharyngeal airway from the top of the nasal cavity to the bottom of the hypopharynx.

### 6.3 Dynamic Characteristics of Unhealthy Upper Airways

This section describes the construction and simulation of real unhealthy UA models including air and soft tissues (uvula and tongue) for OSA patients. It also provides summaries for the obtained results and holds comparisons between the dynamic characteristics of OSA patients.

#### 6.3.1 Unhealthy UA Models

Twelve patients sent back their signed consent forms, however two of them were excluded from the study as one had to withdraw from the study for personal reasons and another patient was off shore at the time of data collection. Therefore the final sample consisted of 10 participants (7 males and 3 females). The demographic data for the ten OSA participants is summarized in Table 6.1 including the age, gender, weight, height, BMI and ethnicity.

**Table 6.1: Demographic data for OSA patients**

Patient ID	Age (Years)	Gender	Weight (kg)	Height (m)	BMI (kg/m <sup>2</sup> )	Ethnicity
1	43	M	86.0	1.72	29.1	Asian
2	60	M	89.4	1.76	28.9	Caucasian English
3	42	F	180.8	1.71	61.8	NZ European
4	60	M	116.1	1.82	35.1	European
5	54	M	98.9	1.72	33.4	European
6	48	M	113.6	1.71	38.9	White European
7	60	M	117.5	1.81	36.1	NZ European
8	62	F	84.5	1.60	33.0	NZ European
9	66	M	108.8	1.75	35.5	NZ European
10	55	F	99.3	1.71	34.0	NZ European
Mean $\pm$ SD	55.0 $\pm$ 8.2				36.6 $\pm$ 9.4	

The isolated airway models were constructed for all patients from the collected MRI data using 3D-DOCTOR software following the same procedure described in section 5.3.1. Figure 6.1 shows a sample of the resulting unhealthy UA models isolated from the rest of the airway.



**Figure 6.1: Unhealthy UA model isolated from the rest of the airway**

Measurements of the UA were determined including airway volume and air gaps at the rear of the uvula and tongue at the mid-sagittal plane (MSP) using the tools of 3D-DOCTOR software; and are summarized in Table 6.2.

**Table 6.2: UA volume and air gaps for all OSA patients**

Patient ID	Air Volume (mm <sup>3</sup> )	Min. gap rear of tongue at MSP (mm)	Min. gap rear of uvula at MSP (mm)
1	16346.2	7.2	5.4
2	11608.8	6.0	6.6
3	16383.4	10.2	8.4
4	33307.1	7.2	6.6
5	18452.9	8.7	6.3
6	31067.7	10.1	5.0
7	19246.8	6.8	7.2
8	8691.9	7.2	7.5
9	22272.3	12.5	6.8
10	10923.5	6.3	4.5
Mean $\pm$ SD	18830.1 $\pm$ 8172.5	8.2 $\pm$ 2.1	6.4 $\pm$ 1.2

### 6.3.2 Dynamic Characteristics of Unhealthy Uvula Models

Unhealthy uvula models were constructed and simulated using the same procedure described in section 5.3.2. The following material properties were used based on the information reported in the background (Chapter 1) [24]:

- $\rho = 1040 \text{ kg/m}^3$
- $\nu = 0.45$
- $E = 25 \text{ kPa}$  (normal control value)

Simulations were conducted on the Abaqus software for different values of E as described previously in section 5.3.2. Values obtained from 3D-DOCTOR software for the volume of the unhealthy uvula models are summarized in Table 6.3.

**Table 6.3: Volumes of the unhealthy uvula models**

Patient ID	Uvula Volume (mm <sup>3</sup> )
1	1589.5
2	1755.8
3	1870.8
4	1913.2
5	2453.3
6	1893.1
7	2105.9
8	1947.3
9	2086.6
10	1813.5
Mean $\pm$ SD	1942.9 $\pm$ 234.0

### Results for an Apneic Patient

This participant has been using variable pressure CPAP for 6 years, his CPAP is 11-13 Cm H<sub>2</sub>O. The ENT specialist reported that this patient has a deviated nasal septum, narrow UA, very large tongue (Mallampati III) and large tonsils. Airway blockage was observed at the rear of the tongue during the ENT examination. The geometry of the uvula model for this patient is shown in Figure 6.2 and the first three mode shapes for E = 25 kPa (normal control value) are given in Figure 6.3.

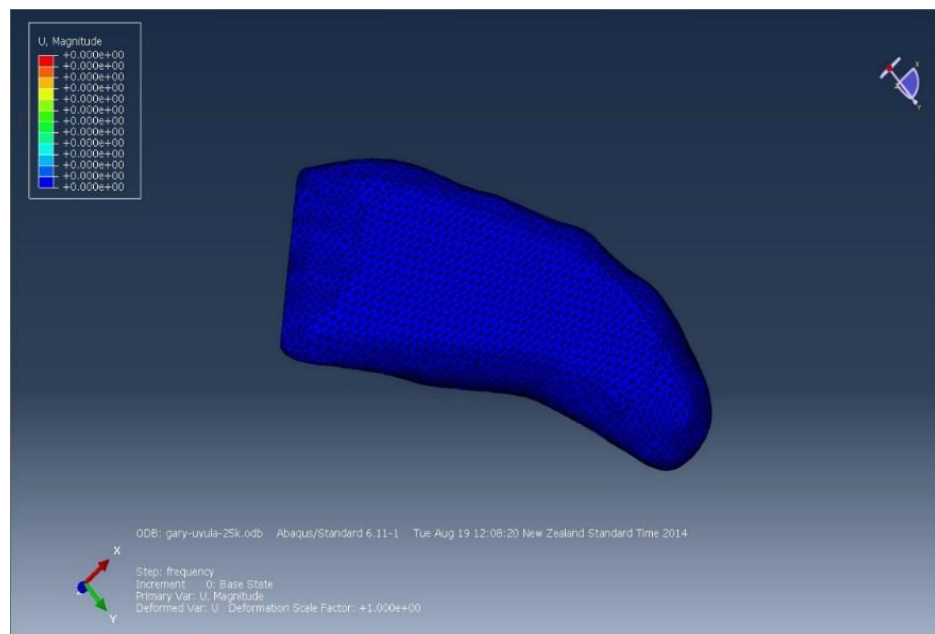
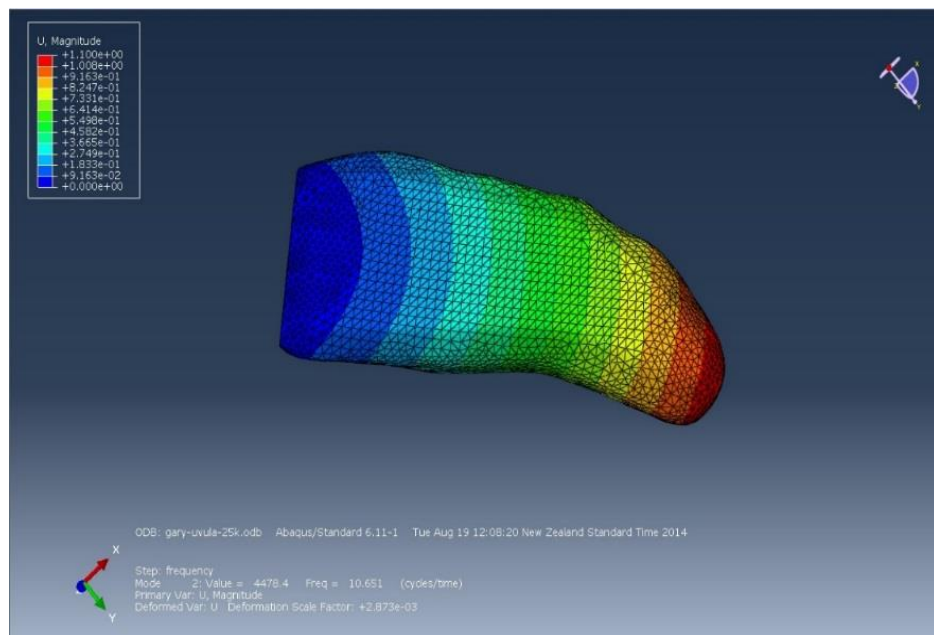
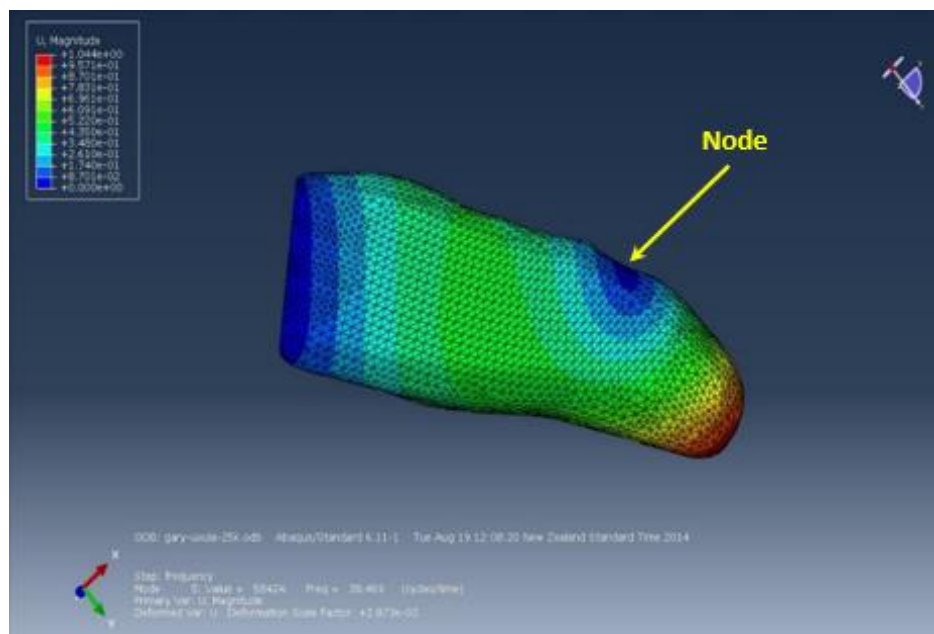


**Figure 6.2: Geometry of an unhealthy uvula model isolated from the airway**

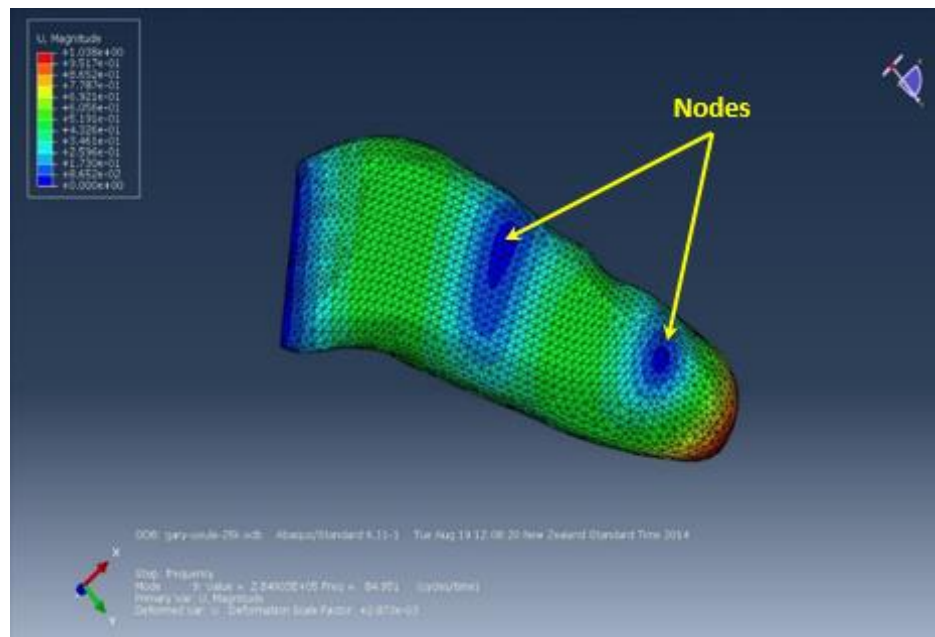


(a) First mode shape



(b) Second mode shape





(c) Third mode shape

**Figure 6.3: Mode shapes for an unhealthy uvula model;  $E = 25$  kPa**

The results for the first three natural frequencies for different values of  $E$  for an unhealthy uvula model are summarized in Table 6.4, and plotted in Figure 6.4.

**Table 6.4: Natural frequencies for an unhealthy uvula for different values of  $E$**

$E$ (Pa)	$f_{n1}$ (Hz)	$f_{n2}$ (Hz)	$f_{n3}$ (Hz)
0	0	0	0
2500	3.4	12.2	26.9
5000	4.8	17.2	38.0
10000	6.7	24.3	53.7
15000	8.3	29.8	65.8
20000	9.5	34.4	76.0
25000	10.7	38.5	85.0
30000	11.7	42.1	93.1
35000	12.6	45.5	100.5
40000	13.5	48.7	107.5
45000	14.3	51.6	114.0
50000	15.1	54.4	120.1

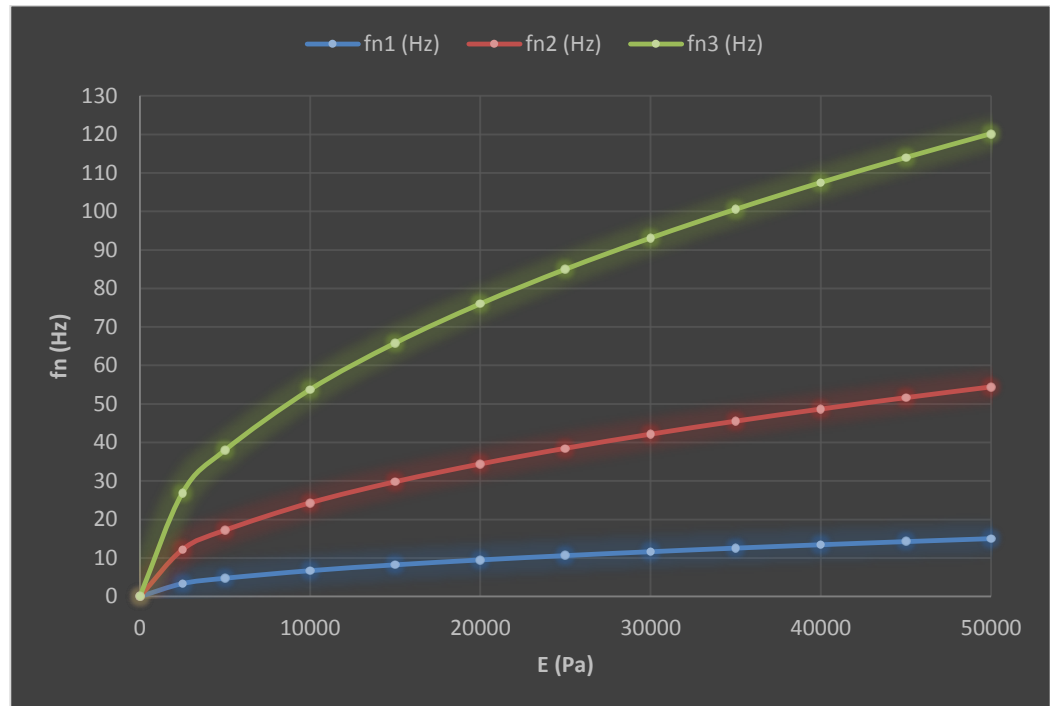


**Figure 6.4: Relationship between E (Pa) and  $f_n$  (Hz) for an unhealthy uvula model**

The procedure for determining the natural frequencies for the unhealthy uvula models using the Abaqus software, which was explained in detail at the beginning of this section (6.3.2), was repeated for all models. Values for the first, second and third natural frequencies for all unhealthy uvula models are summarized in Tables 6.5, 6.6 and 6.7; respectively. Summaries for the reports obtained from the ENT specialist about the UA condition and the current CPAP for all OSA patients are given in Appendix D.

**Table 6.5: Values of the first natural frequencies for all unhealthy uvula models**

<b>E(Pa)</b>	<b>Patient 1</b>	<b>Patient 2</b>	<b>Patient 3</b>	<b>Patient 4</b>	<b>Patient 5</b>	<b>Patient 6</b>	<b>Patient 7</b>	<b>Patient 8</b>	<b>Patient 9</b>	<b>Patient 10</b>
2500	3.4	5.0	2.0	2.5	3.5	2.6	2.5	4.2	3.2	3.2
5000	4.8	7.0	2.8	3.5	4.9	3.7	3.5	5.9	4.6	4.6
10000	6.7	9.9	4.0	5.0	7.0	5.2	4.9	8.4	6.4	6.4
15000	8.3	12.1	4.8	6.1	8.6	6.4	6.0	10.3	7.9	7.9
20000	9.5	14.0	5.6	7.1	9.9	7.4	7.0	11.9	9.1	9.1
25000	10.7	15.7	6.3	7.9	11.0	8.2	7.8	13.3	10.2	10.2
30000	11.7	17.2	6.9	8.7	12.1	9.0	8.6	14.5	11.2	11.1
35000	12.6	18.5	7.4	9.4	13.1	9.8	9.2	15.7	12.1	12.0
40000	13.5	19.8	7.9	10.0	14.0	10.4	9.9	16.8	12.9	12.9
45000	14.3	21.0	8.4	10.6	14.8	11.1	10.5	17.8	13.7	13.6
50000	15.1	22.1	8.8	11.2	15.6	11.7	11.0	18.8	14.4	14.4

Mean  $\pm$  SD = 10.1  $\pm$  2.8 for E = 25 kPa

**Table 6.6: Values of the second natural frequencies for all unhealthy uvula models**

<b>E(Pa)</b>	<b>Patient 1</b>	<b>Patient 2</b>	<b>Patient 3</b>	<b>Patient 4</b>	<b>Patient 5</b>	<b>Patient 6</b>	<b>Patient 7</b>	<b>Patient 8</b>	<b>Patient 9</b>	<b>Patient 10</b>
2500	12.2	14.6	8.5	11.4	10.9	10.2	8.9	13.5	11.5	13.7
5000	17.2	20.6	12.0	16.1	15.4	14.4	12.6	19.1	16.3	19.4
10000	24.3	29.2	17.0	22.8	21.8	20.3	17.8	27.0	23.0	27.5
15000	29.8	35.7	20.9	27.9	26.7	24.9	21.8	33.1	28.1	33.7
20000	34.4	41.2	24.1	32.3	30.9	28.8	25.1	38.2	32.5	38.9
25000	38.5	46.1	26.9	36.1	34.5	32.1	28.1	42.7	36.3	43.5
30000	42.1	50.5	29.5	39.5	37.8	35.2	30.8	46.8	39.8	47.6
35000	45.5	54.6	31.9	42.7	40.8	38.0	33.2	50.5	43.0	51.4
40000	48.7	58.3	34.1	45.6	43.7	40.7	35.5	54.0	46.0	55.0
45000	51.6	61.9	36.1	48.4	46.3	43.1	37.7	57.3	48.7	58.3
50000	54.4	65.2	38.1	51.0	48.8	45.5	39.7	60.4	51.4	61.4

Mean  $\pm$  SD = 36.5  $\pm$  6.4 for E = 25 kPa

**Table 6.7: Values of the third natural frequencies for all unhealthy uvula models**

<b>E(Pa)</b>	<b>Patient 1</b>	<b>Patient 2</b>	<b>Patient 3</b>	<b>Patient 4</b>	<b>Patient 5</b>	<b>Patient 6</b>	<b>Patient 7</b>	<b>Patient 8</b>	<b>Patient 9</b>	<b>Patient 10</b>
2500	26.7	31.1	24.0	28.0	24.7	23.7	20.6	29.4	26.1	34.3
5000	38.0	43.9	34.0	39.6	35.0	33.5	29.1	41.6	36.9	48.5
10000	53.7	62.1	48.1	56.0	49.5	47.4	41.2	58.8	52.2	68.6
15000	65.8	76.1	58.9	68.6	60.6	58.1	50.4	72.0	64.0	84.0
20000	76.0	87.8	68.0	79.2	70.0	67.1	58.2	83.1	73.9	97.0
25000	85.0	98.2	76.0	88.6	78.2	75.0	65.1	92.9	82.6	108.4
30000	93.1	107.5	83.2	97.0	85.7	82.1	71.3	101.8	90.5	118.7
35000	100.5	116.2	89.9	104.8	92.6	88.7	77.0	109.9	97.7	128.3
40000	107.5	124.2	96.1	112.0	98.9	94.8	82.4	117.5	104.5	137.1
45000	114.0	131.7	101.9	118.8	104.9	100.6	87.4	124.7	110.8	145.4
50000	120.1	138.8	107.5	125.3	110.6	106.0	92.1	131.4	116.8	153.3

Mean  $\pm$  SD = 85.0  $\pm$  12.6 for E = 25 kPa

### 6.3.3 Dynamic Characteristics of Unhealthy Isolated Tongue Models

The Isolated unhealthy tongue models for OSA patients were accurately constructed and simulated using the same procedure described in section 5.3.3, where  $\rho = 1040 \text{ kg/m}^3$ ,  $\nu = 0.499$  and  $E = 15 \text{ kPa}$  as the normal control value [24].

Simulations were conducted on the Abaqus software for different values of  $E$  to cover the effects of different ages, races, genders and sleeping positions and/or stages; as discussed in section 5.3.3. Values obtained from 3D-DOCTOR software for the volume of the unhealthy tongue models are summarized in Table 6.8.

**Table 6.8: Volumes of unhealthy tongue models**

Patient ID	Tongue Volume ( $\text{mm}^3$ )
1	126697.7
2	119450.9
3	N/A
4	140334.4
5	141087.3
6	118929.9
7	130563.8
8	104140.1
9	125025.7
10	114629.8
Mean $\pm$ SD	124540.0 $\pm$ 11917.4

The data in Table 6.8 indicates that the tongue volume for patient 3 is not available. This is because the participant was using a mouth retainer and her tongue geometry could not be accurately detected by the MRI scanner, as seen by the highlights in Figure 6.5. Therefore the following results show the outcomes of nine unhealthy tongue models only.



**Figure 6.5: MRI image of the MSP for patient 3**

The geometry of an unhealthy tongue model isolated from the airway is shown in Figure 6.6 and the first three mode shapes are given in Figure 6.7 for  $E = 15 \text{ kPa}$

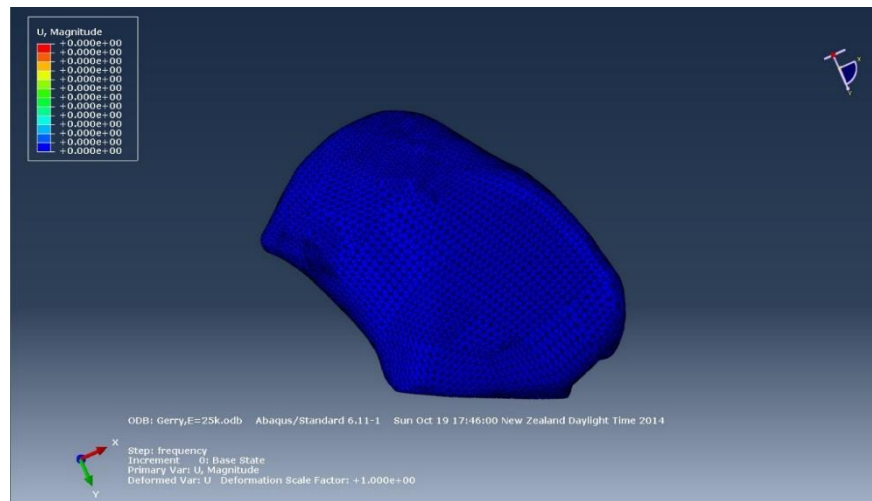
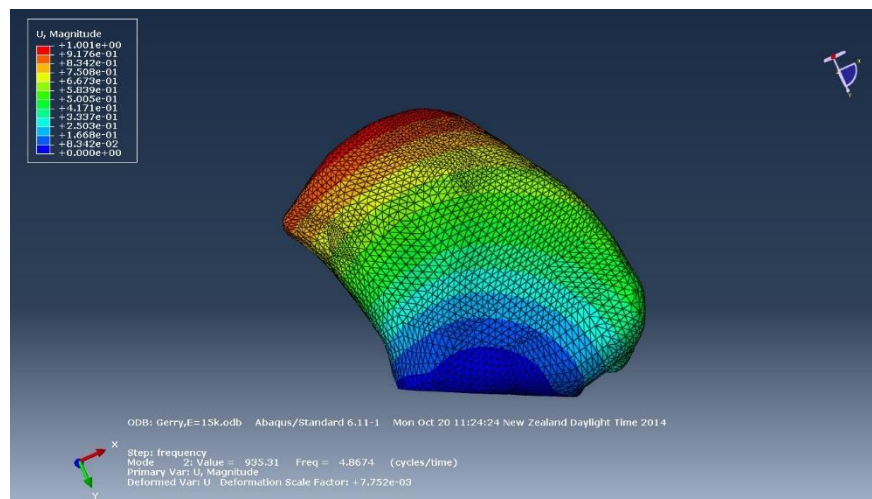
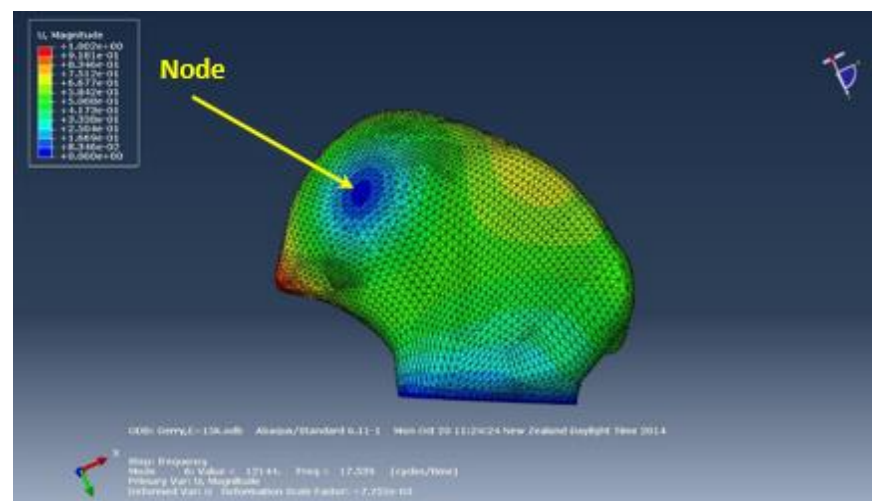


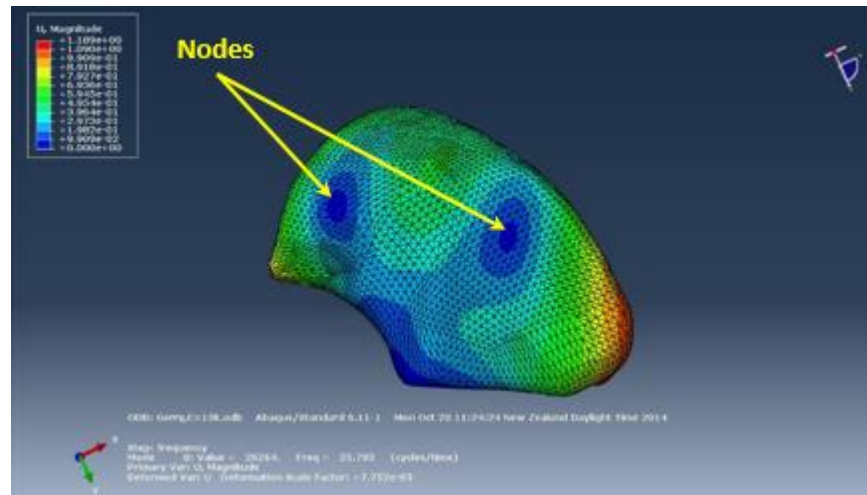
**Figure 6.6: Geometry of an unhealthy tongue model isolated from the airway**



**(a) First mode shape**



**(b) Second mode shape**



(c) Third mode shape

**Figure 6.7: Mode shapes on an unhealthy tongue model;  $E = 15$  kPa**

The results for the first three natural frequencies  $f_n$  for different values of  $E$  for an unhealthy tongue model are summarized in Table 6.9, and plotted in Figure 6.8.

**Table 6.9: Natural frequencies of an unhealthy tongue for different values of  $E$**

$E$ (Pa)	$f_{n1}$ (Hz)	$f_{n2}$ (Hz)	$f_{n3}$ (Hz)
0	0	0	0
2500	2.0	7.2	10.5
5000	2.8	10.1	14.9
10000	4.0	14.3	21.1
15000	4.9	17.5	25.8
20000	5.6	20.3	29.8
25000	6.3	22.6	33.3
30000	6.9	24.8	36.5
35000	7.4	26.8	39.4
40000	8.0	28.6	42.1
45000	8.4	30.4	44.7
50000	8.9	32.0	47.1

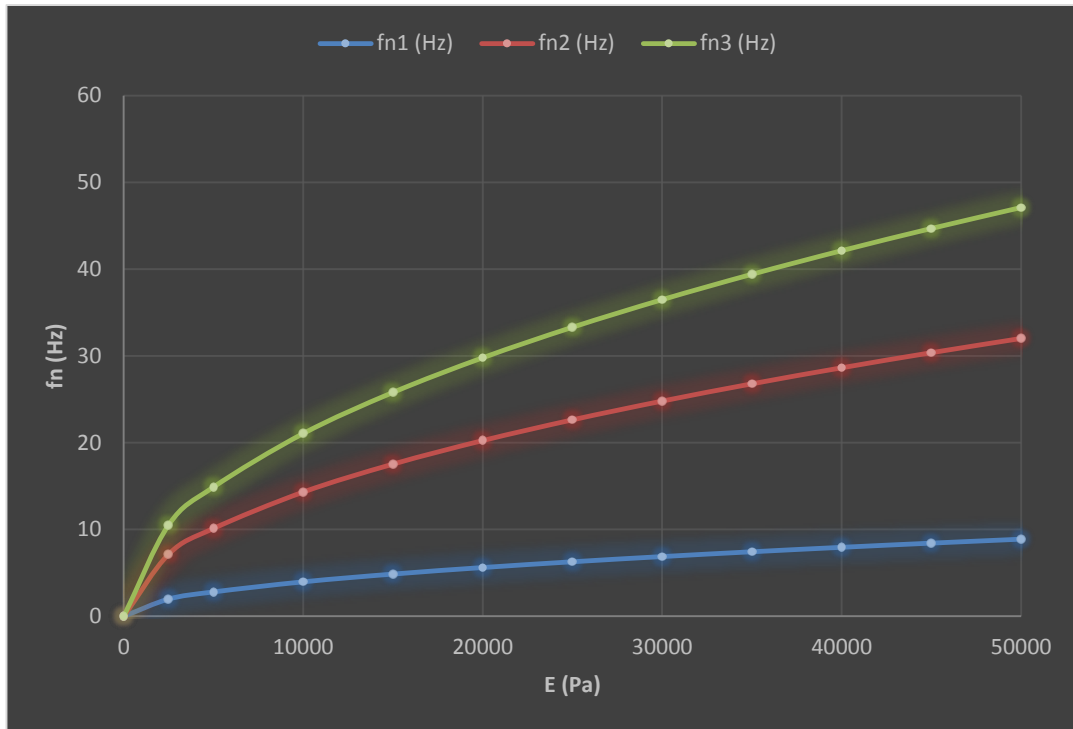


**Figure 6.8: Relationship between E (Pa) and  $f_n$  (Hz) for an unhealthy tongue model**

The procedure for determining the natural frequencies for the isolated unhealthy tongue models using the Abaqus software, which was explained in detail at the beginning of this section (6.3.3), was repeated for all models. Values for the first, second and third natural frequencies for all unhealthy tongue models are summarized in Tables 6.10, 6.11 and 6.12; respectively with the exception of patient 3.

Mean values for the natural frequencies for the unhealthy tongue models are given below each table for the normal control value of  $E = 15$  kPa as well as for  $E = 25$  kPa for the comparison with the obtained results of the isolated uvula models given in section 6.3.2.



**Table 6.10: Values of the first natural frequencies for all unhealthy tongue models**

<b>E(Pa)</b>	<b>Patient 1</b>	<b>Patient 2</b>	<b>Patient 4</b>	<b>Patient 5</b>	<b>Patient 6</b>	<b>Patient 7</b>	<b>Patient 8</b>	<b>Patient 9</b>	<b>Patient 10</b>
2500	2.0	2.3	2.0	2.2	2.4	1.9	1.9	2.2	2.4
5000	2.8	3.2	2.8	3.1	3.4	2.6	2.8	3.2	3.4
10000	4.0	4.5	4.0	4.4	4.9	3.7	3.9	4.5	4.8
15000	4.9	5.5	4.9	5.4	6.0	4.6	4.8	5.5	5.9
20000	5.6	6.4	5.6	6.2	6.9	5.3	5.5	6.3	6.8
25000	6.3	7.1	6.3	6.9	7.7	5.9	6.1	7.1	7.6
30000	6.9	7.8	6.9	7.6	8.4	6.4	6.7	7.7	8.3
35000	7.9	8.4	7.5	8.2	9.1	7.0	7.3	8.3	9.0
40000	8.0	9.1	8.0	8.8	9.7	7.4	7.8	8.9	9.6
45000	8.4	9.6	8.5	9.3	10.3	7.9	8.2	9.5	10.2
50000	8.9	10.1	8.9	9.8	10.9	8.3	8.7	10.0	10.8

Mean  $\pm$  SD = 5.3  $\pm$  0.5 for E = 15 kPa and 6.8  $\pm$  0.7 for E = 25 kPa

**Table 6.11: Values of the second natural frequencies for all unhealthy tongue models**

<b>E(Pa)</b>	<b>Patient 1</b>	<b>Patient 2</b>	<b>Patient 4</b>	<b>Patient 5</b>	<b>Patient 6</b>	<b>Patient 7</b>	<b>Patient 8</b>	<b>Patient 9</b>	<b>Patient 10</b>
2500	7.2	7.2	6.9	6.7	7.8	6.7	7.5	7.4	8.1
5000	10.1	10.2	9.7	9.5	11.0	9.5	10.6	10.5	11.5
10000	14.3	14.4	13.8	13.4	15.5	13.5	15.0	14.9	16.2
15000	17.5	17.7	16.9	16.4	19.0	16.5	18.4	18.2	19.9
20000	20.3	20.4	19.5	19.0	21.9	19.0	21.2	21.1	23.0
25000	22.6	22.8	21.8	21.2	24.5	21.3	23.7	23.5	25.7
30000	24.8	25.0	23.9	23.2	26.8	23.3	26.0	25.8	28.1
35000	26.8	27.0	25.8	25.1	29.0	25.2	28.0	27.9	30.4
40000	28.6	28.8	27.5	26.8	31.0	26.9	30.0	29.8	32.5
45000	30.4	30.6	29.2	28.4	32.9	28.6	31.8	31.6	34.4
50000	32.0	32.2	30.8	30.0	34.6	30.1	33.5	33.3	36.3

Mean  $\pm$  SD = 17.8  $\pm$  1.2 for E = 15 kPa and 23.0  $\pm$  1.5 for E = 25 kPa

**Table 6.12: Values of the third natural frequencies for all unhealthy tongue models**

<b>E(Pa)</b>	<b>Patient 1</b>	<b>Patient 2</b>	<b>Patient 4</b>	<b>Patient 5</b>	<b>Patient 6</b>	<b>Patient 7</b>	<b>Patient 8</b>	<b>Patient 9</b>	<b>Patient 10</b>
2500	10.5	10.6	11.7	11.2	13.4	11.8	11.1	11.3	12.0
5000	14.9	14.9	16.6	15.8	18.9	16.7	15.7	16.0	17.0
10000	21.1	21.1	23.4	22.3	26.7	23.7	22.1	22.6	24.0
15000	25.8	25.8	28.7	27.4	32.8	29.0	27.1	27.7	29.4
20000	29.8	29.8	33.1	31.6	37.8	33.4	31.3	31.9	33.9
25000	33.3	33.4	37.0	35.3	42.3	37.4	35.0	35.7	38.0
30000	36.5	36.5	40.6	38.7	46.3	41.0	38.3	39.1	41.6
35000	39.4	39.5	43.8	41.8	50.0	44.2	41.4	42.3	44.9
40000	42.1	42.2	46.8	44.7	53.5	47.3	44.3	45.2	48.0
45000	44.7	44.7	49.7	47.4	56.7	50.2	47.0	47.9	50.9
50000	47.1	47.2	52.4	49.9	59.8	52.9	49.5	50.5	53.7

Mean  $\pm$  SD = 28.2  $\pm$  2.1 for E = 15 kPa and 36.4  $\pm$  2.8 for E = 25 kPa

## **6.4 Summary for Unhealthy Airway Models**

This section contains the following:

1. Summary of the obtained volumes for the unhealthy air, uvula and tongue models.
2. Comparisons between the obtained results for the unhealthy tongue and uvula models; for each subject specific.
3. Comparisons between the obtained results for all unhealthy uvula models for different subjects.
4. Comparisons between the obtained results for all unhealthy tongue models for different subjects.
5. Overall conclusion.

### **6.4.1 Summary for Unhealthy UA Volumes**

Volumes for the entire unhealthy UA, tongue, uvula and air models were summarized in Table 6.13 as well as the percentage which each element occupies of the total UA volume. The data in this table does not include the value for the tongue volume of patient 3 as she was using a mouth retainer and therefore the MRI scanner could not detect accurate images for her tongues, this was explained previously in section 6.3.3.

The obtained results in Table 6.13 for OSA patients show that their total UA volume have the range of 114779.3-175554.7 mm<sup>3</sup> ( $145592.8 \pm 17341.6$  mm<sup>3</sup>) from which the tongue occupies  $85.9 \pm 4.2\%$ , uvula occupies  $1.34 \pm 0.18\%$  and air occupies only  $12.8 \pm 4.3\%$  of the total UA volume. Also, the obtained results show that the range of the minimum air gaps at the rear of the uvula and tongue in the MSP were  $6.4 \pm 1.2$  mm and  $8.2 \pm 2.1$  mm, respectively.

**Table 6.13: Volumes and percentages of the total UA volume, OSA patients**

Patient ID	Tongue V (mm <sup>3</sup> )	Uvula V (mm <sup>3</sup> )	Air V (mm <sup>3</sup> )	Total V (mm <sup>3</sup> )	%Tongue V	%Uvula V	%Air V
<b>1</b>	126697.7	1589.5	16346.2	144633.4	87.6	1.1	11.3
<b>2</b>	119450.9	1755.8	11608.8	132815.5	89.9	1.3	8.8
<b>3</b>	N/A	1870.8	16383.4	N/A	N/A	N/A	N/A
<b>4</b>	140334.4	1913.2	33307.1	175554.7	79.9	1.1	19.0
<b>5</b>	141087.3	2453.3	18452.9	161993.5	87.1	1.5	11.4
<b>6</b>	118929.9	1893.1	31067.7	151890.7	78.3	1.2	20.5
<b>7</b>	130563.8	2105.9	19246.8	151916.5	85.9	1.4	12.7
<b>8</b>	104140.1	1947.3	8691.9	114779.3	90.7	1.7	7.6
<b>9</b>	125025.7	2086.6	22272.3	149384.6	83.7	1.4	14.9
<b>10</b>	114629.8	1813.5	10923.5	127366.8	90.0	1.4	8.6
<b>Mean ± SD</b>	124540.0 ± 11917.4	1942.9 ± 234.0	18830.1 ± 8172.5	145592.8 ± 17341.6	85.9 ± 4.2	1.3 ± 0.2	12.8 ± 4.3

### 6.4.2 Comparison between Unhealthy Uvula and Tongue Models

In order to compare between the obtained results for the unhealthy uvula and tongue models, the figures describing the relationship between  $f_n$  and  $E$  for each patient specific are combined together into one figure. A sample of the combined figures is given in Figure 6.9 for patient 1.

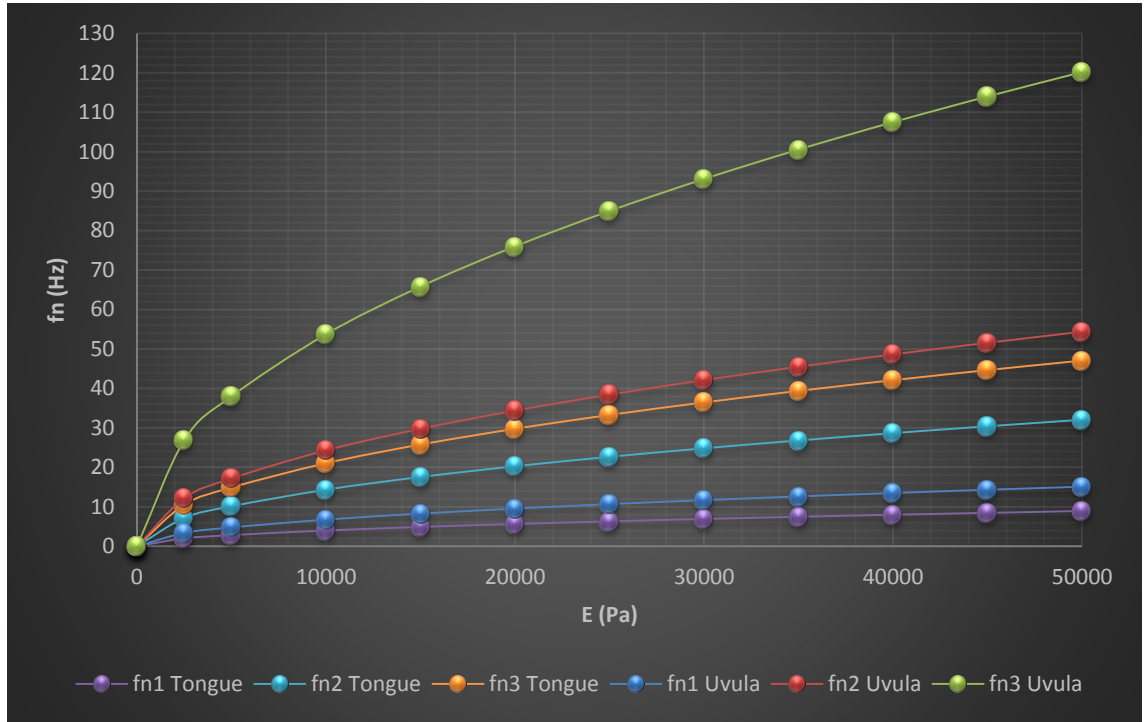


**Figure 6.9: Combined figure for unhealthy uvula and tongue models; patient 1**

The same was done for all the patients, with the exception of patient 3 who was using a mouth retainer and consequently no tongue model could be constructed for her, as explained in section 6.3.3. The combined figures for the rest of the patients are given in appendix D, from which we have concluded the following for each patient specific:

1. The first natural frequencies for the unhealthy uvula and tongue models are very close to one another.
2. The second natural frequencies for the unhealthy uvula and tongue models are close to one another but not as close as the results obtained from the healthy models.
3. The third natural frequencies for the unhealthy uvula and tongue are relatively different.
4. The first and second natural frequencies fall within the reported values in previous findings [497-500, 502].

### 6.4.3 Results for All Unhealthy Uvula Models

Figure 6.10 combines all the results for the unhealthy uvula models which represent the relationship between  $E$  and  $f_n$  for all unhealthy uvula models. The bottom group of line graphs represents the first natural frequencies, the middle group represents the second natural frequencies and the top group of line graphs represents the third natural frequencies.

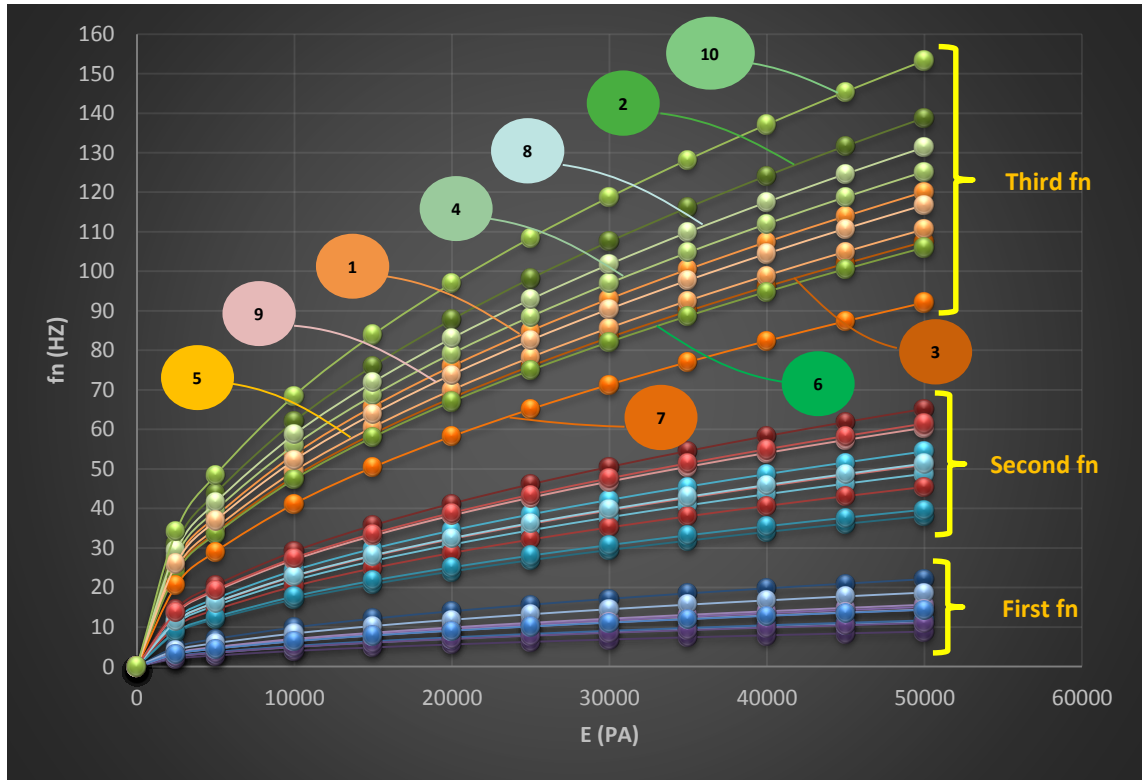


**Figure 6.10: Results for all unhealthy uvula models**

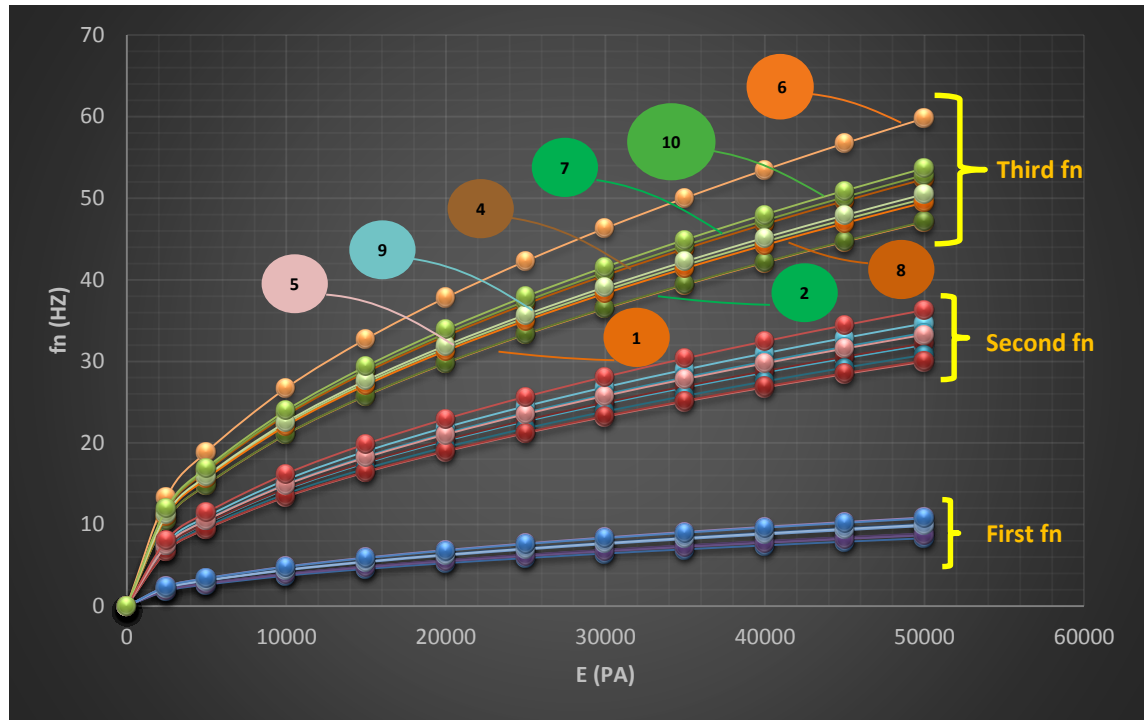
(Numbers on graph indicate patient ID)

Figure 6.10 shows that the values for the first natural frequency for all the patients are very close to one another and fall within the values reported in the previous findings [497-500, 502], the same applies to most of the obtained values for the second natural frequency but they are not as close to one another; while most of the obtained values for the third natural frequencies fall outside the reported values.

### 6.4.4 Results for All Unhealthy Tongue Models

Figure 6.11 combines all the results for the unhealthy tongue models which represent the relationship between  $E$  and  $f_n$  for all the unhealthy tongue models. The bottom group of line graphs represents the first natural frequencies, the middle group

represents the second natural frequencies and the top group of line graphs represents the third natural frequencies



**Figure 6.11: Results for all unhealthy tongue models**

(Numbers on graph indicate patient ID)

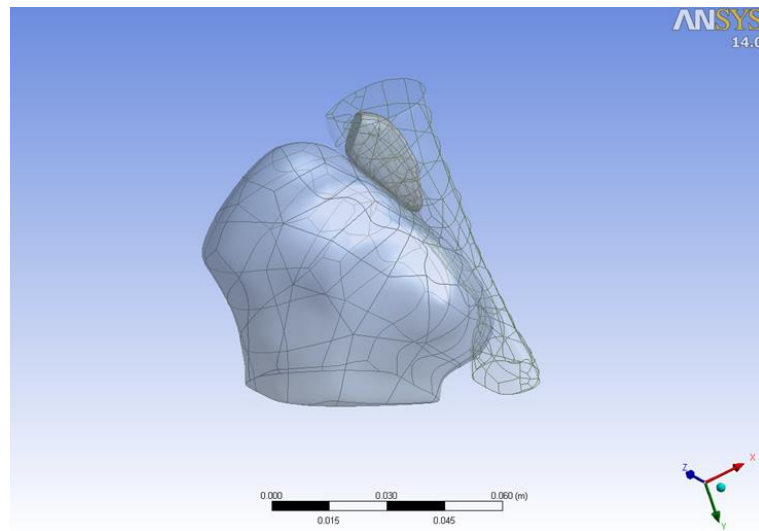
Figure 6.10 shows that the values for the first and second natural frequencies for all the unhealthy tongue models are very close to one another and fall within the values reported in the previous findings [497-500, 502]. The values for the third natural frequency are also very close to one another and fall within these reported values for  $E \leq 35$  kPa. Some of the obtained frequencies for  $E > 35$  kPa have fallen outside the reported range.

## 6.5 One Way Fluid-Structure Interaction (FSI)

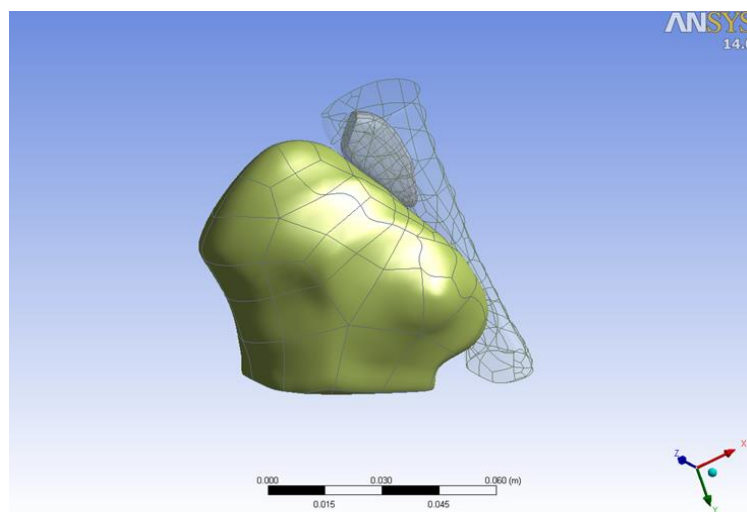
This section investigates the interaction between the airflow through the UA and the deformations of the soft tissues by following the one-way FSI modelling procedure given in section 3.6.

The geometries of the constructed UA models were very complex and contain many irregular surfaces, and could not be successfully imported into the ANSYS DM. Therefore, in order to study the interaction between the airflow and the soft tissues, a simplified UA model that can be easily imported into the ANSYS DM was designed using the collected MRI data of an apneic patient by using 3D-DOCTOR software. This

geometry of the simplified model is still very close to the real upper airway. The geometry of the tongue and uvula models remained the same and only the air cavity was slightly simplified as shown in Figure 6.12.

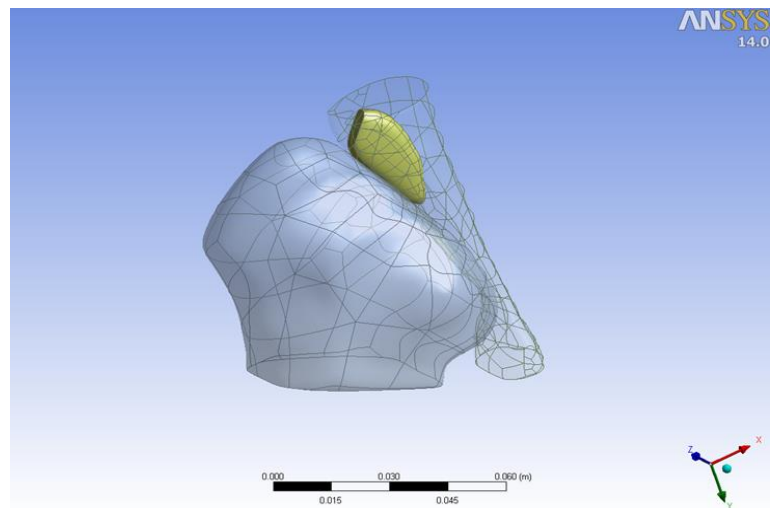


(a)

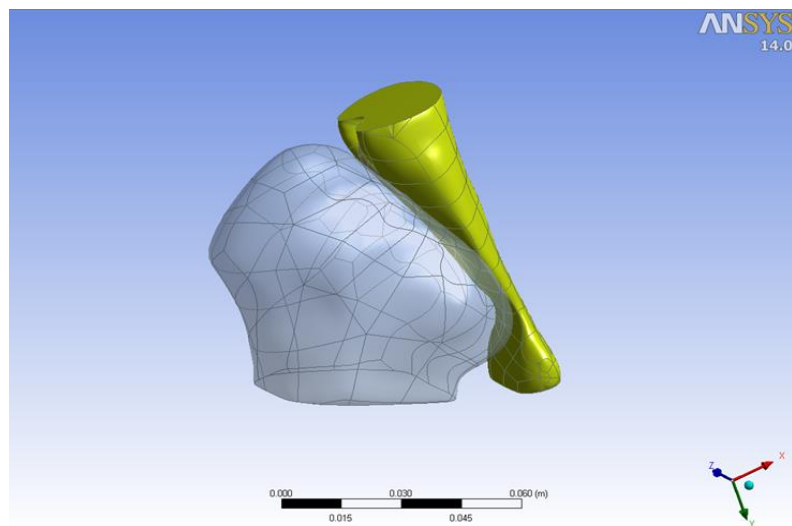


(b)

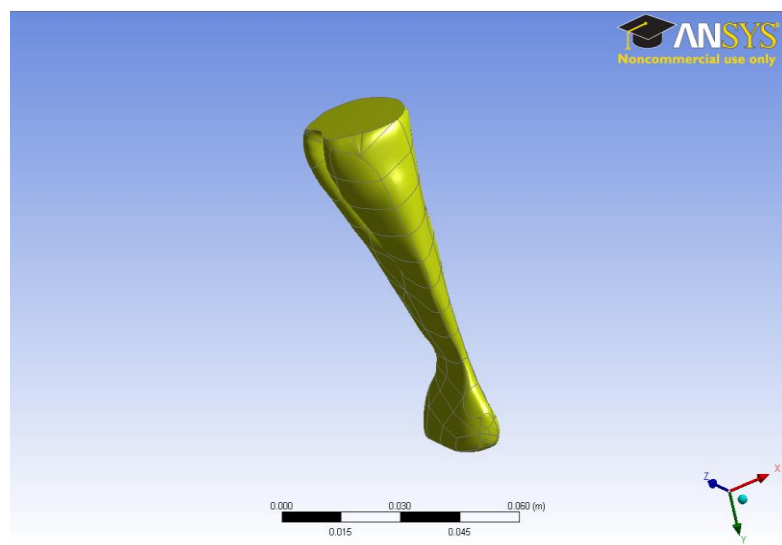




(c)



(d)



(e)

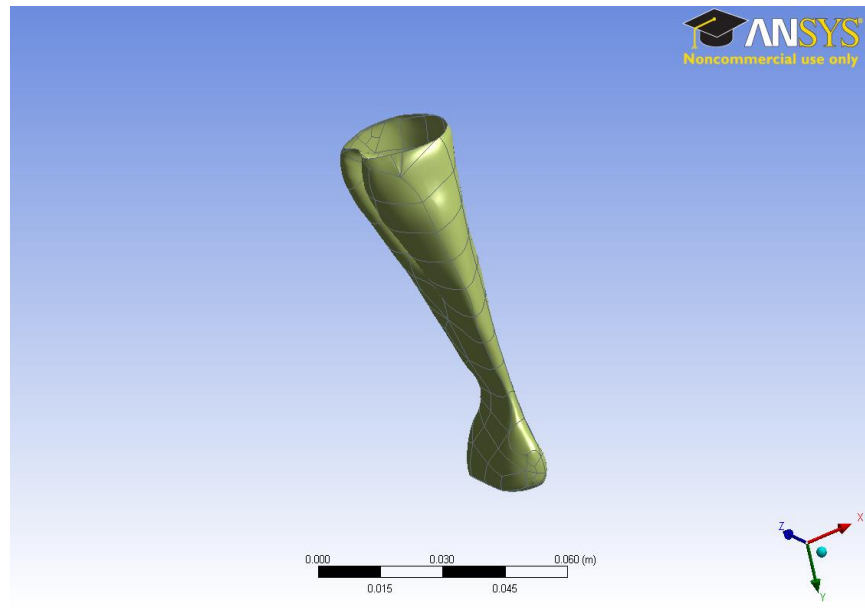
**Figure 6.12: (a) Complete UA, (b) Tongue, (c) Uvula, (d) & (e) Air**

Figure 6.12, (e) shows the simplified air model which is solved by the CFD methods using the Fluid Flow (CFX) Modeller on the ANSYS Workbench. The FSI method on the ANSYS Workbench can investigate the interaction between two models only, however in this study the region of interest in the UA contains three models, the air, the uvula and the tongue; therefore the soft tissues had to be replaced with one material that can produce the deformations of those tissues. By investigating the available materials on the engineering data on the ANSYS Workbench, we have found a rubber material which has very close properties to those of the soft tissues as well as having a hyper elastic behaviour to produce the expected deformations of the soft tissues when excited by the breath cycle. The properties for the rubber material are:

- Density:  $\rho = 1000 \text{ kg/m}^3$
- Temperature:  $T = 38 \text{ }^\circ\text{C}$
- Hyper-elastic behaviour: Mooney-Rivlin 2 Parameter, having an incompressibility parameter of  $1.212\text{E-}09 \text{ Pa}^{-1}$ , material constants  $C_{10} = 1.5\text{E+}05 \text{ Pa}$  and  $C_{01} = 15000 \text{ Pa}$ . These material constants are related to the Shear Modulus ( $\mu$ ) by the relationship :

$$\mu = 2(C_{01} + C_{10}) \quad (6.1)$$

Therefore, the soft tissues were replaced by a rubber enclosure (duct) that surrounds the UA model and has the exact internal geometry as the UA model. Simulations were then conducted for different thicknesses of the rubber enclosure by using the one-way FSI method using the Static Structural-Mechanical Modeller on the ANSYS Workbench. This is after importing the obtained pressure distributions from the CFX Modeller to determine the interaction between the airflow and the deformations of the soft tissues (rubber enclosure), as previously described in section 3.6, and explained in detail below. The best results were obtained when a 1 mm thickness rubber duct was used, Figure 6.13.



**Figure 6.13: 1 mm thickness rubber enclosure**

The UA model was imported to the CFX-Meshing to perform meshing by using CFD preference and fine relevance centre was selected with a minimum edge length of  $8.56 \times 10^{-5}$  m. The resulting meshing for the UA model is shown in Figure 6.14 by using Automatic meshing method.

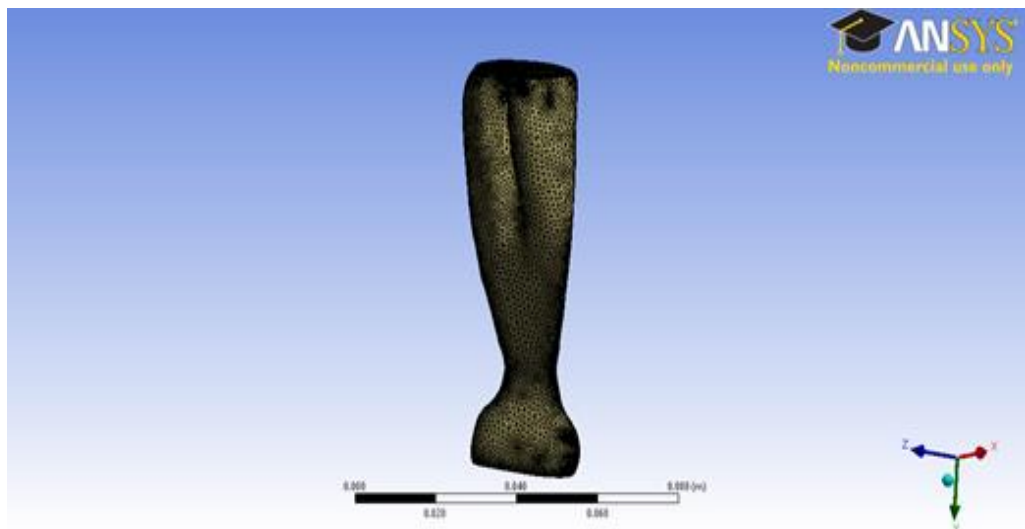


**Figure 6.14: Meshing for the UA model**

The meshing quality for the UA model was validated by the skewness of the meshing, and was found to have an acceptable range of  $6.6 \times 10^{-4}$ -0.938, as shown in Figure 6.15. It is clear that most of the produced UA meshing have a skewness of less than 0.5 which is considered to be a very good meshing quality based on the list described at the end of section 3.7. The number of nodes and elements were 74384 and 389611, respectively.

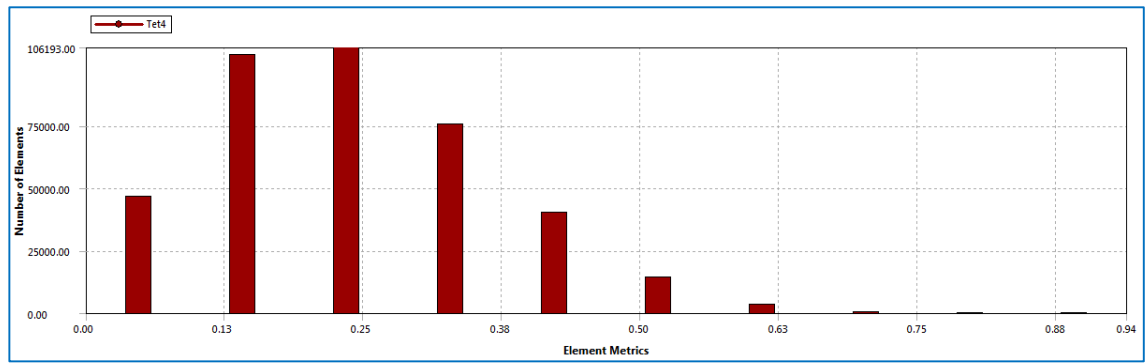


**Figure 6.15: Skewness of the UA meshing**

The meshed UA model was then imported into the CFX-Pre Modeller on the ANSYS Workbench to prepare the solution setup. The material was set to “air ideal gas” with a reference pressure of 1 atm, where the RANS k- $\epsilon$  turbulence model was initially selected.

The rubber duct was then meshed by the Static Structural-Mechanical Modeller on the ANSYS Workbench using mechanical preference and fine relevance centre, with a minimum edge length of  $8.56 \times 10^{-5}$  m. The resulting meshing for the rubber duct model is shown in Figure 6.16 using Quadrilateral meshing method, and Quad/Tri for the free faces.

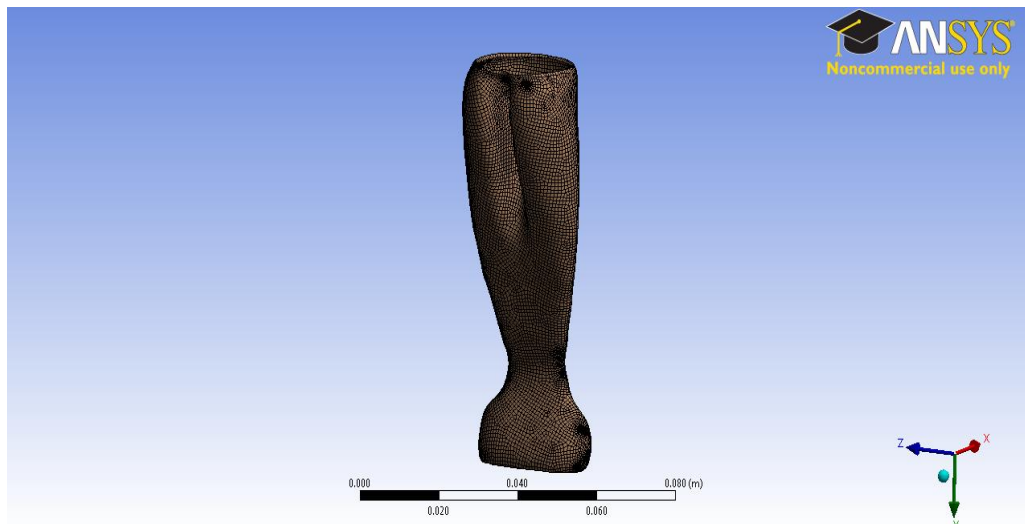


**Figure 6.16: Rubber duct meshing**

The meshing quality for the rubber duct was validated by the skewness of the meshing and was found to have an acceptable range of  $3.05 \times 10^{-5}$ -0.83, as shown in Figure 6.17. It is clear that most of the produced meshing for the rubber duct have a skewness less than

0.25 which is considered to be an excellent meshing quality based on the list described at the end of section 3.7. The number of nodes and elements were 13948 and 13917, respectively.

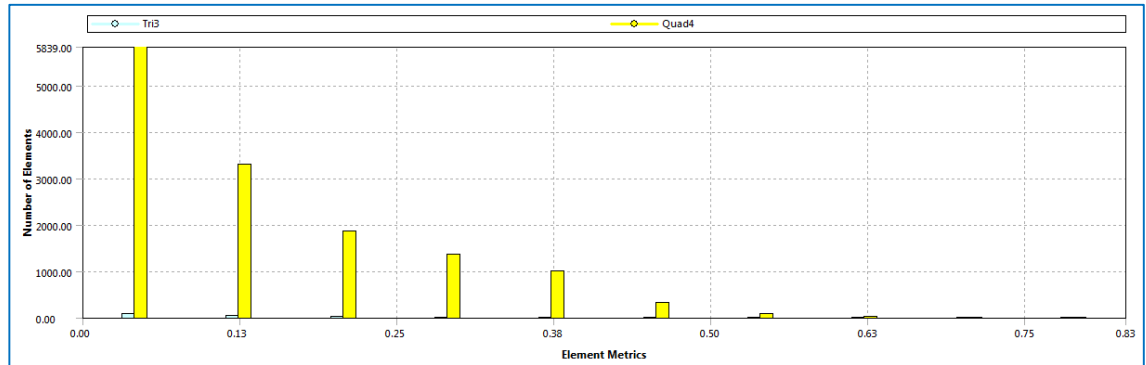


**Figure 6.17: Skewness of the rubber duct meshing**

Many simulations were conducted during inspiration and expiration with different boundary conditions until the UA collapse occurred in both breathing phases (inspiration and expiration). Based on the outcomes of previous studies, the inspiratory esophageal pressure ranges from -25 to -35 Cm H<sub>2</sub>O during the apneic events [25], and the pharyngeal pressure ranges from -5 to 5 Cm H<sub>2</sub>O for the healthy subjects and -14 to 15 Cm H<sub>2</sub>O for OSA patients [551]. In another study, the esophageal pressure was reported to range between -30 and 5 Cm H<sub>2</sub>O [552]. Thus, the boundary conditions were chosen to fulfil these values.

### 6.5.1 Results from RANS k-ε Turbulence Model

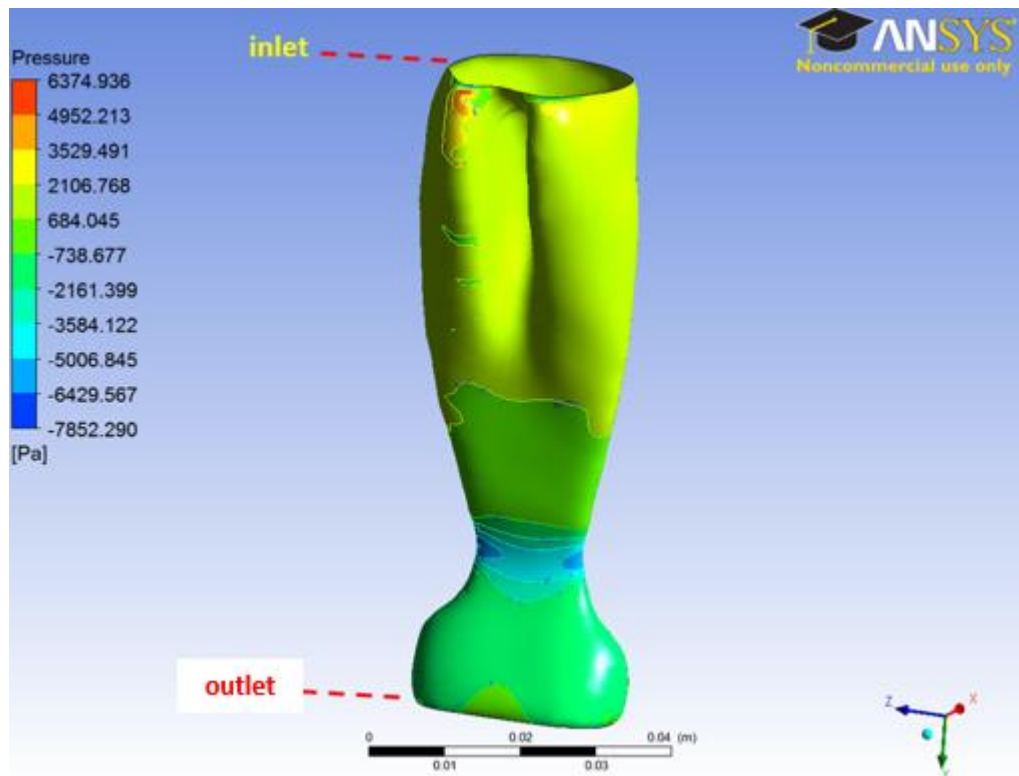
Simulations were conducted during the expiratory and inspiratory breathing phases as described below.

#### (I) Inspiration

After many simulations using different boundary conditions at the inlet and the outlet, collapse was detected during inspiration at the rear of the tongue when:

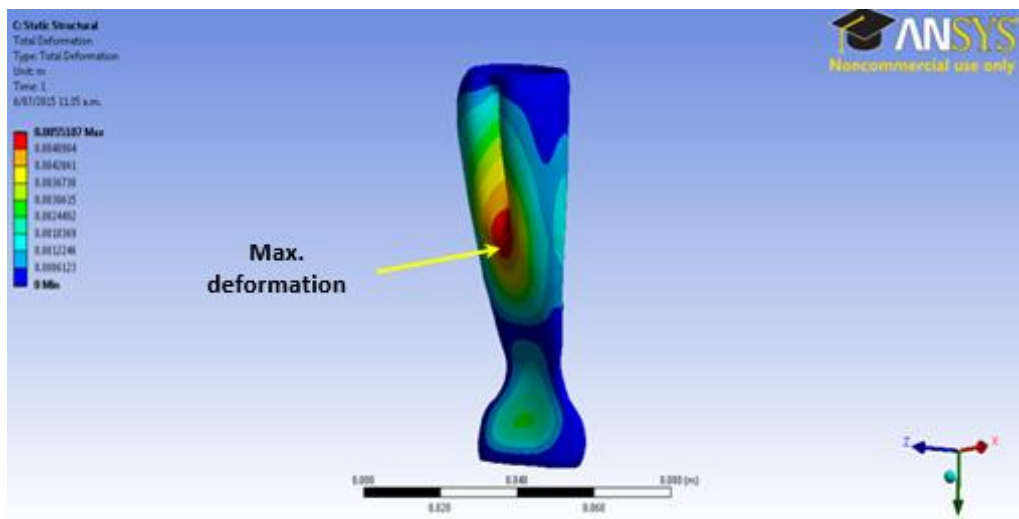
$$P_{in} = 0.9 \text{ kPa} \approx 9 \text{ Cm H}_2\text{O}, \text{ and } P_{out} = -0.8 \text{ kPa} \approx -8 \text{ Cm H}_2\text{O}$$

Figure 6.18 shows the resulting UA pressure distribution during the inspiratory breathing phase under the indicated boundary conditions.

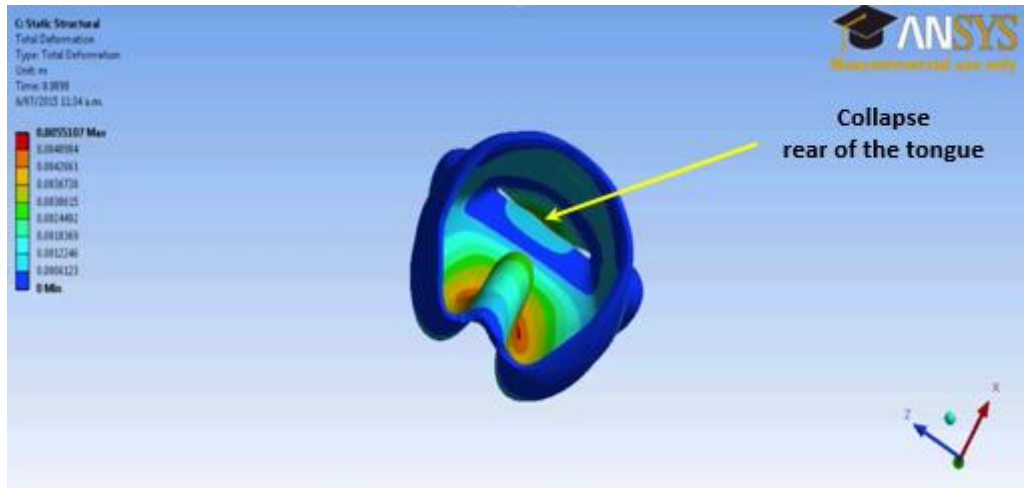


**Figure 6.18: UA pressure distribution during inspiration**

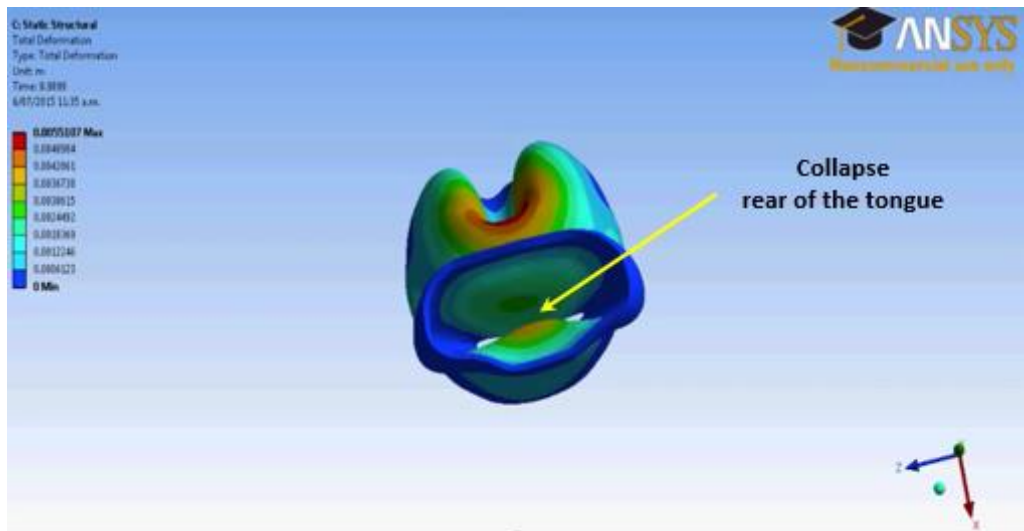
The obtained pressure distribution was then imported to the Static Structural-Mechanical Modeller on the ANSYS Workbench to determine the interaction between the airflow and the enclosure. Figure 6.19 shows the detected deformations of the rubber enclosure, where the UA collapse was detected at the rear of the tongue.



**(a)**



(b)



(c)

**Figure 6.19: Deformations and collapse of the rubber enclosure during inspiration  
(a) front, (b) top and (c) bottom views**

The maximum deformation was found to be 5.5 mm at the rear of the uvula as coloured in red in Figure 6.19 (a) and collapse was detected at the rear of the tongue which agrees with the previous findings which reported that the entering pressurized air during inspiration pushes the uvula away from the airway walls and the airway collapses at the rear of the tongue [24].

Other simulations were conducted to investigate the effects of the pressure oscillations (PO) superimposed on the CPAP for the same aforementioned boundary conditions at the inlet and the outlet. The PO were applied at the inlet according to the following equations:

$$P_{in} = 0.8 + 0.1 \sin(\omega t) \text{ kPa} \quad (6.2)$$

$$\omega = 2\pi f \text{ rad/s}, f = 40 \text{ Hz} \quad (6.3)$$

Figures 6.20 and 6.21 show the resulting UA pressure distribution and the deformations of the rubber enclosure, respectively under the effect of the PO during inspiration.

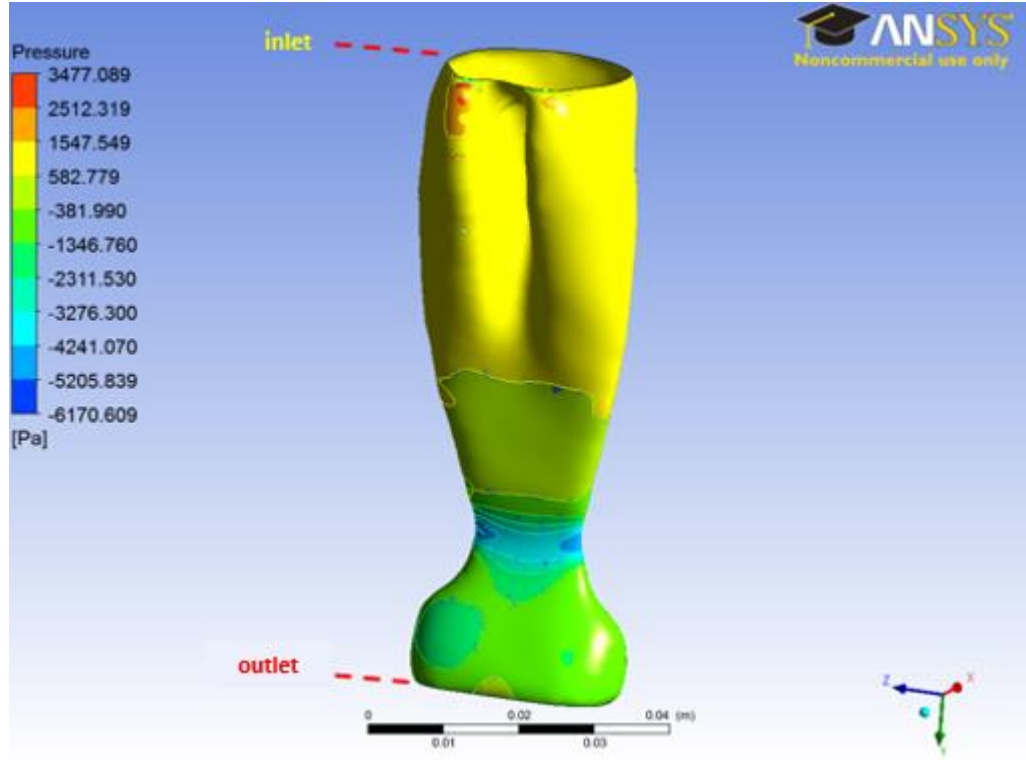
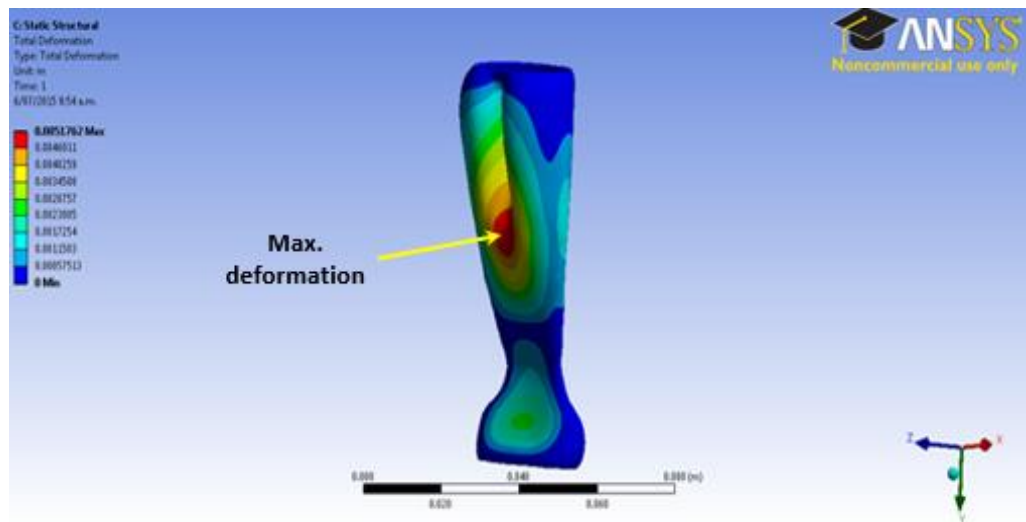
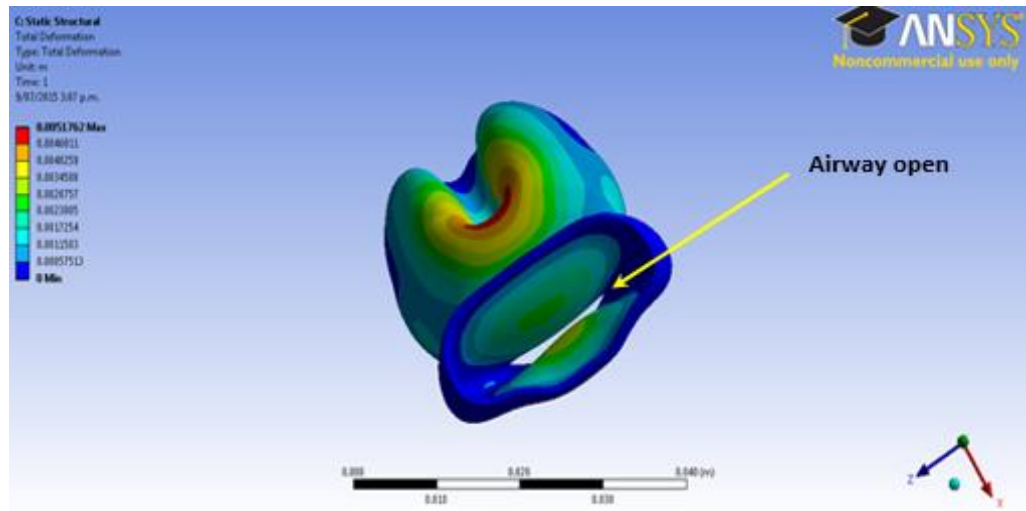


**Figure 6.20: UA pressure distribution during inspiration under PO**



(a)





(b)

**Figure 6.21: Deformations of the rubber enclosure during inspiration (a) front and (b) bottom views under PO**

The maximum deformation is 5.2 mm which is approximately the same deformation obtained without the use of the PO.

The above figures show that the UA pressure distribution with the use of PO (Figure 6.20) is much lower than the obtained results without the use of the PO (Figure 6.18), and despite the fact that the maximum deformation is approximately the same with or without the use of the PO, collapse was detected in Figure 6.19 while the airway is open with no sign of collapse with the use of the PO superimposed on CPAP as shown in Figure 6.21. Thus the use of the PO resulted in lower pressure distributions in the UA and prevented the occurrence of UA collapse.

## (II) Expiration

After many simulations using different boundary conditions at the inlet and the outlet, collapse was detected at the rear of the uvula when  $P_{in} = 2 \text{ kPa} \approx 20 \text{ Cm H}_2\text{O}$ , and  $P_{out} = -0.4 \text{ kPa} \approx -4 \text{ Cm H}_2\text{O}$ .

Figures 6.22 and 6.23 show the resulting UA pressure distribution and deformations of the rubber enclosure during expiration, respectively.

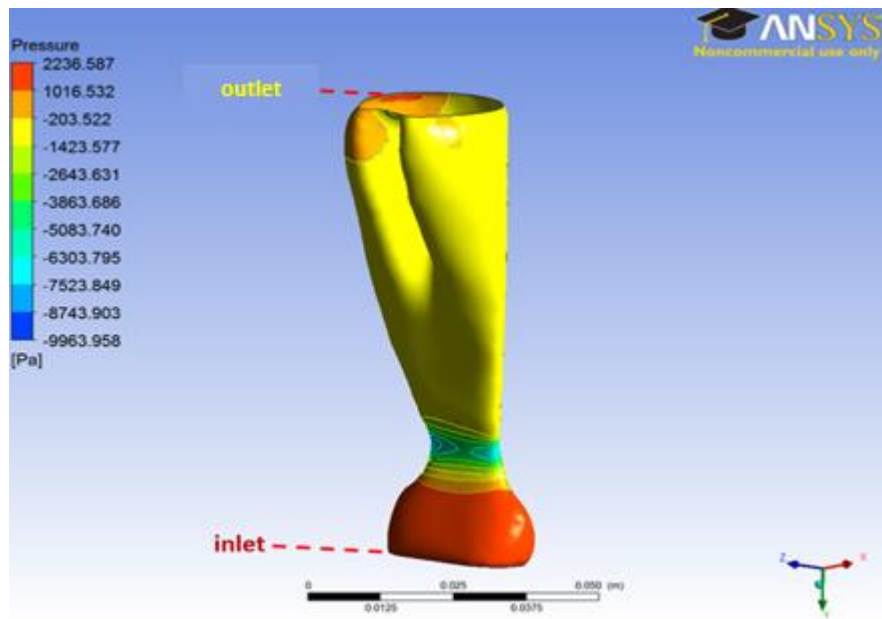
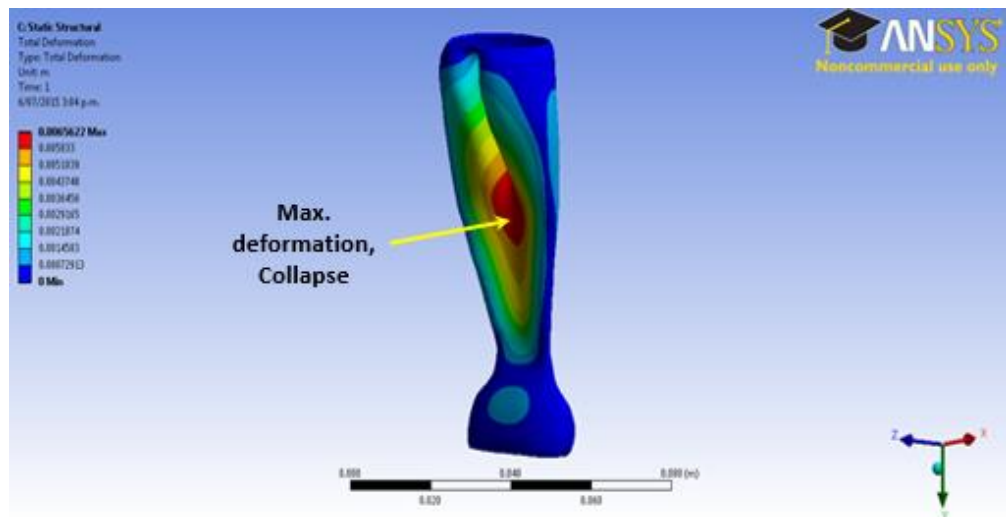
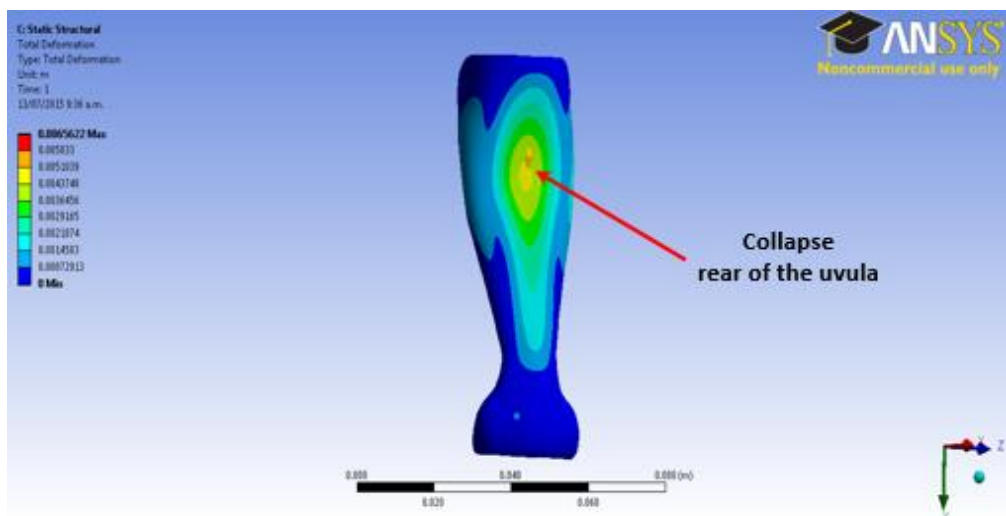


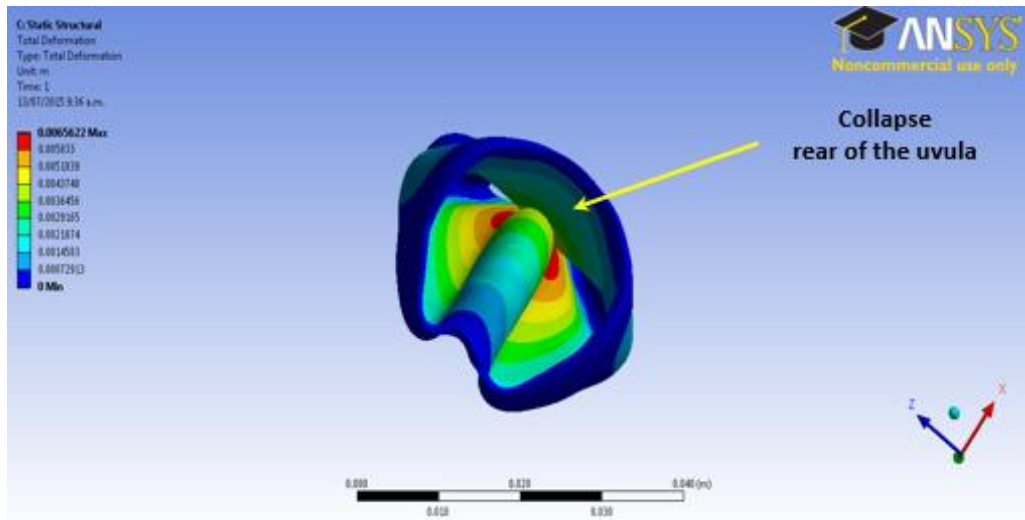
Figure 6.22: UA pressure distribution during expiration



(a)



(b)



(c)

**Figure 6.23: Deformations and collapse of the rubber enclosure during expiration**  
(a) front, (b) rear and (c) top views

If the CPAP is used to prevent the UA collapse with  $P_{\text{out}} = P_{\text{CPAP}} = 0.9 \text{ kPa} \approx 9 \text{ Cm H}_2\text{O}$  and the same inlet pressure ( $P_{\text{in}} = 2 \text{ kPa} \approx 20 \text{ Cm H}_2\text{O}$ ), the pressure distribution is shown in Figure 6.24 and the resulting deformations of the rubber enclosure are given in Figure 6.25 indicating no sign of UA collapse.

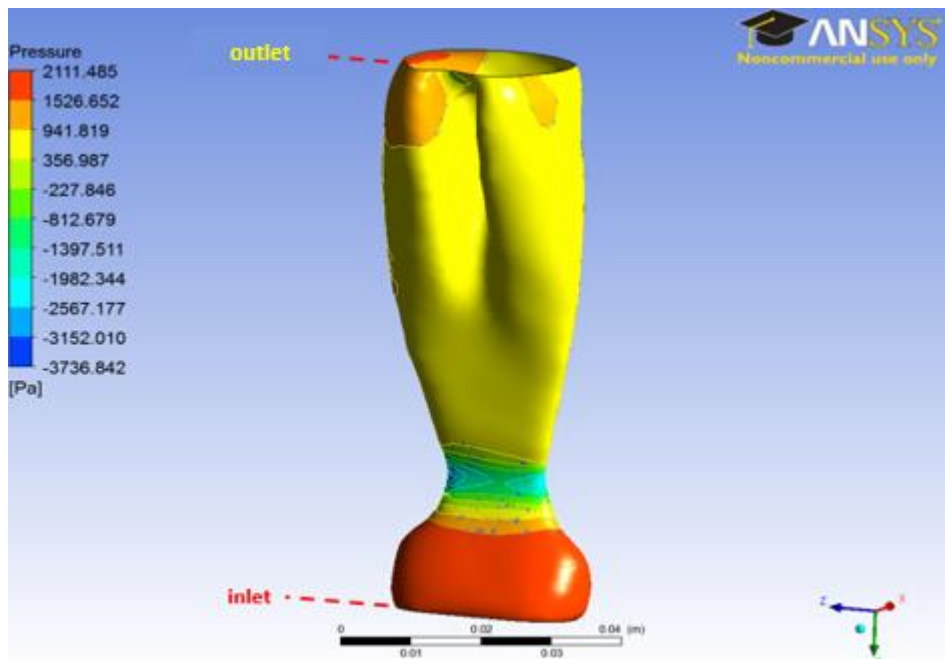
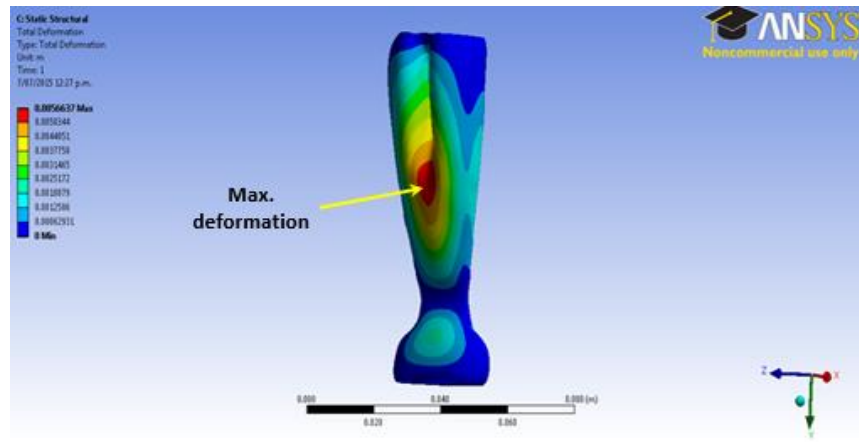
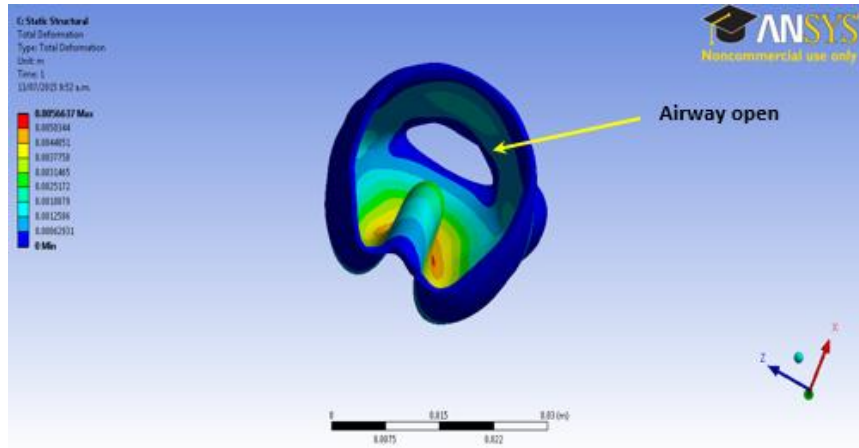


**Figure 6.24: Pressure distribution during expiration with CPAP**



(a)



(b)

**Figure 6.25: Deformations of the rubber enclosure during expiration (a) front view and (b) top view, with CPAP**

Other simulations were conducted to investigate the effects of the PO superimposed on the CPAP with the same boundary conditions at the inlet and the outlet as described previously. The PO were applied at the outlet according to the following equations:

$$P_{\text{out}} = 0.8 + 0.1 \sin(\omega t) \text{ kPa} \quad (6.4)$$

$$\omega = 2\pi f \text{ rad/s, } f = 40 \text{ Hz} \quad (6.5)$$

Figures 6.26 and 6.27 show the resulting air pressure distribution and deformations of the rubber enclosure, respectively under the effect of the PO during expiration.

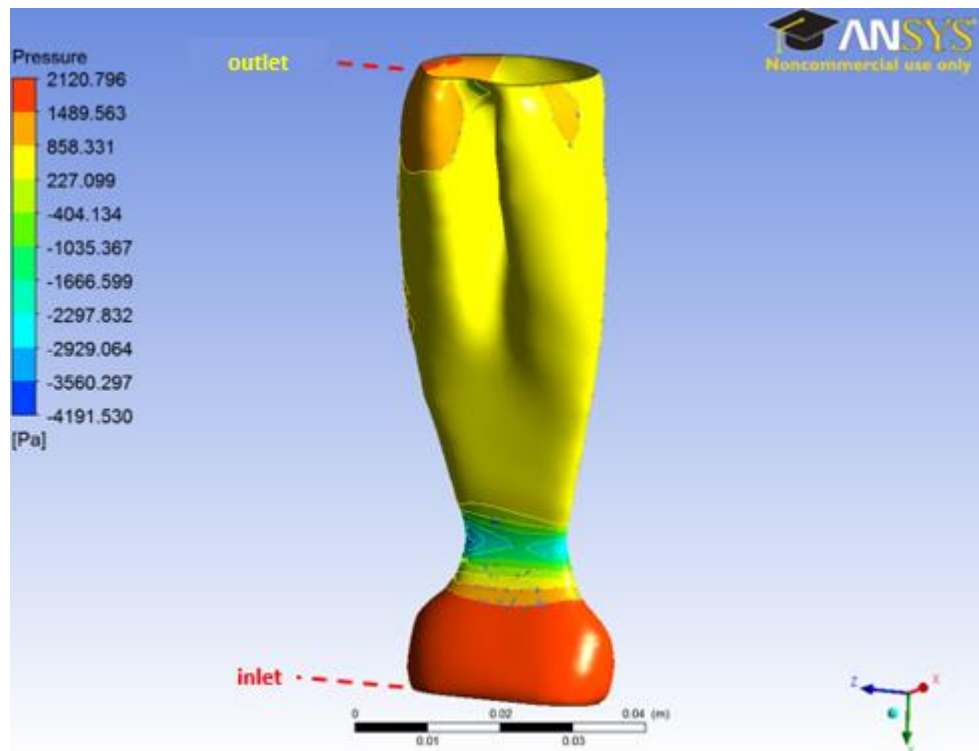
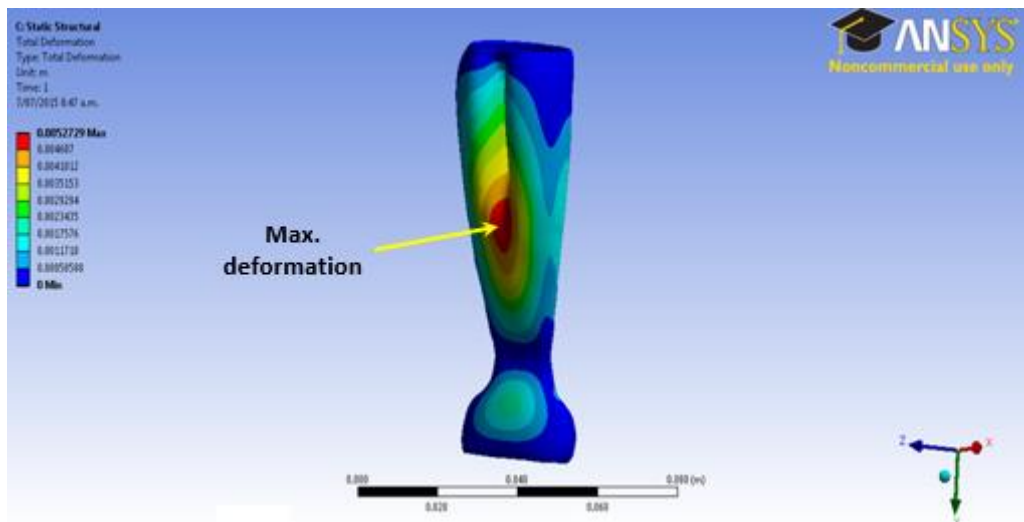
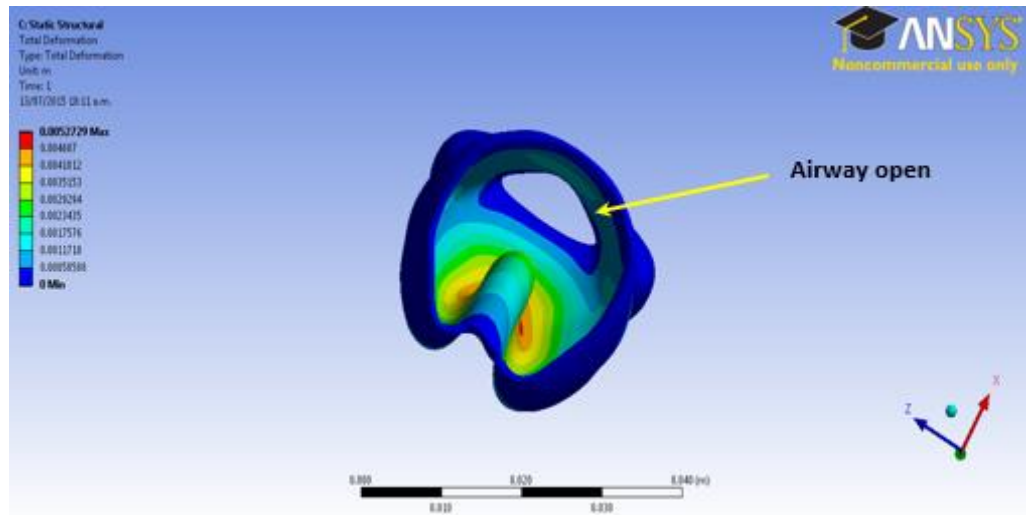


Figure 6.26: Pressure distribution during expiration under PO



(a)



(b)

**Figure 6.27: Deformations of the rubber enclosure during expiration (a) front and (b) top views, under PO**

The maximum deformation without the use of the PO (Figure 6.25) is 5.7 mm and 5.3 mm with the use of the PO (Figure 6.27) which is approximately the same. Also Figures 6.24 and 6.26 show that the maximum positive pressure is approximately the same however the maximum negative (suction) pressure is higher with the use of PO.

Although these results were very promising but the obtained UA pressure distributions were high, therefore the RANS with  $k-\omega$  Shear Stress Transport (SST) turbulence model was used as it is considered to be the best RANS model due to its high ability in describing the viscous effects near the airway walls [377, 379, 529, 534]. The resulting UA pressure distributions were reasonable and much lower than the obtained results from the  $k-\epsilon$  turbulence model.

## 6.5.2 Results from RANS SST Turbulence Model

### (I) Inspiration

In the following simulations the same boundary conditions that we have used for the  $k-\epsilon$  turbulence model were used. The UA pressure distribution and deformations of the rubber enclosure are given in Figures 6.28 and 6.29; respectively.

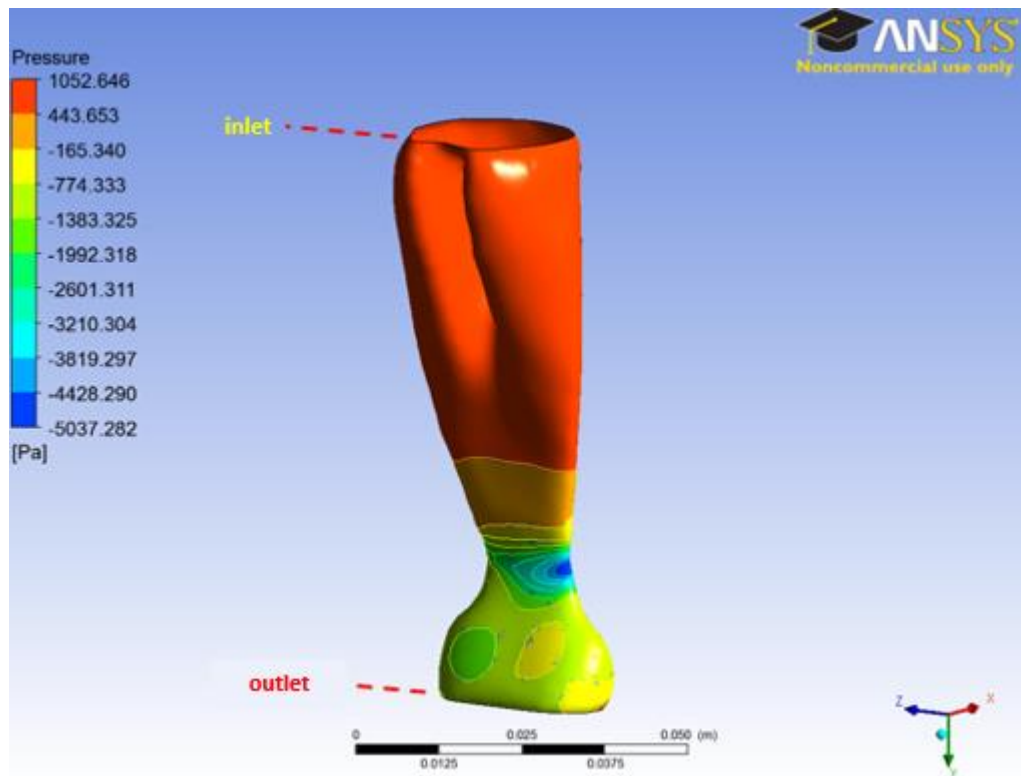


**Figure 6.28: UA pressure distribution during inspiration, SST**

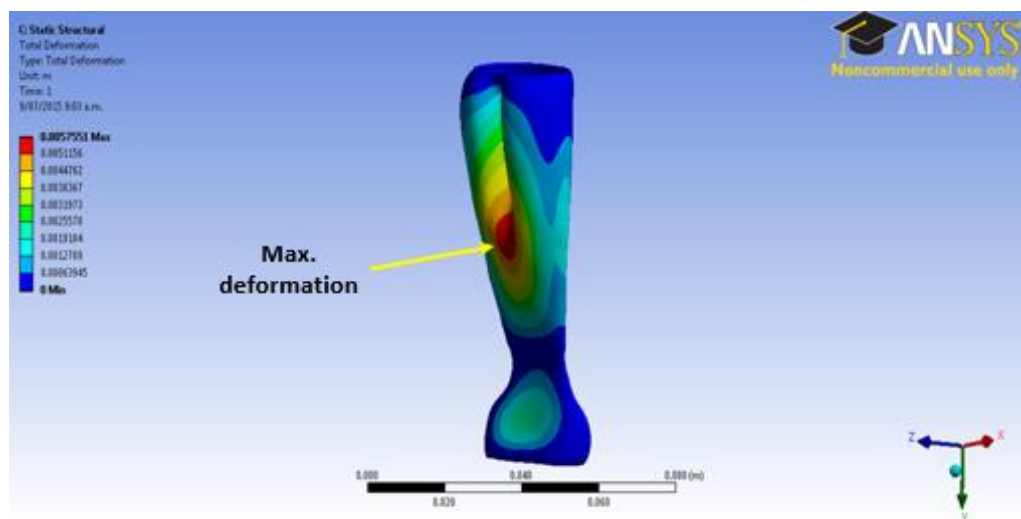


**Figure 6.29: Deformations of the rubber enclosure during inspiration, SST**

Comparisons between Figure 6.18 and Figure 6.28 shows that the resulting UA pressure distribution using the SST turbulence model yield much lower pressure distribution than the k- $\epsilon$  turbulence model. Also comparisons between Figure 6.19 and Figure 6.29 shows no big difference in the maximum deformation obtained from the two turbulence models. The maximum deformation was 5.5 mm with k- $\epsilon$  model and became 5.8 mm with the SST



model. No collapse was detected with the use of SST model under these boundary conditions, therefore new simulations were conducted until collapse was detected when  $P_{in} = 1 \text{ kPa} \approx 10 \text{ Cm H}_2\text{O}$ ,  $P_{out} = -1.1 \text{ kPa} \approx -11 \text{ Cm H}_2\text{O}$ , Figures 6.30 and 6.31.

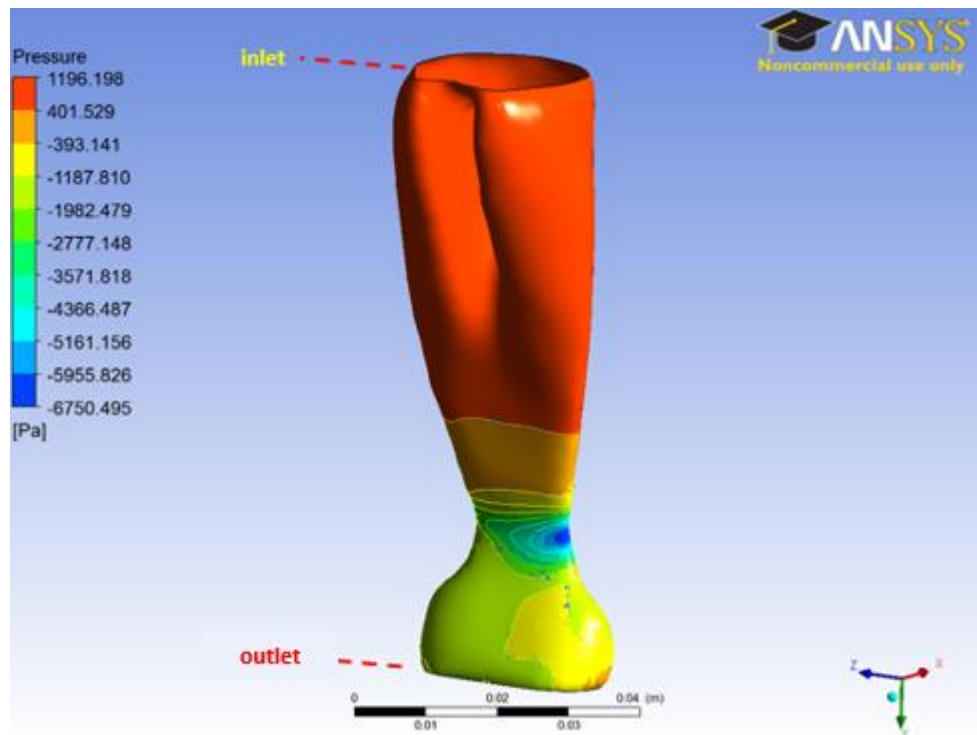
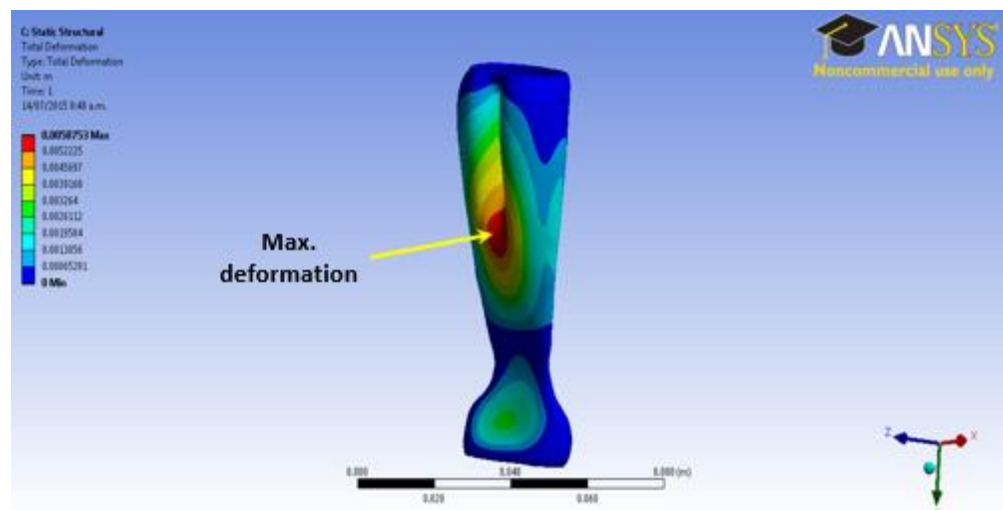
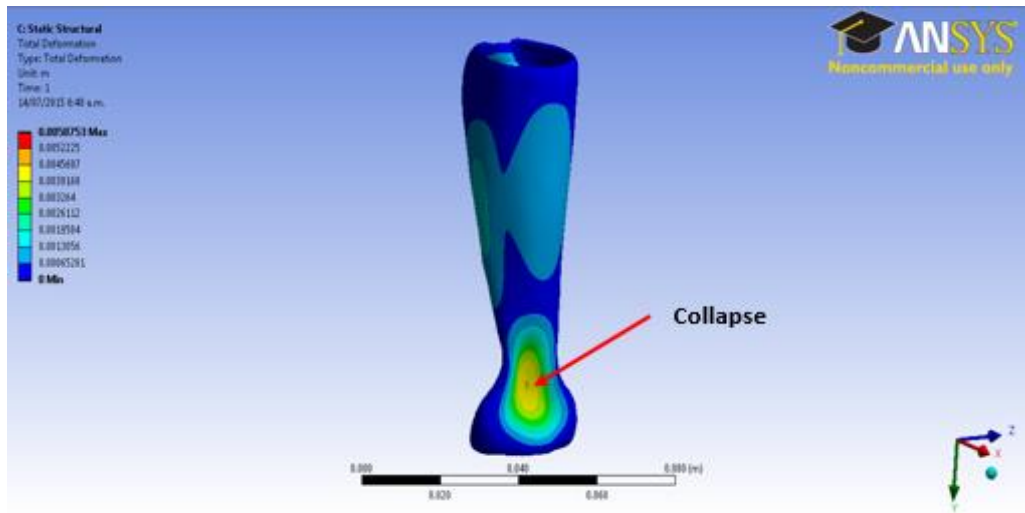


**Figure 6.30: UA pressure distribution during inspiration, SST**

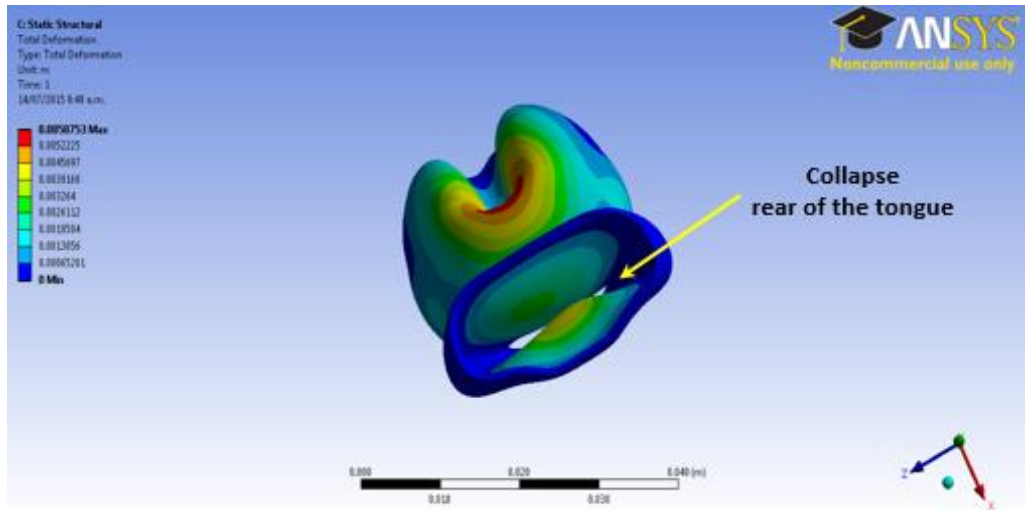


(a)





(b)



(c)

**Figure 6.31: Deformations and collapse of the rubber enclosure during inspiration (a) front, (b) rear and (c) bottom views, SST**

It is noticed that the obtained pressure distribution during inspiration using the SST turbulence model with higher pressure at the inlet and lower pressure at the outlet ( $P_{in} = 1 \text{ kPa} \approx 10 \text{ Cm H}_2\text{O}$ ,  $P_{out} = -1.1 \text{ kPa} \approx -11 \text{ Cm H}_2\text{O}$ ) is much lower than the obtained pressure distribution using the RANS  $k-\epsilon$  turbulence model with  $P_{in} = 0.9 \text{ kPa} \approx 9 \text{ Cm H}_2\text{O}$ , and  $P_{out} = -0.8 \text{ kPa} \approx -8 \text{ Cm H}_2\text{O}$ . These results show that the SST turbulence model is favoured in simulating the UA in comparison to the  $k-\epsilon$  turbulence model.

To investigate the effects of the PO superimposed on the CPAP, PO were applied at the inlet according to the following equations for the same boundary conditions applied at the outlet:

$$P_{in} = 0.9 + 0.1 \sin(\omega t) \text{ kPa} \quad (6.6)$$

$$\omega = 2\pi f \text{ rad/s}, f = 40 \text{ Hz} \quad (6.7)$$

Figures 6.32 and 6.33 show the resulting UA pressure distribution and deformations of the rubber enclosure, respectively under the effect of the PO during inspiration.

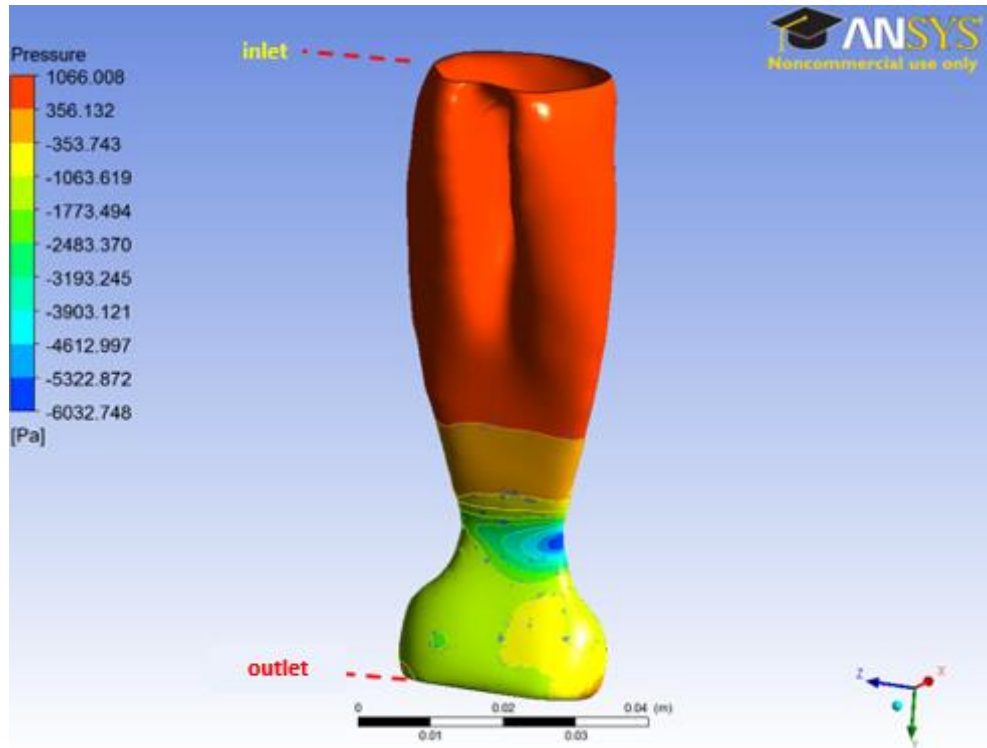
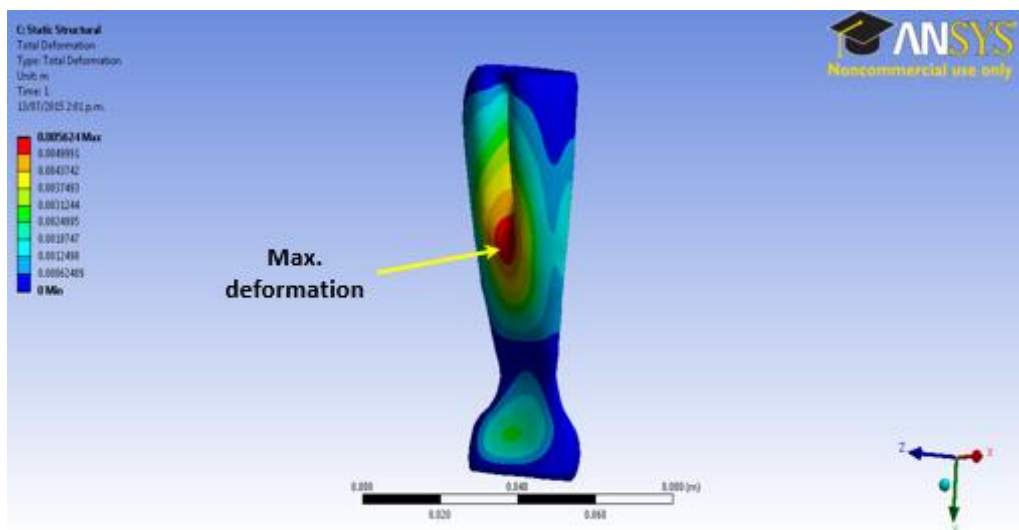
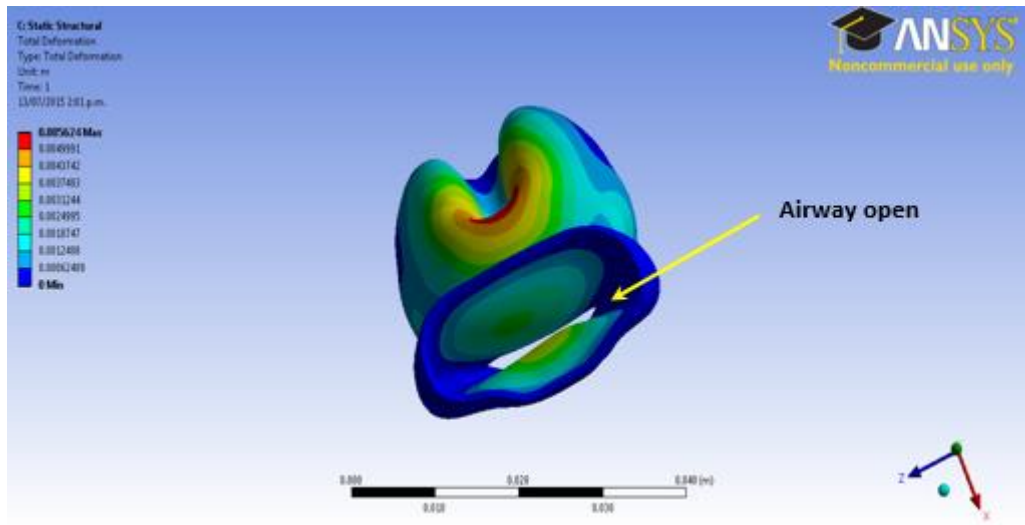


**Figure 6.32: UA pressure distribution during inspiration under PO, SST**



(a)



(b)

**Figure 6.33: Deformations of the rubber enclosure during inspiration (a) front and (b) bottom views, SST under PO**

Comparisons between the obtained UA pressure distributions before and after using the PO (Figures 6.30 and 6.32), it is clear that the use of the PO resulted in much lower UA pressure distributions and consequently prevented the occurrence of collapse. Also the maximum deformation of the rubber enclosure is approximately the same as shown in Figures 6.31 and 6.33.

## (II) Expiration

Using the same boundary conditions that were used for the k- $\epsilon$  turbulence model, where  $P_{in} = 2 \text{ kPa} \approx 20 \text{ Cm H}_2\text{O}$ , and  $P_{out} = -0.4 \text{ kPa} \approx -4 \text{ Cm H}_2\text{O}$ . The UA pressure distribution and the deformations of the rubber enclosure are given in Figures 6.34 and 6.35, respectively, and collapse was detected at the rear of the uvula.

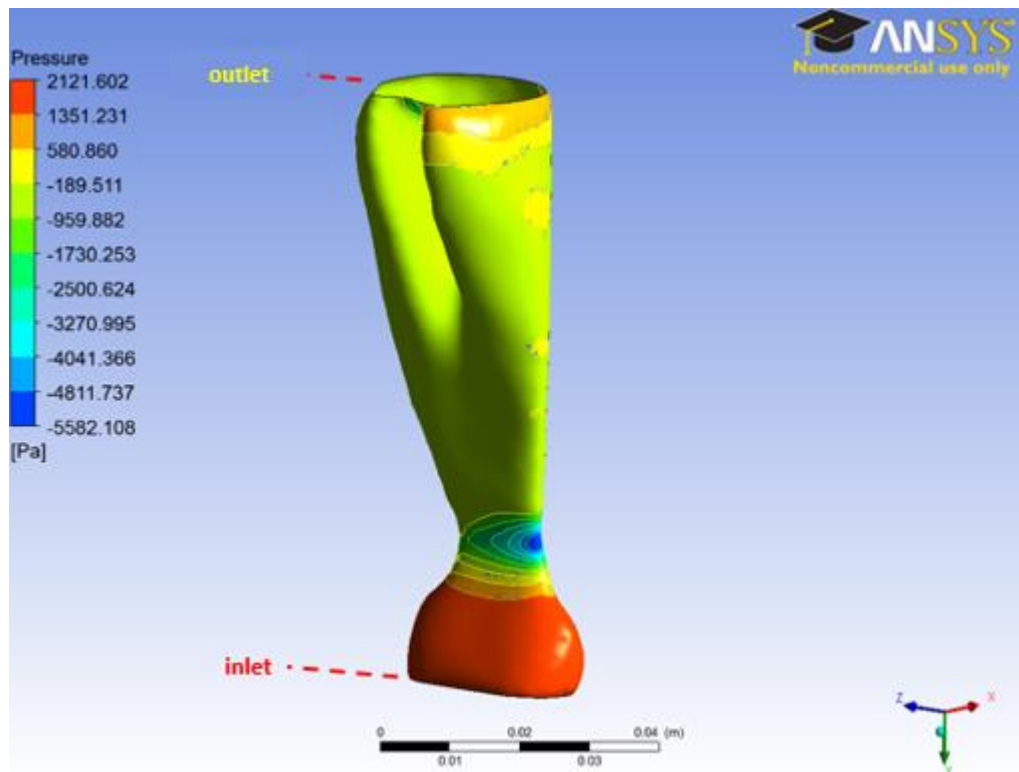
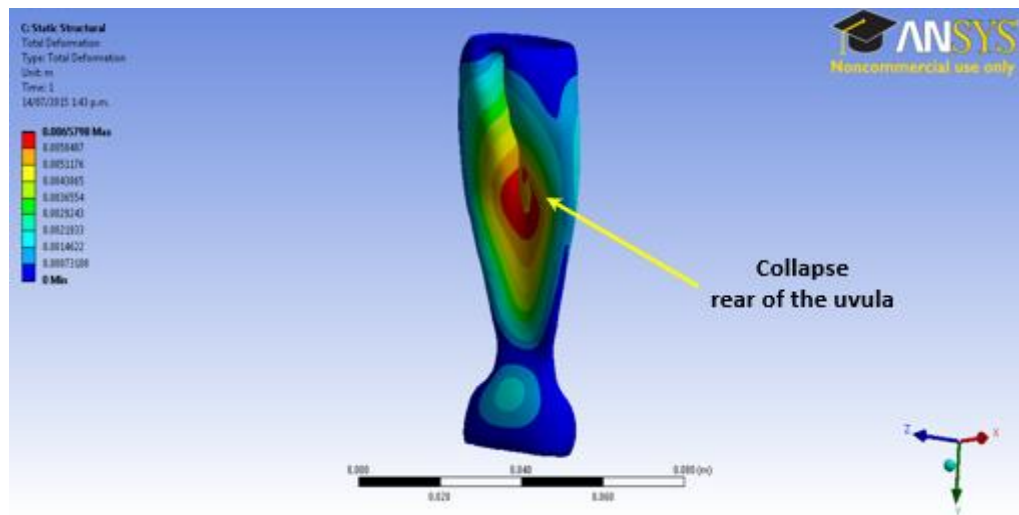
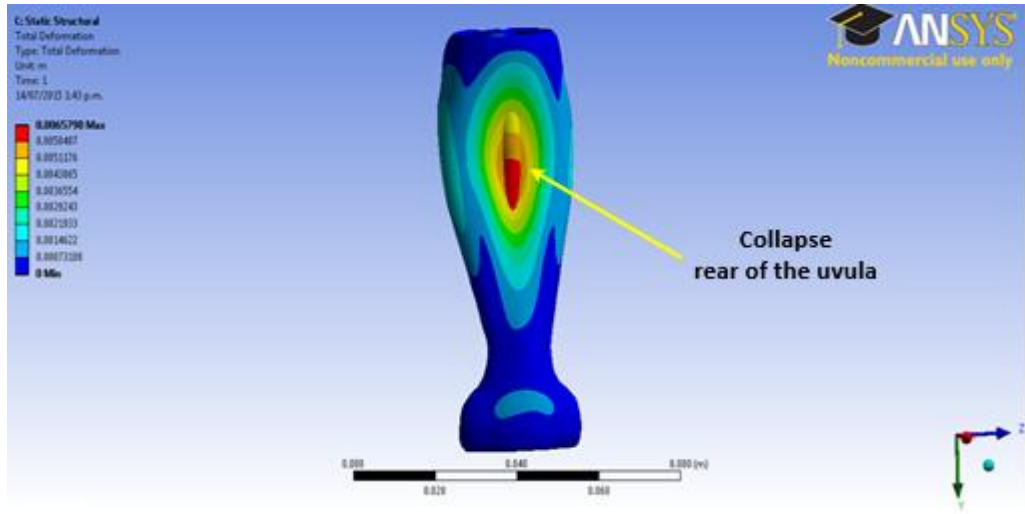


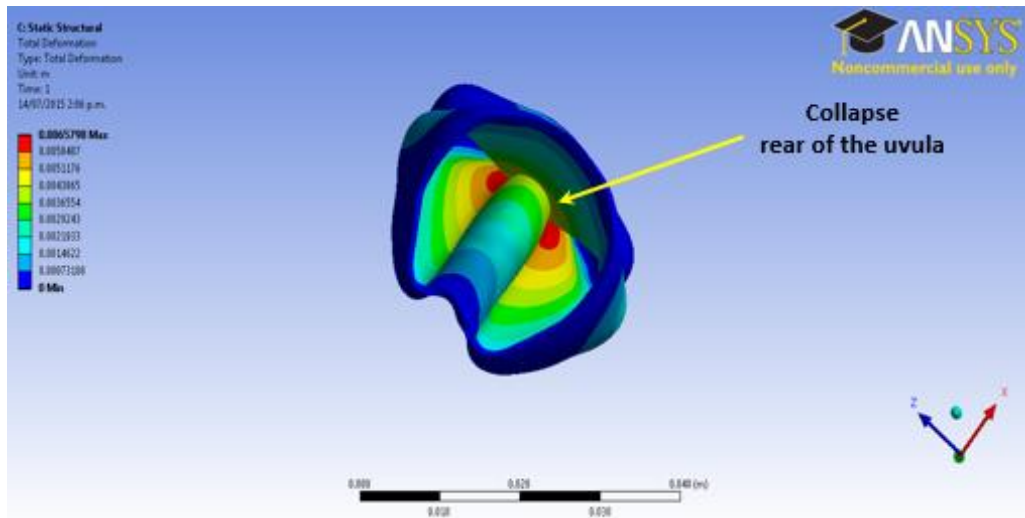
Figure 6.34: UA pressure distribution during expiration, SST



(a)



(b)



(c)

**Figure 6.35: Deformations and collapse of the rubber enclosure during expiration  
(a) front, (b) rear and (c) top views, SST**

The obtained maximum deformation is approximately the same as that of the  $k-\epsilon$  turbulence model, however the UA pressure distribution is much less than the obtained results from the  $k-\epsilon$  turbulence model.

If the CPAP is used to prevent the UA collapse with  $P_{out} = P_{CPAP} = 0.9 \text{ kPa} \approx 9 \text{ Cm H}_2\text{O}$  and the same inlet pressure of  $P_{in} = 2 \text{ kPa} \approx 20 \text{ Cm H}_2\text{O}$ , the UA pressure distribution is

shown in Figure 6.36 and the resulting deformations of the rubber enclosure are given in Figure 6.37 indicating no sign of UA collapse.

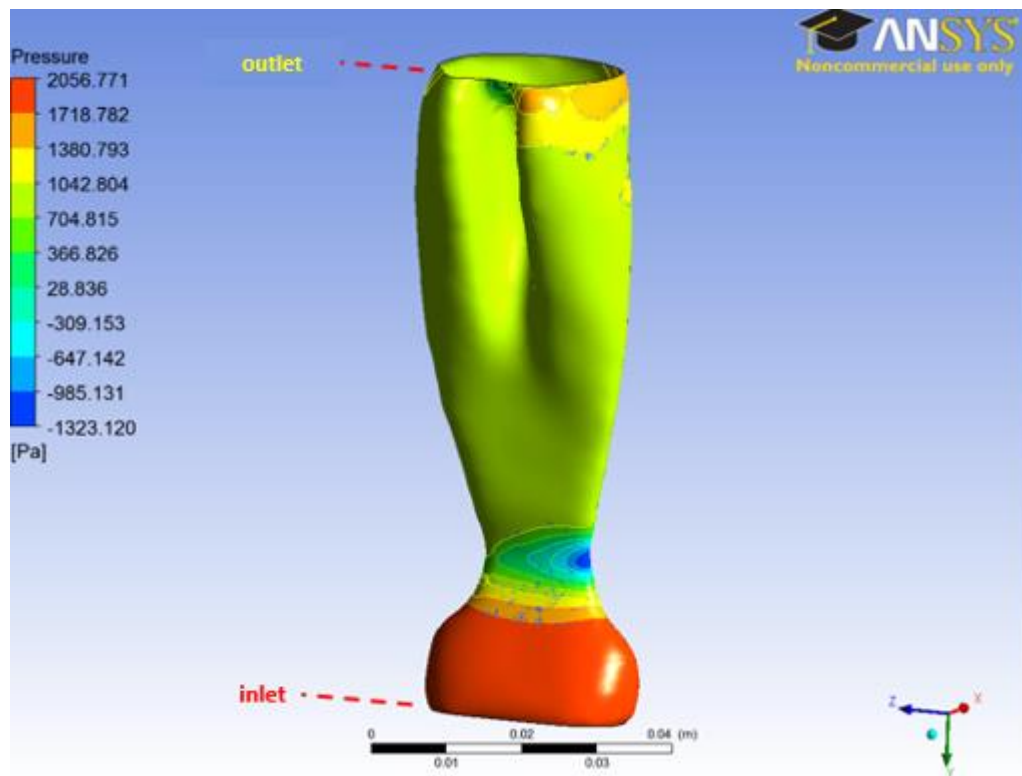
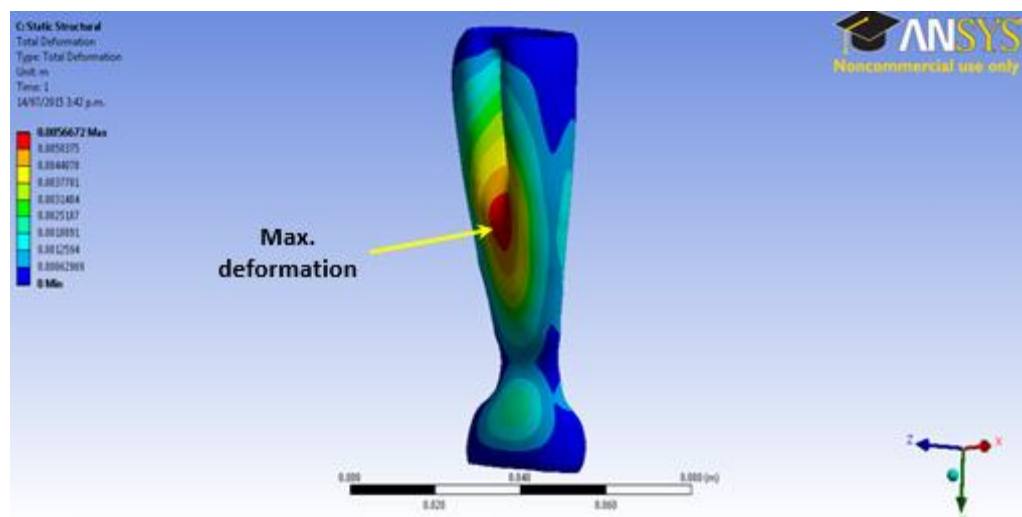
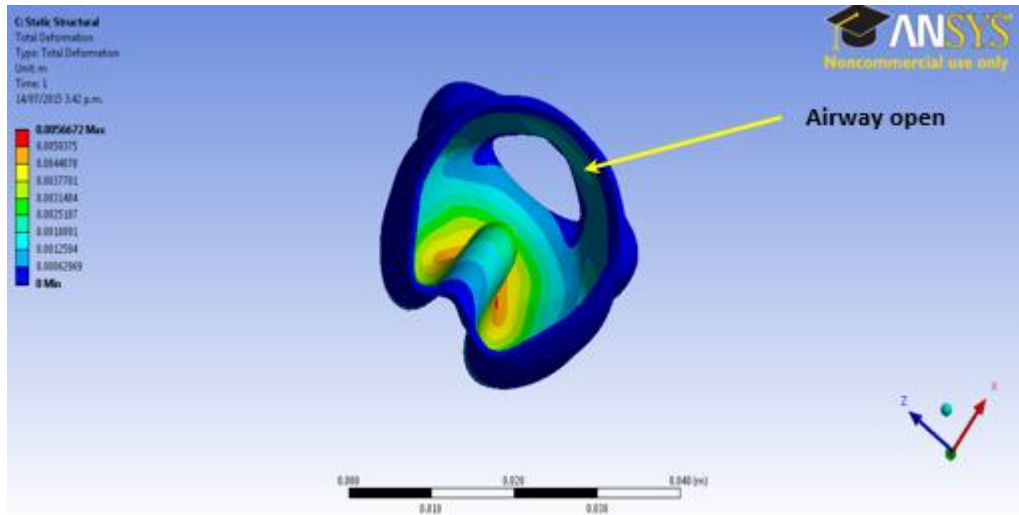


**Figure 6.36: Pressure distribution during expiration, SST with CPAP**



(a)



(b)

**Figure 6.37: Deformations of the rubber enclosure during expiration (a) front and (b) top views, SST with CPAP**

These results show that the maximum deformation is approximately the same when using the two turbulence models, however the SST model resulted in much lower pressure distributions.

To investigate the effects of the PO superimposed on the CPAP, PO were applied at the outlet according to the following equations with the same boundary conditions at the inlet:

$$P_{\text{out}} = 0.8 + 0.1 \sin(\omega t) \text{ kPa} \quad (6.8)$$

$$\omega = 2\pi f \text{ rad/s}, f = 40 \text{ Hz} \quad (6.9)$$

The results of the UA pressure distribution and the deformations of the rubber enclosure are given in Figures 6.38 and 6.39, respectively.



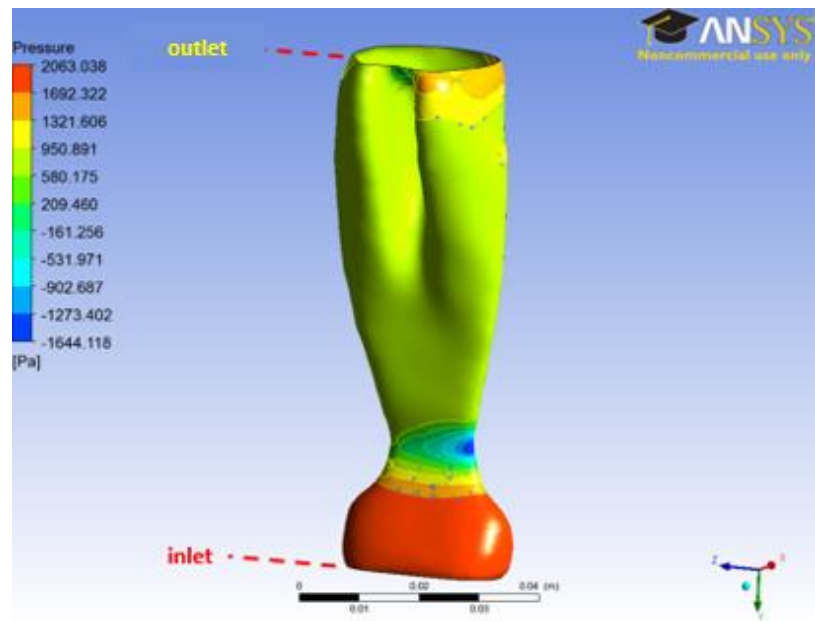
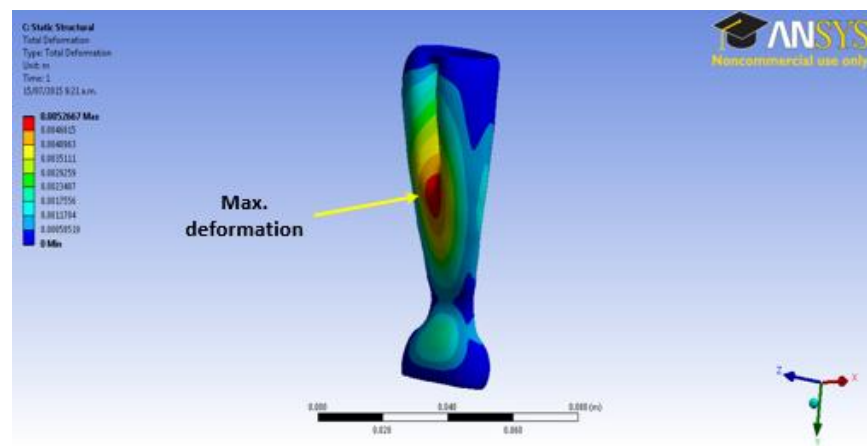
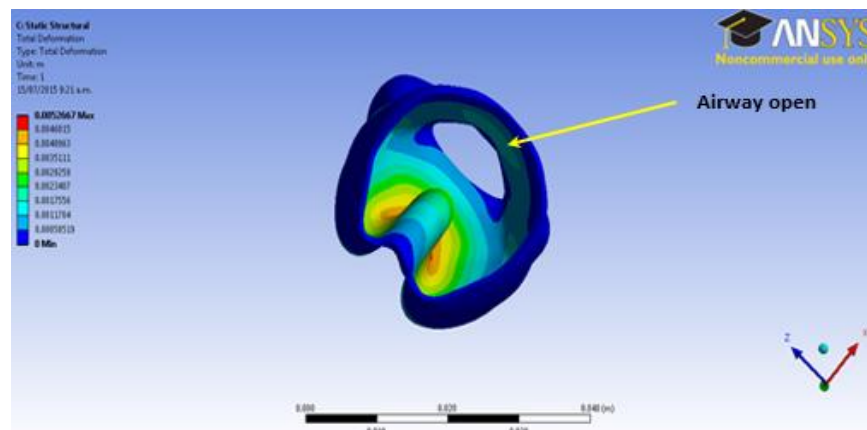


Figure 6.38: UA pressure distribution during expiration under PO, SST



(a)



(b)

Figure 6.39: Deformations of the rubber enclosure during expiration (a) front view and (b) top view, SST under PO



These results show that the obtained maximum deformation during expiration is approximately the same when using the CPAP alone and when the PO were superimposed on the CPAP and the maximum positive UA pressure is approximately the same, however the maximum negative pressure is higher when the PO were superimposed in comparison to the use of the CPAP alone.

### **6.5.3 Conclusions**

From the obtained results we have concluded that:

1. The obtained closing pressures fall within the reported pharyngeal pressures [25, 551, 552].
2. The use of the CPAP prevented the occurrence of UA collapse during inspiration and expiration.
3. The use of the PO superimposed on the CPAP prevented the occurrence of collapse at lower pressures when compared with the obtained values when using the conventional CPAP alone, especially during inspiration.
4. The use of the SST turbulence model resulted in more reasonable pressure distributions and closer to reality in comparison to the results obtained from the k- $\epsilon$  turbulence model.

## **6.6 Closure**

This chapter investigated the dynamic characteristics of the unhealthy UA models and presented the results of using the FE, CFD and FSI methods in determining the dynamic response, UA pressure distributions and the interaction between the airflow and the deformations of the soft tissues; respectively. Also, this chapter investigated the conditions of collapse and the effects of using the PO superimposed on the CPAP during inspiratory and expiratory breathing phases. The obtained results will be experimentally validated in the next chapter which represents a full explanation of the experimental setups, the produced UA models made of silicon rubber and gelatine to determine the deformations of the soft tissues when excited by the breath cycle, and also investigate the effects of the PO when superimposed on the CPAP on the performance of the UA.

## Chapter 7

### Experimental Setup and Validation

#### 7.1 Introduction

The outcomes of the theoretical modelling need to be physically validated to support the outcomes of the project and to prove the validity of the used modelling techniques. Unfortunately there is no available equipment which can be used to capture clear images of the human UA to detect and analyse the deformations of the soft tissues during normal sleeping conditions or when using the CPAP. Therefore, an experimental setup is needed as a replacement for the physical validation to detect the deformations of the soft tissues.

This chapter presents a detailed explanation of the components of the experimental setup that was constructed to fulfil the requirements described previously in section 3.7, which is given in section 7.2. Section 7.3 explains the UA experimental modelling and describes the used simplified models for the UA, tongue and uvula.

#### 7.2 Experimental Setup

The purpose of this setup is to simulate the human UA respiratory system to detect the resulting deformations of the soft tissues when excited by the breath cycle. The setup consists of a computer and two main parts: (A) Lung Simulator and (B) UA Respiration Simulator, Figure 7.1.

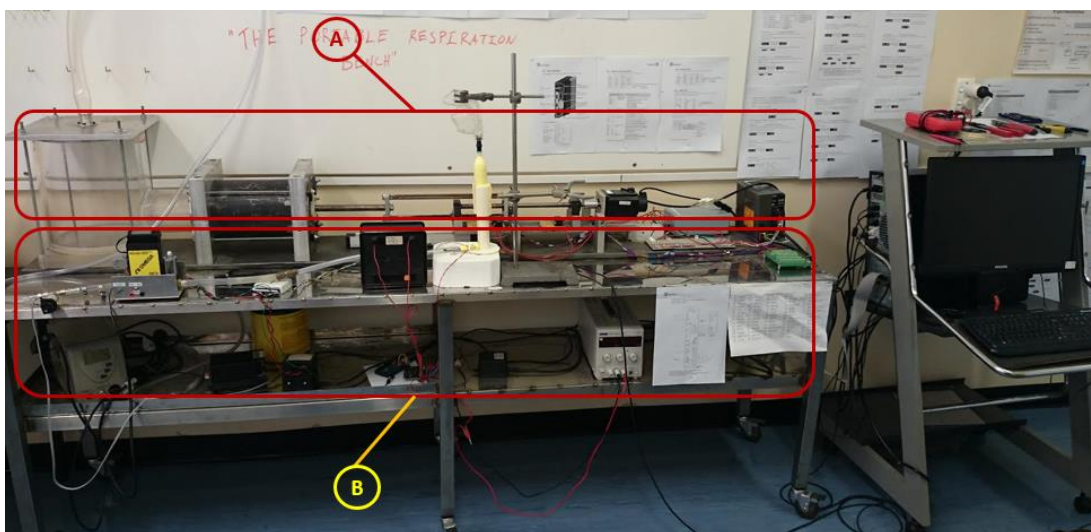


**Figure 7.1: Experimental setup; (A) Lung and (B) UA Respiration simulators**

This setup is capable of producing the human breath cycle with different flow rates to cover the changes that may occur in different ages, genders, ethnicities, and different sleeping stages and/or positions. The setup includes a computer which gives the input signals to the lung simulator and UA simulator, accordingly the lung simulator starts delivering the breath cycle to the UA simulator based on the received input signal from the computer, then the heater starts heating up the upcoming air from the lung simulator to deliver it to the UA model with the same human breathing conditions. This process is summarized in the following two diagrams, Figures 7.2 and 7.3.

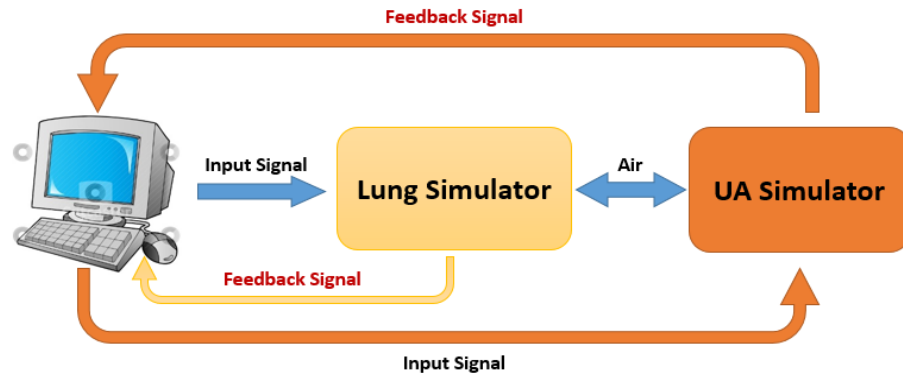


**Figure 7.2: Diagram showing how the setup works**

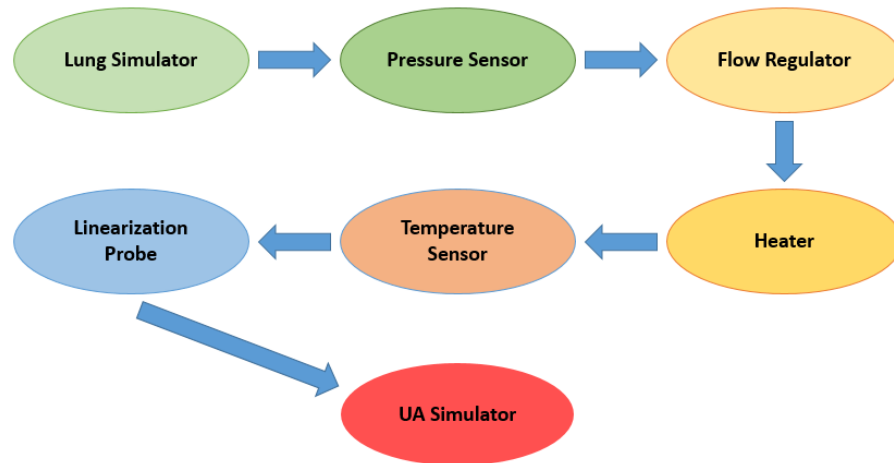


**Figure 7.3: Diagram showing the sequence of the connected items**

Each part of this setup consists of some components and will be discussed in details as follows.

### 7.2.1 Computer

A computer equipped with LabView software (National Instruments, Version 6, 2014) was used to monitor the obtained data (temperature, flow rate and pressure) and

specify the flow conditions (temperature set point and airflow rate). It also displays charts for the pressure, mass flow rate and temperature.

The LabView interface is divided in two parts, the block diagram (Figure 7.4) and the front panel (Figure 7.5). The block diagram is used to prepare the regulation and data acquisition scheme before running the program. Any required changes (such as the temperature set point and air mass flow rate) can be done easily by using the front panel.

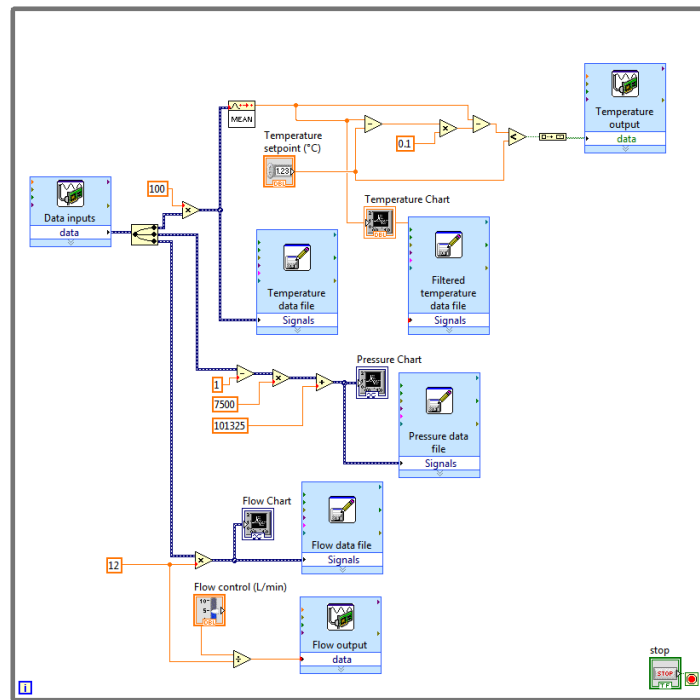


**Figure 7.4: Block diagram**

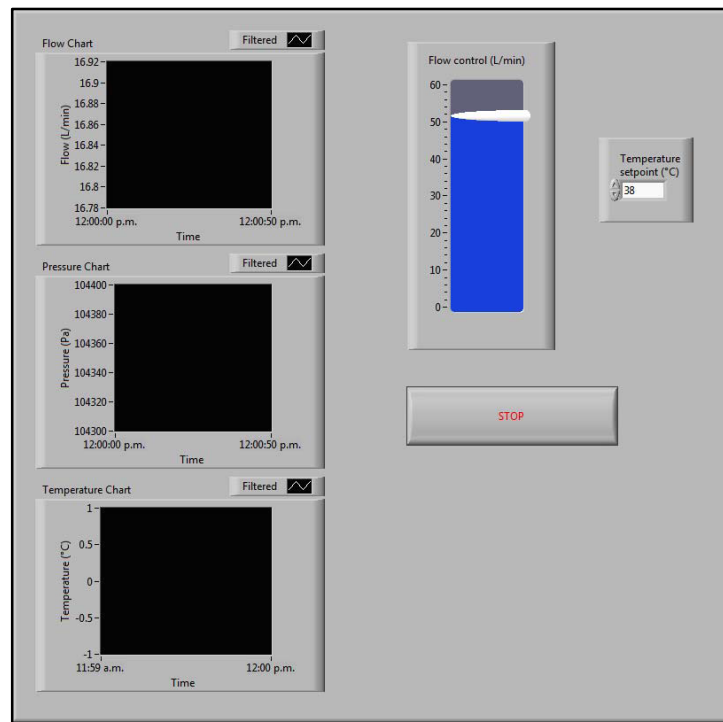


**Figure 7.5: Front panel**

### 7.2.2 Lung Simulator

This simulator was designed and developed at the Institute of Biomedical Technologies (IBTec) prior to the beginning of the current research. It provides the same conditions of the airflow coming from the lungs into the UA system. The only disadvantage of this lung simulator was the fact that it is very difficult to heat it up to obtain the same temperature coming from the real lungs which is approximately 38 °C. It consists of the following:

1. Data Acquisition Board: (model CB-68LP, National Instruments) is used to transfer the data signals from the computer to the setup and vice versa, Figure 7.6.

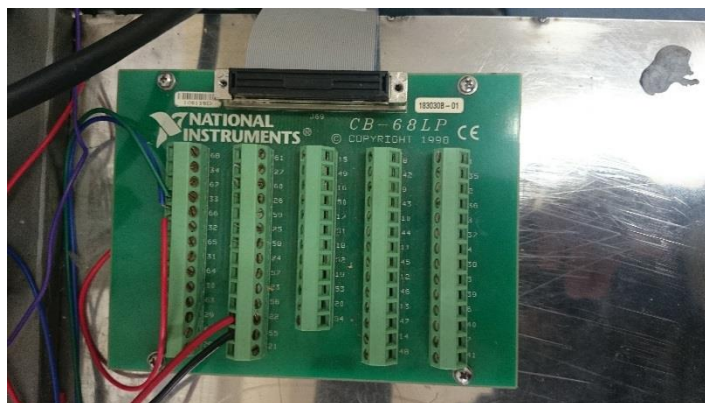


**Figure 7.6: Data acquisition board**

2. **Servo Amplifier:** (model RYC751D3-VVT2) is used to reduce the mechanical vibrations in the system and deliver the signals from the computer to the servo motor, Figure 7.7.



**Figure 7.7: Servo amplifier**

3. **Power Supply Unit:** a 24 volt DC power supply that provides a continuous power supply to the amplifier and motor, Figure 7.8.



**Figure 7.8: Power supply**

4. **Relay:** (model G2RL-1E 24DC, Omron) is an electro-mechanical relay that switches the lung simulator on and off once the screw follower comes in contact with the stop switches, Figure 7.9.

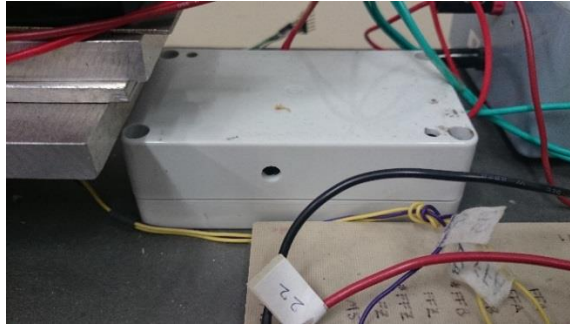


**Figure 7.9: Electro-mechanical relay**

5. **Servo Motor:** (model GYS751DC2-T2A) it receives the computer signal via the amplifier to move the piston forward and backward to simulate the exhaling and inhaling breathing phases, respectively; Figure 7.10.



**Figure 7.10: Servo motor**

6. **Stop Switches and Screw Follower:** when the screw follower makes contact with the stop switches (model PN4-GK48, Sicatron), the relay cuts off the power coming from the power supply to the motor which stops the motor instantly, Figure 7.11.



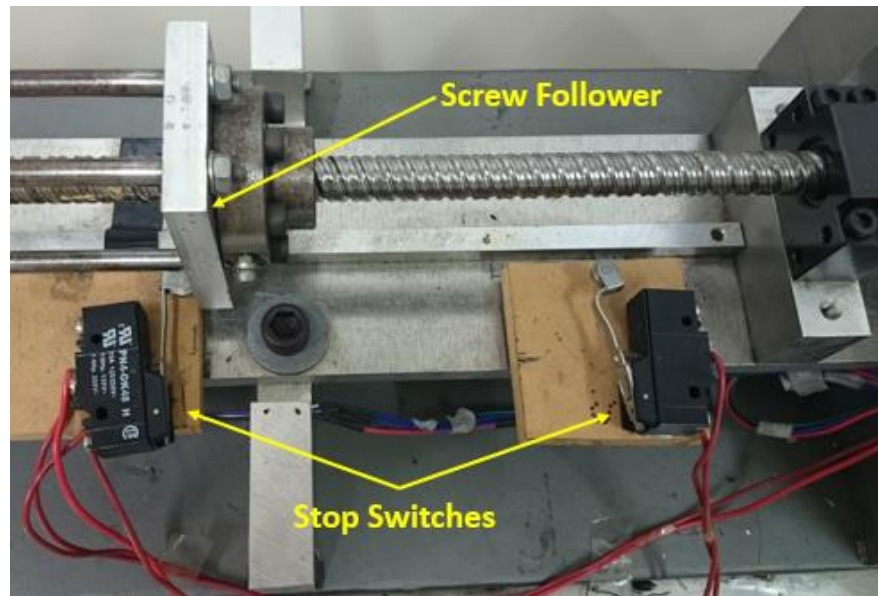


**Figure 7.11: Stop switches and screw follower**

7. **Piston/Cylinder Compartment:** is used to provide pressurized air based on the breathing cycle specified by the LabView code on the computer. It is controlled by the servo motor, Figure 7.12.

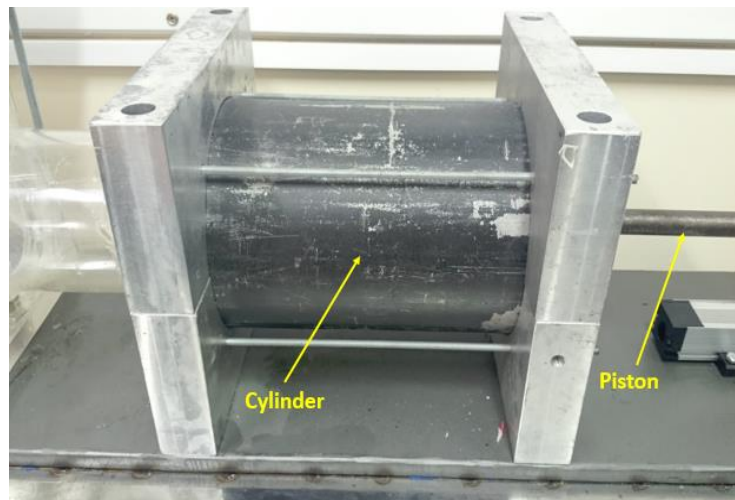


**Figure 7.12: Piston/Cylinder compartment**

8. **Chamber:** is used to collect the pressurized air from the lung simulator and direct it to the UA simulator and vice versa during exhaling and inhaling, respectively, Figure 7.13.



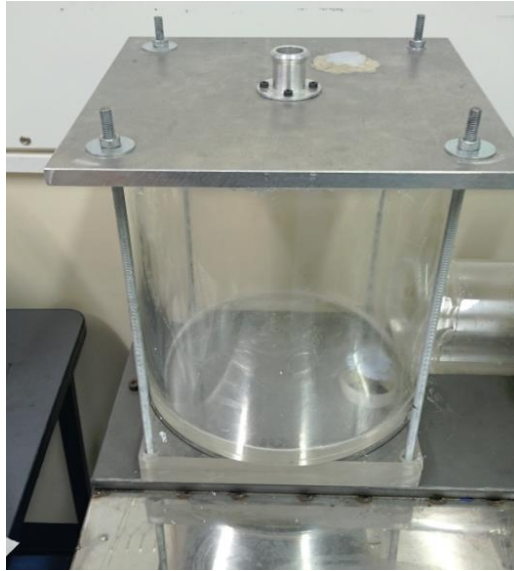


**Figure 7.13: Chamber**

### **7.2.3 UA Simulator**

This setup was built to control the flow rate, pressure and temperature of the airflow. The first few experiments showed that the temperature can be regulated with an error of  $0.0532 \pm 0.2$  °C. The flow can be automatically controlled via a digital flow controller using a PID controller code programmed on the LabView software. The pressure can be manually controlled through a pressure regulator if the UA simulator is to be used alone without being connected to the lung simulator. A divergent-convergent probe (nozzle) was designed and used to laminarise the flow before entering the UA model. The UA simulator consists of the following:

1. **Pressure sensor (transducer):** (Impress Sensors & Systems, serial number 139516) it converts the detected pressures into analogue signals in order to record the obtained pressure data on the computer and allow the user to read these values using LabView software. The pressure transducer can measure the pressure range of 0-0.3 bars above the atmospheric pressure, Figure 7.14.



**Figure 7.14: Pressure transducer**

2. **Flow Controller:** A digital flow controller (Omega, model FMA5400/5500) is used to measure and/or regulate the airflow. It can regulate the airflow from 0-60 L/min (Figure 7.15). It has a built-in electromagnetic valve to maintain a constant flow rate regardless of the variations in the inlet or the outlet pressures, when needed. The set point can be controlled remotely by an analogue 0-5V DC signal which can easily be controlled using LabView software.



**Figure 7.15: Flow controller**

3. **Temperature Sensor:** it is inserted inside the tube between the heater and the laminarisation probe to detect the temperature signals with an accuracy of  $\pm 0.2^{\circ}\text{C}$ , Figure 7.16. A microprocessor and a PID controller were used to keep the system's temperature at the set-point value which can be easily specified using the LabView software.

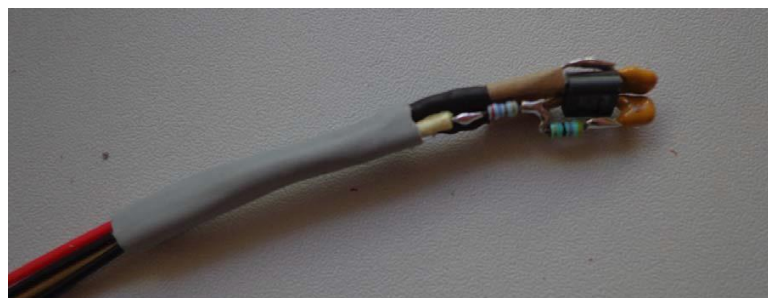


**Figure 7.16: Temperature sensor**

4. **Heater:** Air coming from human lungs should have a temperature of  $38^{\circ}\text{C}$ , and since the experiments were going to be running at room temperature (around  $20^{\circ}\text{C}$ ), therefore a heating element was needed to deliver the air to the UA with a temperature similar to that coming from the real human lungs. Therefore, two heating elements connected in series were used; each element has a power of 35 Watts. These heating elements were kept in a protection box, Figure 7.17, to avoid any possible contact with people or other components of the setup as their temperature can reach  $200^{\circ}\text{C}$ . The heater needs a voltage of 12-14 Volts (depending on the required temperature) which is provided by a power supply unit described later.



**Figure 7.17: Heater**

5. **Laminarisation Probe:** to minimise the calculation errors due to the turbulence in the airflow, a divergent-convergent probe was designed and produced using 3D-printing to laminarise the airflow coming from the lungs (entering from the right) to the UA (from the left). This probe is shown in Figure 7.18.



**Figure 7.18: Laminarisation probe**

6. **Power Supply Units:** two power supply units are used in this setup, the first one supplies voltage and current to the heater and the microprocessor, Figure 7.19 (a);

while the second one supplies voltage and current to the pressure transducer, Figure 7.19 (b).



(a)



(b)

**Figure 7.19: Power supply units**

**7. Data Acquisition Board:** (model is NI USB-6008, National Instrument) is connected to the computer via a USB cable, Figure 7.20, and is responsible for acquiring the signals of the temperature, flow rate and pressure from the setup and convert these analogue signals into digital signals that can be delivered to the computer for data monitoring.



**Figure 7.20: Data acquisition board**

8. **Microprocessor:** (Arduino Mega 2560) is used to control the operation of the heater to smoothly reach the temperature set point by delivering the signals from the computer to the heater via the driving motor described below, Figure 7.21.



**Figure 7.21: Microprocessor**

9. **DC Motor Driver:** (DFRobot DR-0018) is used to deliver the appropriate amount of power to the heater to smoothly reach the required set point temperature, Figure 7.22.



**Figure 7.22: DC motor driver**



### 7.3 UA Experimental Modelling

The collected MRI images were used to construct accurate UA models for the healthy and unhealthy participants using 3D-DOCTOR software as discussed previously. In order to validate the obtained results from simulations, a hollow transparent rig was designed and constructed which has an air cavity of the same geometry as that of a real UA model obtained from the collected MRI. Therefore a three dimensional accurate model consisting of the UA, tongue and uvula was constructed and 3D-printed, as shown in Figure 7.23.

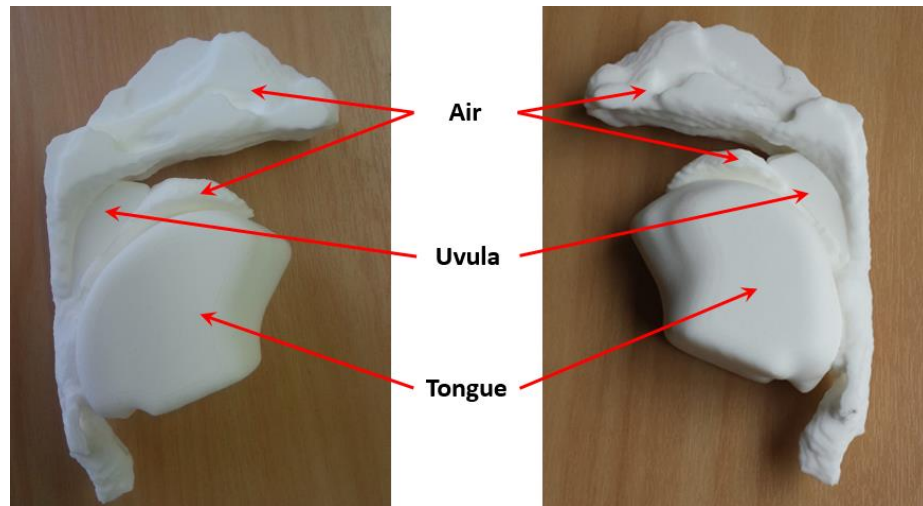


**Figure 7.23: Accurate UA model**

After investigation and consultation on how this rig could be produced, vacuum forming was the best way to produce it. Unfortunately this accurate rig could not be produced because the UA geometry is so complicated and contains many irregular surfaces. Therefore, a simplified UA model, which can be produced from the available resources, was designed and 3D-printed as shown in Figure 7.24.

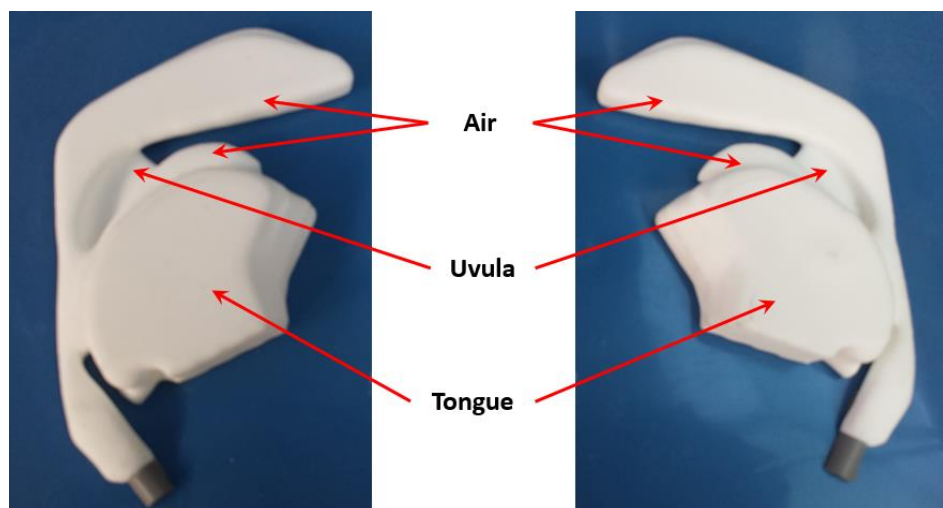


**Figure 7.24: Simplified UA model**

This simplified model was then used to produce the required transparent rig using vacuum forming as shown in Figure 7.25.

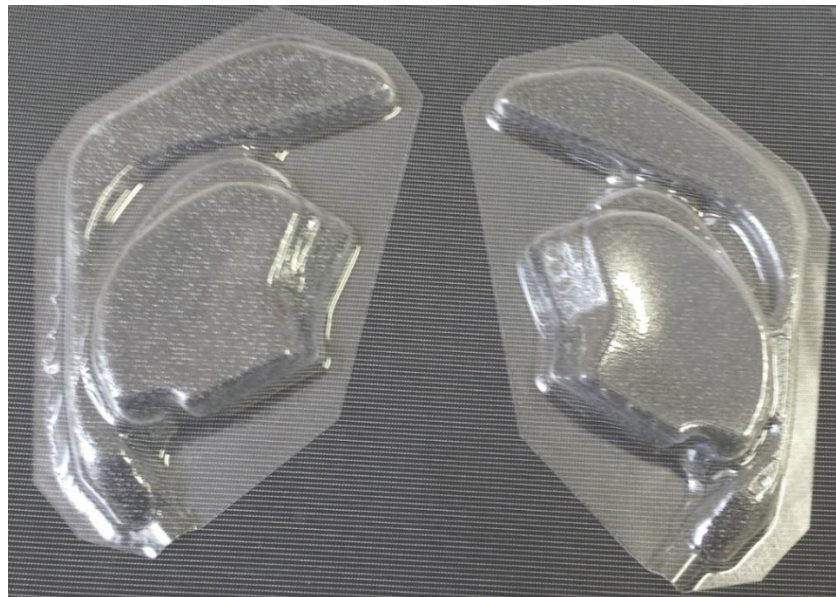


**Figure 7.25: Transparent rig using vacuum forming**

Also tongue and uvula models were needed to be used in experimental validation, the main concern was to find materials having similar properties as those of the real human soft tissues. Therefore moulds for the tongue and uvula were prepared and produced by using 3D-printing and were then used to produce uvula and tongue models made of different materials as described next.

### **7.3.1 Silicon Rubber Models**

Uvula and tongue models made out of silicon rubbers were produced, however the silicon models were very hard compared with the real soft tissues. Models made out of a mixture of two silicon rubber materials were then produced and the resulting models were softer than the first trial, and shown in Figure 7.26.



(a)



(b)

**Figure 7.26: Silicon models for (a) Tongue and (b) Uvula**

The silicon models for the tongue and uvula are made of the same material but with different colours. A compression test was conducted using TA.XT Plus Texture Analyzer (Texture Technologies Corp, Hamilton, MA, USA) to determine the density and the modulus of elasticity of the new material. The obtained density is  $\rho = 1030 \text{ kg/m}^3$  which is very close to that of the soft tissues ( $\rho = 1000 \text{ kg/m}^3$ ). The stress-strain relationship for the produced silicon material is shown in Figure 7.27.

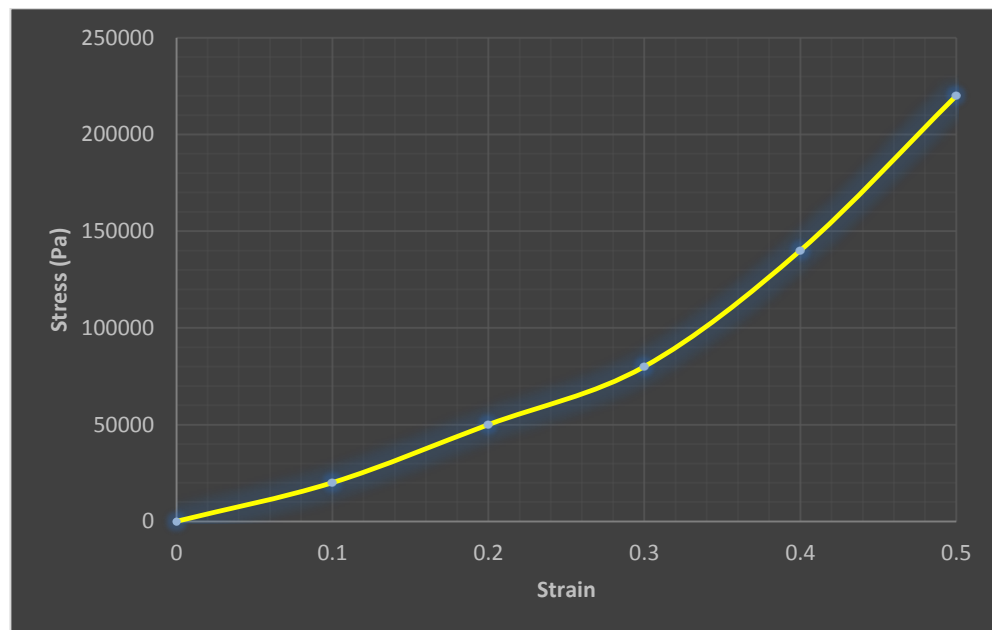


**Figure 7.27: Stress-Strain relationship of silicon rubber**

Figure 7.27 indicates that the relationship is non-linear, therefore piece-wise linear continuous curve fitting was done to determine the value for the modulus of elasticity of the produced soft material, as shown in Figure 7.28.



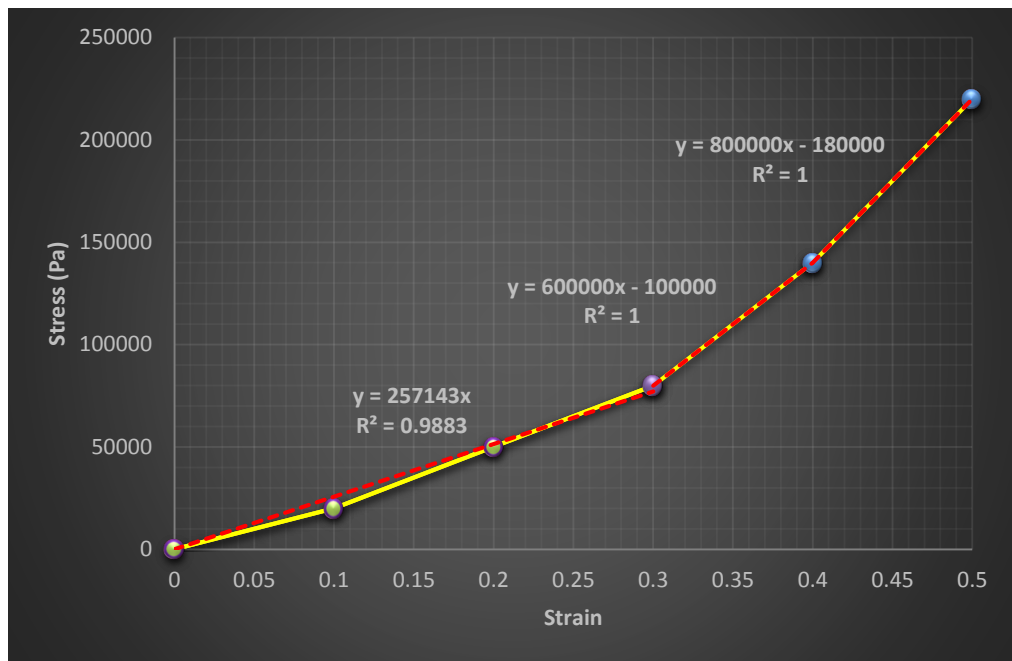


**Figure 7.28: Curve fitting for silicon model**

From Figure 7.28, the modulus of elasticity for the produced silicon rubber material was found to have the value of  $E = 257$  kPa, which is much higher than the range of  $E$  for the real soft tissues (10-35 kPa) as previously used in Chapter 5. The tongue and uvula models were then inserted inside the transparent rig and the model was ready to simulate the UA, as shown in Figure 7.29.

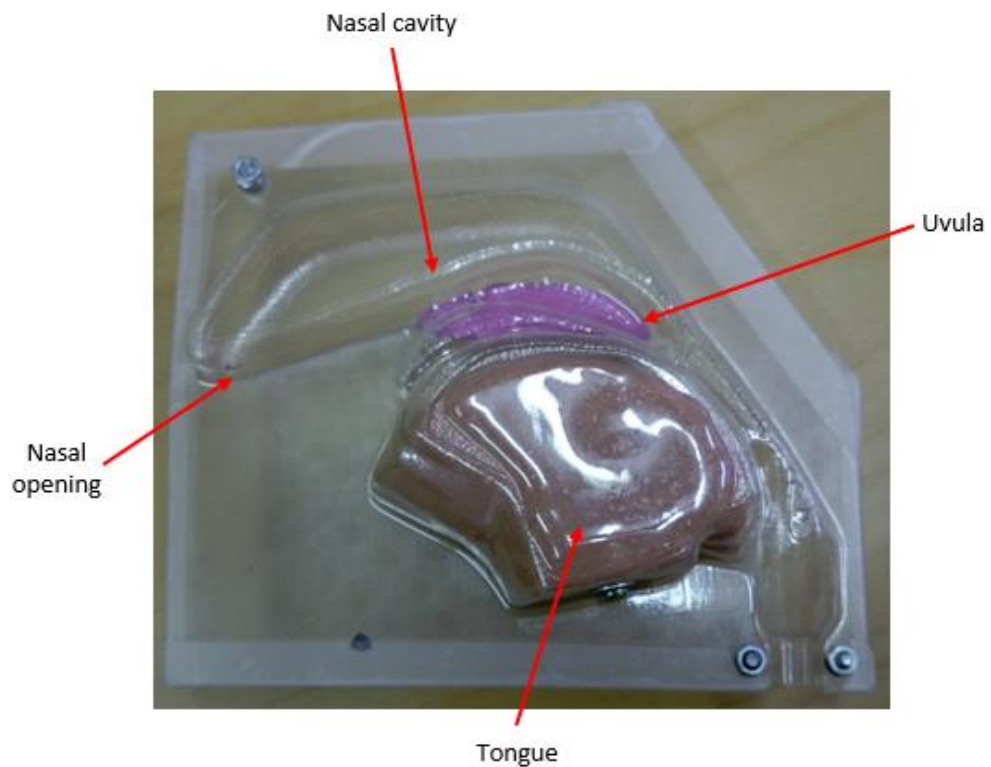


**Figure 7.29: Complete UA with silicon rubber models**

This model was then connected to the laminearisation probe at the end of the experimental setup. Experiments were conducted for both the upright and supine positions to detect the resulting deformations of the tongue and uvula models when excited by the breath cycle. Figures 7.30 and 7.31 show the detected deformations in both positions.

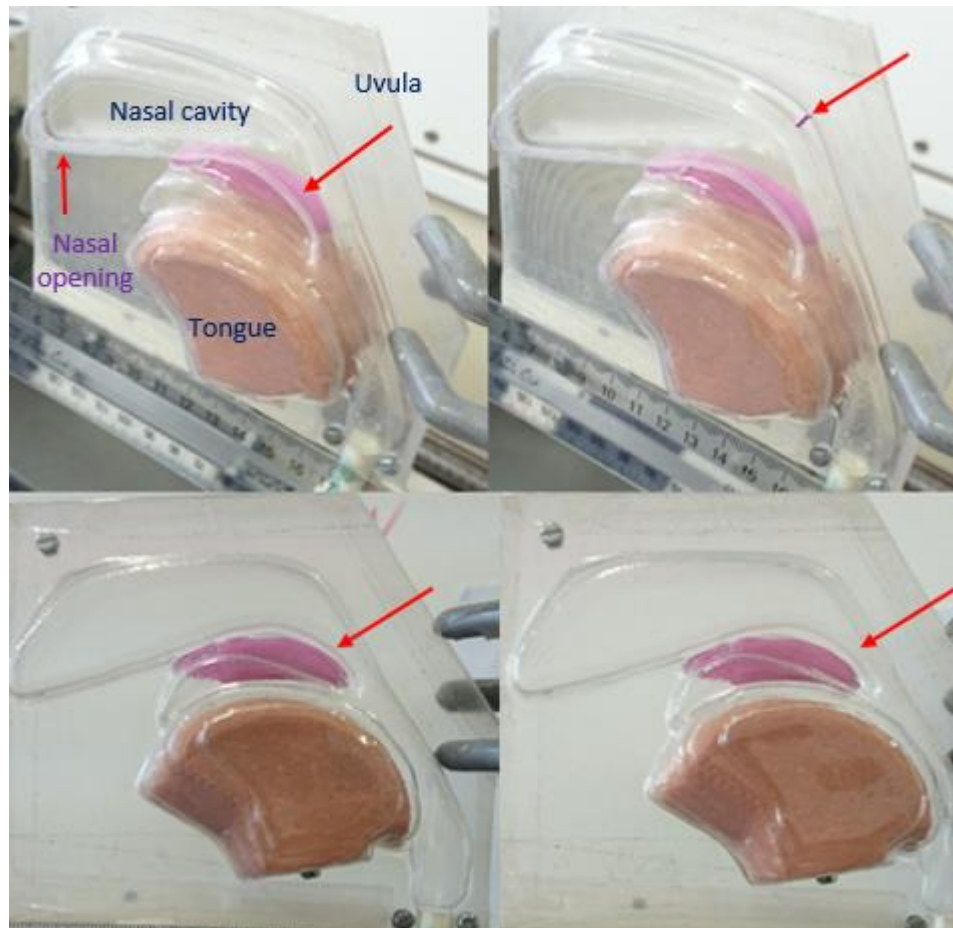


**Figure 7.30: Deformations of silicon models, upright position**

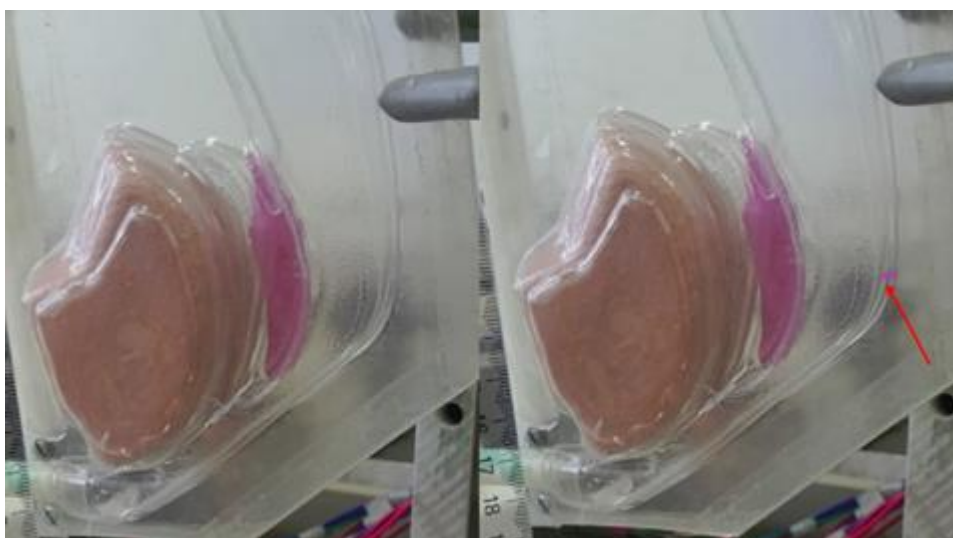


**Figure 7.31: Deformations of silicon models, supine position**

The detected maximum flow rates during inspiration and expiration were -9.6 and 29.7 L/m, respectively for the upright position; -9 and 31.3 L/m, respectively for the supine position.

The images were processed using ImageJ 1.43u software, National Institute of Health, USA. The maximum deformation for the upright position was approximately 1.8 mm produced by the uvula and the rig had an approximate maximum lateral deformation of 5.2 mm. For the supine position, the rig had a maximum lateral deformation of approximately 2.2 mm which is highlighted in the right image of Figure 7.31, however no obvious deformations were detected for the uvula and tongue models, which is expected to be related to the fact that the used silicon material is much harder than the real soft tissues. These results show that the lateral deformation of the rig is larger in the upright position compared to the supine position, which indicates that the airway becomes less responsive in the supine position.

These results were not satisfactory as the detected deformations were less than the obtained results from FSI simulations, and also from the fact that the modulus of elasticity of the obtained material is much higher than the value range of the real soft tissues. Therefore a softer material was required to be looked for and used to produce softer uvula and tongue models.

### 7.3.2 Gelatine Models

A specimen made out of a water-based gelatine (which is softer than the silicon rubber) was produced and a compression test was done using the same tester described in section 7.3.1. The density was found to have the value of  $\rho = 1150 \text{ kg/m}^3$ , and the stress-strain relationship is shown in Figure 7.32.

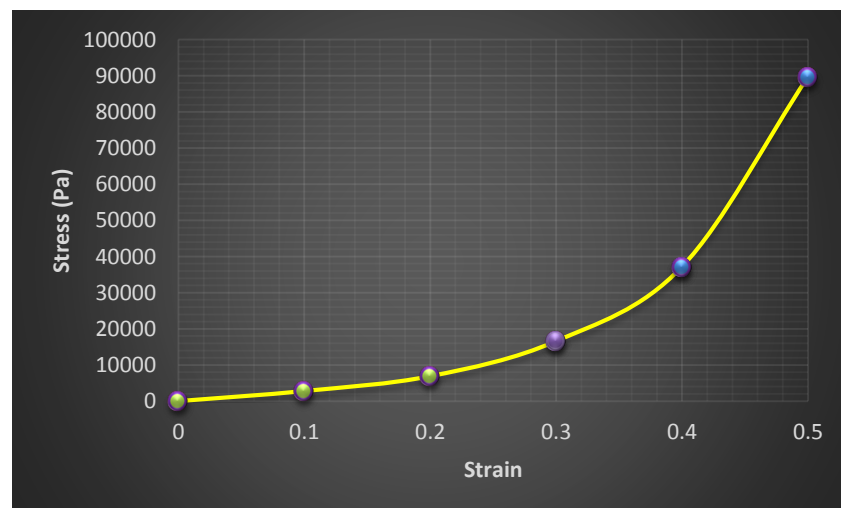


**Figure 7.32: Stress-strain relationship for gelatine material**

The relationship was non-linear, thus piece-wise linear continuous curve fitting was done to determine the value of the modulus of elasticity, as shown in Figure 7.33.

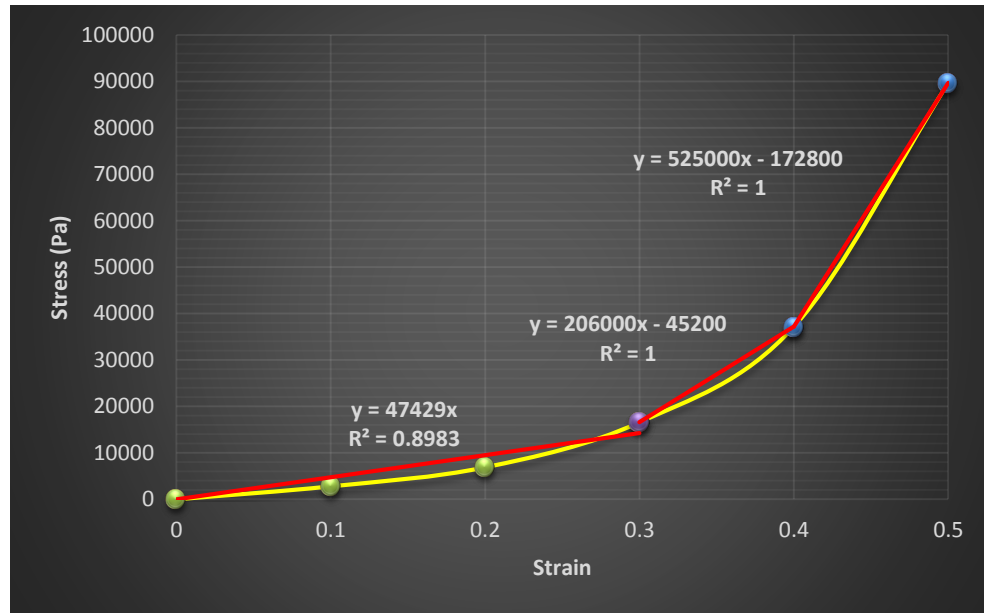


**Figure 7.33: Curve fitting for gelatine model**

From Figure 7.33, the modulus of elasticity for the gelatine material was determined to be approximately  $E = 47$  kPa, which is still higher than the value range of the real soft tissues (10-35 kPa) but softer than the silicon rubber mixture. The natural frequencies of the used gelatine tongue and uvula models were determined by using the Abaqus software. Table 7.1 summarizes the values of the obtained natural frequencies.

**Table 7.1: Natural frequencies for the used gelatine models**

$E = 47$ kPa	$f_{n1}$ (Hz)	$f_{n2}$ (Hz)	$f_{n3}$ (Hz)
<b>Tongue</b>	10.0	31.9	55.1
<b>Uvula</b>	11.3	44.1	102.8

The obtained values for the material properties of the gelatine and the natural frequencies of the gelatine models are very close to the values for the human soft tissues given in Chapters 5 and 6. Therefore, models for the uvula and tongue were produced from the gelatine using the same technique described previously, Figure 7.34. It is noted that the gelatine models were used to be preserved in an air-tight container in a dry and cool environment to make sure that the water content remains the same until all the experiments were conducted.



(a)



(b)

**Figure 7.34: Gelatine (a) Tongue and (b) Uvula models**

The gelatine tongue and uvula models were then inserted into the rig, as shown in Figure 7.35.

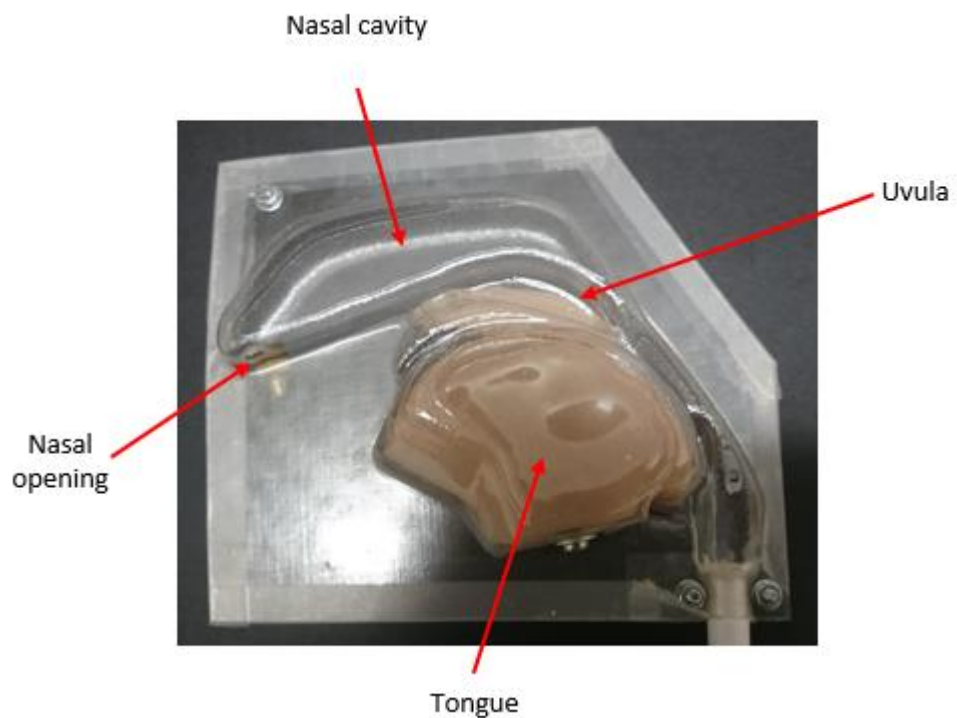


**Figure 7.35: Complete UA with gelatine models**

Experiments were then conducted to detect the deformations of the gelatine models with and without the use of the CPAP, and before and after the use of the PO superimposed to the CPAP.



### (I) Gelatine Models without CPAP

Experiments were conducted for both the upright and supine positions to detect the resulting deformations of the gelatine tongue and uvula models when excited by the breath cycle. Figures 7.36 and 7.37 show the air gap at the rear of the uvula in both positions before running the experiment.

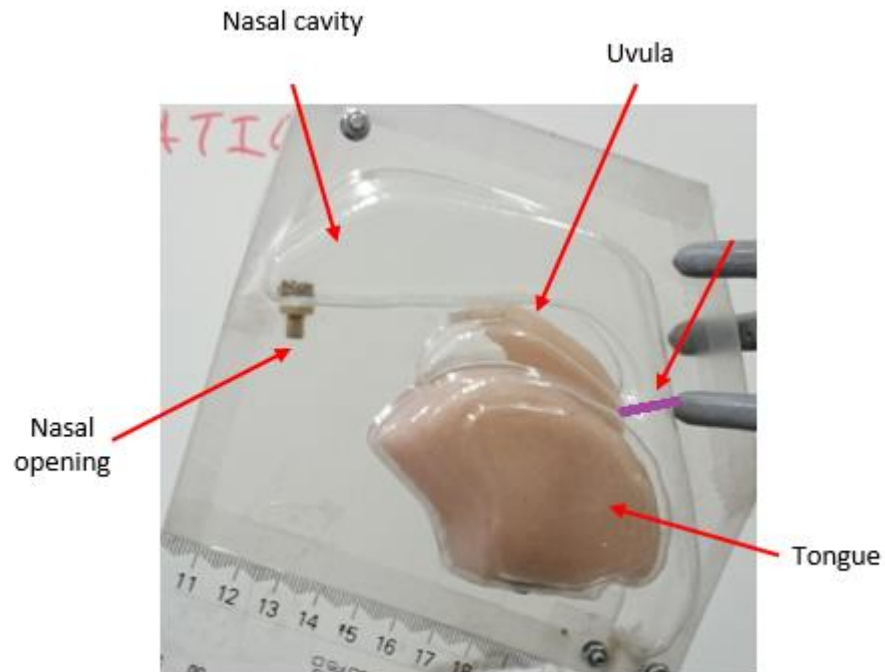


**Figure 7.36: Air gap at the rear of the uvula, upright position**

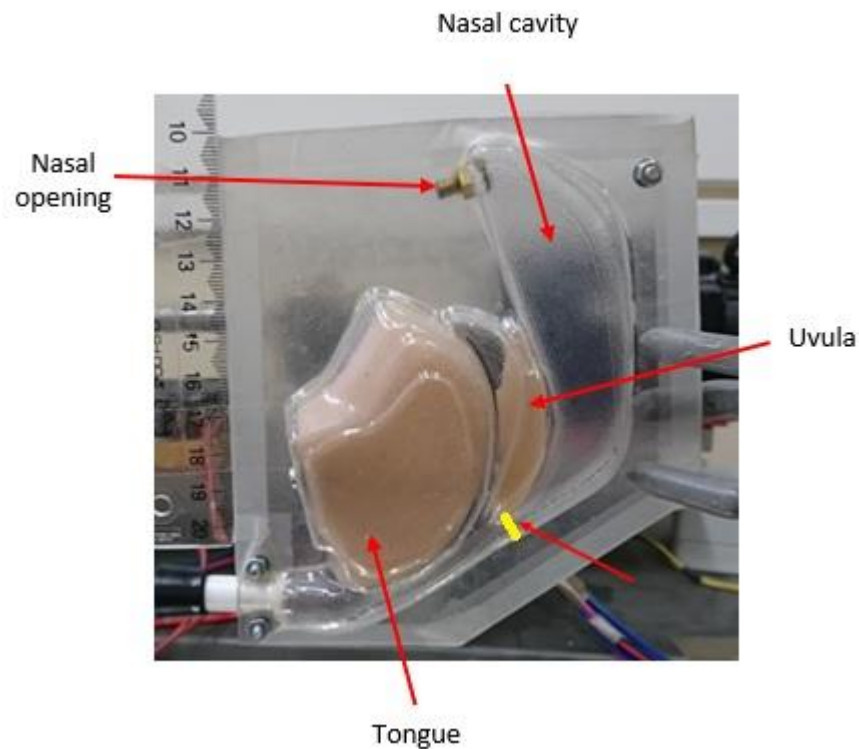


**Figure 7.37: Air gap at the rear of the uvula, supine position**

The highlighted distance in Figure 7.36 represents the minimum air gap at the rear of the uvula in the upright position before the excitation, which was determined by the ImageJ 1.43u software and was found to be around 12.3 mm. For the supine position, this distance was 5.8 mm only as shown by the yellow highlight in Figure 7.37. These values show that the air gap at the rear of the uvula reduced by a distance of 6.5 mm when the model was placed in the supine position, which simulates what occurs in real human upper airways as a result of gravity and muscle relaxation when patients sleep in supine position.

When the setup started exciting the models with the breath cycle, the rig had a maximum lateral deformation of 4.3 mm, Figure 7.38, however no obvious deformations of the uvula were detected in the upright position as the gelatine uvula model was resting on the tongue during the experiments as shown in Figure 7.36.

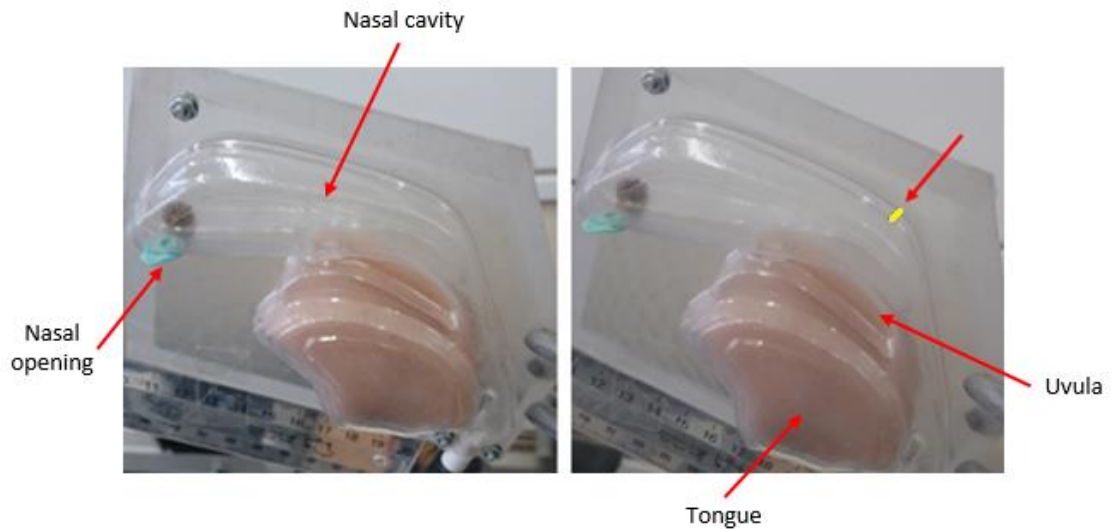


**Figure 7.38: Deformations of the gelatine models, upright position**

For the supine position, Figure 7.39, the initial distance between the tip of the uvula and the airway wall was 5.8 mm as highlighted in Figure 7.39, (a); and when the model was excited by the breath cycle it moved towards the airway and thus reducing that distance to 3.9 mm, Figure 7.39, (b), which shows that the uvula had a maximum deformation of 1.9 mm.

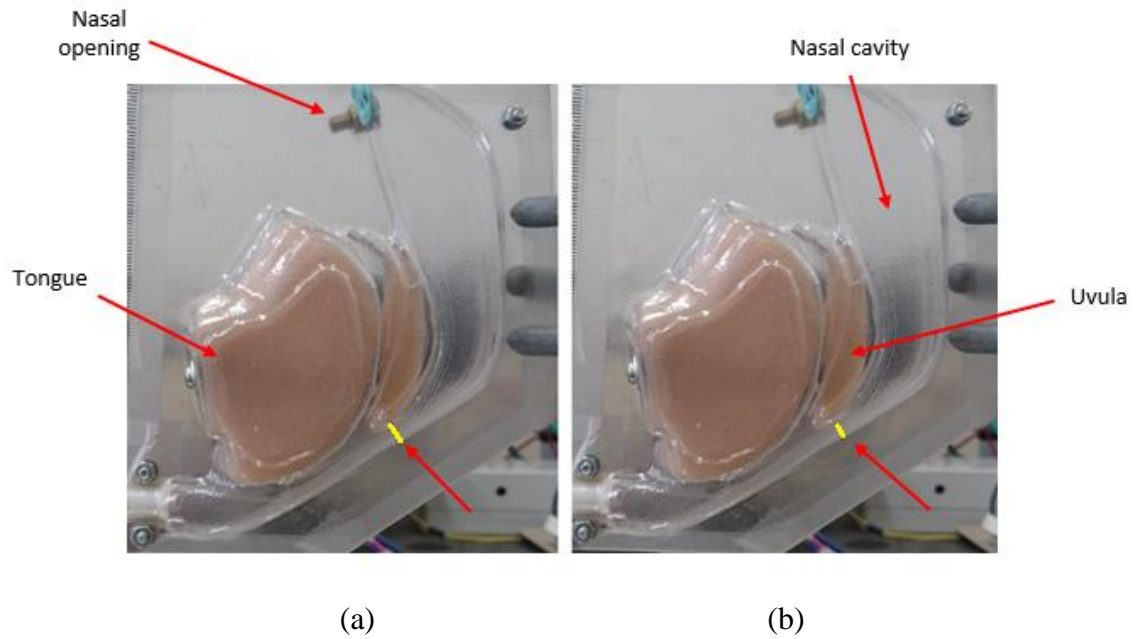


**Figure 7.39: Deformations of the gelatine models, supine position**

The maximum lateral deflection of the rig was measured and found to be 2.5 mm, as shown by the highlighted distance in Figure 7.40 (b).

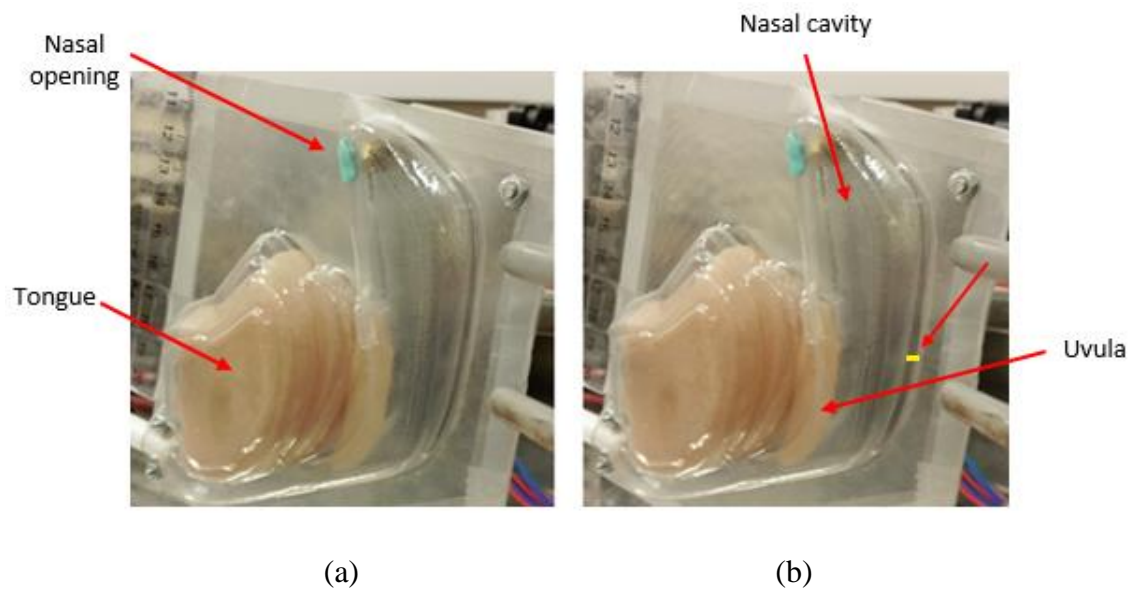


**Figure 7.40: Lateral deformations of the rig, supine position**

## (II) Gelatine Models with CPAP

Experiments were conducted with the CPAP connected to the rig from one nasal opening while the other opening was blocked using a glue tack. The CPAP was set to 4 Cm H<sub>2</sub>O. The reading of the flow rate on the CPAP was 66 L/m before being connected to the rig, then dropped to 2 L/m once connected. When the setup started working, the flow rate reading on the CPAP fluctuated between 4-6 L/m, where the value of 6 L/m was



recorded at the end of the inspiratory breathing phase and the value of 4 L/m was recorded at the end of the expiratory breathing phase. The maximum lateral deformation of the rig in the upright position was 7.7 mm, as highlighted in Figure 7.41, (b).

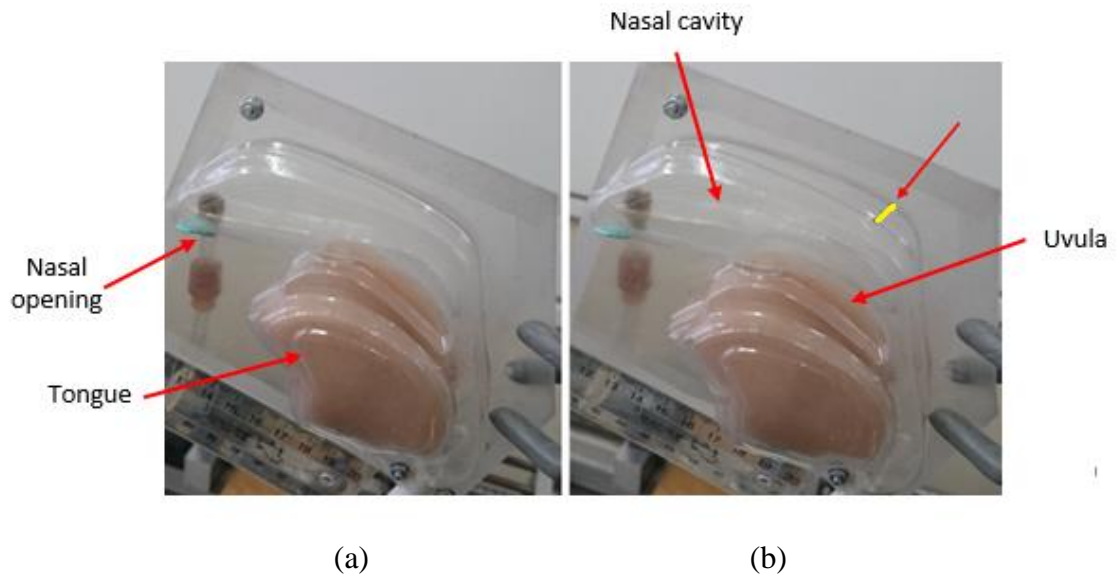


**Figure 7.41: Lateral Deformations of the rig in the upright position (a) zero deformation, (b) maximum deformation; 4 Cm H<sub>2</sub>O**

For the supine position, Figure 7.42, the maximum lateral deformation of the rig was 7.1 mm which is highlighted in Figure 7.42 (b); while Figure 7.42 (a) shows the zero deformation case.

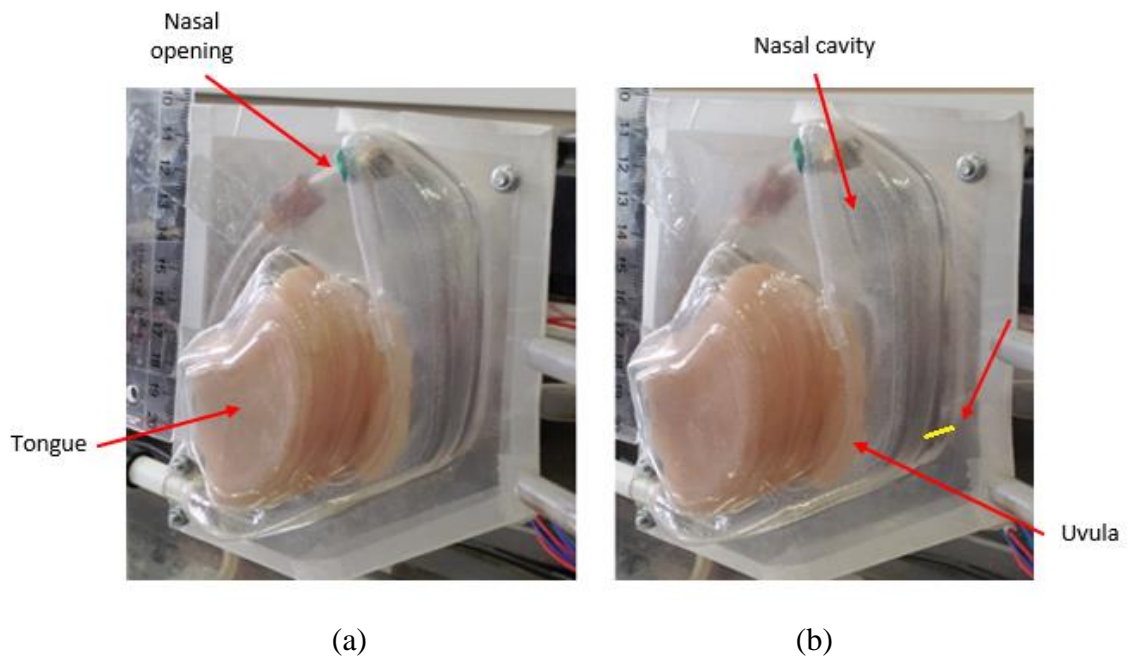


**Figure 7.42: Lateral deformations of the rig in supine position (a) zero deformation, (b) maximum deformation; 4 Cm H<sub>2</sub>O**

The deformations of the uvula could not be accurately detected from Figure 7.42, therefore more photos were taken to show the resulting deformations of the uvula as shown in Figure 7.43.

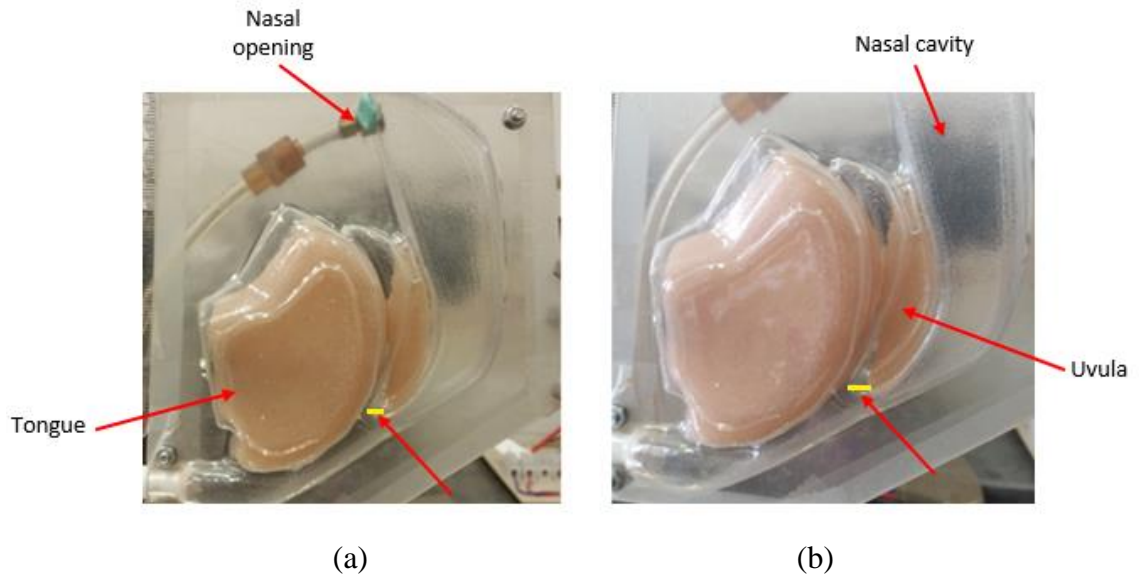


**Figure 7.43: Deformations of the uvula in the supine position (a) zero deformation, (b) maximum deformation; 4 Cm H<sub>2</sub>O**

The highlighted distance in Figure 7.43 (a) before excitation was measured and found to be 2.3 mm, while after excitation it was 4.5 mm which is the highlighted distance in Figure 7.43 (b). This means that the maximum deformation of the uvula is approximately 2.2 mm which is larger than the detected value without the use of the CPAP which was only 1.9 mm.

The same above procedure was repeated for a CPAP of 5 Cm H<sub>2</sub>O. The reading of the flow rate on the CPAP was 74 L/m before being connected to the rig, then dropped to 2 L/m once connected. When the setup started working, the flow rate fluctuated between 4-6 L/m, where the value of 6 L/m was recorded at the end of the inspiration and the value of 4 L/m was recorded at the end of the expiratory breathing phase. The maximum lateral deformation of the rig in the upright position was 8.1 mm, as highlighted in Figure 7.44 (b).

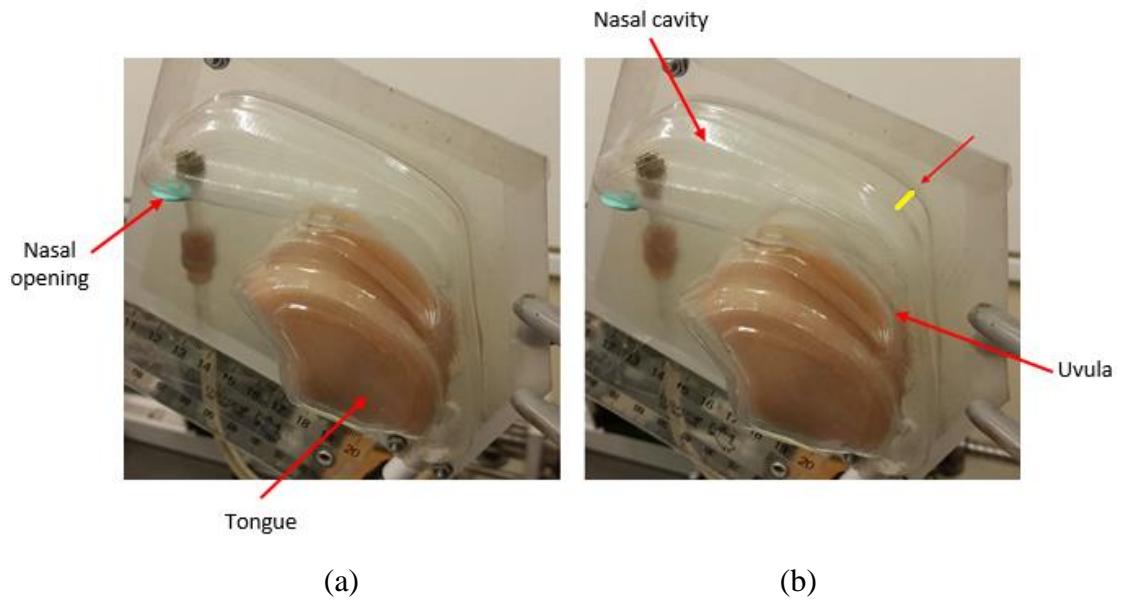


**Figure 7.44: Lateral deformations of the rig in the upright position (a) zero deformation, (b) maximum deformation; 5 Cm H<sub>2</sub>O**

For the supine position, the maximum lateral deformation of the rig was 7.3 mm which is highlighted in Figure 7.45; while the maximum deformation of the uvula was approximately 2.3 mm as seen in Figure 7.46 (b). Table 7.2 summarizes the obtained results before and after using the CPAP.

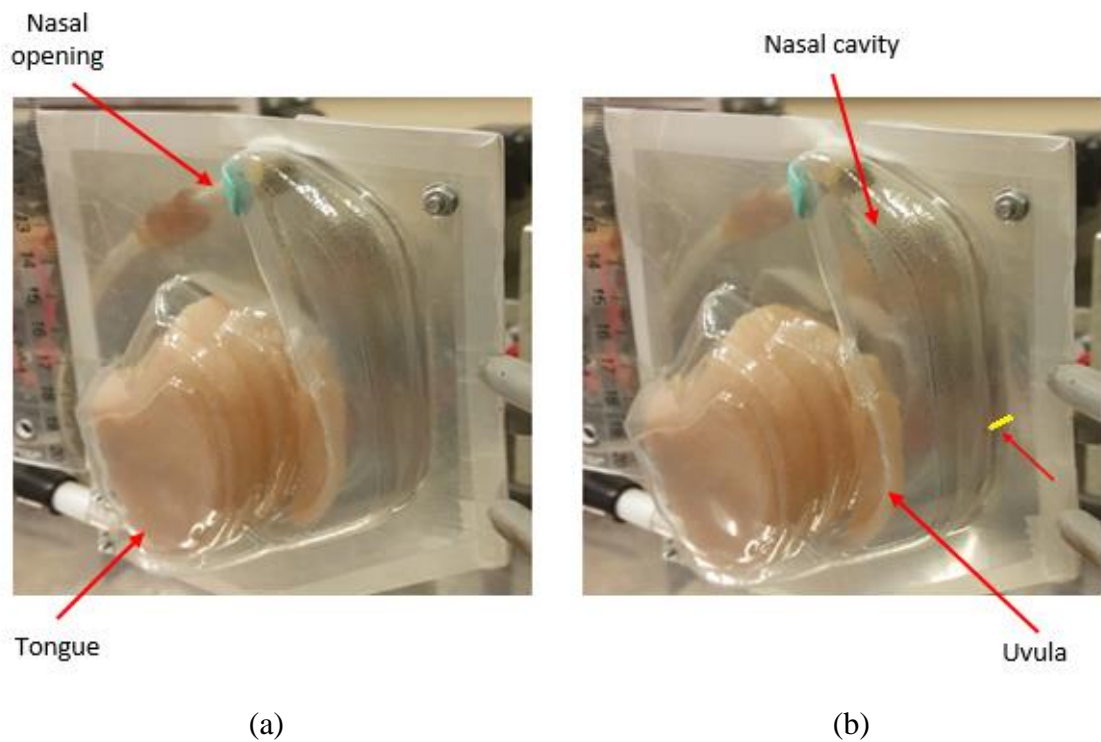


**Figure 7.45: Lateral deformations of the rig in supine position (a) zero deformation and (b) maximum deformation; 5 Cm H<sub>2</sub>O**

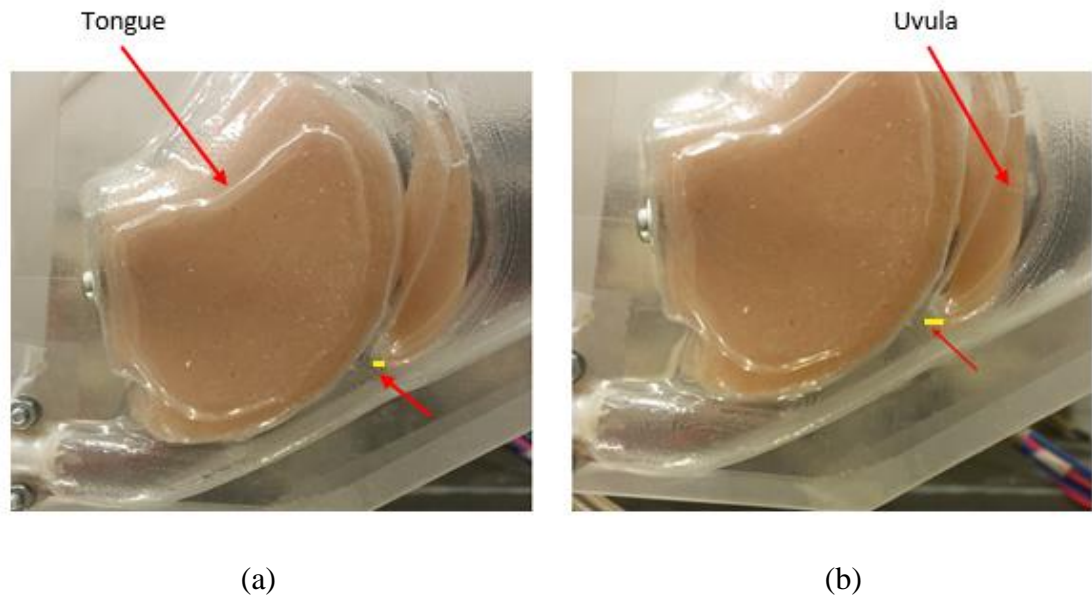


**Figure 7.46: Deformations of the uvula, supine position (a) zero deformation, (b) maximum deformation; 5 Cm H<sub>2</sub>O**

**Table 7.2: Summary of the obtained deformations with and without the CPAP**

Max. Deformation (mm)	Without CPAP	With CPAP	
		4 Cm H <sub>2</sub> O	5 Cm H <sub>2</sub> O
Uvula, upright position	0	0	0
Uvula, supine position	1.9	2.2	2.3
Rig, upright position	4.3	7.7	8.1
Rig, supine position	2.5	7.1	7.3

The data in Table 7.2 shows that the maximum lateral deformations of the rig in the upright position with and without the use of the CPAP are larger than the obtained deformations in the supine position; which means that the airway becomes less responsive to external excitation while in supine position. These data also show that the deformations of the uvula in the supine position with the use of the CPAP are larger than the case without using the CPAP. Also all the deformations increase with increasing the used CPAP pressure.

### (III) Effect of PO

Experiments were conducted to investigate the effects of the PO when superimposed on the CPAP, by using the SmartShaker (model K2004E01, The Modal



Shop, Inc.), Figure 7.47, which can provide the oscillations with different amplitudes and frequencies; which are pre-set by a signal or function generator.



**Figure 7.47: Modal Shop SmartShaker**

A signal generator (Tektronix, model number AFG3022B), Figure 7.48, was used to provide the excitation signal to the SmartShaker. Calibration has been done at earlier stages and showed that when this signal generator provide a signal with an amplitude of 50 mVolts, the shaker produces a pressure equivalent to 1 Cm H<sub>2</sub>O.



**Figure 7.48: Tektronix signal generator**

The CPAP and the SmartShaker were connected to the UA model via a Y-shaped connection, Figure 7.49, and experiments were conducted for CPAP of 4 Cm H<sub>2</sub>O and a frequency of 30 and 40 Hz with an amplitude of 50 mVolts on the SmartShaker; which is equivalent to 5 Cm H<sub>2</sub>O in order to compare between the results before and after using the PO when using the same value for the total static pressure of 5 Cm H<sub>2</sub>O.

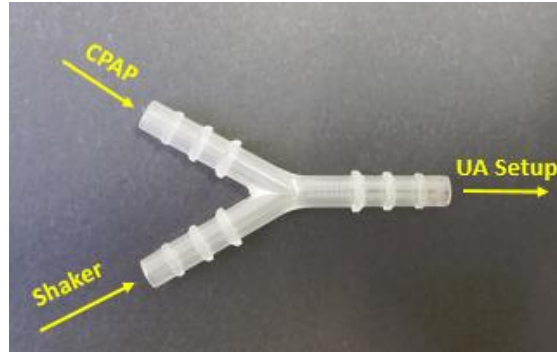


**Figure 7.49: Y-shaped connection**

Experiments were conducted in both the upright and supine positions for a frequency of 30 and 40 Hz, as described below.

#### **(I) Upright Position**

The maximum lateral deformation of the rig was 9.3 mm for  $f = 30$  Hz, and 13.3 mm for  $f = 40$  Hz as shown by the highlighted deformations in Figures 7.50 and 7.51; respectively.

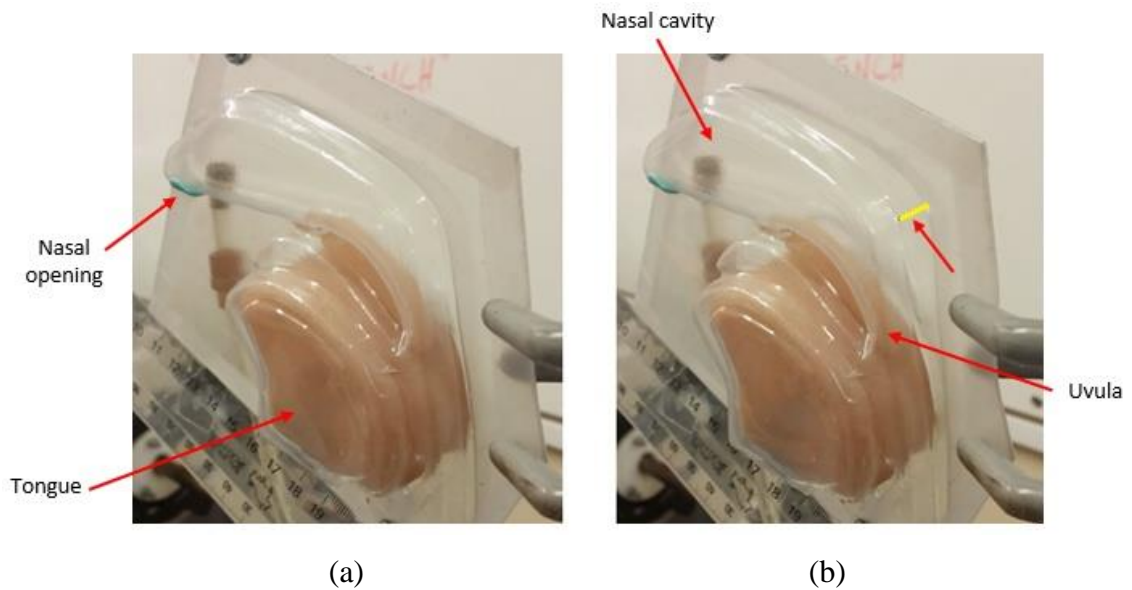


**Figure 7.50: Lateral deformations of the rig in the upright position (a) zero and (b) maximum deformation; 4 Cm H<sub>2</sub>O + 1 Cm H<sub>2</sub>O with PO,  $f = 30$  Hz**

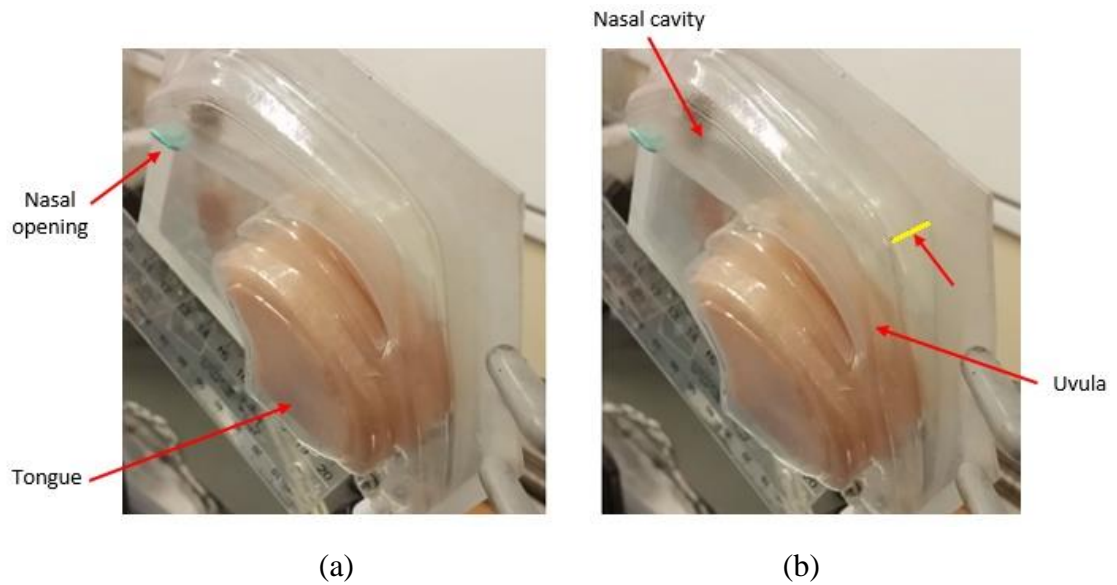


**Figure 7.51: Lateral deformations of the rig in the upright position (a) zero and (b) maximum deformation; 4 Cm H<sub>2</sub>O + 1 Cm H<sub>2</sub>O with PO,  $f = 40$  Hz**

## (II) Supine Position

The maximum lateral deformation of the rig was 7.7 mm for  $f = 30$  Hz, and 8.6 mm for  $f = 40$  Hz as shown by the highlighted deformations in Figure 7.52 and 7.53; respectively.

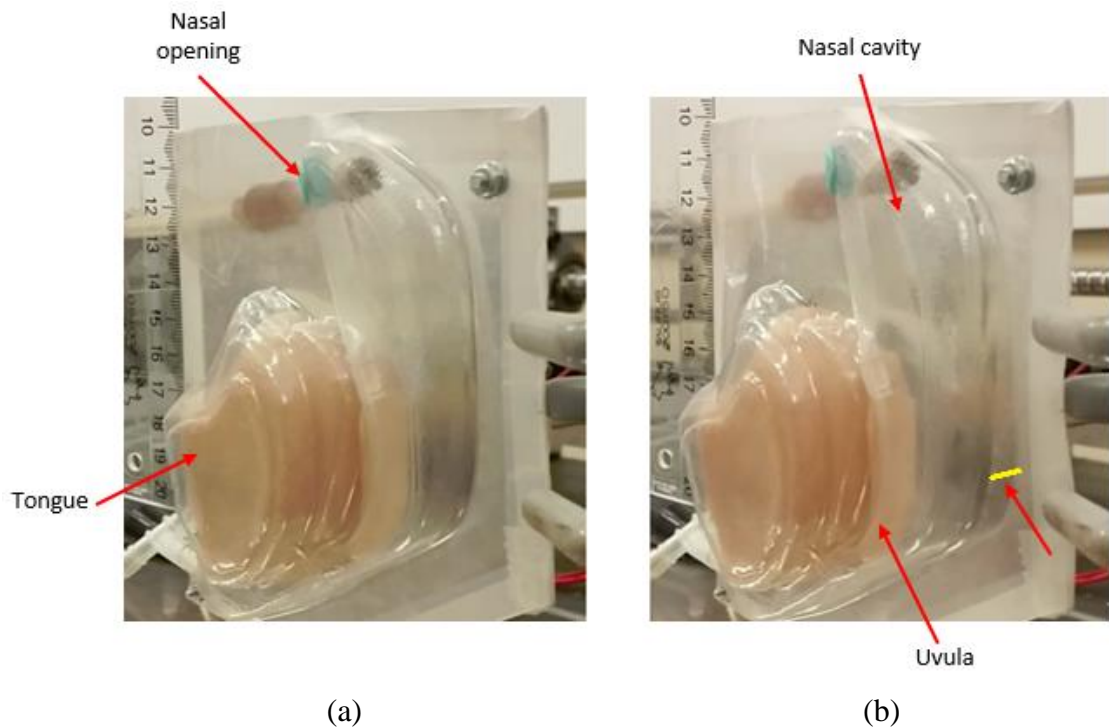


**Figure 7.52: Lateral deformations of the rig in supine position (a) zero and (b) maximum deformations; 4 Cm H<sub>2</sub>O + 1 Cm H<sub>2</sub>O with PO,  $f = 30$  Hz**

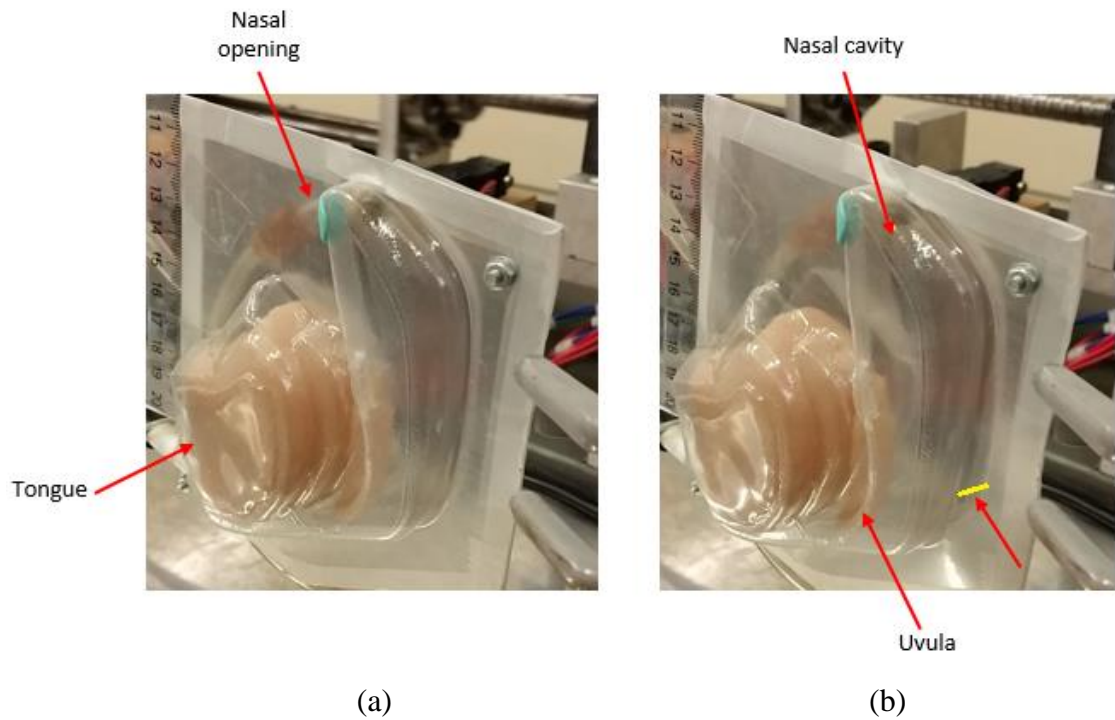


**Figure 7.53: Lateral deformations of the rig in supine position (a) zero and (b) maximum deformations; 4 Cm H<sub>2</sub>O + 1 Cm H<sub>2</sub>O with PO,  $f = 40$  Hz**

For  $f = 40$  Hz, the maximum deformation of the uvula was determined by the highlighted distance in Figure 7.54, which was 2.2 mm and 4.9 mm, before and after the excitation; respectively. Therefore the maximum deformation of the uvula was 2.7 mm. For  $f = 30$  Hz, the maximum deformation of the uvula models was 2.5 mm.

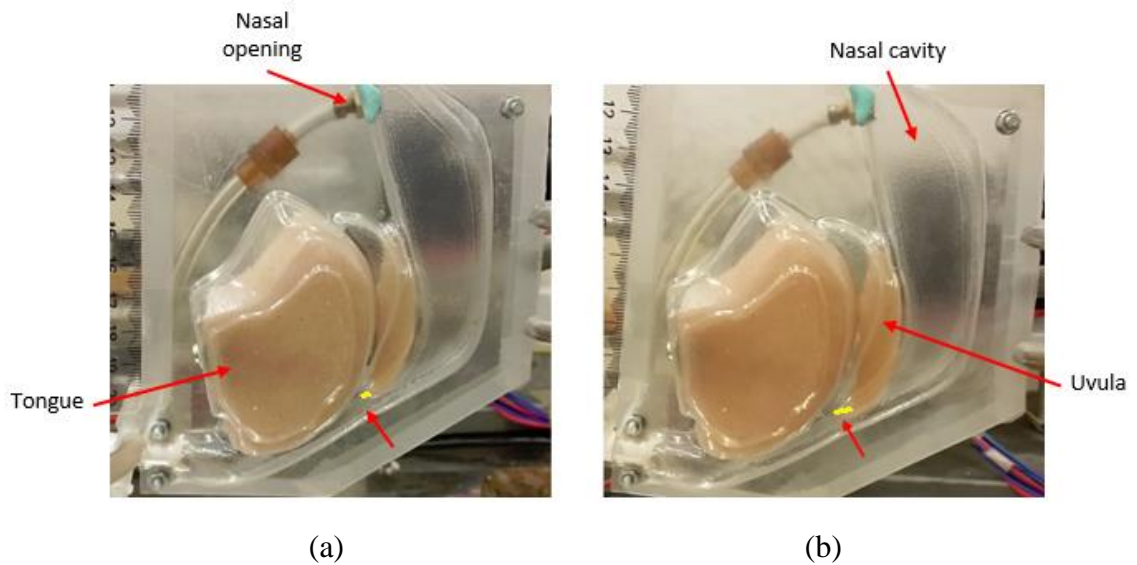


**Figure 7.54: Deformations of the uvula, supine position (a) zero and (b) maximum deformation; 4 Cm H<sub>2</sub>O + 1 Cm H<sub>2</sub>O with PO,  $f = 40$  Hz**



The obtained values for the maximum lateral deformations of the rig and the deformations of the uvula are summarized in Table 7.3 before and after using the PO.

**Table 7.3: Summary of the obtained deformations**

Max. Deformation (mm)	CPAP alone, 5 Cm H <sub>2</sub> O	CPAP with PO	
		30 Hz	40 Hz
Uvula, upright position	0	0	0
Uvula, supine position	2.3	2.5	2.7
Rig, upright position	8.1	9.3	13.3
Rig, supine position	7.3	7.7	8.6

#### 7.4 Closure

This chapter described the experimental setup, and provided a detailed description of its components. It also described the experimental modelling of the UA system using silicon and gelatine materials. Also, this chapter presented the resulting deformations before and after using the CPAP, as well as the resulting deformations when using the PO superimposed on the CPAP in both the upright and supine positions. The next chapter will discuss and summarise all the obtained results and hold comparisons between the results of the healthy subjects and OSA patients. It will also describe the recommendations and the proposed future work.

## **Chapter 8**

### **Discussion and Future Work**

#### **8.1 Introduction**

This chapter discusses the main outcomes of this study and explains the proposed future work. Section 8.2 describes the obtained results from the conducted study on ten morbid obese OSA patients promoted for bariatric surgery before and after surgical intervention. Section 8.3 discusses the results of investigating the dynamic characteristics of healthy and unhealthy upper airways examined in Chapters 5 and 6, respectively. The conditions of collapse and the effects of PO on the UA are discussed in section 8.4. Section 8.5 discusses the experimental results obtained in Chapter 7, and the proposed future work is presented in section 8.6.

A comparison between the obtained theoretical and experimental results were meant to be conducted, however the experimental UA model differs from the real model in many aspects such as:

- The elasticity of the gelatine models (used in experimental modelling) is remarkably larger than that of the real soft tissues (used in theoretical modelling).
- The purpose of the theoretical modelling was to determine the conditions of the UA collapse as well as the performance of the UA when the CPAP is used to prevent the collapse with and without using the PO superimposed on the CPAP; while the experimental modelling focused only on determining the deformations of the UA before and after using the CPAP with and without the use of the PO with no detected sign of UA collapse (due to different material properties between the materials used in the experimental modelling and those used in the theoretical modelling), therefore the boundary conditions at the outlet were not the same in the two modelling techniques due to flow limitations, and consequently the detected deformations of the uvula and tongue models from both modelling methods were relatively different.
- The elasticity of the used silicon duct in the theoretical modelling is very different from the used plastic sheet in producing the rig used in the experimental setup.
- Also, many attempts trying to produce a rig with the same geometry as that of a real UA were unsuccessful, this is due to the very irregular geometry of the real model.

- The UA walls and soft tissues were represented in the simulations by one enclosure, while the experimental rig consisted of separate models for the UA walls, tongue and uvula which included all the boundary conditions and consequently shows the difference between the two models.

Therefore, this section holds comparisons between the obtained theoretical results in the healthy and unhealthy groups, and discuss the effect of using the PO on the performance of the UA theoretically and experimentally to prove that the trend of using the PO to keep the airway open at lower pressures is successful. No comparisons between the obtained theoretical and experimental results were possible due to the aforementioned reasons.

## **8.2     Bariatric Surgery**

The outcomes of this preliminary study with 10 subjects show that bariatric surgery has succeeded to improve the:

- Upper airway volume (V),
- Body mass index (BMI),
- Volume body mass index (VBMI), and
- Apnea/hypopnea index (AHI).

The obtained data and results are summarized in Table 8.1. These results suggest that bariatric surgery may be effective for middle-aged (under the age of 50) morbid obese patients diagnosed with moderate-to-severe OSA. For this group the surgery reduced weight and resolved OSA symptoms.

Also, the outcomes of this study suggest that the newly introduced parameter, VBMI, may be used to evaluate the success of the surgical intervention for morbid obese OSA patients below the age of 60, replacing the relatively expensive and time consuming follow up PSGs especially for those who cannot afford the co-pay of such follow ups.

**Table 8.1: Summary of the obtained data and results for bariatric surgery, B-Baseline, M-Months**

Patient ID	Age	BMI (kg/m <sup>2</sup> )			AHI (events/hr)			V (mm <sup>3</sup> )			VBMI (m <sup>3</sup> /(kg/m <sup>2</sup> )) $\times 10^{-9}$		
		B	6M	12M	B	6M	12M	B	6M	12M	B	6M	12M
1	58	48.3	36.2	33.8	73	37	29	14907.1	15202.9	16642.9	322.7	420.0	492.4
2	39	60.3	40.7	32.8	63	9	1	12575.8	14842.1	16442.3	208.2	364.7	501.3
3	28	54.7	35.3	28.8	22	0	0	12638.7	15715.2	16942.5	231.1	445.2	588.3
4	31	51.4	33.5	33.3	2	3	4	40441.5	23533.8	22914.2	786.8	702.5	688.1
5	60	40.0	29.3	26.6	34	44	N/A	14143.1	10813.2	16682.3	353.6	369.1	627.2
6	41	50.4	34.9	30.0	29	12	0	23982.1	24486.2	24059.6	475.8	701.6	802.0
7	54	36.7	25.5	23.2	32	19	N/A	22593.5	29894.5	24157.3	594.6	1172.3	1041.3
8	49	44.5	34.7	34.6	95	5	N/A	8715.9	10597.9	13129.5	186.2	305.4	379.5
9	30	47.6	33.3	30.8	16	5	0	9033.3	14967.8	12313.3	189.8	449.5	399.8
10	62	47.1	33.3	28.9	15	23	N/A	11289.4	17432.0	19338.7	227.2	523.5	669.2
Mean $\pm$ SD		48.5 $\pm$ 6.5	33.7 $\pm$ 4.0	30.3 $\pm$ 3.6	38.1 $\pm$ 29.4	15.7 $\pm$ 15.0	5.6 $\pm$ 10.2	17032.0 $\pm$ 9691.8	17748.6 $\pm$ 6258.5	18262.3 $\pm$ 4256.6	357.6 $\pm$ 202.4	545.4 $\pm$ 258.0	618.9 $\pm$ 198.7

### **8.2.1 Recommendations and Future Work for Bariatric Surgery**

The constructed three dimensional models need to be simulated using the computational fluid dynamics methods (CFD) to investigate the UA characteristics and predict the conditions of collapse. Also a larger number of participants of both genders needs to be recruited to demonstrate the outcomes of this research and investigate the effectiveness of bariatric surgery especially in the male gender which is considered as a main risk factor for OSA.

For patients with age range 50-60 years, it is recommended to collect follow up CT and PSG data at longer time intervals postoperatively to check the long term outcomes of the surgical intervention (due to slower response of the UA muscles in this age group). Finally, for patients who are 60 years of age and older, pharmaceutical research is required to develop effective drugs that can stimulate and improve the response of their UA muscles and consequently improve the outcomes of the surgery to alleviate OSA symptoms in addition to the noticeable improvements in their BMI.

## **8.3 Dynamic Characteristics of Healthy and Unhealthy Upper Airways**

This section sets comparisons and correlations between the UA parameters in the healthy and unhealthy subjects obtained in Chapters 5 and 6; including the volumes of air, tongue, uvula and the entire UA, as well as the air gaps at the rear of the uvula and tongue at the MSP. Also comparisons between the natural frequencies of healthy and unhealthy tongue and uvula models are presented, as well as the correlation between the UA volume and the BMI in both groups.

The obtained results from Chapters 5 and 6 are summarized in Table 8.2 for discussion and comparison purposes; and will be discussed thoroughly in sections 8.3.1 to 8.3.8.

**Table 8.2: Summary of the obtained results for healthy and unhealthy subjects**

	Healthy Subjects	OSA Patients
Age (years)	31.1 ± 10.1	55.0 ± 8.2
BMI (kg/m <sup>2</sup> )	25.4 ± 1.5 (overweight)	36.6 ± 9.4 (morbid obese)
Min. gap/tongue (mm)	7.7 ± 4.2	8.2 ± 2.1
Min. gap/uvula (mm)	5.2 ± 2.8	6.4 ± 1.2
First f <sub>n</sub> (Hz), uvula	9.5 ± 0.7 (E = 25 kPa)	10.1 ± 2.8 (E = 25 kPa)
Second f <sub>n</sub> (Hz), uvula	34.0 ± 2.7 (E = 25 kPa)	36.5 ± 6.4
Third f <sub>n</sub> (Hz), uvula	75.7 ± 10.0 (E = 25 kPa)	85.0 ± 12.6
First f <sub>n</sub> (Hz), tongue	6.7 ± 1.0 (E = 15 kPa) 8.7 ± 1.3 (E = 25 kPa)	5.3 ± 0.5 (E = 15 kPa) 6.8 ± 0.7 (E = 25 kPa)
Second f <sub>n</sub> (Hz), tongue	21.9 ± 1.4 (E = 15 kPa) 28.2 ± 1.8 (E = 25 kPa)	17.8 ± 1.2 (E = 15 kPa) 23.0 ± 1.5 (E = 25 kPa)
Third f <sub>n</sub> (Hz), tongue	34.1 ± 1.0 (E = 15 kPa) 44.0 ± 1.2 (E = 25 kPa)	28.2 ± 2.1 (E = 15 kPa) 36.4 ± 2.8 (E = 25 kPa)
Air volume (mm <sup>3</sup> )	7824.0-18803.1 (12272.4 ± 4161.6)	8691.9-33307.1 (18830.1 ± 8172.5)
Uvula volume (mm <sup>3</sup> )	941.0-1667.0 (1250.4 ± 248.0)	1589.5-2453.3 (1942.9 ± 234.0)
Tongue volume (mm <sup>3</sup> )	56594.6-81243.6 (66536.2 ± 10097.5)	104140.1-126697.7 (124540.0 ± 11917.4)
Total volume (mm <sup>3</sup> )	68498.5-90415.7 (78151.2 ± 10146.7)	114779.3-175554.7 (145592.8 ± 17341.6)
% V <sub>tongue</sub> /V <sub>total</sub>	81.8-89.9 (85.0 ± 3.4)	78.3-90.7 (85.9 ± 4.2)
% V <sub>uvula</sub> /V <sub>total</sub>	1.3-1.9 (1.6 ± 0.2)	1.1-1.7 (1.3 ± 0.2)
% V <sub>air</sub> /V <sub>total</sub>	8.7-16.8 (13.5 ± 3.4)	7.6-20.5 (12.8 ± 4.3)

### 8.3.1 Air Volume

The values of the air volume for the healthy subjects and OSA patients were 12272.4±4161.6 mm<sup>3</sup> (13.5±3.4% of the entire UA volume) and 18830.1±8172.5 mm<sup>3</sup> (12.8±4.3% of the entire UA volume), respectively; which shows that the participating OSA patients seem to have larger air volume in comparison to the healthy participants, however there is no remarkable difference between the two groups in regards to the

percentages at which the air models occupy from the UA. The fact that the participating OSA patients have larger air volumes compared to the healthy participants contradicts the previous findings which have reported that OSA patients have narrower airways compared to the healthy subjects. These results suggest that air volume is not the main contributor to the UA obstruction and/or collapse.

### **8.3.2 Tongue Volume**

The values of the tongue volume were  $66536.2 \pm 10097.5 \text{ mm}^3$  ( $85.0 \pm 3.4\%$  of the entire UA volume) and  $124540.0 \pm 11917.4 \text{ mm}^3$  ( $85.9 \pm 4.2\%$  of the entire UA volume) for the healthy subjects and OSA patients, respectively; which shows that the participating OSA patients have extremely larger tongues than their healthy counterparts, while there is no big difference between the two groups in regards to the percentages that the tongue models occupy from the UA.

### **8.3.3 Uvula Volume**

The values of the uvula volume were  $1250.4 \pm 248.0 \text{ mm}^3$  ( $1.57 \pm 0.23\%$  of the entire UA volume) for the healthy subjects and  $1942.9 \pm 234.0 \text{ mm}^3$  ( $1.3 \pm 0.2\%$  of the entire UA volume) for the OSA patients, which shows that the OSA participants have extremely larger uvulas than their healthy counterparts but with relatively less percentage to the entire UA volume.

### **8.3.4 Entire UA Volume**

The values of the entire UA volume were  $78151.2 \pm 10146.7 \text{ mm}^3$  for the healthy subjects and  $145592.8 \pm 17341.6 \text{ mm}^3$  for the OSA patients, which shows that the participating OSA patients have larger total UA volumes than the healthy participants.

### **8.3.5 Air Gaps at the Rear of the Mouth**

The values of the minimum air gaps at the rear of the uvula and tongue at the MSP were  $5.2 \pm 2.8 \text{ mm}$  and  $7.7 \pm 4.2 \text{ mm}$ , respectively for the healthy subjects;  $6.4 \pm 1.2 \text{ mm}$  and  $8.2 \pm 2.1 \text{ mm}$ , respectively for the OSA patients. These results show that the OSA participants have relatively larger air gaps at the rear of uvula and tongue. This suggests that air gap is not the main contributor for UA collapse.

### **8.3.6 Natural Frequency**

The normal control values of the first natural frequency for the uvula ( $E = 25 \text{ kPa}$ ) and tongue ( $E = 15 \text{ kPa}$ ) were  $9.5 \pm 0.7 \text{ Hz}$  and  $6.7 \pm 1.0 \text{ Hz}$ , respectively for the healthy subjects;  $10.1 \pm 2.8 \text{ Hz}$  and  $5.3 \pm 0.5 \text{ Hz}$ , respectively for the OSA patients. These results

show no big difference in the obtained natural frequencies for the uvula and tongue models between the two participating groups. The results also show that the natural frequencies for the unhealthy uvula models are slightly higher than the obtained values for the healthy uvula models, while the opposite is noticed for the tongue models as the natural frequencies of the unhealthy tongue models are less than the obtained results from the healthy models.

### 8.3.7 BMI

The participating OSA group is classified as morbid obese, while the healthy group was overweight; which demonstrates the fact that obesity is a major risk factor for OSA [148-154] and that OSA prevalence is much higher in the obese subjects [286-288].

### 8.3.8 VBMI

The above results may be misleading as the two groups have huge differences such as age range, ethnicities, body size and weight categories (the healthy group is classified as overweight while the unhealthy group is morbid obese). Therefore the VBMI was used, which was firstly introduced by us in Chapter 4 to combine the changes in the UA characteristics to the size of the body. It is defined as the ratio of an element ( $\text{mm}^3$ ) to the BMI ( $\text{kg}/\text{m}^2$ ). Table 8.3 summarizes the obtained values for the VBMI.

**Table 8.3: VBMI for healthy and unhealthy subjects**

<b>VBMI</b> <b>[<math>\text{mm}^3/(\text{kg}/\text{m}^2)</math>]</b>	<b>Healthy Subjects</b>	<b>OSA Patients</b>
<b>Air</b>	290.9-793.4 ( $486.3 \pm 175.3$ )	263.4-951.6 ( $527.7 \pm 226.6$ )
<b>Uvula</b>	37.8-60.2 ( $49.0 \pm 7.8$ )	48.7-73.4 ( $55.2 \pm 10.9$ )
<b>Tongue</b>	2143.7-3072.3 ( $2627.5 \pm 383.3$ )	3057.3-4353.9 ( $3716.0 \pm 479.5$ )

This work demonstrates that OSA patients compared with healthy subjects have: (I) slightly larger  $(\text{VBMI})_{\text{uvula}}$ ; (II) larger  $(\text{VBMI})_{\text{air}}$  and (III) much larger  $(\text{VBMI})_{\text{tongue}}$ . These outcomes support the fact that the air volume is not the main contributor for UA collapse and show that the obstruction and collapse episodes (apneic events) are caused by the large size of the tongue and uvula.

The modulus of elasticity of the soft tissues for OSA patients might be less than those for the healthy subjects as they become very loose and could block the airway easily during



sleep, and from the background (Chapter 1) the modulus of elasticity for the healthy uvula and tongue were 25 and 15 kPa; respectively. Therefore throughout this conclusion we will focus on a range of values for E around those normal control values; particularly we will consider the range of E to be 20-30 kPa for the uvula; and 10-20 kPa for the tongue in order to cover the different sleeping positions and/or stages (where the muscles relax, which means that E will be less than that during wakefulness). Also to cover the changes in E that might occur due to different genders, races, ages and BMI.

After investigating the results for the uvula, tongue and the combinations between them we have concluded:

1. The range for the natural frequencies which stimulate both the uvula and tongue models is 5-40 Hz.
2. For each subject specific, the first and second natural frequencies of the uvula and tongue models are very close to one another, which indicates that they can be stimulated at the same time with approximately the same frequencies.
3. The natural frequencies for the unhealthy uvula models are slightly higher than those for the healthy models.
4. The natural frequencies for the unhealthy tongue models are slightly less than those for the healthy models.
5. The first and second natural frequencies for all the unhealthy uvula and tongue models are very close to one another and fall within the values reported in the previous findings [497-500, 502].
6. The third natural frequencies for the healthy and unhealthy uvula models are relatively different and higher than the reported frequency range [497-500, 502].
7. The third natural frequencies for the healthy and unhealthy tongue models are very close to one another and fall within the reported frequency range [497-500, 502].
8. For each patient specific, the first and second natural frequencies for the unhealthy uvula and tongue models are close to one another but not as close as the results obtained from the healthy models.
9. The third natural frequencies for the uvula and tongue are relatively different in the two participating groups (healthy and unhealthy).

10. The minimum air gaps at the rear of the uvula and tongue, and the UA volume are larger in the apneic group than the healthy participating group, which indicates that these two factors may not be responsible for the UA collapse.
11. The volumes of the uvula and tongue models in the apneic patients are much larger than those of the healthy subjects, which may contribute to the UA collapse.

#### **8.4 Collapse and the Effects of PO on the UA**

The conducted simulations in Chapter 6 have succeeded in detecting the UA collapse during inspiration and expiration using the CFX Modeller on the ANSYS Workbench to determine the pressure distributions for the air model inside the UA, as well as using one way FSI by using the Static-Structural Modeller on the ANSYS Workbench to determine the resulting UA deformations. The conditions for collapse were determined by using two turbulence models, k- $\epsilon$  and SST. The results show that the SST turbulence model has resulted in better and more reasonable pressure distributions when compared with the k- $\epsilon$  model; which recommends the use of the SST turbulence model to determine the dynamic characteristics of the UA in similar future studies. The results also show that the obtained conditions of collapse fall within the previously reported values of the esophageal pressures, and suggest that the use of one-way FSI method is recommended in determining the dynamic characteristics of human upper airways.

After determining the conditions of collapse, the boundary conditions at the nasal cavity were changed to simulate the use of the CPAP to prevent the UA collapse, and the results showed that there was no sign for any obstruction or collapse with the use of the CPAP.

The effects of the pressure oscillations on the performance of the UA were also investigated and the results suggest that the use of the PO superimposed on the CPAP has succeeded in keeping the airway open with no sign of collapse and at lower pressure distributions compared to the obtained pressure distributions using the CPAP alone.

From the obtained results we have concluded that:

1. The obtained closing pressures fall within the reported pharyngeal pressures [25, 551, 552].
2. The use of the CPAP prevented the occurrence of UA collapse during inspiration and expiration.

3. The use of the PO superimposed on the CPAP prevented the occurrence of collapse at lower pressures when compared with the obtained values using the conventional CPAP alone, especially during inspiration.
4. The use of SST turbulence model resulted in more reasonable pressure distributions and closer to reality compared to the obtained results from the k- $\epsilon$  turbulence model, and consequently the SST turbulence model is recommended to be used in future similar studies.

## **8.5 Experimental Results**

The obtained results from the conducted experiments described in Chapter 7 show the following:

1. The resulting deformations of the rig and the uvula with the use of the CPAP are larger than those without using the CPAP.
2. The resulting deformations in the upright position are larger than the obtained values in the supine position, which suggests that the UA becomes less responsive in the supine position.
3. The resulting deformations increase with increasing the CPAP, which indicates that the CPAP can successfully stimulate the UA.
4. The use of the PO superimposed on the CPAP has resulted in larger deformations compared with using the CPAP alone, which indicates that the UA can be stimulated more with the use of the PO.
5. The resulting deformations increase with increasing the frequency of the used PO, which indicates that the UA can be stimulated more when using the PO with higher frequencies for the same amplitude.
6. The obtained experimental results from Chapter 8 in addition to the theoretical results of Chapter 6 show that the use of the PO has resulted in larger deformations at lower UA pressure distributions, which indicates that the use of the PO can keep the UA open at much lower pressure distributions compared to the obtained results when using the CPAP alone, which in turn will reduce patient's rejection and consequently increase the CPAP marketability.

## **8.6 Conclusions**

This thesis has met the objectives specified in section 2.6 as follows:

1. The biomechanical changes of the dynamic characteristics of the UA before and after bariatric surgery were thoroughly investigated and new parameters were introduced. The outcomes suggest that bariatric surgery is a good treatment in losing weight and alleviating OSA symptoms in morbid obese OSA patients under 50 years of age.
2. The dynamic characteristics of healthy and unhealthy upper airways were investigated and compared. The outcomes show that the sizes of the uvula and tongue in the apneic patients are significantly larger than those of the healthy subjects ( $p < 0.05$ ), which may contribute to the UA collapse.
3. The conditions of the UA collapse in the unhealthy airways were successfully determined during inspiration and expiration by using the FSI method on the ANSYS Workbench. The outcomes show that the UA collapse occurs at the rear of the uvula during expiration and rear of the tongue during inspiration.
4. The effects of using the CPAP to prevent the UA collapse were investigated and discussed, and the use of the CPAP has successfully prevented the UA collapse.
5. The effects of using the PO superimposed on the CPAP were investigated, and the use of the PO has successfully prevented the UA collapse at lower CPAP pressures compared to the case of using the CPAP alone and consequently resulted in lower pressure distributions inside the UA.

## **8.7 Future Work**

It is believed that the outcomes of this project can be further used in the following:

1. Use the same FSI modelling procedure to simulate the rest of the constructed unhealthy models and prepare a report describing all the UA characteristics of each patient, which might be very useful in better understanding of their upper airways.
2. The project can be further improved if a funding is available for the purpose of buying a full licence of Mimics software, which is believed to be capable of simulating the constructed models without the need for any simplification.
3. Start a new phase of the project which is to modify the design of the current CPAP by superimposing the PO onto it, in order to keep the airway open at lower pressures and consequently minimise patients' rejection, which in turn may result in a new patent.
4. If possible, recruit OSA patients for clinical trials of the new CPAP after the modifications.

5. More accurate models need to be produced using the advantage of advances in 3D printing.
6. Repeat the simulations using the two-way-FSI methods to investigate if there is any difference in regards to the conditions of collapse, resulting deformations and the effect of PO on the performance of the UA compared to the obtained results from the one-way-FSI methods.
7. Conduct simulations including the viscoelastic behaviour of the soft tissues, which was meant to be included in this research from the beginning but since the viscoelastic properties are subject specific and change with different positions for the same subject and consequently should be changed for each patient, and due to time limitations we were not able to include these properties in this study.

## References

1. Flenley, D.C., *Sleep in chronic obstructive lung disease*. Clinics in Chest Medicine, 1985. **6**(4): p. 651-661.
2. Partinen, M., A. Jamieson, and C. Guilleminault, *Long-term outcome for obstructive sleep apnea syndrome patients. Mortality*. Chest, 1988. **94**(6): p. 1200-1204.
3. Campos-Rodriguez, F., et al., *Mortality in obstructive sleep apnea-hypopnea patients treated with positive airway pressure*. Chest, 2005. **128**(2): p. 624-633.
4. Mitler, M.M., et al., *Catastrophes, sleep, and public policy: Consensus report*. Sleep, 1988. **11**(1): p. 100-109.
5. Roth, T. and T.A. Roehrs, *Etiologies and sequelae of excessive daytime sleepiness*. Clinical Therapeutics, 1996. **18**(4): p. 562-576.
6. Leger, D., *The cost of sleep-related accidents: A report for the National Commission on Sleep Disorders Research*. Sleep, 1994. **17**(1): p. 84-93.
7. Briones, B., et al., *Relationship between sleepiness and general health status*. Sleep, 1996. **19**(7): p. 583-588.
8. Baldwin, C.M., et al., *The association of sleep-disordered breathing and sleep symptoms with quality of life in the sleep heart health study*. Sleep, 2001. **24**(1): p. 96-105.
9. Vorona, R.D. and J.C. Ware, *Sleep disordered breathing and driving risk*. Current Opinion in Pulmonary Medicine, 2002. **8**(6): p. 506-510.
10. Yang, E.H., et al., *Sleep apnea and quality of life*. Sleep, 2000. **23**(4): p. 535-541.
11. Hui, D.S.C., et al., *Effects of augmented continuous positive airway pressure education and support on compliance and outcome in a Chinese population*. Chest, 2000. **117**(5): p. 1410-1416.
12. Hoy, C.J., et al., *Can intensive support improve continuous positive airway pressure use in patients with the sleep apnea/hypopnea syndrome?* American Journal of Respiratory and Critical Care Medicine, 1999. **159**(4 1): p. 1096-1100.
13. D'Ambrosio, C., T. Bowman, and V. Mohsenin, *Quality of life in patients with obstructive sleep apnea: Effect of nasal continuous positive airway pressure - A prospective study*. Chest, 1999. **115**(1): p. 123-129.
14. Meslier, N., et al., *A French survey of 3,225 patients treated with CPAP for obstructive sleep apnoea: Benefits, tolerance compliance and quality of life*. European Respiratory Journal, 1998. **12**(1): p. 185-192.
15. Bolitschek, J., et al., *Impact of nasal continuous positive airway pressure treatment on quality of life in patients with obstructive sleep apnoea*. European Respiratory Journal, 1998. **11**(4): p. 890-894.
16. Young, T., P.E. Peppard, and D.J. Gottlieb, *Epidemiology of obstructive sleep apnea: A population health perspective*. American Journal of Respiratory and Critical Care Medicine, 2002. **165**(9): p. 1217-1239.

17. Flemons, W.W., et al., *Sleep-related breathing disorders in adults: Recommendations for syndrome definition and measurement techniques in clinical research*. Sleep, 1999. **22**(5): p. 667-689.
18. Ciftci, T.U., O. Kokturk, and S. Ozkan, *Apnea-Hypopnea Indexes Calculated Using Different Hypopnea Definitions and Their Relationship to Major Symptoms*. Sleep and Breathing, 2004. **8**(3): p. 141-146.
19. Fan, Y., et al., *Computational fluid dynamics analysis on the upper airways of obstructive sleep apnea using patient - specific models*. IAENG International Journal of Computer Science, 2011. **38**(4): p. 401-408.
20. Young, T., et al., *The occurrence of sleep-disordered breathing among middle-aged adults*. New England Journal of Medicine, 1993. **328**(17): p. 1230-1235.
21. Wright, J., et al., *Health effects of obstructive sleep apnoea and the effectiveness of continuous positive airways pressure: A systematic review of the research evidence*. British Medical Journal, 1997. **314**(7084): p. 851-860.
22. Ayappa, I. and D.M. Rapoport, *The upper airway in sleep: Physiology of the pharynx*. Sleep Medicine Reviews, 2003. **7**(1): p. 9-33.
23. Boudewyns, A., et al., *Does socially disturbing snoring and/or excessive daytime sleepiness warrant polysomnography?* Clinical Otolaryngology and Allied Sciences, 1997. **22**(5): p. 403-407.
24. Mylavarapu, G., et al. *Fluid structure interaction analysis in human upper airways to understand sleep apnea*. 2010.
25. Mihaescu, M., et al., *Computational modeling of upper airway before and after adenotonsillectomy for obstructive sleep apnea*. Laryngoscope, 2008. **118**(2): p. 360-362.
26. Malhotra, A. and D.P. White, *Obstructive sleep apnoea*. Lancet, 2002. **360**(9328): p. 237-245.
27. Meoli, A.L., et al., *Hypopnea in sleep-disordered breathing in adults*. Sleep, 2001. **24**(4): p. 469-470.
28. Guilleminault, C., A. Tilkian, and W.C. Dement, *The sleep apnea syndromes*. Annual Review of Medicine, 1976. **27**: p. 465-489.
29. Kuna, S.T. and G. Sant'Ambrogio, *Pathophysiology of upper airway closure during sleep*. Journal of the American Medical Association, 1991. **266**(10): p. 1384-1389.
30. Weitzman, E.D., et al., *The Hypersomnia Sleep-Apnea Syndrome: site and mechanism of upper airway obstruction*. Transactions of the American Neurological Association, 1977. **102**: p. 150-153.
31. Gastaut, H., C.A. Tassinari, and B. Duron, *Polygraphic study of the episodic diurnal and nocturnal (hypnic and respiratory) manifestations of the pickwick syndrome*. Brain Research, 1966. **1**(2): p. 167-186.
32. Olson, L.G., et al., *A community study of snoring and sleep-disordered breathing: Symptoms*. American Journal of Respiratory and Critical Care Medicine, 1995. **152**(2): p. 707-710.
33. Bassiri, A.G. and C. Guilleminault, *Clinical features and evaluation of obstructive sleep apnea-hypopnea syndrome*. Principles and Practice of Sleep Medicine, 2000. **3**: p. 869-878.

34. Emsellem, H.A. and K.E. Murtagh, *Sleep apnea and sports performance*. Clinics in Sports Medicine, 2005. **24**(2): p. 329-341.
35. Flegal, K.M., et al., *Prevalence and trends in obesity among US adults, 1999-2000*. Journal of the American Medical Association, 2002. **288**(14): p. 1723-1727.
36. Susarla, S.M., et al., *Biomechanics of the upper airway: Changing concepts in the pathogenesis of obstructive sleep apnea*. International journal of oral and maxillofacial surgery, 2010. **39**(12): p. 1149-1159.
37. Al Lawati, N.M., S.R. Patel, and N.T. Ayas, *Epidemiology, risk factors, and consequences of obstructive sleep apnea and short sleep duration*. Progress in Cardiovascular Diseases, 2009. **51**(4): p. 285-293.
38. Qureshi, A., R.D. Ballard, and H.S. Nelson, *Obstructive sleep apnea*. Journal of Allergy and Clinical Immunology, 2003. **112**(4): p. 643-651.
39. El-Ad, B. and P. Lavie, *Effect of sleep apnea on cognition and mood*. International Review of Psychiatry, 2005. **17**(4): p. 277-282.
40. Terán-Santos, J., A. Jiménez-Gómez, and J. Cordero-Guevara, *The association between sleep apnea and the risk of traffic accidents*. New England Journal of Medicine, 1999. **340**(11): p. 847-851.
41. Yaggi, H.K., et al., *Obstructive sleep apnea as a risk factor for stroke and death*. New England Journal of Medicine, 2005. **353**(19): p. 2034-2041.
42. Wiegand, L. and C.W. Zwillich, *Obstructive sleep apnea*. Disease-a-Month, 1994. **40**(4): p. 203-252.
43. Ho, M.L. and S.D. Brass, *Obstructive sleep apnea*. Neurology international, 2011. **3**(3): p. e15.
44. Phillipson, E.A., *Sleep apnea*. Harrison's principles of internal medicine. 16th ed, 2005: p. 1575.
45. Pasman, J.W., E.M.G. Joosten, and H.J. Wouters, *Increased daytime sleepiness and snoring - obstructive sleep apnea syndrome caused by webbing of the soft palate*. Clinical Neurology and Neurosurgery, 1988. **90**(1): p. 75-78.
46. Zwillich, C.W., et al., *Disturbed sleep and prolonged apnea during nasal obstruction in normal men*. American Review of Respiratory Disease, 1981. **124**(2): p. 158-160.
47. McNicholas, W.T. and S. Ryan, *Obstructive sleep apnoea syndrome: Translating science to clinical practice*. Respiriology, 2006. **11**(2): p. 136-144.
48. Kales, A., C.R. Soldatos, and J.D. Kales, *Taking a sleep history*. American Family Physician, 1980. **22**(2): p. 101-107.
49. Kales, A., A. Vela-Bueno, and J.D. Kales, *Sleep disorders: Sleep apnea and narcolepsy*. Annals of Internal Medicine, 1987. **106**(3): p. 434-443.
50. Lugaresi, E., et al., *Hypersomnia with periodic apnea*. Narcolepsy, 1976: p. 351-366.
51. Guilleminault, C. and W.C. Dement, *Sleep Apnea Syndromes*. KRGF Foundation Series, 1978. **11**.



52. Ead, H., *Meeting the Challenge of Obstructive Sleep Apnea: Developing a Protocol That Guides Perianesthesia Patient Care*. Journal of Perianesthesia Nursing, 2009. **24**(2): p. 103-113.
53. Powell, N.B., et al., *Patterns in pharyngeal airflow associated with sleep-disordered breathing*. Sleep Medicine, 2011. **12**(10): p. 966-974.
54. Hopewell, P.C. and J.F. Murray, *The adult respiratory distress syndrome*. Annual Review of Medicine, 1976. **27**: p. 343-356.
55. Ingbar, D.H. and J.B. Gee, *Pathophysiology and treatment of sleep apnea*. Annual Review of Medicine, 1985. **36**: p. 369-395.
56. Shintani, T., K. Asakura, and A. Kataura, *Adenotonsillar hypertrophy and skeletal morphology of children with obstructive sleep apnea syndrome*. Acta Oto-Laryngologica, Supplement, 1996(523): p. 222-224.
57. Schwab, R.J., et al., *Identification of upper airway anatomic risk factors for obstructive sleep apnea with volumetric magnetic resonance imaging*. American Journal of Respiratory and Critical Care Medicine, 2003. **168**(5): p. 522-530.
58. Do, K.L., et al., *Does tongue size differ between patients with and without sleep-disordered breathing?* Laryngoscope, 2000. **110**(9): p. 1552-1555.
59. Moos, D.D. and J.D. Cuddeford, *Implications of Obstructive Sleep Apnea Syndrome for the Perianesthesia Nurse*. Journal of Perianesthesia Nursing, 2006. **21**(2): p. 103-118.
60. *Practice guidelines for the perioperative management of patients with obstructive sleep apnea: A report by the American Society of Anesthesiologists Task Force on Perioperative Management of Patients with Obstructive Sleep Apnea*. Anesthesiology, 2006. **104**(5): p. 1081-1093.
61. Hamans, E.P.P.M., et al., *Morphometric analysis of the uvula in patients with sleep-related breathing disorders*. European Archives of Oto-Rhino-Laryngology, 2000. **257**(4): p. 232-236.
62. Hoffstein, V., *Snoring*. Principles and Practice of Sleep Medicine, 2000: p. 813-826.
63. Bahammam, A. and M. Kryger, *Decision making in obstructive sleep-disordered breathing: Putting it all together*. Otolaryngologic Clinics of North America, 1999. **32**(2): p. 333-348.
64. Ono, T., *Tongue and upper airway function in subjects with and without obstructive sleep apnea*. Japanese Dental Science Review, 2012: p. In press.
65. White, D.P., *Pathogenesis of obstructive and central sleep apnea*. American Journal of Respiratory and Critical Care Medicine, 2005. **172**(11): p. 1363-1370.
66. Deegan, P.C. and W.T. McNicholas, *Pathophysiology of obstructive sleep apnoea*. European Respiratory Journal, 1995. **8**(7): p. 1161-1178.
67. Svanborg, E., *Impact of obstructive apnea syndrome on upper airway respiratory muscles*. Respiratory Physiology and Neurobiology, 2005. **147**(2-3 SPEC. ISS.): p. 263-272.
68. Wellman, A., et al., *A method for measuring and modeling the physiological traits causing obstructive sleep apnea*. Journal of Applied Physiology, 2011. **110**(6): p. 1627-1637.
69. Benumof, J.L., *Obstructive sleep apnea in the adult obese patient: Implications for airway management*. Journal of Clinical Anesthesia, 2001. **13**(2): p. 144-156.

70. Morrison, D.L., et al., *Pharyngeal narrowing and closing pressures in patients with obstructive sleep apnea*. American Review of Respiratory Disease, 1993. **148**(3): p. 606-611.
71. Hudgel, D.W. and C. Hendricks, *Palate and hypopharynx - Sites of inspiratory narrowing of the upper airway during sleep*. American Review of Respiratory Disease, 1988. **138**(6): p. 1542-1547.
72. *Pharynx*. Available from: <http://nursingmedic.blogspot.co.nz/>.
73. Patil, S.P., et al., *Adult obstructive sleep apnea: Pathophysiology and diagnosis*. Chest, 2007. **132**(1): p. 325-337.
74. Eckert, D.J. and A. Malhotra, *Pathophysiology of adult obstructive sleep apnea*. Proceedings of the American Thoracic Society, 2008. **5**(2): p. 144-153.
75. Fouke, J.M. and K.P. Strohl, *Effect of position and lung volume on upper airway geometry*. Journal of Applied Physiology, 1987. **63**(1): p. 375-380.
76. Strollo Jr, P.J. and R.M. Rogers, *Obstructive sleep apnea*. New England Journal of Medicine, 1996. **334**(2): p. 99-104.
77. Taasan, V.C., A.J. Block, and P.G. Boysen, *Alcohol increases sleep apnea and oxygen desaturation in asymptomatic men*. American Journal of Medicine, 1981. **71**(2): p. 240-245.
78. Guilleminault, C., J. Van den Hoed, and M.M. Mitler, *Clinical overview of the sleep apnea syndromes*. Sleep Apnea Syndromes, 1978: p. 1-46.
79. Tobin, M.J., M.A. Cohn, and M.A. Sackner, *Breathing abnormalities during sleep*. Archives of Internal Medicine, 1983. **143**(6): p. 1221-1228.
80. Coaker, L.A. and S.F. Quan, *Diagnosis and treatment of sleep apnea syndrome in adults*. Arizona Medicine, 1981. **38**(6): p. 446-450.
81. Snyderman, N.L., J.T. Johnson, and C.F. Reynolds Iii, *Evaluation of the adult with sleep apnea*. Annals of Otology, Rhinology and Laryngology, 1983. **92**(5 1): p. 518-520.
82. Chaudhary, B.A. and W.A. Speir Jr, *Sleep apnea syndromes*. Southern medical journal, 1982. **75**(1): p. 39-45.
83. McCoy, K.S., C.F. Koopmann Jr, and L.M. Taussig, *Sleep-related breathing disorders*. American Journal of Otolaryngology - Head and Neck Medicine and Surgery, 1981. **2**(3): p. 228-239.
84. Iber, C., et al., *The AASM manual for the scoring of sleep and associated events: Rules, terminology, and technical specifications*, 2007.
85. Lowenstein, L., et al., *The relationship between obstructive sleep apnea, nocturia, and daytime overactive bladder syndrome in women*. American journal of obstetrics and gynecology, 2008. **198**(5): p. 598.e1-598.e5.
86. *Guideline fifteen: Guidelines for polygraphic assessment of sleep-related disorders (polysomnography)*. Journal of Clinical Neurophysiology, 1994. **11**(1): p. 116-124.
87. Roure, N., et al., *Daytime sleepiness and polysomnography in obstructive sleep apnea patients*. Sleep Medicine, 2008. **9**(7): p. 727-731.
88. Whitelaw, W.A. and K.R. Burgess, *Diagnosis of sleep apnoea: Some critical issues*. Indian Journal of Medical Research, 2010. **131**(2): p. 217-229.

89. Chung, F. and C. Imairengiaye, *Management of sleep apnea in adults*. Canadian Journal of Anesthesia / Journal canadien d'anesthésie, 2002. **49**(0): p. R1-R6.
90. Horner, R.L., *Motor control of the pharyngeal musculature and implications for the pathogenesis of obstructive sleep apnea*. Sleep, 1996. **19**(10): p. 827-853.
91. Remmers, J.E., et al., *Pathogenesis of upper airway occlusion during sleep*. Journal of Applied Physiology Respiratory Environmental and Exercise Physiology, 1978. **44**(6): p. 931-938.
92. Isono, S., et al., *Anatomy of pharynx in patients with obstructive sleep apnea and in normal subjects*. Journal of Applied Physiology, 1997. **82**(4): p. 1319-1326.
93. Koenig, J.S. and B.T. Thach, *Effects of mass loading on the upper airway*. Journal of Applied Physiology, 1988. **64**(6): p. 2124-2131.
94. Kiely, J.L., M. Murphy, and W.T. McNicholas, *Subjective efficacy of nasal CPAP therapy in obstructive sleep apnoea syndrome: A prospective controlled study*. European Respiratory Journal, 1999. **13**(5): p. 1086-1090.
95. Suratt, P.M., P. Dee, and R.L. Atkinson, *Fluoroscopic and computed tomographic features of the pharyngeal airway in obstructive sleep apnea*. American Review of Respiratory Disease, 1983. **127**(4): p. 487-492.
96. *Obstructive Sleep Apnea: Blocked Upper Airway*. 2015 [cited 2015; Available from: <http://www.emedicinehealth.com/script/main/art.asp?articlekey=135675&ref=129801>].
97. Ruehland, W.R., et al., *The new AASM criteria for scoring hypopneas: Impact on the apnea hypopnea index*. Sleep, 2009. **32**(2): p. 150-157.
98. Kryger, M.H., *Management of obstructive sleep apnea-hypopnea syndrome: Overview*. Principles and Practice of Sleep Medicine, 2000: p. 940-954.
99. Guilleminault, C., J. Cumiskey, and W.C. Dement, *Sleep apnea syndrome: recent advances*. Advances in internal medicine, 1980. **26**: p. 347-372.
100. Kryger, M.H., *Monitoring respiratory and cardiac function*. Principles and Practice of Sleep Medicine, 2000: p. 1217-1230.
101. Kushida, C.A., et al., *Practice parameters for the indications for polysomnography and related procedures: An update for 2005*. Sleep, 2005. **28**(4): p. 499-521.
102. Coccagna, G., A. Pollini, and F. Provini, *Cardiovascular disorders and obstructive sleep apnea syndrome*. Clinical and Experimental Hypertension, 2006. **28**(3-4): p. 217-224.
103. Michaelson, P.G., et al., *Validations of a portable home sleep study with twelve-lead polysomnography: Comparisons and insights into a variable gold standard*. Annals of Otology, Rhinology and Laryngology, 2006. **115**(11): p. 802-809.
104. Pevernagie, D., et al., *Treatment of obstructive sleep-disordered breathing with positive airway pressure systems*. European Respiratory Review, 2007. **16**(106): p. 125-131.
105. Seneviratne, U. and K. Puvanendran, *Excessive daytime sleepiness in obstructive sleep apnea: Prevalence, severity, and predictors*. Sleep Medicine, 2004. **5**(4): p. 339-343.
106. Chervin, R.D., *Use of clinical tools and tests in sleep medicine*. Principles and Practice of Sleep Medicine, 2000: p. 535-546.

107. Haines, K.L., et al., *Objective evidence that bariatric surgery improves obesity-related obstructive sleep apnea*. Surgery, 2007. **141**(3): p. 354-358.
108. Prevention, C.f.D.C.a. Centers for Disease Control and Prevention, *Interpretation of BMI for Adults*. 2015 February 23, 2015 [cited 2015 01/03/2015]; Available from: [http://www.cdc.gov/healthyweight/assessing/bmi/adult\\_bmi/index.html](http://www.cdc.gov/healthyweight/assessing/bmi/adult_bmi/index.html).
109. Gami, A.S., S.M. Caples, and V.K. Somers, *Obesity and obstructive sleep apnea*. Endocrinology and Metabolism Clinics of North America, 2003. **32**(4): p. 869-894.
110. Vgontzas, A.N. and A. Kales, *Sleep and its disorders*. 1999. p. 387-400.
111. Mohsenin, V., *Gender differences in the expression of sleep-disordered breathing: Role of upper airway dimensions*. Chest, 2001. **120**(5): p. 1442-1447.
112. Guilleminault, C., et al., *Sleep apnea syndrome. Can it induce hemodynamic changes?* Western Journal of Medicine, 1975. **123**(1): p. 7-16.
113. Abdal, H., J.J. Pizzimenti, and C.C. Purvis, *The eye in sleep apnea syndrome*. Sleep Medicine, 2006. **7**(2): p. 107-15.
114. Lee, R.W.W., et al., *Differences in craniofacial structures and obesity in Caucasian and Chinese patients with obstructive sleep apnea*. Sleep, 2010. **33**(8): p. 1075-1080.
115. Young, T., J. Skatrud, and P.E. Peppard, *Risk Factors for Obstructive Sleep Apnea in Adults*. Journal of the American Medical Association, 2004. **291**(16): p. 2013-2016.
116. Ip, M.S.M., et al., *A community study of sleep-disordered breathing in middle-aged Chinese men in Hong Kong*. Chest, 2001. **119**(1): p. 62-69.
117. Ip, M.S.M., et al., *A Community Study of Sleep-Disordered Breathing in Middle-Aged Chinese Women in Hong Kong: Prevalence and Gender Differences*. Chest, 2004. **125**(1): p. 127-134.
118. Jordan, A.S. and D.P. White, *Pharyngeal motor control and the pathogenesis of obstructive sleep apnea*. Respiratory Physiology and Neurobiology, 2008. **160**(1): p. 1-7.
119. Caballero, P., et al., *CT in the evaluation of the upper airway in healthy subjects and in patients with obstructive sleep apnea syndrome*. Chest, 1998. **113**(1): p. 111-116.
120. Kryger, M.H., *Diagnosis and management of sleep apnea syndrome*. Clinical cornerstone, 2000. **2**(5): p. 39-47.
121. Namen, A.M., et al., *Increased physician-reported sleep apnea: The National Ambulatory Medical Care Survey*. Chest, 2002. **121**(6): p. 1741-1747.
122. Rajagopalan, N., *Obstructive sleep apnea: Not just a sleep disorder*. Journal of Postgraduate Medicine, 2011. **57**(2): p. 168-175.
123. Kales, A., R.J. Cadieux, and E.O. Bixler, *Severe obstructive sleep apnea. I: Onset, clinical course, and characteristics*. Journal of Chronic Diseases, 1985. **38**(5): p. 419-425.
124. Gottlieb, D.J., et al., *Relationship of sleepiness to respiratory disturbance index: The sleep heart health study*. American Journal of Respiratory and Critical Care Medicine, 1999. **159**(2): p. 502-507.
125. Guilleminault, C., F. Eldridge, and W.C. Dement, *Insomnia, narcolepsy, and sleep apneas*. Bulletin de physio-pathologie respiratoire, 1972. **8**(5): p. 1127-1138.

126. Zamagni, M., et al., *Respiratory effort: A factor contributing to sleep propensity in patients with obstructive sleep apnea*. Chest, 1996. **109**(3): p. 651-658.
127. Paiva, T., et al., *Chronic headaches and sleep disorders*. Archives of Internal Medicine, 1997. **157**(15): p. 1701-1705.
128. Davies, R.J.O. and J.R. Stradling, *The relationship between neck circumference, radiographic pharyngeal anatomy, and the obstructive sleep apnoea syndrome*. European Respiratory Journal, 1990. **3**(5): p. 509-514.
129. Stradling, J.R. and J.H. Crosby, *Predictors and prevalence of obstructive sleep apnoea and snoring in 1001 middle aged men*. Thorax, 1991. **46**(2): p. 85-90.
130. Davies, R.J.O., N.J. Ali, and J.R. Stradling, *Neck circumference and other clinical features in the diagnosis of the obstructive sleep apnoea syndrome*. Thorax, 1992. **47**(2): p. 101-105.
131. Kales, A., A.B. Caldwell, and R.J. Cadieux, *Severe obstructive sleep apnea - II: Associated psychopathology and psychosocial consequences*. Journal of Chronic Diseases, 1985. **38**(5): p. 427-434.
132. Blanco Pérez, J.J., et al., *Acromegaly and sleep apnea*. Acromegalia y apnea del sueño, 2004. **40**(8): p. 355-359.
133. Jennum, P. and R. Jensen, *Sleep and headache*. Sleep Medicine Reviews, 2002. **6**(6): p. 471-479.
134. Coleman, R.M., H.P. Roffwarg, and S.J. Kennedy, *Sleep-wake disorders based on a polysomnographic diagnosis. A national cooperative study*. Journal of the American Medical Association, 1982. **247**(7): p. 997-1003.
135. Dement, W.C., M.A. Carskadon, and G. Richardson, *Excessive daytime sleepiness in the sleep apnea syndrome*. Sleep Apnea Syndromes, 1978: p. 23-46.
136. Guilleminault, C., S.J. Connolly, and R.A. Winkle, *Cardiac arrhythmia and conduction disturbances during sleep in 400 patients with sleep apnea syndrome*. American Journal of Cardiology, 1983. **52**(5): p. 490-494.
137. Kim, H.C., et al., *Sleep-disordered breathing and neuropsychological deficits: A population-based study*. American Journal of Respiratory and Critical Care Medicine, 1997. **156**(6): p. 1813-1819.
138. Punjabi, N.M., et al., *Modeling hypersomnolence in sleep-disordered breathing: A novel approach using survival analysis*. American Journal of Respiratory and Critical Care Medicine, 1999. **159**(6): p. 1703-1709.
139. Young, T., et al., *Sleep-disordered breathing and motor vehicle accidents in a population-based sample of employed adults*. Sleep, 1997. **20**(8): p. 608-613.
140. Guilleminault, C., et al., *A cause of excessive daytime sleepiness: The upper airway resistance syndrome*. Chest, 1993. **104**(3): p. 781-787.
141. Morris, L.G.T., et al., *Rapid risk stratification for obstructive sleep apnea, based on snoring severity and body mass index*. Otolaryngology - Head and Neck Surgery, 2008. **139**(5): p. 615-618.
142. Koskenvuo, M., M. Partinen, and J. Kaprio, *Snoring and disease*. Annals of Clinical Research, 1985. **17**(5): p. 247-251.

143. Bearpark, H., et al., *Snoring and sleep apnea: A population study in Australian men*. American Journal of Respiratory and Critical Care Medicine, 1995. **151**(5): p. 1459-1465.
144. FitzGerald, M.P., M. Mulligan, and S. Parthasarathy, *Nocturic frequency is related to severity of obstructive sleep apnea, improves with continuous positive airways treatment*. American journal of obstetrics and gynecology, 2006. **194**(5): p. 1399-1403.
145. Oztura, I., D. Kaynak, and H.C. Kaynak, *Nocturia in sleep-disordered breathing*. Sleep Medicine, 2006. **7**(4): p. 362-367.
146. Hedner, J., L. Grote, and D. Zou, *Pharmacological treatment of sleep apnea: Current situation and future strategies*. Sleep Medicine Reviews, 2008. **12**(1): p. 33-47.
147. Tilkian, A.G., C. Guilleminault, and J.S. Schroeder, *Sleep-induced apnea syndrome. Prevalence of cardiac arrhythmias and their reversal after tracheostomy*. American Journal of Medicine, 1977. **63**(3): p. 348-358.
148. Strobel, R.J. and R.C. Rosen, *Obesity and weight loss in obstructive sleep apnea: A critical review*. Sleep, 1996. **19**(2): p. 104-115.
149. Thurnheer, R., P.K. Wraith, and N.J. Douglas, *Influence of age and gender on upper airway resistance in NREM and REM sleep*. Journal of Applied Physiology, 2001. **90**(3): p. 981-988.
150. Pillar, G. and N. Shehadeh, *Abdominal fat and sleep apnea: the chicken or the egg?* Diabetes Care, 2008. **31**(2): p. S303-S309.
151. Cottam, D.R., et al., *The chronic inflammatory hypothesis for the morbidity associated with morbid obesity: Implications and effect of weight loss*. Obesity Surgery, 2004. **14**(5): p. 589-600.
152. Young, T., P.E. Peppard, and S. Taheri, *Excess weight and sleep-disordered breathing*. Journal of Applied Physiology, 2005. **99**(4): p. 1592-1599.
153. Strohl, K.P. and S. Redline, *Recognition of obstructive sleep apnea*. American Journal of Respiratory and Critical Care Medicine, 1996. **154**(2): p. 279-289.
154. Stanchina, M.L., et al., *The influence of lung volume on pharyngeal mechanics, collapsibility, and genioglossus muscle activation during sleep*. Sleep, 2003. **26**(7): p. 851-856.
155. Bixler, E.O., et al., *Effects of age on sleep apnea in men. I. Prevalence and severity*. American Journal of Respiratory and Critical Care Medicine, 1998. **157**(1): p. 144-148.
156. Redline, S., *Epidemiology of sleep-disordered breathing*. Seminars in Respiratory and Critical Care Medicine, 1998. **19**(2): p. 113-122.
157. Schwartz, A.R., et al., *Obesity and obstructive sleep apnea: Pathogenic mechanisms and therapeutic approaches*. Proceedings of the American Thoracic Society, 2008. **5**(2): p. 185-192.
158. Wolk, R., A.S.M. Shamsuzzaman, and V.K. Somers, *Obesity, Sleep Apnea, and Hypertension*. Hypertension, 2003. **42**(6): p. 1067-1074.
159. García-Río, F., et al., *Sleep apnea and hypertension: The role of peripheral chemoreceptors and the sympathetic system*. Chest, 2000. **117**(5): p. 1417-1425.
160. Lavie, P., P. Herer, and V. Hoffstein, *Obstructive sleep apnoea syndrome as a risk factor for hypertension: Population study*. British Medical Journal, 2000. **320**(7233): p. 479-482.

161. Rosenow, F., et al., *Sleep apnoea in treated acromegaly: Relative frequency and predisposing factors*. Clinical Endocrinology, 1996. **45**(5): p. 563-569.
162. Mestrón, A., et al., *Epidemiology, clinical characteristics, outcome, morbidity and mortality in acromegaly based on the Spanish Acromegaly Registry (Registro Español de Acromegalia, REA)*. European Journal of Endocrinology, 2004. **151**(4): p. 439-446.
163. Issa, F.G. and C.E. Sullivan, *Alcohol, snoring and sleep apnoea*. Journal of Neurology Neurosurgery and Psychiatry, 1982. **45**(4): p. 353-359.
164. Scrima, L., et al., *Increased severity of obstructive sleep apnea after bedtime alcohol ingestion: Diagnostic potential and proposed mechanism of action*. Sleep, 1982. **5**(4): p. 318-328.
165. Mitler, M.M., et al., *Bedtime ethanol increases resistance of upper airways and produces sleep apneas in asymptomatic snorers*. Alcoholism: Clinical and Experimental Research, 1988. **12**(6): p. 801-805.
166. Krol, R.C., S.L. Knuth, and D. Bartlett Jr, *Selective reduction of genioglossal muscle activity by alcohol in normal human subjects*. American Review of Respiratory Disease, 1984. **129**(2): p. 247-250.
167. Leiter, J.C., S.L. Knuth, and D. Bartlett Jr, *The effect of sleep deprivation on activity of the genioglossus muscle*. American Review of Respiratory Disease, 1985. **132**(6): p. 1242-1245.
168. Leiter, J.C., et al., *The effect of diazepam on genioglossal muscle activity in normal human subjects*. American Review of Respiratory Disease, 1985. **132**(2): p. 216-219.
169. Nishino, T., et al., *Comparison of changes in the hypoglossal and the phrenic nerve activity in response to increasing depth of anesthesia in cats*. Anesthesiology, 1984. **60**(1): p. 19-24.
170. Carskadon, M.A., et al., *Effects of menopause and nasal occlusion on breathing during sleep*. American Journal of Respiratory and Critical Care Medicine, 1997. **155**(1): p. 205-210.
171. Mirza, N. and D.C. Lanza, *The nasal airway and obstructed breathing during sleep*. Otolaryngologic Clinics of North America, 1999. **32**(2): p. 243-262.
172. Lofaso, F., et al., *Nasal obstruction as a risk factor for sleep apnoea syndrome*. European Respiratory Journal, 2000. **16**(4): p. 639-643.
173. Young, T., L. Finn, and M. Palta, *Chronic nasal congestion at night is a risk factor for snoring in a population-based cohort study*. Archives of Internal Medicine, 2001. **161**(12): p. 1514-1519.
174. Mortimore, I.L., et al., *Neck and total body fat deposition in nonobese and obese patients with sleep apnea compared with that in control subjects*. American Journal of Respiratory and Critical Care Medicine, 1998. **157**(1): p. 280-283.
175. Bresnitz, E.A., R. Goldberg, and R.M. Kosinski, *Epidemiology of obstructive sleep apnea*. Epidemiologic Reviews, 1994. **16**(2): p. 210-227.
176. Willett, W.C., W.H. Dietz, and G.A. Colditz, *Guidelines for healthy weight*. New England Journal of Medicine, 1999. **341**(6): p. 427-434.
177. Flemons, W.W., et al., *Likelihood ratios for a sleep apnea clinical prediction rule*. American Journal of Respiratory and Critical Care Medicine, 1994. **150**(5 I): p. 1279-1285.

178. Tsai, W.H., et al., *A decision rule for diagnostic testing in obstructive sleep apnea*. American Journal of Respiratory and Critical Care Medicine, 2003. **167**(10): p. 1427-1432.
179. Marin, J.M., et al., *Long-term cardiovascular outcomes in men with obstructive sleep apnoea-hypopnoea with or without treatment with continuous positive airway pressure: An observational study*. Lancet, 2005. **365**(9464): p. 1046-1053.
180. Peppard, P.E., et al., *Prospective study of the association between sleep-disordered breathing and hypertension*. New England Journal of Medicine, 2000. **342**(19): p. 1378-1384.
181. Javier Nieto, F., et al., *Association of sleep-disordered breathing sleep apnea, and hypertension in a large community-based study*. Journal of the American Medical Association, 2000. **283**(14): p. 1829-1836.
182. Partinen, M. and W.T. McNicholas, *Epidemiology, morbidity and mortality of the sleep apnoea syndrome*. European Respiratory Monograph, 1998. **3**(10): p. 63-74.
183. Orr, W.C. and R.J. Martin, *Obstructive sleep apnea associated with tonsillar hypertrophy in adults*. Archives of Internal Medicine, 1981. **141**(8): p. 990-992.
184. Mezon, B.J., et al., *Sleep apnea in acromegaly*. American Journal of Medicine, 1980. **69**(4): p. 615-618.
185. Perks, W.H., P.M. Horrocks, and R.A. Cooper, *Sleep apnoea in acromegaly*. British Medical Journal, 1980. **280**(6218): p. 894-897.
186. Perks, W.H., R.A. Cooper, and S. Bradbury, *Sleep apnoea in Scheie's syndrome*. Thorax, 1980. **35**(2): p. 85-91.
187. Zorick, F., Roth, T., Kramer, M., and Fless, H., *Exacerbation of upper airway sleep apnea by lymphatic lymphoma*. Chest, 1980. **77**: p. 689-690.
188. Gleeson, K., C.W. Zwillich, and D.P. White, *The influence of increasing ventilatory effort on arousal from sleep*. American Review of Respiratory Disease, 1990. **142**(2): p. 295-300.
189. Benlloch, E., et al., *Ventilatory pattern at rest and response to hypercapnic stimulation in patients with obstructive sleep apnoea syndrome*. Respiration, 1995. **62**(1): p. 4-9.
190. Ayas, N.T., R. Brown, and S.A. Shea, *Hypercapnia can induce arousal from sleep in the absence of altered respiratory mechanoreception*. American Journal of Respiratory and Critical Care Medicine, 2000. **162**(3 1): p. 1004-1008.
191. Vanuxem, D., et al., *Impairment of muscle energy metabolism in patients with sleep apnoea syndrome*. Respiratory Medicine, 1997. **91**(9): p. 551-557.
192. Alonso-Fernández, A., et al., *Obstructive sleep apnoea-hypoapnoea syndrome reversibly depresses cardiac response to exercise*. European Heart Journal, 2006. **27**(2): p. 207-215.
193. Przybyłowski, T., et al., *Exercise capacity in patients with obstructive sleep apnea syndrome*. Journal of Physiology and Pharmacology, 2007. **58**(SUPPL. 5): p. 563-574.
194. Coccagna, G., et al., *Continuous recording of the pulmonary and systemic arterial pressure during sleep in syndromes of hypersomnia with periodic breathing*. Bulletin de physiopathologie respiratoire, 1972. **8**(5): p. 1159-1172.
195. Onal, E. and M. Lopata, *Periodic breathing and the pathogenesis of occlusive sleep apneas*. American Review of Respiratory Disease, 1982. **126**(4): p. 676-680.



196. Rowe, L.D., et al., *Continuous measurements of skin surface oxygen and carbon dioxide tensions in obstructive sleep apnea*. Laryngoscope, 1980. **90**(11 I): p. 1797-1803.
197. Tilkian, A.G., C. Guilleminault, and J.S. Schroeder, *Hemodynamics in sleep induced apnea. Studies during wakefulness and sleep*. Annals of Internal Medicine, 1976. **85**(6): p. 714-719.
198. Coughlin, S.R., et al., *Obstructive sleep apnoea is independently associated with an increased prevalence of metabolic syndrome*. European Heart Journal, 2004. **25**(9): p. 735-741.
199. Dyken, M.E., et al., *Investigating the relationship between stroke and obstructive sleep apnea*. Stroke, 1996. **27**(3): p. 401-407.
200. Bassetti, C. and M.S. Aldrich, *Sleep apnea in acute cerebrovascular diseases: Final report on 128 patients*. Sleep, 1999. **22**(2): p. 217-223.
201. Wolk, R. and V.K. Somers, *Cardiovascular consequences of obstructive sleep apnea*. Clinics in Chest Medicine, 2003. **24**(2): p. 195-205.
202. Franklin, K.A., et al., *Sleep apnoea and nocturnal angina*. Lancet, 1995. **345**(8957): p. 1085-1087.
203. Gami, A.S., et al., *Day-night pattern of sudden death in obstructive sleep apnea*. New England Journal of Medicine, 2005. **352**(12): p. 1206-1214.
204. Carlson, J.T., et al., *Augmented resting sympathetic activity in awake patients with obstructive sleep apnea*. Chest, 1993. **103**(6): p. 1763-1768.
205. Hoffstein, V. and S. Mateika, *Cardiac arrhythmias, snoring, and sleep apnea*. Chest, 1994. **106**(2): p. 466-471.
206. Javaheri, S., *Effects of continuous positive airway pressure on sleep apnea and ventricular irritability in patients with heart failure*. Circulation, 2000. **101**(4): p. 392-397.
207. Harbison, J., P. O'Reilly, and W.T. McNicholas, *Cardiac rhythm disturbances in the obstructive sleep apnea syndrome: Effects of nasal continuous positive airway pressure therapy*. Chest, 2000. **118**(3): p. 591-595.
208. Wolk, R., T. Kara, and V.K. Somers, *Sleep-disordered breathing and cardiovascular disease*. Circulation, 2003. **108**(1): p. 9-12.
209. McNicholas, W.T. and M.R. Bonsignore, *Sleep apnoea as an independent risk for cardiovascular disease: Current evidence, basic mechanisms and research priorities*. European Respiratory Journal, 2007. **29**(1): p. 156-178.
210. Somers, V.K., et al., *Sleep Apnea and Cardiovascular Disease. An American Heart Association/American College of Cardiology Foundation Scientific Statement From the American Heart Association Council for High Blood Pressure Research Professional Education Committee, Council on Clinical Cardiology, Stroke Council, and Council on Cardiovascular Nursing In Collaboration With the National Heart, Lung*. Journal of the American College of Cardiology, 2008. **52**(8): p. 686-717.
211. Reichmuth, K.J., et al., *Association of sleep apnea and type II diabetes: A population-based study*. American Journal of Respiratory and Critical Care Medicine, 2005. **172**(12): p. 1590-1595.

212. Vgontzas, A.N., et al., *Sleep apnea and daytime sleepiness and fatigue: Relationship to visceral obesity, insulin resistance, and hypercytokinemia*. Journal of Clinical Endocrinology and Metabolism, 2000. **85**(3): p. 1151-1158.
213. Elmasry, A., et al., *Sleep-disordered breathing and glucose metabolism in hypertensive men: A population-based study*. Journal of Internal Medicine, 2001. **249**(2): p. 153-161.
214. Grote, L., et al., *Sleep-related breathing disorder is an independent risk factor for systemic hypertension*. American Journal of Respiratory and Critical Care Medicine, 1999. **160**(6): p. 1875-1882.
215. Arzt, M., et al., *Association of sleep-disordered breathing and the occurrence of stroke*. American Journal of Respiratory and Critical Care Medicine, 2005. **172**(11): p. 1447-1451.
216. Parish, J.M. and J.W. Shepard Jr, *Cardiovascular effects of sleep disorders*. Chest, 1990. **97**(5): p. 1220-1226.
217. Hla, K.M., et al., *Sleep apnea and hypertension: A population-based study*. Annals of Internal Medicine, 1994. **120**(5): p. 382-388.
218. Pepperell, J.C.T., et al., *Ambulatory blood pressure after therapeutic and subtherapeutic nasal continuous positive airway pressure for obstructive sleep apnoea: A randomised parallel trial*. Lancet, 2002. **359**(9302): p. 204-210.
219. Faccenda, J.F., et al., *Randomized placebo-controlled trial of continuous positive airway pressure on blood pressure in the sleep apnea-hypopnea syndrome*. American Journal of Respiratory and Critical Care Medicine, 2001. **163**(2): p. 344-348.
220. Nithiarasu, P., et al., *Steady flow through a realistic human upper airway geometry*. International Journal for Numerical Methods in Fluids, 2008. **57**(5): p. 631-651.
221. Neau, J.P., et al., *Stroke and sleep apnoea: Cause or consequence?* Sleep Medicine Reviews, 2002. **6**(6): p. 457-469.
222. Partinen, M. and H. Palomaki, *Snoring and cerebral infarction*. Lancet, 1985. **2**(8468): p. 1325-1326.
223. Hu, F.B., et al., *Snoring and risk of cardiovascular disease in women*. Journal of the American College of Cardiology, 2000. **35**(2): p. 308-313.
224. Hermann, D.M. and C.L. Bassetti, *Sleep-disordered breathing and stroke*. Current Opinion in Neurology, 2003. **16**(1): p. 87-90.
225. He, J., et al., *Mortality and apnea index in obstructive sleep apnea. Experience in 385 male patients*. Chest, 1988. **94**(1): p. 9-14.
226. Lavie, P., et al., *Mortality in sleep apnea patients: A multivariate analysis of risk factors*. Sleep, 1995. **18**(3): p. 149-157.
227. Shahar, E., et al., *Sleep-disordered breathing and cardiovascular disease: Cross-sectional results of the sleep heart health study*. American Journal of Respiratory and Critical Care Medicine, 2001. **163**(1): p. 19-25.
228. Peker, Y., et al., *Respiratory disturbance index: An independent predictor of mortality in coronary artery disease*. American Journal of Respiratory and Critical Care Medicine, 2000. **162**(1): p. 81-86.

229. Shivalkar, B., et al., *Obstructive sleep apnea syndrome: more insights on structural and functional cardiac alterations, and the effects of treatment with continuous positive airway pressure*. Journal of the American College of Cardiology, 2006. **47**(7): p. 1433-1439.
230. Garvey, J.F., C.T. Taylor, and W.T. McNicholas, *Cardiovascular disease in obstructive sleep apnoea syndrome: The role of intermittent hypoxia and inflammation*. European Respiratory Journal, 2009. **33**(5): p. 1195-1205.
231. Shamsuzzaman, A.S.M., B.J. Gersh, and V.K. Somers, *Obstructive Sleep Apnea: Implications for Cardiac and Vascular Disease*. Journal of the American Medical Association, 2003. **290**(14): p. 1906-1914.
232. Schäfer, H., et al., *Obstructive sleep apnea as a risk marker in coronary artery disease*. Cardiology, 1999. **92**(2): p. 79-84.
233. Bradley, T.D., R. Rutherford, and R.F. Grossman, *Role of daytime hypoxemia in the pathogenesis of right heart failure in the obstructive sleep apnea syndrome*. American Review of Respiratory Disease, 1985. **131**(6): p. 835-839.
234. Parati, G., C. Lombardi, and K. Narkiewicz, *Sleep apnea: Epidemiology, pathophysiology, and relationship to cardiovascular risk*. American Journal of Physiology - Regulatory Integrative and Comparative Physiology, 2007. **293**(4): p. R1671-R1683.
235. Young, T., et al., *Sleep disordered breathing and mortality: Eighteen-year follow-up of the wisconsin sleep cohort*. Sleep, 2008. **31**(8): p. 1071-1078.
236. Moee, T., et al., *Sleep-disordered breathing and coronary artery disease: Long-term prognosis*. American Journal of Respiratory and Critical Care Medicine, 2001. **164**(10 I): p. 1910-1913.
237. Young, T., et al., *Population-based study of sleep-disordered breathing as a risk factor for hypertension*. Archives of Internal Medicine, 1997. **157**(15): p. 1746-1752.
238. Barbe, F., et al., *Automobile accidents in patients with sleep apnea syndrome: An epidemiological and mechanistic study*. American Journal of Respiratory and Critical Care Medicine, 1998. **158**(1): p. 18-22.
239. Findley, L.J., M.E. Unverzagt, and P.M. Suratt, *Automobile accidents involving patients with obstructive sleep apnea*. American Review of Respiratory Disease, 1988. **138**(2): p. 337-340.
240. Jureyda, S. and D.W. Shucard, *Obstructive sleep apnea—an overview of the disorder and its consequences*. Seminars in Orthodontics, 2004. **10**(1): p. 63-72.
241. Sassani, A., et al., *Reducing motor-vehicle collisions, costs, and fatalities by treating obstructive sleep apnea syndrome*. Sleep, 2004. **27**(3): p. 453-458.
242. Masa, J.F., et al., *Habitually sleepy drivers have a high frequency of automobile crashes associated with respiratory disorders during sleep*. American Journal of Respiratory and Critical Care Medicine, 2000. **162**(4 I): p. 1407-1412.
243. Findley, L.J., et al., *Treatment with nasal CPAP decreases automobile accidents in patients with sleep apnea*. American Journal of Respiratory and Critical Care Medicine, 2000. **161**(3 I): p. 857-859.
244. Young, T., et al., *Predictors of sleep-disordered breathing in community-dwelling adults: The Sleep Heart Health Study*. Archives of Internal Medicine, 2002. **162**(8): p. 893-900.

245. Collop, N.A., *The significance of sleep-disordered breathing and obstructive sleep apnea in the elderly*. Chest, 1997. **112**(4): p. 867-868.
246. Launois, S.H., J.L. Pépin, and P. Lévy, *Sleep apnea in the elderly: A specific entity?* Sleep Medicine Reviews, 2007. **11**(2): p. 87-97.
247. White, D.P., et al., *Pharyngeal resistance in normal humans: Influence of gender, age, and obesity*. Journal of Applied Physiology, 1985. **58**(2): p. 365-371.
248. Ancoli-Israel, S., et al., *Sleep-disordered breathing in community-dwelling elderly*. Sleep, 1991. **14**(6): p. 486-495.
249. Barthel, S.W. and M. Strome, *Snoring, obstructive sleep apnea, and surgery*. Medical Clinics of North America, 1999. **83**(1): p. 85-96.
250. Cutler, M.J., et al., *Sleep apnea: From the nose to the heart*. Journal of the American Board of Family Practice, 2002. **15**(2): p. 128-141.
251. Arter, J.L., D.S. Chi, and M. Girish, *Obstructive sleep apnea, inflammation, and cardiopulmonary disease*. Front Biosci, 2004. **9**: p. 2892-2900.
252. Kapur, V., et al., *The medical cost of undiagnosed sleep apnea*. Sleep, 1999. **22**(6): p. 749-755.
253. Block, A.J., et al., *Sleep apnea, hypopnea and oxygen desaturation in normal subjects. A strong male predominance*. New England Journal of Medicine, 1979. **300**(10): p. 513-517.
254. Quintana-Gallego, E., et al., *Gender differences in obstructive sleep apnea syndrome: A clinical study of 1166 patients*. Respiratory Medicine, 2004. **98**(10): p. 984-989.
255. Carter Iii, R. and D.E. Watenpaugh, *Obesity and obstructive sleep apnea: Or is it OSA and obesity?* Pathophysiology : the official journal of the International Society for Pathophysiology / ISP, 2008. **15**(2): p. 71-77.
256. Bixler, E.O., et al., *Prevalence of sleep-disordered breathing in women: Effects of gender*. American Journal of Respiratory and Critical Care Medicine, 2001. **163**(3 I): p. 608-613.
257. Redline, S., et al., *Gender differences in sleep disordered breathing in a community-based sample*. American Journal of Respiratory and Critical Care Medicine, 1994. **149**(3 I): p. 722-726.
258. Guilleminault, C., et al., *Women and the obstructive sleep apnea syndrome*. Chest, 1988. **93**(1): p. 104-109.
259. Schwab, R.J., *Sex differences and sleep apnoea*. Thorax, 1999. **54**(4): p. 284-285.
260. O'Connor, C., K.S. Thornley, and P.J. Hanly, *Gender differences in the polysomnographic features of obstructive sleep apnea*. American Journal of Respiratory and Critical Care Medicine, 2000. **161**(5): p. 1465-1472.
261. Ware, J.C., R.H. McBrayer, and J.A. Scott, *Influence of sex and age on duration and frequency of sleep apnea events*. Sleep, 2000. **23**(2): p. 165-170.
262. Young, T., et al., *Estimation of the clinically diagnosed proportion of sleep apnea syndrome in middle-aged men and women*. Sleep, 1997. **20**(9): p. 705-706.
263. Jennum, P. and R.L. Riha, *Epidemiology of sleep apnoea/hypopnoea syndrome and sleep-disordered breathing*. European Respiratory Journal, 2009. **33**(4): p. 907-914.

264. Stierer, T. and N.M. Punjabi, *Demographics and diagnosis of obstructive sleep apnea*. Anesthesiology Clinics of North America, 2005. **23**(3): p. 405-420.
265. Vagiakis, E., et al., *Gender differences on polysomnographic findings in Greek subjects with obstructive sleep apnea syndrome*. Sleep Medicine, 2006. **7**(5): p. 424-430.
266. Jordan, A.S., et al., *Respiratory control stability and upper airway collapsibility in men and women with obstructive sleep apnea*. Journal of Applied Physiology, 2005. **99**(5): p. 2020-2027.
267. Hader, C., et al., *Sleep disordered breathing in the elderly: Comparison of women and men*. Journal of Physiology and Pharmacology, 2005. **56**(SUPPL. 4): p. 85-91.
268. Millman, R.P., et al., *Body fat distribution and sleep apnea severity in women*. Chest, 1995. **107**(2): p. 362-366.
269. Leech, J.A., et al., *A comparison of men and women with occlusive sleep apnea syndrome*. Chest, 1988. **94**(5): p. 983-988.
270. Shahar, E., et al., *Hormone replacement therapy and sleep-disordered breathing*. American Journal of Respiratory and Critical Care Medicine, 2003. **167**(9): p. 1186-1192.
271. Young, T., et al., *Menopausal status and sleep-disordered breathing in the Wisconsin Sleep Cohort Study*. American Journal of Respiratory and Critical Care Medicine, 2003. **167**(9): p. 1181-1185.
272. Block, A.J., J.W. Wynne, and P.G. Baysen, *Menopause, medroxyprogesterone and breathing during sleep*. American Journal of Medicine, 1981. **70**(3): p. 506-510.
273. Wilhoit, S.C. and P.M. Suratt, *Obstructive sleep apnea in premenopausal women. A comparison with men and with postmenopausal women*. Chest, 1987. **91**(5): p. 654-658.
274. Durán, J., et al., *Obstructive sleep apnea-hypopnea and related clinical features in a population-based sample of subjects aged 30 to 70 yr*. American Journal of Respiratory and Critical Care Medicine, 2001. **163**(3 I): p. 685-689.
275. Fisher, D., et al., *Long-term follow-up of untreated patients with sleep apnoea syndrome*. Respiratory Medicine, 2002. **96**(5): p. 337-343.
276. Tishler, P.V., et al., *Incidence of Sleep-Disordered Breathing in an Urban Adult Population: The Relative Importance of Risk Factors in the Development of Sleep-Disordered Breathing*. Journal of the American Medical Association, 2003. **289**(17): p. 2230-2237.
277. Lopez-Jimenez, F., et al., *Obstructive sleep apnea: Implications for cardiac and vascular disease*. Chest, 2008. **133**(3): p. 793-804.
278. Kalra, M. and R. Chakraborty, *Genetic susceptibility to obstructive sleep apnea in the obese child*. Sleep Medicine, 2007. **8**(2): p. 169-175.
279. Bixler, E.O., et al., *Blood pressure associated with sleep-disordered breathing in a population sample of children*. Hypertension, 2008. **52**(5): p. 841-846.
280. Guilleminault, C., R. Korobkin, and R. Winkle, *A review of 50 children with obstructive sleep apnea syndrome*. Lung, 1981. **159**(5): p. 275-287.
281. Rosen, C.L., L. D'Andrea, and G.G. Haddad, *Adult criteria for obstructive sleep apnea do not identify children with serious obstruction*. American Review of Respiratory Disease, 1992. **146**(5): p. 1231-1234.

282. Thach, B.T., *Sleep apnea in infancy and childhood*. Medical Clinics of North America, 1985. **69**(6): p. 1289-1315.
283. Ali, N.J., D.J. Pitson, and J.R. Stradling, *Snoring, sleep disturbance, and behaviour in 4-5 year olds*. Archives of Disease in Childhood, 1993. **68**(3): p. 360-366.
284. Xu, C., et al., *Computational fluid dynamics modeling of the upper airway of children with obstructive sleep apnea syndrome in steady flow*. Journal of Biomechanics, 2006. **39**(11): p. 2043-2054.
285. Fietze, I., et al., *Management of obstructive sleep apnea in Europe*. Sleep Medicine, 2011. **12**(2): p. 190-197.
286. Frey, W.C. and J. Pilcher, *Obstructive Sleep-Related Breathing Disorders in Patients Evaluated for Bariatric Surgery*. Obesity Surgery, 2003. **13**(5): p. 676-683.
287. Hallowell, P.T., et al., *Potentially life-threatening sleep apnea is unrecognized without aggressive evaluation*. The American journal of surgery, 2007. **193**(3): p. 364-367.
288. Lopez, P.P., et al., *Prevalence of sleep apnea in morbidly obese patients who presented for weight loss surgery evaluation: more evidence for routine screening for obstructive sleep apnea before weight loss surgery*. The American surgeon, 2008. **74**(9): p. 834-838.
289. Naimark, A. and R.M. Cherniack, *Compliance of the respiratory system and its components in health and obesity*. Journal of Applied Physiology, 1960. **15**: p. 377-382.
290. Zerah, F., et al., *Effects of obesity on respiratory resistance*. Chest, 1993. **103**(5): p. 1470-1476.
291. Sampson, M.G. and A. Grassino, *Neuromechanical properties in obese patients during carbon dioxide rebreathing*. American Journal of Medicine, 1983. **75**(1): p. 81-90.
292. Fleetham, J.A., *Upper airway imaging in relationship to obstructive sleep apnea*. Clinics in Chest Medicine, 1992. **13**(3): p. 399-416.
293. Kyzer, S. and I. Charuzi, *Obstructive sleep apnea in the obese*. World Journal of Surgery, 1998. **22**(9): p. 998-1001.
294. Mallory Jr, G.B., D.H. Fiser, and R. Jackson, *Sleep-associated breathing disorders in morbidly obese children and adolescents*. The Journal of Pediatrics, 1989. **115**(6): p. 892-897.
295. Silvestri, J.M., et al., *Polysomnography in obese children with a history of sleep-associated breathing disorders*. Pediatric Pulmonology, 1993. **16**(2): p. 124-129.
296. Marcus, C.L., et al., *Evaluation of pulmonary function and polysomnography in obese children and adolescents*. Pediatric Pulmonology, 1996. **21**(3): p. 176-183.
297. Redline, S., et al., *Risk Factors for Sleep-disordered Breathing in Children*. American Journal of Respiratory and Critical Care Medicine, 1999. **159**(5): p. 1527-1532.
298. Valencia-Flores, M., et al., *Prevalence of sleep apnea and electrocardiographic disturbances in morbidly obese patients*. Obesity Research, 2000. **8**(3): p. 262-269.
299. Peppard, P.E., et al., *Longitudinal study of moderate weight change and sleep-disordered breathing*. Journal of the American Medical Association, 2000. **284**(23): p. 3015-3021.
300. Resta, O., et al., *Sleep-related breathing disorders, loud snoring and excessive daytime sleepiness in obese subjects*. International Journal of Obesity, 2001. **25**(5): p. 669-675.

301. Lacasse, Y., C. Godbout, and F. Sériès, *Independent validation of the Sleep Apnoea Quality of Life Index*. Thorax, 2002. **57**(6): p. 483-488.
302. Moore, P., et al., *Association between polysomnographic sleep measures and health-related quality of life in obstructive sleep apnea*. Journal of Sleep Research, 2001. **10**(4): p. 303-308.
303. Glinski, J., S. Wetzler, and E. Goodman, *The psychology of gastric bypass surgery*. Obesity Surgery, 2001. **11**(5): p. 581-588.
304. Friedman, K.E., et al., *Body image partially mediates the relationship between obesity and psychological distress*. Obesity Research, 2002. **10**(1): p. 33-41.
305. Dixon, J.B., L.M. Schachter, and P.E. O'Brien, *Predicting sleep apnea and excessive day sleepiness in the severely obese: Indicators for polysomnography*. Chest, 2003. **123**(4): p. 1134-1141.
306. O'Keeffe, T. and E.J. Patterson, *Evidence Supporting Routine Polysomnography before Bariatric Surgery*. Obesity Surgery, 2004. **14**(1): p. 23-26.
307. Fritscher, L.G., et al., *Obesity and obstructive sleep apnea-hypopnea syndrome: the impact of bariatric surgery*. Obesity surgery : the official journal of the American Society for Bariatric Surgery and of the Obesity Surgery Society of Australia and New Zealand, 2007. **17**(1): p. 95-99.
308. Verhulst, S.L., et al., *Sleep-disordered breathing in overweight and obese children and adolescents: Prevalence, characteristics and the role of fat distribution*. Archives of Disease in Childhood, 2007. **92**(3): p. 205-208.
309. Maclel Santos, M.E.S., et al., *Obstructive sleep apnea-hypopnea syndrome-the role of bariatric and maxillofacial surgeries*. Obesity Surgery, 2009. **19**(6): p. 796-801.
310. Ancoli-Israel, S., et al., *Sleep-disordered breathing in African-American elderly*. American Journal of Respiratory and Critical Care Medicine, 1995. **152**(6 1): p. 1946-1949.
311. Palmer, L.J., et al., *Whole genome scan for obstructive sleep apnea and obesity in African-American families*. American Journal of Respiratory and Critical Care Medicine, 2004. **169**(12): p. 1314-1321.
312. Villaneuva, A.T.C., et al., *Ethnicity and obstructive sleep apnoea*. Sleep Medicine Reviews, 2005. **9**(6): p. 419-436.
313. Redline, S., et al., *Racial differences in sleep-disordered breathing in African-Americans and Caucasians*. American Journal of Respiratory and Critical Care Medicine, 1997. **155**(1): p. 186-192.
314. Lam, B., D.C.L. Lam, and M.S.M. Ip, *Obstructive sleep apnoea in Asia*. International Journal of Tuberculosis and Lung Disease, 2007. **11**(1): p. 2-11.
315. Sutherland, K., R.W.W. Lee, and P.A. Cistulli, *Obesity and craniofacial structure as risk factors for obstructive sleep apnoea: Impact of ethnicity*. Respiriology, 2012. **17**(2): p. 213-222.
316. Mihaere, K.M., et al., *Obstructive sleep apnea in new zealand adults: prevalence and risk factors among Māori and non-Māori*. Sleep, 2009. **32**(7): p. 949-956.
317. Robson, B., Harris, R. *Hauora Maori standards of Health IV*. Wellington: Te Ropu Rangahau Hauora a Eru Pomare. 2007; Available from: <http://www.hauora.Maori.nz>.

318. Frith, R.W., Cant B. R., *Obstructive sleep apnoea in Auckland: diagnosis and treatment*. New Zealand Medical Journal, 1985. **98**: p. 745-748.
319. Baldwin D. R., K., J., Troy, K., et al, *Comparative clinical and physiological features of Māori, Pacific Islanders and Europeans with sleep related breathing disorders*. Respiriology, 1998. **3**: p. 253-260.
320. Gentles, D.G.R., et al., *Blood pressure prevalences and levels for a multicultural population in Auckland, New Zealand: Results from the Diabetes, Heart and Health Survey 2002/2003*. New Zealand Medical Journal, 2006. **119**(1245).
321. Firestone, R.T., K. Mihaere, and P.H. Gander, *Obstructive sleep apnoea among professional taxi drivers: A pilot study*. Accident Analysis and Prevention, 2009. **41**(3): p. 552-556.
322. Tipene-Leach, D., Stewart, A., Beaglehole, R., *Coronary heart disease mortality in Auckland Maori and Europeans*. New Zealand Medical Journal, 1991. **104**(906): p. 55-57.
323. Paine, S.J., R.B. Harris, and K.M. Mihaere, *Managing obstructive sleep apnoea and achieving equity: Implications for health services*. New Zealand Medical Journal, 2011. **124**(1334): p. 97-104.
324. Dryson, E., et al., *The relationship between body mass index and socioeconomic status in New Zealand: ethnic and occupational factors*. New Zealand Medical Journal, 1992. **105**(936): p. 233-235.
325. Tuomilehto, H.P.I., et al., *Lifestyle intervention with weight reduction: First-line treatment in mild obstructive sleep apnea*. American Journal of Respiratory and Critical Care Medicine, 2009. **179**(4): p. 320-327.
326. Li, K.K., et al., *Overview of phase I surgery for obstructive sleep apnea syndrome*. Ear, Nose and Throat Journal, 1999. **78**(11): p. 836-845.
327. Harman, E., J. Wynne, and A. Block, *The effect of weight loss on sleep-disordered breathing and oxygen desaturation in morbidly obese men*. Chest, 1982. **82**(3): p. 291-294.
328. Jenkinson, C., et al., *Comparison of therapeutic and subtherapeutic nasal continuous positive airway pressure for obstructive sleep apnoea: A randomised prospective parallel trial*. Lancet, 1999. **353**(9170): p. 2100-2105.
329. Montserrat, J.M., et al., *Effectiveness of CPAP treatment in daytime function in sleep apnea syndrome: A randomized controlled study with an optimized placebo*. American Journal of Respiratory and Critical Care Medicine, 2001. **164**(4): p. 608-613.
330. Conway, W.A., Zorick, F., Piccione, P., Roth, T., *Protriptylline in the treatment of sleep apnea*. Thorax, 1982. **37**: p. 49-53.
331. Lin, C.M., T.M. Davidson, and S. Ancoli-Israel, *Gender differences in obstructive sleep apnea and treatment implications*. Sleep Medicine Reviews, 2008. **12**(6): p. 481-496.
332. Thorpy, M., Chesson, A., and Derderian, S., *Practice parameters for the treatment of obstructive sleep apnea in adults: The efficacy of surgical modifications of the upper airway*. Sleep, 1996. **19**(2): p. 152-155.
333. Friedman, M., et al., *Effect of improved nasal breathing on obstructive sleep apnea*. Otolaryngology - Head and Neck Surgery, 2000. **122**(1): p. 71-74.



334. Verse, T., J.T. Maurer, and W. Pirsig, *Effect of nasal surgery on sleep-related breathing disorders*. Laryngoscope, 2002. **112**(1): p. 64-68.
335. Guilleminault, C., et al., *Is obstructive sleep apnea syndrome a neurological disorder? A continuous positive airway pressure follow-up study*. Annals of Neurology, 2005. **58**(6): p. 880-887.
336. Schmidt-Nowara, W., et al., *Oral appliances for the treatment of snoring and obstructive sleep apnea: A review*. Sleep, 1995. **18**(6): p. 501-510.
337. Marti, S., et al., *Mortality in severe sleep apnoea/hypopnoea syndrome patients: Impact of treatment*. European Respiratory Journal, 2002. **20**(6): p. 1511-1518.
338. Li, K.K., *Surgical therapy for adult obstructive sleep apnea*. Sleep Medicine Reviews, 2005. **9**(3): p. 201-209.
339. Fijita, S., Conway, W., Zorick, F., and Roth, T., *Surgical correction of anatomic abnormalities of obstructive sleep apnea syndrome: uvulopalatopharyngoplasty*. Otolaryngol Head Neck Surg, 1981. **89**: p. 923-934.
340. Fujita, S., et al., *Surgical correction of anatomic abnormalities in obstructive sleep apnea syndrome: Uvulopalatopharyngoplasty*. Otolaryngology - Head and Neck Surgery, 1981. **89**(6): p. 923-934.
341. Riley, R.W., N. Powell, and C. Guilleminault, *Current surgical concepts for treating obstructive sleep apnea syndrome*. Journal of Oral and Maxillofacial Surgery, 1987. **45**(2): p. 149-157.
342. Sher, A.E., *Surgical management of obstructive sleep apnea*. Progress in Cardiovascular Diseases, 1999. **41**(5): p. 387-396.
343. Sher, A.E., K.B. Schechtman, and J.F. Piccirillo, *The efficacy of surgical modifications of the upper airway in adults with obstructive sleep apnea syndrome*. Sleep, 1996. **19**(2): p. 156-177.
344. Rivlin, J., V. Hoffstein, and J. Kalbfleisch, *Upper airway morphology in patients with idiopathic obstructive sleep apnea*. American Review of Respiratory Disease, 1984. **129**(3): p. 355-360.
345. Powell, N., et al., *A reversible uvulopalatal flap for snoring and sleep apnea syndrome*. Sleep, 1996. **19**(7): p. 593-599.
346. Kamami, Y.V., *Laser CO2 for snoring. Preliminary results*. Acta Oto-Rhino-Laryngologica Belgica, 1990. **44**(4): p. 451-456.
347. Kamami, Y.V., *Outpatient treatment of sleep apnea syndrome with CO2 laser: Laser-assisted UPPP*. Journal of Otolaryngology, 1994. **23**(6): p. 395-398.
348. Cheng, D.S.T., et al., *Carbon dioxide laser surgery for snoring: Results in 192 patients*. Otolaryngology - Head and Neck Surgery, 1998. **118**(4): p. 486-489.
349. Astor, F.C., et al., *Analysis of short-term outcome after office-based laser-assisted uvulopalatoplasty*. Otolaryngology - Head and Neck Surgery, 1998. **118**(4): p. 478-480.
350. Littner, M., et al., *Practice parameters for the use of laser-assisted uvulopalatoplasty: An update for 2000*. Sleep, 2001. **24**(5): p. 603-619.

351. Riley, R.W., N.B. Powell, and C. Guilleminault, *Obstructive sleep apnea and the hyoid: A revised surgical procedure*. Otolaryngology - Head and Neck Surgery, 1994. **111**(6): p. 717-721.
352. Riley, R.W., N.B. Powell, and C. Guilleminault, *Inferior mandibular osteotomy and hyoid myotomy suspension for obstructive sleep apnea: a review of 55 patients*. Journal of Oral and Maxillofacial Surgery, 1989. **47**(2): p. 159-164.
353. Verse, T., A. Baisch, and K. Hörmann, *Multi-level surgery for obstructive sleep apnea. Preliminary objective results*. Multi-level-chirurgie bei obstruktiver schlafapnoe. Erste objektive ergebnisse, 2004. **83**(8): p. 516-522.
354. Bettega, G., et al., *Obstructive sleep apnea syndrome: Fifty-one consecutive patients treated by maxillofacial surgery*. American Journal of Respiratory and Critical Care Medicine, 2000. **162**(2 1): p. 641-649.
355. Hsu, P.P. and R.H. Brett, *Multiple level pharyngeal surgery for obstructive sleep apnoea*. Singapore Medical Journal, 2001. **42**(4): p. 160-164.
356. Neruntarat, C., *Genioglossus advancement and hyoid myotomy under local anesthesia*. Otolaryngology - Head and Neck Surgery, 2003. **129**(1): p. 85-91.
357. Lee, N.R., et al., *Staged surgical treatment of obstructive sleep apnea syndrome: A review of 35 patients*. Journal of Oral and Maxillofacial Surgery, 1999. **57**(4): p. 382-385.
358. Prinsell, J.R., *Maxillomandibular advancement surgery in a site-specific treatment approach for obstructive sleep apnea in 50 consecutive patients*. Chest, 1999. **116**(6): p. 1519-1529.
359. Powell, N.B., *Contemporary surgery for obstructive sleep apnea syndrome*. Clinical and Experimental Otorhinolaryngology, 2009. **2**(3): p. 107-114.
360. Riley, R.W., N.B. Powell, and C. Guilleminault, *Maxillofacial surgery and nasal CPAP: A comparison of treatment for obstructive sleep apnea syndrome*. Chest, 1990. **98**(6): p. 1421-1425.
361. Yu, C.C., et al., *Computational fluid dynamic study on obstructive sleep apnea syndrome treated with maxillomandibular advancement*. Journal of Craniofacial Surgery, 2009. **20**(2): p. 426-430.
362. Huynh, J., K.B. Kim, and M. McQuilling, *Pharyngeal airflow analysis in obstructive sleep apnea patients pre-and post-maxillomandibular advancement surgery*. Journal of Fluids Engineering, Transactions of the ASME, 2009. **131**(9): p. 91-101.
363. Li, K.K., et al., *Overview of phase II surgery for obstructive sleep apnea syndrome*. Ear, Nose and Throat Journal, 1999. **78**(11): p. 851-857.
364. Won, C.H.J., K.K. Li, and C. Guilleminault, *Surgical treatment of obstructive sleep apnea: Upper airway and maxillomandibular surgery*. Proceedings of the American Thoracic Society, 2008. **5**(2): p. 193-199.
365. Abbey, N.C., Cooper, K.R., and Kwentus, J.A., *Benefit of nasal CPAP in obstructive sleep apnea is due to positive pharyngeal pressure*. Sleep, 1989. **12**: p. 420-422.
366. Li, K.K., et al., *Obstructive sleep apnea surgery: Patient perspective and polysomnographic results*. Otolaryngology - Head and Neck Surgery, 2000. **123**(5): p. 572-575.

367. Waite, P.D., et al., *Maxillomandibular advancement surgery in 23 patients with obstructive sleep apnea syndrome*. Journal of Oral and Maxillofacial Surgery, 1989. **47**(12): p. 1256-1261.
368. Waite, P.D. and S.M. Shettar, *Maxillomandibular advancement surgery: A cure for obstructive sleep apnea syndrome*. Oral Maxillofac Surg Clin North Am, 1995. **7**(2): p. 327-336.
369. Riley, R.W., N.B. Powell, and C. Guilleminault, *Maxillofacial surgery and obstructive sleep apnea: A review of 80 patients*. Otolaryngology - Head and Neck Surgery, 1989. **101**(3): p. 353-361.
370. Riley, R.W., N.B. Powell, and C. Guilleminault, *Obstructive sleep apnea syndrome: A review of 306 consecutively treated surgical patients*. Otolaryngology - Head and Neck Surgery, 1993. **108**(2): p. 117-125.
371. Kuo, P.C., R.A. West, and D.S. Bloomquist, *The effect of mandibular osteotomy in three patients with hypersomnia sleep apnea*. Oral Surgery Oral Medicine and Oral Pathology, 1979. **48**(5): p. 385-392.
372. De Backer, J.W., et al., *Functional imaging using computational fluid dynamics to predict treatment success of mandibular advancement devices in sleep-disordered breathing*. Journal of Biomechanics, 2007. **40**(16): p. 3708-3714.
373. Van Holsbeke, C., et al., *Anatomical and functional changes in the upper airways of sleep apnea patients due to mandibular repositioning: A large scale study*. Journal of Biomechanics, 2011. **44**(3): p. 442-449.
374. Powell, N.B., et al., *Radiofrequency volumetric reduction of the tongue: A porcine pilot study for the treatment of obstructive sleep apnea syndrome*. Chest, 1997. **111**(5): p. 1348-1355.
375. Powell, N.B., et al., *Radiofrequency volumetric tissue reduction of the palate in subjects with sleep-disordered breathing*. Chest, 1998. **113**(5): p. 1163-1174.
376. Li, K.K., et al., *Temperature-controlled radiofrequency tongue base reduction for sleep-disordered breathing: Long-term outcomes*. Otolaryngology - Head and Neck Surgery, 2002. **127**(3): p. 230-234.
377. Menter, F.R., *Two-equation eddy-viscosity turbulence models for engineering applications*. AIAA Journal, 1994. **32**(8): p. 1598-1605.
378. Mihaescu, M., et al., *Large Eddy simulation and Reynolds-Averaged Navier-Stokes modeling of flow in a realistic pharyngeal airway model: An investigation of obstructive sleep apnea*. Journal of Biomechanics, 2008. **41**(10): p. 303-309.
379. Suh, J. and S.H. Frankel, *Comparing turbulence models for flow through a rigid glottal model*. Journal of the Acoustical Society of America, 2008. **123**(3): p. 1237-1240.
380. Karason, K., et al., *Relief of cardiorespiratory symptoms and increased physical activity after surgically induced weight loss: results from the Swedish Obese Subjects study*. Archives of internal medicine, 2000. **160**(12): p. 1797-1802.
381. Rasheid, S., et al., *Gastric Bypass is an Effective Treatment for Obstructive Sleep Apnea in Patients with Clinically Significant Obesity*. Obesity Surgery, 2003. **13**(1): p. 58-61.
382. Kalra, M., et al., *Obstructive sleep apnea in extremely overweight adolescents undergoing bariatric surgery*. Obesity Research, 2005. **13**(7): p. 1175-1179.

383. Dixon, J.B., L.M. Schachter, and P.E. O'Brien, *Polysomnography before and after weight loss in obese patients with severe sleep apnea*. International Journal of Obesity, 2005. **29**(9): p. 1048-1054.
384. Bakker, J.P., et al., *Pilot study of the effects of bariatric surgery and continuous positive airway pressure treatment on vascular function in obese subjects with obstructive sleep apnoea*. Internal Medicine Journal, 2013. **43**(9): p. 993-998.
385. Busetto, L., et al., *Obstructive sleep apnea syndrome in morbid obesity: effects of intragastric balloon*. Chest Journal, 2005. **128**(2): p. 618-623.
386. Valencia-Flores, M., et al., *Effect of bariatric surgery on obstructive sleep apnea and hypopnea syndrome, electrocardiogram, and pulmonary arterial pressure*. Obesity Surgery, 2004. **14**(6): p. 755-762.
387. Charuzi, I., et al., *Sleep apnea syndrome in the morbidly obese undergoing bariatric surgery*. Gastroenterology clinics of North America, 1987. **16**(3): p. 517-519.
388. Fritscher, L.G., et al., *Bariatric surgery in the treatment of obstructive sleep apnea in morbidly obese patients*. Respiration, 2007. **74**(6): p. 647-652.
389. Ulfberg, J. and R. Thuman, *A Non-Urologic Cause of Nocturia and Enuresis - Obstructive Sleep Apnea Syndrome (OSAS)*. Scandinavian Journal of Urology and Nephrology, 1996. **30**(2): p. 135-137.
390. Smith, P.L., et al., *Indications and standards for use of nasal continuous positive airway pressure (CPAP) in sleep apnea syndromes*. American Journal of Respiratory and Critical Care Medicine, 1994. **150**(6 I): p. 1738-1745.
391. Ballester, E., et al., *Evidence of the effectiveness of continuous positive airway pressure in the treatment of sleep apnea/hypopnea syndrome*. American Journal of Respiratory and Critical Care Medicine, 1999. **159**(2): p. 495-501.
392. Loube, D.I., et al., *Indications for positive airway pressure treatment of adult obstructive sleep apnea patients: A consensus statement*. Chest, 1999. **115**(3): p. 863-866.
393. Grunstein, R. and C. Sullivan, *Continuous positive airway pressure for sleep breathing disorders*. Principles and Practice of Sleep Medicine, 2000: p. 894-912.
394. Hack, M., et al., *Randomised prospective parallel trial of therapeutic versus subtherapeutic nasal continuous positive airway pressure on simulated steering performance in patients with obstructive sleep apnoea*. Thorax, 2000. **55**(3): p. 224-231.
395. Giles, T.L., et al., *Continuous positive airways pressure for obstructive sleep apnoea in adults*. Cochrane database of systematic reviews (Online), 2006(1).
396. Kushida, C.A., et al., *Practice parameters for the use of continuous and bilevel positive airway pressure devices to treat adult patients with sleep-related breathing disorders*. Sleep, 2006. **29**(3): p. 375-380.
397. Johnson, J.T., Gluckman, J. L., Sanders, M. M., *Management of obstructive sleep apnea*. Taylor and Francis, London, 2002.
398. Roux, F.J. and J. Hilbert, *Continuous positive airway pressure: New generations*. Clinics in Chest Medicine, 2003. **24**(2): p. 315-342.

399. Whitelaw, W.A., R.F. Brant, and W.W. Flemons, *Clinical usefulness of home oximetry compared with polysomnography for assessment of sleep apnea*. American Journal of Respiratory and Critical Care Medicine, 2005. **171**(2): p. 188-193.
400. Littner, M., et al., *Practice parameters for the use of auto-titrating continuous positive airway pressure devices for titrating pressures and treating adult patients with obstructive sleep apnea syndrome: An American Academy of Sleep Medicine report*. Sleep, 2002. **25**(2): p. 143-147.
401. Berthon-Jones, M., et al., *Feasibility of a self-setting CPAP machine*. Sleep, 1993. **16**(8 SUPPL.): p. S120-S123.
402. Berry, R.B., J.M. Parish, and K.M. Hartse, *The use of auto-titrating continuous positive airway pressure for treatment of adult obstructive sleep apnea: An American Academy of Sleep Medicine review*. Sleep, 2002. **25**(2): p. 148-173.
403. Teschler, H., et al., *Automated continuous positive airway pressure titration for obstructive sleep apnea syndrome*. American Journal of Respiratory and Critical Care Medicine, 1996. **154**(3 1): p. 734-740.
404. Senn, O., et al., *Randomized Short-term Trial of Two AutoCPAP Devices versus Fixed Continuous Positive Airway Pressure for the Treatment of Sleep Apnea*. American Journal of Respiratory and Critical Care Medicine, 2003. **168**(12): p. 1506-1511.
405. Stammnitz, A., et al., *Automatic CPAP titration with different self-setting devices in patients with obstructive sleep apnoea*. European Respiratory Journal, 2004. **24**(2): p. 273-278.
406. Pevernagie, D.A., et al., *Efficacy of flow- vs impedance-guided autoadjustable continuous positive airway pressure: A randomized cross-over trial*. Chest, 2004. **126**(1): p. 25-30.
407. Scharf, M.B., et al., *Computerized adjustable versus fixed NCPAP treatment of obstructive sleep apnea*. Sleep, 1996. **19**(6): p. 491-496.
408. Konermann, M., et al., *Use of conventional and self-adjusting nasal continuous positive airway pressure for treatment of severe obstructive sleep apnea syndrome: A comparative study*. Chest, 1998. **113**(3): p. 714-718.
409. Boudewyns, A., et al., *Two months follow up of auto-CPAP treatment in patients with obstructive sleep apnoea*. Thorax, 1999. **54**(2): p. 147-149.
410. D'Ortho, M.P., et al., *Constant vs automatic continuous positive airway pressure therapy: Home evaluation*. Chest, 2000. **118**(4): p. 1010-1017.
411. Planès, C., et al., *Efficacy and cost of home-initiated auto-nCPAP versus conventional nCPAP*. Sleep, 2003. **26**(2): p. 156-160.
412. Meurice, J.C., I. Marc, and F. Sériès, *Efficacy of auto-CPAP in the treatment of obstructive sleep apnea/hypopnea syndrome*. American Journal of Respiratory and Critical Care Medicine, 1996. **153**(2): p. 794-798.
413. Hussain, S.F., et al., *A randomized trial of auto-titrating CPAP and fixed CPAP in the treatment of obstructive sleep apnea-hypopnea*. Respiratory Medicine, 2004. **98**(4): p. 330-333.
414. Ficker, J.H., et al., *An auto-continuous positive airway pressure device controlled exclusively by the forced oscillation technique*. European Respiratory Journal, 2000. **16**(5): p. 914-920.

415. Randerath, W.J., et al., *Autoadjusting CPAP therapy based on impedance efficacy, compliance and acceptance*. American Journal of Respiratory and Critical Care Medicine, 2001. **163**(3 I): p. 652-657.
416. Teschler, H., et al., *Two months auto-adjusting versus conventional nCPAP for obstructive sleep apnoea syndrome*. European Respiratory Journal, 2000. **15**(6): p. 990-995.
417. Massie, C.A., et al., *Comparison between automatic and fixed positive airway pressure therapy in the home*. American Journal of Respiratory and Critical Care Medicine, 2003. **167**(1): p. 20-23.
418. Hudgel, D.W. and C. Fung, *A long-term randomized, cross-over comparison of auto-titrating and standard nasal continuous airway pressure*. Sleep, 2000. **23**(5): p. 645-648.
419. Marrone, O., et al., *Preference for fixed or automatic CPAP in patients with obstructive sleep apnea syndrome*. Sleep Medicine, 2004. **5**(3): p. 247-251.
420. Hukins, C., *Comparative study of autotitrating and fixed-pressure CPAP in the home: A randomized, single-blind crossover trial*. Sleep, 2004. **27**(8): p. 1512-1517.
421. Rodenstein, D.O., *Automatically controlled continuous positive airway pressure. A bright past, a dubious future*. European Respiratory Journal, 2000. **15**(6): p. 985-987.
422. Lowe, A.A., *Oral appliances for sleep breathing disorders*. Principles and Practice of Sleep Medicine, 2000: p. 929-939.
423. Rapoport, D.M., et al., *Reversal of the 'Pickwickian syndrome' by long-term use of nocturnal nasal-airway pressure*. New England Journal of Medicine, 1982. **307**(15): p. 931-933.
424. Randerath, W.J., et al., *An individually adjustable oral appliance vs continuous positive airway pressure in mild-to-moderate obstructive sleep apnea syndrome*. Chest, 2002. **122**(2): p. 569-575.
425. Engleman, H.M., et al., *Randomized crossover trial of two treatments for sleep apnea/hypopnea syndrome: Continuous positive airway pressure and mandibular repositioning splint*. American Journal of Respiratory and Critical Care Medicine, 2002. **166**(6): p. 855-859.
426. Sullivan, C.E., et al., *Reversal of obstructive sleep apnoea by continuous positive airway pressure applied through the nares*. Lancet, 1981. **1**(8225): p. 862-865.
427. Gay, P., et al., *Evaluation of positive airway pressure treatment for sleep related breathing disorders in adults: A review by the positive airway pressure task force of the Standards of Practice Committee of the American Academy of Sleep Medicine*. Sleep, 2006. **29**(3): p. 381-401.
428. Kramer, N.R., A.E. Bonitati, and R.P. Millman, *Enuresis and obstructive sleep apnea in adults*. Chest, 1998. **114**(2): p. 634-637.
429. Gold, A.R. and A.R. Schwartz, *The pharyngeal critical pressure: The whys and hows of using nasal continuous positive airway pressure diagnostically*. Chest, 1996. **110**(4): p. 1077-1088.
430. Iber, C., et al., *Single night studies in obstructive sleep apnea*. Sleep, 1991. **14**(5): p. 383-385.
431. Berry, R.B. and A.J. Block, *Positive nasal airway pressure eliminates snoring as well as obstructive sleep apnea*. Chest, 1984. **85**(1): p. 15-20.

432. McArdle, N. and N.J. Douglas, *Effect of continuous positive airway pressure on sleep architecture in the sleep apnea-hypopnea syndrome: A randomized controlled trial*. American Journal of Respiratory and Critical Care Medicine, 2001. **164**(8 I): p. 1459-1463.
433. Lamphere, J., et al., *Recovery of alertness after CPAP in apnea*. Chest, 1989. **96**(6): p. 1364-1367.
434. Pichel, F., et al., *Health-related quality of life in patients with obstructive sleep apnea: Effects of long-term positive airway pressure treatment*. Respiratory Medicine, 2004. **98**(10): p. 968-976.
435. Findley, L.J., et al., *Driving simulator performance in patients with sleep apnea*. American Review of Respiratory Disease, 1989. **140**(2 I): p. 529-530.
436. George, C.F.P., *Driving and automobile crashes in patients with obstructive sleep apnoea/hypopnoea syndrome*. Thorax, 2004. **59**(9): p. 804-807.
437. Worsnop, C.J., R.J. Pierce, and M. Naughton, *Systemic hypertension and obstructive sleep apnea*. Sleep, 1993. **16**(8 SUPPL.): p. S148-S149.
438. Bahammam, A., et al., *Health care utilization in males with obstructive sleep apnea syndrome two years after diagnosis and treatment*. Sleep, 1999. **22**(6): p. 740-747.
439. Oliver, Z. and V. Hoffstein, *Predicting effective continuous positive airway pressure*. Chest, 2000. **117**(4): p. 1061-1064.
440. Patel, S.R., et al., *Continuous positive airway pressure therapy for treating sleepiness in a diverse population with obstructive sleep apnea results of a meta-analysis*. Archives of Internal Medicine, 2003. **163**(5): p. 565-571.
441. Marshall, N.S., et al., *Continuous positive airway pressure reduces daytime sleepiness in mild to moderate obstructive sleep apnoea: A meta-analysis*. Thorax, 2006. **61**(5): p. 430-434.
442. Lam, B., et al., *Randomised study of three non-surgical treatments in mild to moderate obstructive sleep apnoea*. Thorax, 2007. **62**(4): p. 354-359.
443. Noda, A., et al., *Continuous positive airway pressure improves daytime baroreflex sensitivity and nitric oxide production in patients with moderate to severe obstructive sleep apnea syndrome*. Hypertension Research, 2007. **30**(8): p. 669-676.
444. Bayram, N.A., et al., *Effects of continuous positive airway pressure therapy on right ventricular function assessment by tissue Doppler imaging in patients with obstructive sleep apnea syndrome*. Echocardiography, 2008. **25**(10): p. 1071-1078.
445. Chesson A.L, Jr., et al., *Practice parameters for the indications for polysomnography and related procedures*. Sleep, 1997. **20**(6): p. 406-422.
446. Kushida, C.A., et al., *Clinical guidelines for the manual titration of positive airway pressure in patients with obstructive sleep apnea*. Journal of Clinical Sleep Medicine, 2008. **4**(2): p. 157-171.
447. Foster, G.E., et al., *Effects of continuous positive airway pressure on cerebral vascular response to hypoxia in patients with obstructive sleep apnea*. American Journal of Respiratory and Critical Care Medicine, 2007. **175**(7): p. 720-725.
448. Bowie, R.A., et al., *The effect of continuous positive airway pressure on cerebral blood flow velocity in awake volunteers*. Anesthesia and analgesia, 2001. **92**(2): p. 415-417.

449. Palomaki, H., et al., *Snoring as a risk factor for sleep-related brain infarction*. Stroke, 1989. **20**(10): p. 1311-1315.
450. Spriggs, D.A., et al., *Snoring increases the risk of stroke and adversely affects prognosis*. Quarterly Journal of Medicine, 1992. **83**(303): p. 555-562.
451. Mohsenin, V., *Sleep-related breathing disorders and risk of Stroke*. Stroke, 2001. **32**(6): p. 1271-1278.
452. Hoffstein, V. and J.P. Szalai, *Predictive value of clinical features in diagnosing obstructive sleep apnea*. Sleep, 1993. **16**(2): p. 118-122.
453. Pepin, J.L., et al., *Side effects of nasal continuous positive airway pressure in sleep apnea syndrome: Study of 193 patients in two French sleep centers*. Chest, 1995. **107**(2): p. 375-381.
454. Brander, P.E., M. Soirinsuo, and P. Lohela, *Nasopharyngeal symptoms in patients with obstructive sleep apnea syndrome. Effect of nasal CPAP treatment*. Respiration, 1999. **66**(2): p. 128-135.
455. Series, F., I.M.Y. Cormier, and J. La Forge, *Required levels of nasal continuous positive airway pressure during treatment of obstructive sleep apnoea*. European Respiratory Journal, 1994. **7**(10): p. 1776-1781.
456. Collard, P., et al., *Compliance with nasal CPAP in obstructive sleep apnea patients*. Sleep Medicine Reviews, 1997. **1**(1): p. 33-44.
457. Kribbs, N.B., et al., *Objective measurement of patterns of nasal CPAP use by patients with obstructive sleep apnea*. American Review of Respiratory Disease, 1993. **147**(4): p. 887-895.
458. Berthon-Jones, M., et al., *Nasal continuous positive airway pressure treatment: Current realities and future*. Sleep, 1996. **19**(9 SUPPL.): p. S131-S135.
459. Meurice, J.C., et al., *Predictive factors of long-term compliance with nasal continuous positive airway pressure treatment in sleep apnea syndrome*. Chest, 1994. **105**(2): p. 429-433.
460. Zozula, R., R. Rosen, and B. Phillips, *Compliance with continuous positive airway pressure therapy: Assessing and improving treatment outcomes*. Current Opinion in Pulmonary Medicine, 2001. **7**(6): p. 391-398.
461. Vgontzas, A.N., et al., *Obesity without sleep apnea is associated with daytime sleepiness*. Archives of Internal Medicine, 1998. **158**(12): p. 1333-1337.
462. Barnes, M., et al., *Efficacy of positive airway pressure and oral appliance in mild to moderate obstructive sleep apnea*. American Journal of Respiratory and Critical Care Medicine, 2004. **170**(6): p. 656-664.
463. Frigg, A., et al., *Reduction in Co-morbidities 4 Years after Laparoscopic Adjustable Gastric Banding*. Obesity Surgery, 2004. **14**(2): p. 216-223.
464. Simard, B., et al., *Asthma and sleep apnea in patients with morbid obesity: Outcome after bariatric surgery*. Obesity Surgery, 2004. **14**(10): p. 1381-1388.
465. Lankford, D.A., C.D. Proctor, and R. Richard, *Continuous positive airway pressure (CPAP) changes in bariatric surgery patients undergoing rapid weight loss*. Obesity Surgery, 2005. **15**(3): p. 336-341.



466. Sugerman, H.J., et al., *Long-term effects of gastric surgery for treating respiratory insufficiency of obesity*. American Journal of Clinical Nutrition, 1992. **55**(2 SUPPL.): p. 597S-601S.
467. Pillar, G., R. Peled, and P. Lavie, *Recurrence of sleep apnea without concomitant weight increase 7.5 years after weight reduction surgery*. Chest, 1994. **106**(6): p. 1702-1704.
468. Charuzi, I., et al., *The effect of surgical weight reduction on sleep quality in obesity-related sleep apnea syndrome*. Surgery, 1985. **97**(5): p. 535-538.
469. Scheuller, M. and D. Weider, *Bariatric Surgery for Treatment of Sleep Apnea Syndrome in 15 Morbidly Obese Patients: Long-Term Results*. Otolaryngology -- Head and Neck Surgery, 2001. **125**(4): p. 299-302.
470. Guardiano, S.A., et al., *The long-term results of gastric bypass on indexes of sleep apnea\**. CHEST Journal, 2003. **124**(4): p. 1615-1619.
471. Peiser, J., et al., *Sleep apnea syndrome in the morbidly obese as an indication for weight reduction surgery*. Annals of surgery, 1984. **199**(1): p. 112-115.
472. Rubinstein, I., et al., *Improvement in upper airway function after weight loss in patients with obstructive sleep apnea*. American Review of Respiratory Disease, 1988. **138**(5): p. 1192-1195.
473. Summers, C.L., J.R. Stradling, and R.M. Baddeley, *Treatment of sleep apnoea by vertical gastropasty*. British Journal of Surgery, 1990. **77**(11): p. 1271-1272.
474. Schwartz, A.R., et al., *Effect of Weight Loss on Upper Airway Collapsibility in Obstructive Sleep Apnea*. American Review of Respiratory Disease, 1991. **144**(3\_pt\_1): p. 494-498.
475. Smith, D.K., Leonard, S. B., Greene, J. M., et al, *Physician's and dietitian's role in obese care*. Flor Med Assoc, 1992. **79**: p. 385-387.
476. Charuzi, I., et al., *Bariatric surgery in morbidly obese sleep-apnea patients: Short- and long-term follow-up*. American Journal of Clinical Nutrition, 1992. **55**(2 SUPPL.): p. 594S-596S.
477. Dhabuwala, A., R.J. Cannan, and R.S. Stubbs, *Improvement in co-morbidities following weight loss from gastric bypass surgery*. Obesity Surgery, 2000. **10**(5): p. 428-435.
478. Dixon, J.B., L.M. Schachter, and P.E. O'Brien, *Sleep disturbance and obesity: Changes following surgically induced weight loss*. Archives of Internal Medicine, 2001. **161**(1): p. 102-106.
479. Scheuller, M. and D. Weider, *Bariatric surgery for treatment of sleep apnea syndrome in 15 morbidly obese patients: Long-term results*. Otolaryngology - Head and Neck Surgery, 2001. **125**(4): p. 299-302.
480. Sugerman, H.J., et al., *Bariatric surgery for severely obese adolescents*. Journal of Gastrointestinal Surgery, 2003. **7**(1): p. 102-108.
481. Valencia-Flores, M., et al., *Effect of Bariatric Surgery on Obstructive Sleep Apnea and Hypopnea Syndrome, Electrocardiogram, and Pulmonary Arterial Pressure*. Obesity Surgery, 2004. **14**(6): p. 755-762.
482. Buchwald, H., et al., *Bariatric surgery: A systematic review and meta-analysis*. Journal of the American Medical Association, 2004. **292**(14): p. 1724-1737.

483. Dolan, K., et al., *A Comparison of Laparoscopic Adjustable Gastric Banding and Biliopancreatic Diversion in Superobesity*. Obesity Surgery, 2004. **14**(2): p. 165-169.
484. Flancbaum, L. and S. Belsley, *Factors affecting morbidity and mortality of roux-en-Y gastric bypass for clinically severe obesity: An analysis of 1,000 consecutive open cases by a single surgeon*. Journal of Gastrointestinal Surgery, 2007. **11**(4): p. 500-507.
485. Kuzniar, T.J. and T.I. Morgenthaler, *A patient with obstructive sleep apnea undergoing bariatric surgery*. Journal of Clinical Sleep Medicine, 2008. **4**(3): p. 279-280.
486. Nguyen, N.T., et al., *Improvement of restrictive and obstructive pulmonary mechanics following laparoscopic bariatric surgery*. Surgical Endoscopy and Other Interventional Techniques, 2009. **23**(4): p. 808-812.
487. Sharkey, K.M., et al., *Predicting obstructive sleep apnea among women candidates for bariatric surgery*. Journal of Women's Health, 2010. **19**(10): p. 1833-1841.
488. Sareli, A.E., et al., *Obstructive sleep apnea in patients undergoing bariatric surgery - A tertiary center experience*. Obesity Surgery, 2011. **21**(3): p. 316-327.
489. Ravesloot, M.J.L., et al., *Obstructive sleep apnea is underrecognized and underdiagnosed in patients undergoing bariatric surgery*. European Archives of Oto-Rhino-Laryngology, 2012. **269**(7): p. 1865-1871.
490. Ravesloot, M.J.L., et al., *Assessment of the effect of bariatric surgery on obstructive sleep apnea at two postoperative intervals*. Obesity Surgery, 2013: p. 1-10.
491. Mezzanotte, W.S., D.J. Tangel, and D.P. White, *Waking genioglossal electromyogram in sleep apnea patients versus normal controls (a neuromuscular compensatory mechanism)*. Journal of Clinical Investigation, 1992. **89**(5): p. 1571-1579.
492. Van der Touw, T., et al., *Respiratory-related activity of soft palate muscles: Augmentation by negative upper airway pressure*. Journal of Applied Physiology, 1994. **76**(1): p. 424-432.
493. Mortimore, I.L., R. Mathur, and N.J. Douglas, *Effect of posture, route of respiration, and negative pressure on palatal muscle activity in humans*. Journal of Applied Physiology, 1995. **79**(2): p. 448-454.
494. Henke, K.G., *Upper airway muscle activity and upper airway resistance in young adults during sleep*. Journal of Applied Physiology, 1998. **84**(2): p. 486-491.
495. Fogel, R.B., et al., *The effect of sleep onset on upper airway muscle activity in patients with sleep apnoea versus controls*. Journal of Physiology, 2005. **564**(2): p. 549-562.
496. Lo, Y.L., et al., *Influence of wakefulness on pharyngeal airway muscle activity*. Thorax, 2007. **62**(9): p. 799-805.
497. Robin, I.G., *Snoring*. Proceedings of the Royal Society of Medicine, 1968. **61**(6): p. 575-582.
498. Plowman, L., et al., *Waking and genioglossus muscle responses to upper airway pressure oscillation in sleeping dogs*. Journal of Applied Physiology, 1990. **68**(6): p. 2564-2573.
499. Zhang, S. and O.P. Mathew, *Response of laryngeal mechanoreceptors to high-frequency pressure oscillation*. Journal of Applied Physiology, 1992. **73**(1): p. 219-223.
500. Henke, K.G. and C.E. Sullivan, *Effects of high-frequency oscillating pressures on upper airway muscles in humans*. Journal of Applied Physiology, 1993. **75**(2): p. 856-862.

501. Brancatisano, A., et al., *Influence of upper airway pressure oscillations on soft palate muscle electromyographic activity*. Journal of Applied Physiology, 1996. **81**(3): p. 1190-1196.
502. Eastwood, P.R., et al., *Inhibition of inspiratory motor output by high-frequency low-pressure oscillations in the upper airway of sleeping dogs*. Journal of Physiology, 1999. **517**(1): p. 259-271.
503. Badia, J.R., et al., *Forced oscillation measurements do not affect upper airway muscle tone or sleep in clinical studies*. European Respiratory Journal, 2001. **18**(2): p. 335-339.
504. Larsson, H., et al., *Temperature thresholds in the oropharynx of patients with obstructive sleep apnea syndrome*. American Review of Respiratory Disease, 1992. **146**(5): p. 1246-1249.
505. Deegan, P.C., E. Mulloy, and W.T. McNicholas, *Topical oropharyngeal anesthesia in patients with obstructive sleep apnea*. American Journal of Respiratory and Critical Care Medicine, 1995. **151**(4): p. 1108-1112.
506. Vanderveken, O.M., et al., *Quantification of pharyngeal patency in patients with sleep-disordered breathing*. ORL; journal for oto-rhino-laryngology and its related specialties, 2005. **67**(3): p. 168-179.
507. Morrell, M.J., et al., *Progressive retropalatal narrowing preceding obstructive apnea*. American Journal of Respiratory and Critical Care Medicine, 1998. **158**(6): p. 1974-1981.
508. Mihaescu, M., et al., *Unsteady laryngeal airflow simulations of the intra-glottal vortical structures*. Journal of the Acoustical Society of America, 2010. **127**(1): p. 435-444.
509. Mihaescu, M., et al., *Computational fluid dynamics analysis of upper airway reconstructed from magnetic resonance imaging data*. Annals of Otology, Rhinology and Laryngology, 2008. **117**(4): p. 303-309.
510. Sung, S.J., et al., *Customized three-dimensional computational fluid dynamics simulation of the upper airway of obstructive sleep apnea*. Angle Orthodontist, 2006. **76**(5): p. 791-799.
511. De Backer, J.W., et al., *Flow analyses in the lower airways: Patient-specific model and boundary conditions*. Medical Engineering and Physics, 2008. **30**(7): p. 872-879.
512. Fan, Y., et al., *Computational study on obstructive sleep apnea syndrome using patient - specific models*, in *Lecture Notes in Engineering and Computer Science: Proceedings of the World Congress on Engineering 2011*: London, UK. p. 2632-2635.
513. Gambaruto, A.M., D.J. Taylor, and D.J. Doorly, *Modelling nasal air flow using a Fourier descriptor representation of geometry*. International Journal for Numerical Methods in Fluids, 2009. **59**(11): p. 1259-1283.
514. Jeong, S.J., W.S. Kim, and S.J. Sung, *Numerical investigation on the flow characteristics and aerodynamic force of the upper airway of patient with obstructive sleep apnea using computational fluid dynamics*. Medical Engineering and Physics, 2007. **29**(6): p. 637-651.
515. Keyhani, K., P.W. Scherer, and M.M. Mozell, *Numerical simulation of airflow in the human nasal cavity*. Journal of Biomechanical Engineering, 1995. **117**(4): p. 429-441.
516. Mihaescu, M., et al., *Large Eddy simulation and Reynolds-Averaged Navier-Stokes modeling of flow in a realistic pharyngeal airway model: An investigation of obstructive sleep apnea*. Journal of Biomechanics, 2008. **41**(10): p. 2279-2288.

517. Mylavarapu, G., et al., *Validation of computational fluid dynamics methodology used for human upper airway flow simulations*. Journal of Biomechanics, 2009. **42**(10): p. 1553-1559.
518. Stuck, B.A. and J.T. Maurer, *Airway evaluation in obstructive sleep apnea*. Sleep Medicine Reviews, 2008. **12**(6): p. 411-436.
519. Vos, W., et al., *Correlation between severity of sleep apnea and upper airway morphology based on advanced anatomical and functional imaging*. Journal of Biomechanics, 2007. **40**(10): p. 2207-2213.
520. Wang, K., et al. *Numerical simulation of air flow in the human nasal cavity*. 2005.
521. Weinhold, I. and G. Mlynski, *Numerical simulation of airflow in the human nose*. European Archives of Oto-Rhino-Laryngology, 2004. **261**(8): p. 452-455.
522. Yang, X.L., Y. Liu, and H.Y. Luo, *Respiratory flow in obstructed airways*. Journal of Biomechanics, 2006. **39**(15): p. 2743-2751.
523. Luo, X.Y., et al., *LES modelling of flow in a simple airway model*. Medical Engineering and Physics, 2004. **26**(5): p. 403-413.
524. Marzo, A., X.Y. Luo, and C.D. Bertram, *Three-dimensional collapse and steady flow in thick-walled flexible tubes*. Journal of Fluids and Structures, 2005. **20**(6 SPEC. ISS.): p. 817-835.
525. Ku, D.N., *Blood flow in arteries*. Annual Review of Fluid Mechanics, 1997. **29**(1): p. 399-434.
526. Bathe, M. and R.D. Kamm, *A fluid-structure interaction finite element analysis of pulsatile blood flow through a compliant stenotic artery*. Journal of Biomechanical Engineering, 1999. **121**(4): p. 361-369.
527. Allen, G.M., et al., *Computational simulations of airflow in an in vitro model of the pediatric upper airways*. Journal of Biomechanical Engineering, 2004. **126**(5): p. 604-613.
528. Gemci, T., et al., *Computational model of airflow in upper 17 generations of human respiratory tract*. Journal of Biomechanics, 2008. **41**(9): p. 2047-2054.
529. Mihaescu, M., et al., *Large Eddy Simulation of the pharyngeal airflow associated with Obstructive Sleep Apnea Syndrome at pre and post-surgical treatment*. Journal of Biomechanics, 2011. **44**(12): p. 2221-2228.
530. De Backer, J.W., et al., *Novel imaging techniques using computer methods for the evaluation of the upper airway in patients with sleep-disordered breathing: A comprehensive review*. Sleep Medicine Reviews, 2008. **12**(6): p. 437-447.
531. Mylavarapu, G., et al., *Importance of paranasal sinuses in computational modeling of nasal airflow*. 47th AIAA Aerospace Sciences Meeting and Exhibit, 2009.
532. Chouly, F., et al., *Simulation of the Retroglossal Fluid-Structure Interaction During Obstructive Sleep Apnea Biomedical Simulation*, M. Harders and G. Székely, Editors. 2006, Springer Berlin / Heidelberg. p. 48-57.
533. Balint, T.S. and A.D. Lucey, *Sleep Disorders in Microgravity (An Engineering Approach)*, 2003.
534. Wilcox, D.C., *Turbulence Modeling for CFD*. DCW Industries, Inc, ed. . 1993, CA: La Canada.
535. Pope, S.B., *Turbulent flows*. 2000, Cambridge: Cambridge University Press.

536. Zhang, Z. and C. Kleinstreuer, *Low-Reynolds-number turbulent flows in locally constricted conduits: A comparison study*. AIAA Journal, 2003. **41**(5): p. 831-840.
537. Persak, S.C., et al. *Computational fluid dynamics modeling of upper airway during tidal breathing using volume-gated MRI in OSAS and control subjects*. in *36th Annual Northeast Bioengineering Conference*. 2010. NY.
538. Ito, Y., et al., *Patient-specific geometry modeling and mesh generation for simulating Obstructive Sleep Apnea Syndrome cases by Maxillomandibular Advancement*. Mathematics and Computers in Simulation, 2011. **81**(9): p. 1876-1891.
539. Leiter, J.C., *Upper airway shape. Is it important in the pathogenesis of obstructive sleep apnea?* American Journal of Respiratory and Critical Care Medicine, 1996. **153**(3): p. 894-898.
540. Fogel, R.B., A. Malhotra, and D.P. White, *Sleep · 2: Pathophysiology of obstructive sleep apnoea/hypopnoea syndrome*. Thorax, 2004. **59**(2): p. 159-163.
541. Balint, T.S. and A.D. Lucey, *Instability of a cantilevered flexible plate in viscous channel flow*. Journal of Fluids and Structures, 2005. **20**(7 SPEC. ISS.): p. 893-912.
542. Payan, Y., X. Pelorson, and P. Perrier, *Physical modeling of airflow-walls interactions to understand the Sleep Apnea Syndrome*. 2003. p. 261-269.
543. Chouly, F., et al., *Numerical and experimental study of expiratory flow in the case of major upper airway obstructions with fluid-structure interaction*. Journal of Fluids and Structures, 2008. **24**(2): p. 250-269.
544. Malhotra, A., et al., *The male predisposition to pharyngeal collapse: Importance of airway length*. American Journal of Respiratory and Critical Care Medicine, 2002. **166**(10): p. 1388-1395.
545. Able. *3D-DOCTOR Software*. 2015 [cited 2015 30/03/2015]; Available from: <http://www.ablesw.com/3d-doctor/>.
546. ANSYS CFX v14. 2011 [cited 2015; Available from: <http://www.ansys.com/Products/Simulation+Technology/Fluid+Dynamics/Fluid+Dynamics+Products/ANSYS+CFX>.
547. White, F.M. and I. Corfield, *Viscous fluid flow*. Vol. 3. 2006: McGraw-Hill New York.
548. Wiki, M. *Navier-Stokes Equations*. [cited 2015; Available from: [http://www.cfd-online.com/Wiki/Navier-Stokes\\_equations](http://www.cfd-online.com/Wiki/Navier-Stokes_equations).
549. OSR Medical. 2007 [cited 2015; Available from: <http://www.osrmedical.com/en/division-diagnostic/polysomnographie/>.
550. James M. Gere, S.P.T., *Mechanics of materials*. Vol. 4th edition. 1997: Boston : PWS Pub Co.
551. Bijaoui, E.L., et al., *Mechanical properties of the lung and upper airways in patients with sleep-disordered breathing*. American journal of respiratory and critical care medicine, 2002. **165**(8): p. 1055-1061.
552. Tenhunen, M., et al., *Increased respiratory effort during sleep is non-invasively detected with movement sensor*. Sleep and Breathing, 2011. **15**(4): p. 737-746.

## Appendix A

### Mathematical Modelling

#### The Governing Equations for fluid flow

Continuity Equation:

$$\text{div } \vec{V} = 0 \quad (1)$$

$$\therefore \left( \frac{\partial}{\partial x} \underline{i} + \frac{\partial}{\partial y} \underline{j} + \frac{\partial}{\partial z} \underline{k} \right) \cdot (u \underline{i} + v \underline{j} + w \underline{k}) = 0$$

$$\therefore \frac{\partial u}{\partial x} + \frac{\partial v}{\partial y} + \frac{\partial w}{\partial z} = 0 \quad (2)$$

Momentum Equations (Navier-Stokes):

$$(\vec{V} \cdot \text{grad}) \vec{V} = -\frac{1}{\rho} \text{grad } P + \nu \nabla^2 \vec{V} \quad (3)$$

Which can be written as:

$$\frac{D\vec{V}}{Dt} = -\frac{1}{\rho} \text{grad } P + \nu \nabla^2 \vec{V} \quad (4)$$

Equation (4) can be solved by two mathematical techniques presented below in details.

- **First Technique:** From the definition of the total derivative,

$$\frac{D\vec{V}}{Dt} = \frac{\partial \vec{V}}{\partial t} + \frac{d\vec{V}}{dt}$$

$$\therefore \frac{\partial \vec{V}}{\partial t} + \frac{d\vec{V}}{dt} = -\frac{1}{\rho} \text{grad } P + \nu \nabla^2 \vec{V} \quad (5)$$

Also, we have:

$$\frac{\partial \vec{V}}{\partial t} = \frac{\partial u}{\partial t} \underline{i} + \frac{\partial v}{\partial t} \underline{j} + \frac{\partial w}{\partial t} \underline{k} \quad (6)$$

$$\frac{d\vec{V}}{dt} = (\vec{V} \cdot \text{grad } u) \underline{i} + (\vec{V} \cdot \text{grad } v) \underline{j} + (\vec{V} \cdot \text{grad } w) \underline{k} \quad (7)$$

Where:

$\frac{D\vec{V}}{Dt}$  : is the total derivative

$\frac{\partial \vec{V}}{\partial t}$  : is the local (time) derivative

$\frac{d\vec{V}}{dt}$  : is the space (convective) derivative

Also,

$$\begin{aligned}\vec{V} \cdot \text{grad } u &= (u\vec{i} + v\vec{j} + w\vec{k}) \cdot \left( \frac{\partial u}{\partial x}\vec{i} + \frac{\partial u}{\partial y}\vec{j} + \frac{\partial u}{\partial z}\vec{k} \right) = \\ &= u \frac{\partial u}{\partial x} + v \frac{\partial u}{\partial y} + w \frac{\partial u}{\partial z}\end{aligned}\quad (8)$$

$$\begin{aligned}\vec{V} \cdot \text{grad } v &= (u\vec{i} + v\vec{j} + w\vec{k}) \cdot \left( \frac{\partial v}{\partial x}\vec{i} + \frac{\partial v}{\partial y}\vec{j} + \frac{\partial v}{\partial z}\vec{k} \right) = \\ &= u \frac{\partial v}{\partial x} + v \frac{\partial v}{\partial y} + w \frac{\partial v}{\partial z}\end{aligned}\quad (9)$$

$$\begin{aligned}\vec{V} \cdot \text{grad } w &= (u\vec{i} + v\vec{j} + w\vec{k}) \cdot \left( \frac{\partial w}{\partial x}\vec{i} + \frac{\partial w}{\partial y}\vec{j} + \frac{\partial w}{\partial z}\vec{k} \right) = \\ &= u \frac{\partial w}{\partial x} + v \frac{\partial w}{\partial y} + w \frac{\partial w}{\partial z}\end{aligned}\quad (10)$$

Now, substituting from equations (8)-(10) into equation (7); we get:

$$\begin{aligned}& \left( \frac{\partial u}{\partial t}\vec{i} + \frac{\partial v}{\partial t}\vec{j} + \frac{\partial w}{\partial t}\vec{k} \right) + \left( u \frac{\partial u}{\partial x} + v \frac{\partial u}{\partial y} + w \frac{\partial u}{\partial z} \right)\vec{i} + \\ & \left( u \frac{\partial v}{\partial x} + v \frac{\partial v}{\partial y} + w \frac{\partial v}{\partial z} \right)\vec{j} + \left( u \frac{\partial w}{\partial x} + v \frac{\partial w}{\partial y} + w \frac{\partial w}{\partial z} \right)\vec{k} = \\ & -\frac{1}{\rho} \left( \frac{\partial P}{\partial x}\vec{i} + \frac{\partial P}{\partial y}\vec{j} + \frac{\partial P}{\partial z}\vec{k} \right) + v \left[ \left( \frac{\partial^2 u}{\partial x^2} + \frac{\partial^2 u}{\partial y^2} + \frac{\partial^2 u}{\partial z^2} \right)\vec{i} + \right. \\ & \left. \left( \frac{\partial^2 v}{\partial x^2} + \frac{\partial^2 v}{\partial y^2} + \frac{\partial^2 v}{\partial z^2} \right)\vec{j} + \left( \frac{\partial^2 w}{\partial x^2} + \frac{\partial^2 w}{\partial y^2} + \frac{\partial^2 w}{\partial z^2} \right)\vec{k} \right]\end{aligned}\quad (11)$$

Now, separating the above equation yield:

$$\vec{i} \text{ direction} \quad \frac{\partial u}{\partial t} + u \frac{\partial u}{\partial x} + v \frac{\partial u}{\partial y} + w \frac{\partial u}{\partial z} = -\frac{1}{\rho} \frac{\partial P}{\partial x} + v \left( \frac{\partial^2 u}{\partial x^2} + \frac{\partial^2 u}{\partial y^2} + \frac{\partial^2 u}{\partial z^2} \right) \quad (12)$$

$$\vec{j} \text{ direction} \quad \frac{\partial v}{\partial t} + u \frac{\partial v}{\partial x} + v \frac{\partial v}{\partial y} + w \frac{\partial v}{\partial z} = -\frac{1}{\rho} \frac{\partial P}{\partial y} + v \left( \frac{\partial^2 v}{\partial x^2} + \frac{\partial^2 v}{\partial y^2} + \frac{\partial^2 v}{\partial z^2} \right) \quad (13)$$

$$\vec{k} \text{ direction} \quad \frac{\partial w}{\partial t} + u \frac{\partial w}{\partial x} + v \frac{\partial w}{\partial y} + w \frac{\partial w}{\partial z} = -\frac{1}{\rho} \frac{\partial P}{\partial z} + v \left( \frac{\partial^2 w}{\partial x^2} + \frac{\partial^2 w}{\partial y^2} + \frac{\partial^2 w}{\partial z^2} \right) \quad (14)$$

- **Second Technique:** Equation (4) can be rewritten as follows:

$$\begin{aligned}\frac{Du}{Dt}\vec{i} + \frac{Dv}{Dt}\vec{j} + \frac{Dw}{Dt}\vec{k} &= -\frac{1}{\rho} \left( \frac{\partial P}{\partial x}\vec{i} + \frac{\partial P}{\partial y}\vec{j} + \frac{\partial P}{\partial z}\vec{k} \right) + \\ & v \left[ (\nabla^2 u)\vec{i} + (\nabla^2 v)\vec{j} + (\nabla^2 w)\vec{k} \right]\end{aligned}\quad (15)$$

The total derivative is defined as follows:

$$\frac{DA}{Dt} = \frac{\partial A}{\partial t} + \vec{V} \cdot \text{grad } A \quad (16)$$

Where A is any function or quantity

Therefore, equation (15) can be rewritten by using the definition of the total derivative given in equation (16) as follows:

$$\begin{aligned} \underline{i} \text{ direction} \quad \frac{\partial u}{\partial t} + \left( u \underline{i} + v \underline{j} + w \underline{k} \right) \cdot \left( \frac{\partial u}{\partial x} \underline{i} + \frac{\partial u}{\partial y} \underline{j} + \frac{\partial u}{\partial z} \underline{k} \right) &= -\frac{1}{\rho} \frac{\partial P}{\partial x} + \\ &v \left( \frac{\partial^2 u}{\partial x^2} + \frac{\partial^2 u}{\partial y^2} + \frac{\partial^2 u}{\partial z^2} \right) \end{aligned} \quad (17)$$

$$\begin{aligned} \underline{j} \text{ direction} \quad \frac{\partial v}{\partial t} + \left( u \underline{i} + v \underline{j} + w \underline{k} \right) \cdot \left( \frac{\partial v}{\partial x} \underline{i} + \frac{\partial v}{\partial y} \underline{j} + \frac{\partial v}{\partial z} \underline{k} \right) &= -\frac{1}{\rho} \frac{\partial P}{\partial y} + \\ &v \left( \frac{\partial^2 v}{\partial x^2} + \frac{\partial^2 v}{\partial y^2} + \frac{\partial^2 v}{\partial z^2} \right) \end{aligned} \quad (18)$$

$$\begin{aligned} \underline{k} \text{ direction} \quad \frac{\partial w}{\partial t} + \left( u \underline{i} + v \underline{j} + w \underline{k} \right) \cdot \left( \frac{\partial w}{\partial x} \underline{i} + \frac{\partial w}{\partial y} \underline{j} + \frac{\partial w}{\partial z} \underline{k} \right) &= -\frac{1}{\rho} \frac{\partial P}{\partial z} + \\ &v \left( \frac{\partial^2 w}{\partial x^2} + \frac{\partial^2 w}{\partial y^2} + \frac{\partial^2 w}{\partial z^2} \right) \end{aligned} \quad (19)$$

This can be rewritten as follows:

$$\underline{i} \text{ direction} \quad \frac{\partial u}{\partial t} + u \frac{\partial u}{\partial x} + v \frac{\partial u}{\partial y} + w \frac{\partial u}{\partial z} = -\frac{1}{\rho} \frac{\partial P}{\partial x} + v \left( \frac{\partial^2 u}{\partial x^2} + \frac{\partial^2 u}{\partial y^2} + \frac{\partial^2 u}{\partial z^2} \right) \quad (20)$$

$$\underline{j} \text{ direction} \quad \frac{\partial v}{\partial t} + u \frac{\partial v}{\partial x} + v \frac{\partial v}{\partial y} + w \frac{\partial v}{\partial z} = -\frac{1}{\rho} \frac{\partial P}{\partial y} + v \left( \frac{\partial^2 v}{\partial x^2} + \frac{\partial^2 v}{\partial y^2} + \frac{\partial^2 v}{\partial z^2} \right) \quad (21)$$

$$\underline{k} \text{ direction} \quad \frac{\partial w}{\partial t} + u \frac{\partial w}{\partial x} + v \frac{\partial w}{\partial y} + w \frac{\partial w}{\partial z} = -\frac{1}{\rho} \frac{\partial P}{\partial z} + v \left( \frac{\partial^2 w}{\partial x^2} + \frac{\partial^2 w}{\partial y^2} + \frac{\partial^2 w}{\partial z^2} \right) \quad (22)$$

It is clear that equations (20)-(22) are typically the same as equations (12)-(14).

### Transverse Vibration of Uniform Beams

The geometry of the uniform beam is given in Figure (1)

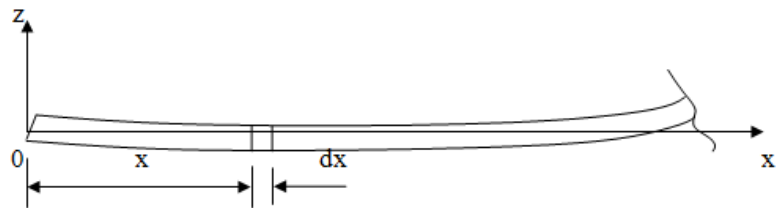


**Figure (1): Beam Geometry**



Consider the thin element of width ( $dx$ ) shown in Figure (2):

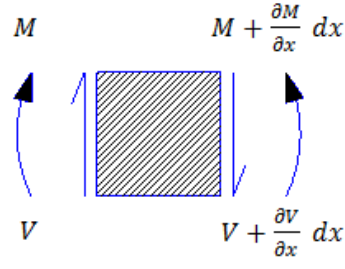


**Figure (2): Element Geometry**

Where:

M: Moment

V: Shear Force

Since the element is under equilibrium, therefore the summation of moments and forces on the element equal to zero

$$\therefore \sum M = 0$$

$$\therefore V dx = \frac{\partial M}{\partial x} dx$$

$$\text{Or } V = \frac{\partial M}{\partial x} \quad (23)$$

$$\therefore \sum F = 0$$

$$\therefore - \frac{\partial V}{\partial x} dx = (dm) \frac{\partial^2 w}{\partial t^2}$$

$$\therefore - \frac{\partial V}{\partial x} dx = \left( \frac{W}{g} \right) dx \frac{\partial^2 w}{\partial t^2}$$

$$\therefore - \frac{\partial V}{\partial x} = \left( \frac{W}{g} \right) \frac{\partial^2 w}{\partial t^2} \quad (24)$$

Where:

w: is the vertical deformation of the beam

W: Weight per unit length of the beam (N/m)

Now substituting from equation (24) in equation (23), we get:

$$\therefore -\frac{\partial^2 M}{\partial x^2} = \left(\frac{W}{g}\right) \frac{\partial^2 w}{\partial t^2} \quad (25)$$

$$\text{And } \because M = EI \frac{\partial^2 w}{\partial x^2} \quad (26)$$

Therefore equation (25) can be written as follows:

$$-\frac{\partial^2}{\partial x^2} \left( EI \frac{\partial^2 w}{\partial x^2} \right) = \left( \frac{W}{g} \right) \frac{\partial^2 w}{\partial t^2}$$

$$\text{Or } -\frac{\partial^2}{\partial x^2} \left( EI \frac{\partial^2 w}{\partial x^2} \right) = m \frac{\partial^2 w}{\partial t^2} \quad (27)$$

Where:

m: is the mass per unit length of the beam =  $\rho A$  (kg/m)

**For uniform beam, E = Constant, and I = Constant**

Therefore equation (27) becomes:

$$-EI \frac{\partial^4 w}{\partial x^4} = m \frac{\partial^2 w}{\partial t^2}$$

$$\text{Or } -EI \frac{d^4 w}{dx^4} = m \frac{d^2 w}{dt^2}$$

$$\therefore -EI \frac{d^4 w}{dx^4} = \rho A \frac{d^2 w}{dt^2} \quad (28)$$

Equation (28) is well known as “Euler-Bernoulli Beam Theory”; and is solved analytically using “Separation of Variables technique as follows:

$$w(x, t) = f(x) \cdot g(t) \quad (29)$$

Differentiating equation (29) four times with respect to (x), we get:

$$\frac{d^4 w}{dx^4} = \frac{d^4 f(x)}{dx^4} \cdot g(t) \quad (30)$$

And differentiating equation (29) twice with respect to (t), we get:

$$\frac{d^2 w}{dx^2} = f(x) \cdot \frac{d^2 g(t)}{dt^2} \quad (31)$$

Now, substitute from equation (30) and equation (31) into equation (28), we get:

$$-(EI) \frac{d^4 f(x)}{dx^4} \cdot g(t) = (\rho A) \cdot f(x) \cdot \frac{d^2 g(t)}{dt^2}$$

Divide by  $[\rho A \cdot f(x) \cdot g(t)]$ , we get:

$$-\frac{EI}{\rho A g(x)} \cdot \frac{d^4 f(x)}{dx^4} = \frac{1}{g(t)} \cdot \frac{d^2 g(t)}{dt^2} = -\omega_n^2 \quad (32)$$

Where:

$\omega_n$ : The Natural Frequency (rad/sec.)

From equation (32) we can write:

$$\therefore \frac{1}{g(t)} \cdot \frac{d^2 g(t)}{dt^2} = -\omega_n^2$$

$$\text{Or } \frac{d^2 g(t)}{dt^2} + g(t) \omega_n^2 = 0 \quad (33)$$

And

$$\therefore -\frac{EI}{\rho A g(x)} \cdot \frac{d^4 f(x)}{dx^4} = -\omega_n^2$$

$$\therefore \frac{d^4 f(x)}{dx^4} - \frac{\rho A}{EI} \omega_n^2 g(x) = 0 \quad (34)$$

To solve equation (34), the complementary function for this differential equation is given by:

$$m^2 + \omega_n^2 = 0$$

$$\therefore m = \pm i\omega_n = \alpha \pm i\beta$$

Where:

$$\alpha = 0, \beta = \omega_n$$

Therefore, the solution is given by:

$$g(t) = e^0(A \cos \omega_n t + B \sin \omega_n t)$$

$$\therefore g(t) = A \cos \omega_n t + B \sin \omega_n t \quad (35)$$

It is clear that equation (35) needs two initial conditions to evaluate the constants A and B.

Also, to solve equation (32), the complementary function for this differential equation is:

$$m^4 - \frac{\rho A}{EI} \omega_n^2 = 0$$

$$\therefore m^2 = \pm \sqrt{\frac{\rho A}{EI} \omega_n^2}$$

$$\text{For } m^2 = \sqrt{\frac{\rho A}{EI} \omega_n^2}$$

$$\therefore m = \pm \left( \frac{\rho A}{EI} \omega_n^2 \right)^{\frac{1}{4}}$$

$$\text{And for } m^2 = -\sqrt{\frac{\rho A}{EI} \omega_n^2}$$

$$\therefore m = \pm i \left( \frac{\rho A}{EI} \omega_n^2 \right)^{\frac{1}{4}}$$

So, the solution of equation (32) can be written as:

$$f(x) = C e^{\left( \frac{\rho A}{EI} \omega_n^2 \right)^{\frac{1}{4}} x} + D e^{-\left( \frac{\rho A}{EI} \omega_n^2 \right)^{\frac{1}{4}} x} + E \cos \left( \frac{\rho A}{EI} \omega_n^2 \right)^{\frac{1}{4}} x + F \sin \left( \frac{\rho A}{EI} \omega_n^2 \right)^{\frac{1}{4}} x$$

This can be rewritten as:

$$f(x) = C \cosh \lambda_n x + D \sinh \lambda_n x + E \cos \lambda_n x + F \sin \lambda_n x \quad (36)$$

Where:

$$\lambda_n = \left( \frac{\rho A}{EI} \omega_n^2 \right)^{\frac{1}{4}} \quad (37)$$

And C, D, E and F are arbitrary constants

It is clear that equation (36) needs four boundary conditions to evaluate the arbitrary constants C, D, E and F.

Recalling that equation (29) was:

$$w(x, t) = f(x) \cdot g(t) \quad (29)$$

Substituting for  $g(t)$  and  $f(x)$  from equations (35) and (36); respectively we get:

$$w(x, t) = (A \cos \omega_n t + B \sin \omega_n t)(C \cosh \lambda_n x + D \sinh \lambda_n x + E \cos \lambda_n x + F \sin \lambda_n x) \quad (38)$$

Differentiating equation (38) with respect to  $(x)$  we get:

$$\begin{aligned} \frac{dw}{dx} &= (A \cos \omega_n t + B \sin \omega_n t)(C \lambda_n \sinh \lambda_n x + D \lambda_n \cosh \lambda_n x - E \lambda_n \sin \lambda_n x + F \lambda_n \cos \lambda_n x) \\ \therefore \frac{dw}{dx} &= \lambda_n (A \cos \omega_n t + B \sin \omega_n t)(C \sinh \lambda_n x + D \cosh \lambda_n x - E \sin \lambda_n x + F \cos \lambda_n x) \end{aligned} \quad (39)$$

Differentiating equation (39) with respect to  $(x)$ , the second derivative can be written as:

$$\frac{d^2 w}{dx^2} = \lambda_n^2 (A \cos \omega_n t + B \sin \omega_n t)(C \cosh \lambda_n x + D \sinh \lambda_n x - E \cos \lambda_n x - F \sin \lambda_n x) \quad (40)$$

Differentiating equation (40), then the third derivative is given by:

$$\frac{d^3 w}{dx^3} = \lambda_n^3 (A \cos \omega_n t + B \sin \omega_n t)(C \sinh \lambda_n x + D \cosh \lambda_n x + E \sin \lambda_n x - F \cos \lambda_n x) \quad (41)$$

### **Boundary Conditions**

At  $x = 0$

$$w = 0, \quad \frac{dw}{dx} = 0$$

At  $x = L$

$$\frac{d^2 w}{dx^2} = 0 \text{ (No Bending)}, \quad \frac{d^3 w}{dx^3} = 0 \text{ (No Shear)}$$

So, at  $x = 0$  and  $w = 0$ , from equation (38) we get:

$$\begin{aligned} 0 &= (A \cos \omega_n t + B \sin \omega_n t)(C + E) \\ \therefore C + E &= 0 \end{aligned} \quad (42)$$

$$\therefore E = -C$$

Also at  $x = 0$ ,  $\frac{dw}{dx} = 0$ ; substituting into (39) we get:

$$0 = \lambda_n (A \cos \omega_n t + B \sin \omega_n t)(0 + D - 0 + F)$$

$$\text{Therefore, } D + F = 0$$

$$\text{Or } F = -D \quad (43)$$

Now, substituting equations (42) and (43) in equations (38) – (41), we get:

$$w(x, t) = (A \cos \omega_n t + B \sin \omega_n t)[C(\cosh \lambda_n x - \cos \lambda_n x) + D(\sinh \lambda_n x - \sin \lambda_n x)] \quad (44)$$

$$\frac{dw}{dx} = \lambda_n (A \cos \omega_n t + B \sin \omega_n t)[C(\sinh \lambda_n x + \sin \lambda_n x) + D(\cosh \lambda_n x - \cos \lambda_n x)] \quad (45)$$

$$\frac{d^2 w}{dx^2} = \lambda_n^2 (A \cos \omega_n t + B \sin \omega_n t)[C(\cosh \lambda_n x + \cos \lambda_n x) + D(\sinh \lambda_n x + \sin \lambda_n x)] \quad (46)$$

$$\frac{d^3 w}{dx^3} = \lambda_n^3 (A \cos \omega_n t + \sin \omega_n t)[C(\sinh \lambda_n x - \sin \lambda_n x) + D(\cosh \lambda_n x + \cos \lambda_n x)] \quad (47)$$

Now, at  $x = L$ ,  $\frac{d^2 w}{dx^2} = 0$ , from equation (46) we can write:

$$\begin{aligned} 0 &= \lambda_n^2 (A \cos \omega_n t + B \sin \omega_n t)[C(\cosh \lambda_n L + \cos \lambda_n L) + D(\sinh \lambda_n L + \sin \lambda_n L)] \\ \therefore C(\cosh \lambda_n L + \cos \lambda_n L) + D(\sinh \lambda_n L + \sin \lambda_n L) &= 0 \end{aligned} \quad (48)$$

Also, at  $x = L$ ,  $\frac{d^3 w}{dx^3} = 0$ , from equation (47) we can write:

$$\begin{aligned} 0 &= \lambda_n^3 (A \cos \omega_n t + B \sin \omega_n t)[C(\sinh \lambda_n L - \sin \lambda_n L) + D(\cosh \lambda_n L + \cos \lambda_n L)] \\ \therefore C(\sinh \lambda_n L - \sin \lambda_n L) + D(\cosh \lambda_n L + \cos \lambda_n L) &= 0 \end{aligned} \quad (49)$$

Equations (48) and (49) can be written in matrix form as follows:

$$\underbrace{\begin{bmatrix} (\cosh \lambda_n L + \cos \lambda_n L) & (\sinh \lambda_n L + \sin \lambda_n L) \\ (\sinh \lambda_n L - \sin \lambda_n L) & (\cosh \lambda_n L + \cos \lambda_n L) \end{bmatrix}}_{[A]} \begin{bmatrix} C \\ D \end{bmatrix} = 0 \quad (50)$$

And since C and D  $\neq 0$ , therefore:

$$|A| = 0$$

$$\begin{aligned} \therefore (\cosh \lambda_n L + \cos \lambda_n L)^2 - (\sinh^2 \lambda_n L - \sin^2 \lambda_n L) &= 0 \\ \cosh^2 \lambda_n L + 2 \cosh \lambda_n L \cos \lambda_n L + \cos^2 \lambda_n L - & \\ \sinh^2 \lambda_n L + \sin^2 \lambda_n L &= 0 \end{aligned}$$

Rearranging, we get:

$$\begin{aligned} (\cosh^2 \lambda_n L - \sinh^2 \lambda_n L) + (\cos^2 \lambda_n L + \sin^2 \lambda_n L) + \\ 2 \cosh \lambda_n L \cos \lambda_n L = 0 \end{aligned}$$

$$\therefore 1 + 1 + 2 \cosh \lambda_n L \cos \lambda_n L = 0$$

$$2 \cosh \lambda_n L \cos \lambda_n L = -2$$

Therefore,

$$\cosh \lambda_n L \cos \lambda_n L = -1 \quad (51)$$

Which is equivalent to the result of James M. Gere and Stephen P. Timoshenko in their book titled “Mechanics of Materials” [550].

To solve this equation for the values of  $(\lambda_n L)$ , we can rearrange it as follows:

$$\begin{aligned} \cos \lambda_n L &= \frac{-1}{\cosh \lambda_n L} \\ \therefore \cos \lambda_n L &= -\operatorname{sech} \lambda_n L \end{aligned} \quad (52)$$

Now, let

$$y_1 = \cos x \text{ and } y_2 = -\operatorname{sech} x$$

Where  $x = \lambda_n L$

Therefore the solution exists when  $y_1 = y_2$ , which is represented by the points of intersection between the two graphs. These two functions are plotted by using MATLAB software using the code given below.

```
close all; clear all
x=[0:0.001*pi:10];
y=cos(x)
z=-sech(x)
plot(x,y,'r-')
hold on
plot(x,z,'b-')
```

```

xlabel('x')
ylabel('y')
title('\cos (x) . cosh(x) = -1')
set(gca,'XlimMode','manual','YlimMode','manual'); % Fix axes limits
hold on;
[x,y] = ginput(1); % Select a point with the mouse
plot([x x],get(gca,'Ylim'),'k-'); % Plot dashed line
plot(x,y,'r*'); % Mark intersection with red asterisk
disp('Intersection coordinates:');
disp([x y]); % Display the intersection point
[x,y] = ginput(1); % Select a point with the mouse
plot([x x],get(gca,'Ylim'),'k-'); % Plot dashed line
plot(x,y,'r*'); % Mark intersection with red asterisk
disp('Intersection coordinates:');
disp([x y]); % Display the intersection point
[x,y] = ginput(1); % Select a point with the mouse
plot([x x],get(gca,'Ylim'),'k-'); % Plot dashed line
plot(x,y,'r*'); % Mark intersection with red asterisk
disp('Intersection coordinates:');
disp([x y]); % Display the intersection point

```

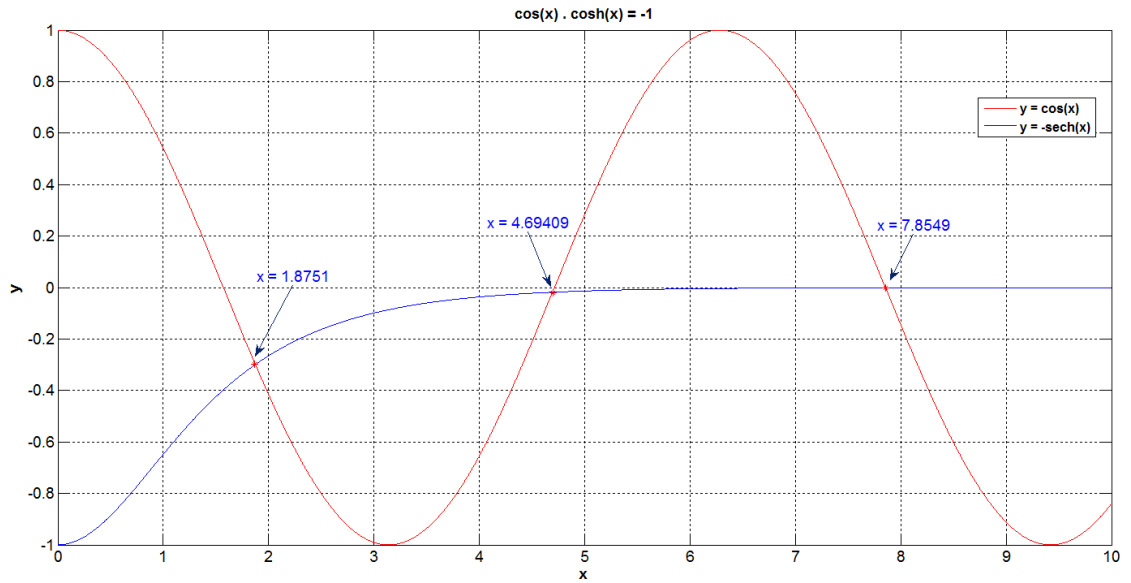


**Figure 3: Solution of Equation (52) using MATLAB software**

From Figure (3), we get:

$$\begin{aligned}
 x_1 &= \lambda_1 L = 1.8751 \\
 x_2 &= \lambda_2 L = 4.69409 \\
 x_3 &= \lambda_3 L = 7.8549
 \end{aligned} \tag{53}$$



These are the values of the first three modes; for higher modes we can use the following formula:

$$\lambda_n L = \frac{(2n-1)}{2} \pi ; n = 3, 4, 5, \dots \quad (54)$$

From these modes we can calculate the values of the corresponding natural frequencies ( $\omega_n$ ); the steps are as follows:

Recalling equation (37):

$$\lambda_n = \left( \frac{\rho A}{EI} \omega_n^2 \right)^{\frac{1}{4}} \quad (37)$$

This can be rewritten as:

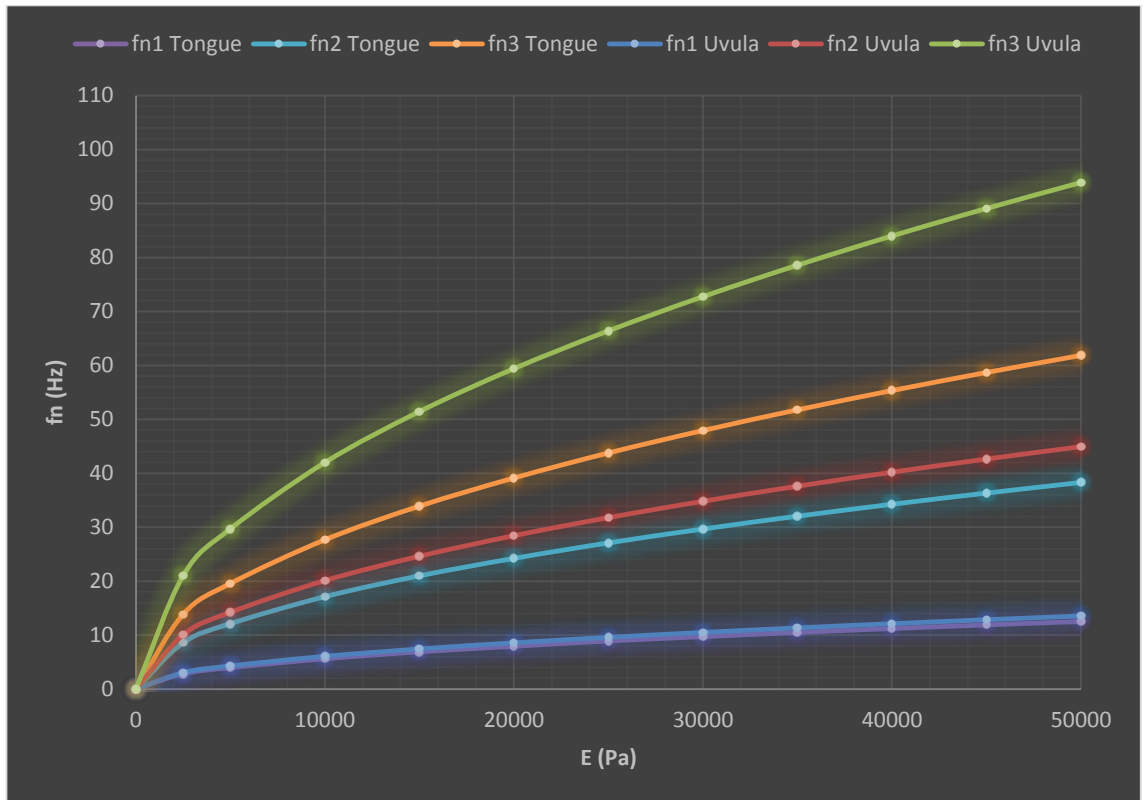
$$\begin{aligned} \lambda_n^4 &= \frac{\rho A}{EI} \omega_n^2 \\ \omega_n^2 &= \frac{EI}{\rho A} \lambda_n^4 \\ \therefore \omega_n &= \lambda_n^2 \sqrt{\frac{EI}{\rho A}} \text{ (rad/sec.)} \\ \omega_n &= \frac{(\lambda_n L)^2}{L^2} \sqrt{\frac{EI}{\rho A}} \text{ (rad/sec.)} \end{aligned} \quad (55)$$

And the frequency in Hz (vibrations/second) is obtained as follows:

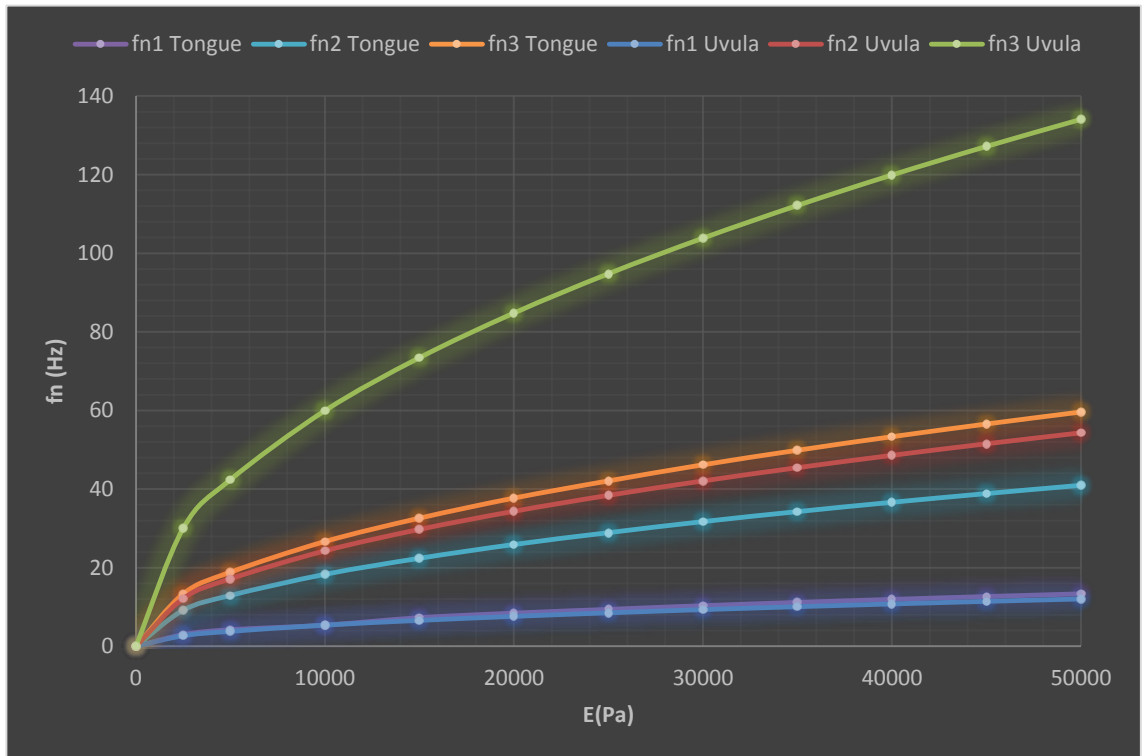
$$f_n = \frac{\omega_n}{2\pi} \text{ (Hz)} \quad (56)$$

## Appendix B

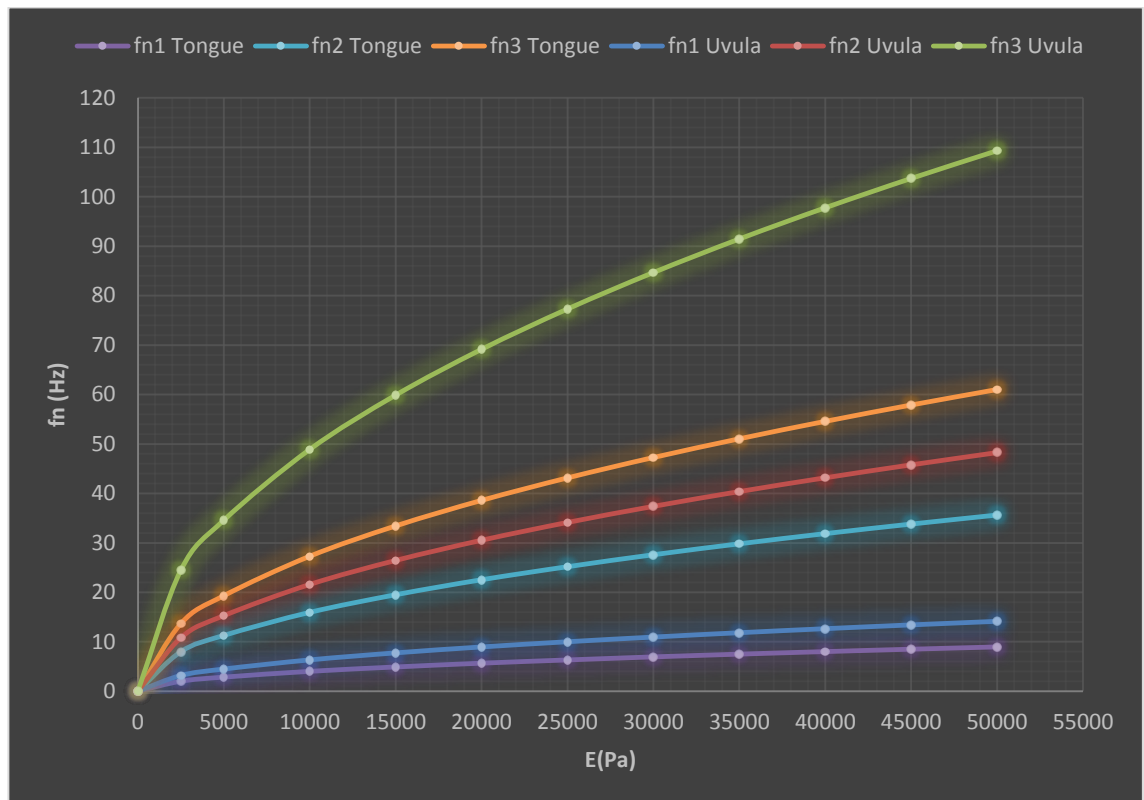
### Combined Figures for Healthy Uvula and Tongue Models



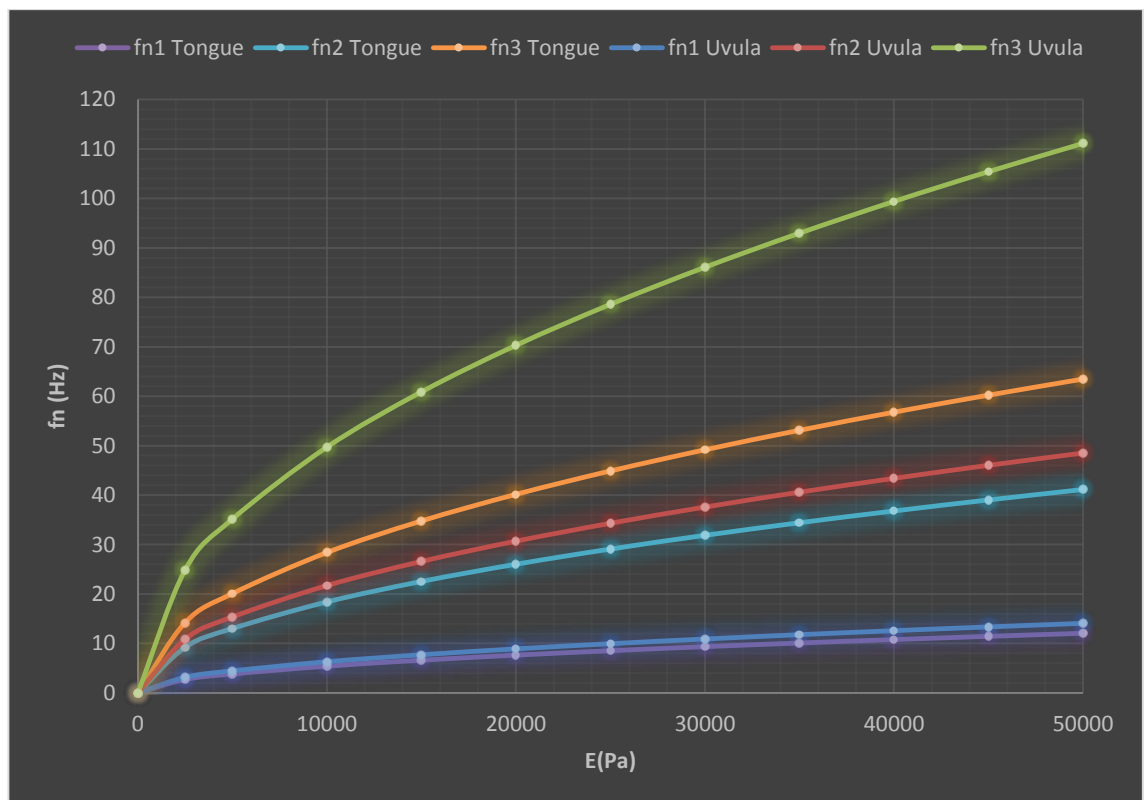
Combined figure for healthy uvula and tongue models; subject 3



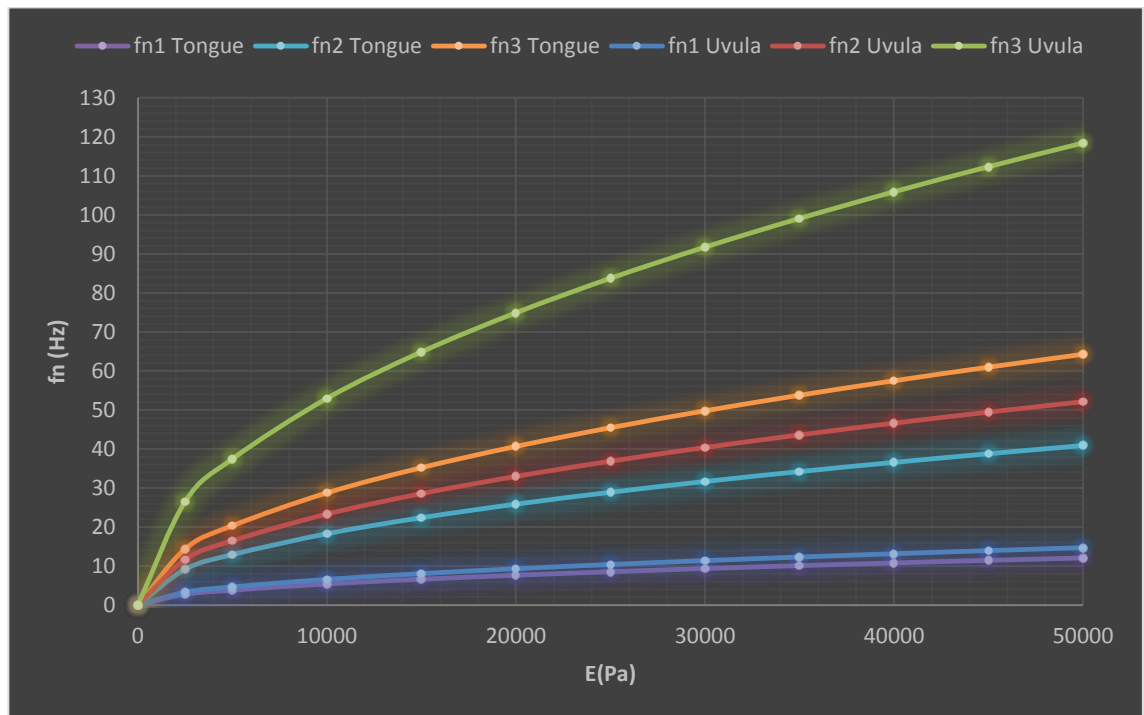
Combined figure for healthy uvula and tongue models; subject 4



Combined figure for healthy uvula and tongue models; subject 6



Combined figure for healthy uvula and tongue models; subject 7



**Combined figure for healthy uvula and tongue models; subject 8**

## Appendix C

### Ethical Approval Letter, PIS, Consent Form



14 January 2014

Ahmed Al-Jumaily  
Faculty of Design and Creative Technologies

Dear Ahmed

Re Ethics Application: 13/355 Understanding upper airway collapse in obstructive sleep apnea patients using CFD modelling.

Thank you for providing evidence as requested, which satisfies the points raised by the AUT University Ethics Committee (AUTE C).

Your ethics application has been approved for three years until 14 January 2017.

As part of the ethics approval process, you are required to submit the following to AUTE C:

- A brief annual progress report using form EA2, which is available online through <http://www.aut.ac.nz/researchethics>. When necessary this form may also be used to request an extension of the approval at least one month prior to its expiry on 14 January 2017;
- A brief report on the status of the project using form EA3, which is available online through <http://www.aut.ac.nz/researchethics>. This report is to be submitted either when the approval expires on 14 January 2017 or on completion of the project.

It is a condition of approval that AUTE C is notified of any adverse events or if the research does not commence. AUTE C approval needs to be sought for any alteration to the research, including any alteration of or addition to any documents that are provided to participants. You are responsible for ensuring that research undertaken under this approval occurs within the parameters outlined in the approved application.

AUTE C grants ethical approval only. If you require management approval from an institution or organisation for your research, then you will need to obtain this. If your research is undertaken within a jurisdiction outside New Zealand, you will need to make the arrangements necessary to meet the legal and ethical requirements that apply there.

To enable us to provide you with efficient service, please use the application number and study title in all correspondence with us. If you have any enquiries about this application, or anything else, please do contact us at [ethics@aut.ac.nz](mailto:ethics@aut.ac.nz).

All the very best with your research,

A handwritten signature in black ink, appearing to read 'K O'Connor'.

Kate O'Connor  
Executive Secretary  
Auckland University of Technology Ethics Committee

Cc: Sherif Ashaat [sherif.ashaat@aut.ac.nz](mailto:sherif.ashaat@aut.ac.nz)

Auckland University of Technology Ethics Committee

WA505F Level 5 WA Building City Campus

Private Bag 92006 Auckland 1142 Ph: +64-9-921-9999 ext 8316 email [ethics@aut.ac.nz](mailto:ethics@aut.ac.nz)

# Participant Information Sheet



## Date Information Sheet Produced:

15 January 2014

**Project Title:** Understanding Upper Airway Collapse in Obstructive Sleep Apnea Patients Using FSI Modelling

## An Invitation

My name is Sherif Ashaat. I hold a Master of Science degree in Engineering Mechanics. I'm doing this research as part of the Doctor of Philosophy degree in Engineering at Auckland University of Technology (AUT).

MRI data of the upper airway geometry are needed for OSA patients to construct and simulate real upper airway models using suitable computer software to investigate the conditions for collapse.

This Participant information Sheet is sent to you to provide further detailed information and to invite you to participate in this research.

If you are an OSA patient, aged 25-65 years, non-smoker, have never had any upper airway surgical intervention, have no upper airway metallic implants, have no pacemaker, not pregnant (if applicable) and interested in participating in this research, please fill in the attached Consent Form and email it to the primary researcher, Sherif Ashaat, [sherif.ashaat@aut.ac.nz](mailto:sherif.ashaat@aut.ac.nz) or post it to the physical address given below before 21 February 2014:

**Address:** Auckland University of Technology, Private Bag 92006, Wellesley Campus, WD304, Auckland, New Zealand

This participation is voluntary, and any participant may withdraw at any time prior to the completion of data collection without being disadvantaged in any way.

## What is the purpose of this research?

Obstructive Sleep apnea (OSA) is considered as one of the most threatening diseases to the quality of life. It is considered as the most worldwide common upper respiratory system ailment and sleep-disorder. OSA occurs due to obstruction (narrowing) in the upper airway region and is characterized by repeated collapse and/or obstruction of the pharyngeal airway during sleep, which requires more breathing effort.

Airway collapse occurs when the forces of the wall muscles are less than the forces generated from the negative pressures during the respiration process. Collapse occurs when the airflow is reduced by 90% or more, or the gap between the soft palate tip and the airway wall is reduced by 75%, which results in reducing the diameter of the pharyngeal airway and in turn increases the airflow resistance.

OSA can lead to many diseases, such as excessive daytime sleepiness, arrhythmias, diabetes, hypertension, stroke, cardiac stroke, cardiovascular disease, low sexual drive in men, and memory loss.

This research aims to improve the understanding of upper airway collapse in OSA patients, which will help in delivering better treatment and reduce the required health care for those patients.

The research will result in the publication of a thesis, as well as research papers that will be published in international journals and refereed conference proceedings.

### **How was I identified and why am I being invited to participate in this research?**

You are included in a group of OSA patients on the records of F & P Healthcare, from which your contact details were available; and you are being invited to participate because you have shown interest in participating in this research upon contact with F & P.

It is desired that all the participants be OSA patients that cover a range of age (25-65 years), both genders, races (ethnicity), disease severity (mild, moderate and severe) and are not under any current form of medication. So the volunteers will be selected to fulfil these criteria. The study excludes OSA patients who have:

- Had any surgical intervention as a treatment for obstructive sleep apnea
- Metallic implants through their upper airways
- Pacemakers

Also, pregnant patients are excluded.

### **What will happen in this research?**

The interested candidates will send their signed Consent Forms to the primary researcher. Then, all the interested participants will be examined by an ear, nose and throat (ENT) specialist who will give a report about their upper airways. A Demographic Form would then be completed to collect data for screening process.

A screening process will then be undertaken to exclude those who are unsuited to undertake this study and to provide the desired population sample variety. *It may be that at this stage you no longer continue the study. If this is the case, all your data will be destroyed.*

The final selected participants will be notified and a mutually agreeable time will be arranged for the study to be undertaken. Given that it takes between 10-20 minutes to recruit participants and another 20 minutes to collect MRI data. The participant will have to give about 1 hour to the project. The data will be gathered according to the following steps:

1. Each participant will assume the recumbent (supine) position within the MRI scanner. The MRI head coil will then be positioned over his/her head
2. After a suitable settling time to enable the participant to settle in, the MRI scanner will record the upper airway geometry
3. The above procedure is repeated for all participants

The obtained data will be analysed using suitable computer software at the Institute of Biomedical Technologies (IBTec).

**What are the discomforts and risks? And How will these discomforts and risks be alleviated?**

MRI techniques have been used in the clinical environment for more than 20 years. No physical discomforts or incapacity have been noted in people who used these techniques. Common MRI side effects are related to the noise generated during testing which include headaches, dizziness, sweating, nausea, fatigue. If experienced, MRI side effects are temporary and mostly caused by the noise during scan. These symptoms commonly disappear upon cessation of scan and if these become a problem then the machine will be turned off immediately.

**What are the benefits?**

This research aims to improve the understanding of upper airway collapse in OSA patients, which will help in delivering better treatment and reduce the required health care for those patients.

The research may result in the publication of a thesis towards a PhD, as well as research papers that will be published in international journals and refereed conference proceedings.

**What compensation is available for injury or negligence?**

In the unlikely event of a physical injury as a result of your participation in this study, rehabilitation and compensation for injury by accident may be available from the Accident Compensation Corporation, providing the incident details satisfy the requirements of the law and the Corporation's regulations.

**How will my privacy be protected?**

The researcher will arrange for private confidential interviews with the interested volunteers. The participants will not be identified in the final report, only aggregate data will be reported in such a form that no individuals or groups can be identified from it.

**What are the costs of participating in this research?**

It takes between 10-20 minutes to recruit participants and another 20 minutes to collect MRI data. The participant will have to give about 1 hour to the project.



**What opportunity do I have to consider this invitation?**

Once you have signed the Consent Form, and it was sent to the primary researcher before the given deadline, the primary researcher will arrange with you for a mutually agreeable time to be examined by an ear, nose and throat (ENT) specialist. A Demographic Form would then be completed to collect data for screening process.

A screening process will then be undertaken to exclude those who are unsuited to undertake this study (according to the exclusion criteria) and to provide the desired population sample variety.

The final sample of participants selected will be notified and a mutually agreeable time will be arranged for the study to be undertaken.

MRI data is scheduled to be collected at The Centre for Advanced MRI (CAMRI), University of Auckland. Times will be arranged later on.

**How do I agree to participate in this research?**

If you agree to participate in this research, please fill in the attached Consent Form and email it to the primary researcher, Sherif Ashaat, [sherif.ashaat@aut.ac.nz](mailto:sherif.ashaat@aut.ac.nz) or post it to the physical address given below before 21 February 2014:

**Address:** Auckland University of Technology, Private Bag 92006, Wellesley Campus, WD304, Auckland, New Zealand.

**Will I receive feedback on the results of this research?**

Yes, the primary researcher, Sherif Ashaat, will email or post the participants with the summary of the research findings.

**What do I do if I have concerns about this research?**

Any concerns regarding the nature of this project should be notified in the first instance to the Project Supervisor.

Name: Prof Ahmed Al-Jumaily

Email: [ahmed.al-jumaily@aut.ac.nz](mailto:ahmed.al-jumaily@aut.ac.nz)

Work Phone: +64 (0) 9 921 9777

Mobile: +64 (0) 21 524 468

Concerns regarding the conduct of the research should be notified to the Executive Secretary of AUTC, Kate O'Connor, [ethics@aut.ac.nz](mailto:ethics@aut.ac.nz), 921 9999 ext 6038

**Whom do I contact for further information about this research?**

***Researcher Contact Details:***

Name: Sherif Ashaat

Email: [sherif.ashaat@aut.ac.nz](mailto:sherif.ashaat@aut.ac.nz)

Mobile: +64 (0) 21 0252 5259

***Project Supervisor Contact Details:***

Name: Prof Ahmed Al-Jumaily

Email: [ahmed.al-jumaily@aut.ac.nz](mailto:ahmed.al-jumaily@aut.ac.nz)

Work Phone: +64 (0) 9 921 9777

Mobile: +64 (0) 21 524 468

***Approved by the Auckland University of Technology Ethics Committee on 14<sup>th</sup> January 2014***  
***AUTEC Reference number 13/355***

# Consent Form



**Project title:** Understanding Upper Airway Collapse in Obstructive Sleep Apnea Patients Using FSI Modelling

**Project Supervisor:** Prof Ahmed Al-Jumaily

**Researcher:** Sherif Ashaat

**Participant Number:** .....

- 
- I have read and understood the information provided about this research project in the Participant Information Sheet dated 15 January 2014.
  - I have had an opportunity to ask questions and to have them answered.
  - I understand that I may withdraw myself or any information that I have provided for this project at any time prior to completion of data collection, without being disadvantaged in any way.
  - I agree to discuss my health condition and answer all questions asked correctly to the best of my knowledge.
  - I am a non-smoker, have had no recent history of upper airway or sinus infection or allergy and do not suffer any respiratory condition but OSA. Also, that I have no upper airway metallic implants, do not have a pacemaker, not pregnant and am not under any current form of medication.
  - I agree to take part in this research and have my upper airway examined by an ear, nose and throat (ENT) specialist to ensure the absence of infection, swelling or other conditions that may influence nasal breathing.
  - I am aware that the collected MRI images and data collected for this project will be maintained for a period of 10 years.
  - I am aware that the MRI images and data collected from this project may be used in journal and conference publications of this research. A summary of this activity and global findings may be given on the Institute of Biomedical Technologies website, [www.aut.ac.nz/ibtec/](http://www.aut.ac.nz/ibtec/), in an anonymous form to overview the research work being undertaken within the institute.
  - I wish to receive a copy of the report from the research. ☐ Yes ☐ No
  - Should other pathologies be detected I understand that the primary researcher will advise me of this in a private and confidential manner. I would also like my medical specialist to be advised. ☐ Yes ☐ No

Participant's Signature: .....

Participant's Name: .....

Participant's Contact Details (if appropriate):

Phone : .....

Email : .....

Address : .....

Date : .....

***Approved by the Auckland University of Technology Ethics Committee on 14 January 2014 AUTEC***

***Reference number 13/355***

*Note: The Participant should retain a copy of this form*

# Demographic Form



**Project title:** Understanding Upper Airway Collapse in Obstructive Sleep Apnea Patients Using FSI Modelling

**Project Supervisor:** Prof Ahmed Al-Jumaily

**Researcher:** Sherif Ashaat **Participant Number:** .....

---

- Age: .....
  - Height: .....
  - Gender: .....
  - Ethnicity: .....
  - Confirmation of non-smoker status ☐ (Please tick)
  - State of Respiratory Health (please tick one) ☐ Poor ☐ Good
  - OSA Severity (please tick one) ☐ Mild ☐ Moderate ☐ Severe
- Date: .....

*Approved by the Auckland University of Technology Ethics Committee on 14<sup>th</sup> January 2014*  
*AUTEC Reference number 13/355*

## **Appendix D**

### **Summaries of the ENT specialist reports for OSA patients**

#### **Report for Patient Number 2**

This participant reported that he has been using CPAP for 5.5 years, his CPAP is 12 Cm H<sub>2</sub>O. He also reported that he is an ex-smoker, and that his tonsils and adenoids were previously removed. The ENT specialist reported that this patient has a good nasal airway, wide oropharynx, large tongue (Mallampati II) which flops back easily and blocks the airway producing snoring.

#### **Report for Patient Number 3**

This participant reported that she has been using CPAP for 7-8 years, her CPAP is 10 Cm H<sub>2</sub>O. The ENT specialist reported that this patient has dry nose, redness and bleeding from the left nostril, very narrow UA, large tongue (Mallampati II), and very narrow airway gap rear of the tongue which may block the airway easily.

#### **Report for Patient Number 4**

This participant reported that he has been using CPAP for 3 years, his CPAP is 11 Cm H<sub>2</sub>O. He also reported that he used to have recurrent sinus infection (which was explained by the ENT to be due to a small hall in the sinus), the back of his throat gets dry sometimes, he takes anti-depressant in the evening to sleep easily, and that he did not have any cold or sore throat since he started using the CPAP. Also, the patient reported that he tried to use a mouth guard to pull the tongue forward preventing airway blockage and he felt good using it but it was pressing on some teeth and that is why he stopped using it. Skin marks on his face were noticed as a result from using the CPAP mask every day. The ENT specialist reported that there is a slight nasal septum deviation to the left, large tongue (Mallampati II), tonsils and soft palate are not swollen and narrow airway gap at the rear of the tongue and epiglottis which may block the airway easily.

#### **Report for Patient Number 5**

This participant reported that he has been using CPAP for 3 years, his CPAP is 11 Cm H<sub>2</sub>O (using nostril inserts), and that he has been diagnosed with both CSA and OSA. Also he reported that he had a nasal septum straightening surgery in 1995, his nose gets congested quite easily from one side, and that the CPAP mask leaves marks on his nose from being used on daily basis. The ENT specialist reported that there is a small hall in the middle of

the nasal septum (from the previous surgery), large tongue (Mallampati II) and narrow airway gap rear of the tongue which may block the airway easily.

#### **Report for Patient Number 6**

This participant reported that he has been using CPAP for 3 years, his CPAP is 7 Cm H<sub>2</sub>O. He also reported to have recurrent bleeding from his left nostril. The ENT specialist reported that the patient has a good nasal airway, the soft palate is not swollen, there is a crust inside the left nostril (where the bleeding comes from) and very large tongue (Mallampati III) which flops back easily and may block the airway easily.

#### **Report for Patient Number 7**

This participant reported that he has been using CPAP for 3 years, his CPAP is 12 Cm H<sub>2</sub>O. The ENT specialist reported that the patient has a normal looking nose with slightly narrow nasal cavity from the right, the soft palate is swollen due to daily use of CPAP, and large tongue (Mallampati II) which flops back easily and may block the airway easily

#### **Report for Patient Number 8**

This participant reported that she has been using CPAP for 5 years, her CPAP is 4 Cm H<sub>2</sub>O. The ENT specialist reported that the patient has a narrow nasal airway, swollen nose from inside and large tongue (Mallampati II) which flops back easily and may block the airway easily.

#### **Report for Patient Number 9**

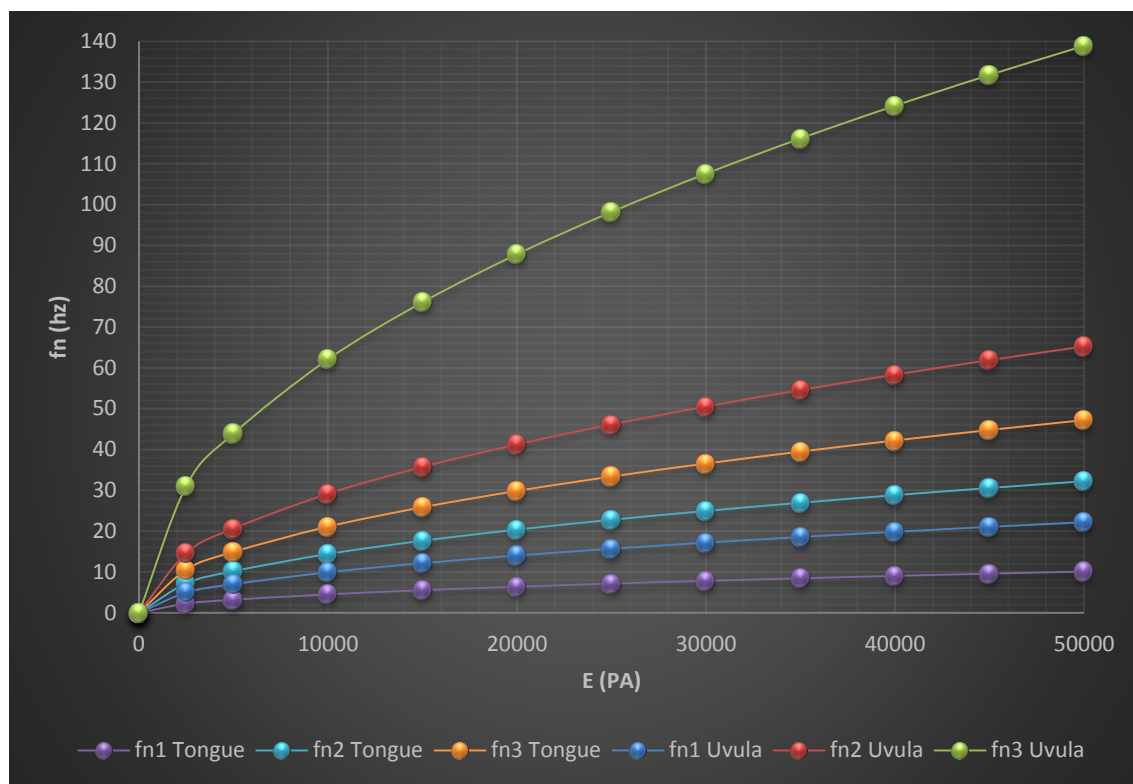
This participant reported that he has been using APAP for 7 years, the pressure starts at 6 Cm H<sub>2</sub>O and changes accordingly. He reported that he broke his nose when he was 15 while playing basketball and that is why his nose is distorted. Also he reported that some crust accumulates inside the left nostril and easily blocks that side of the nose (he uses an ointment to get rid of that crust). He has recurrent nasal bleeding, and he is diagnosed to be diabetic (not using insulin) but when he started using the metformin the nasal blockage disappeared. The ENT specialist reported that the patient has a good nasal airway on both sides and large tongue (Mallampati II) which flops back easily and may block the airway easily.

#### **Report for Patient Number 10**

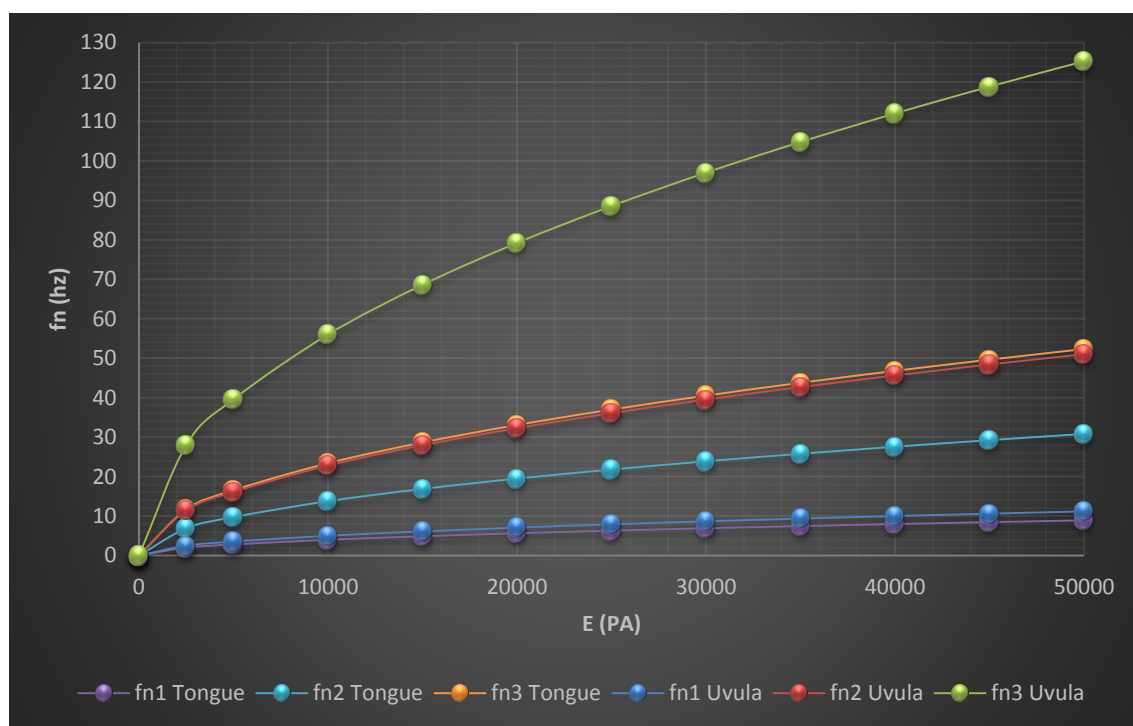
This participant reported that she has been using CPAP for 6 months, her CPAP is 6 Cm H<sub>2</sub>O. The ENT specialist reported that the patient has a good nasal airway on both

sides and very large tongue (Mallampati III) which flops back easily and may block the airway easily.

### **Combined Figures for Unhealthy Uvula and Tongue Models**

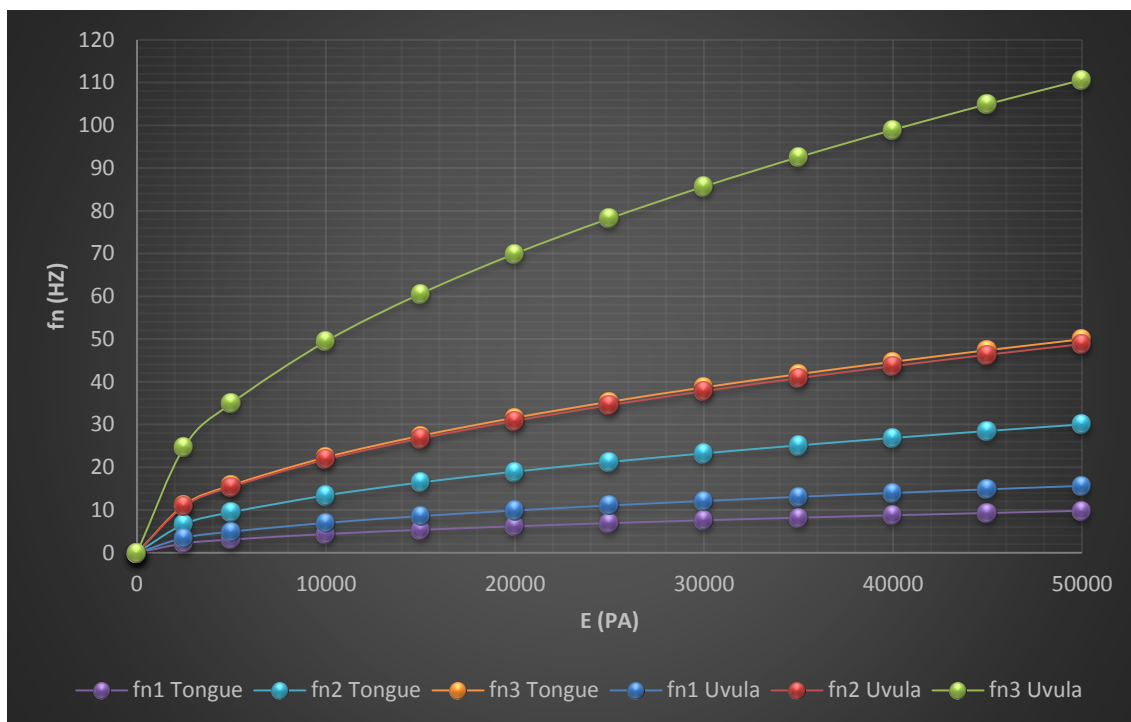


**Combined figure for unhealthy uvula and tongue models; patient 2**

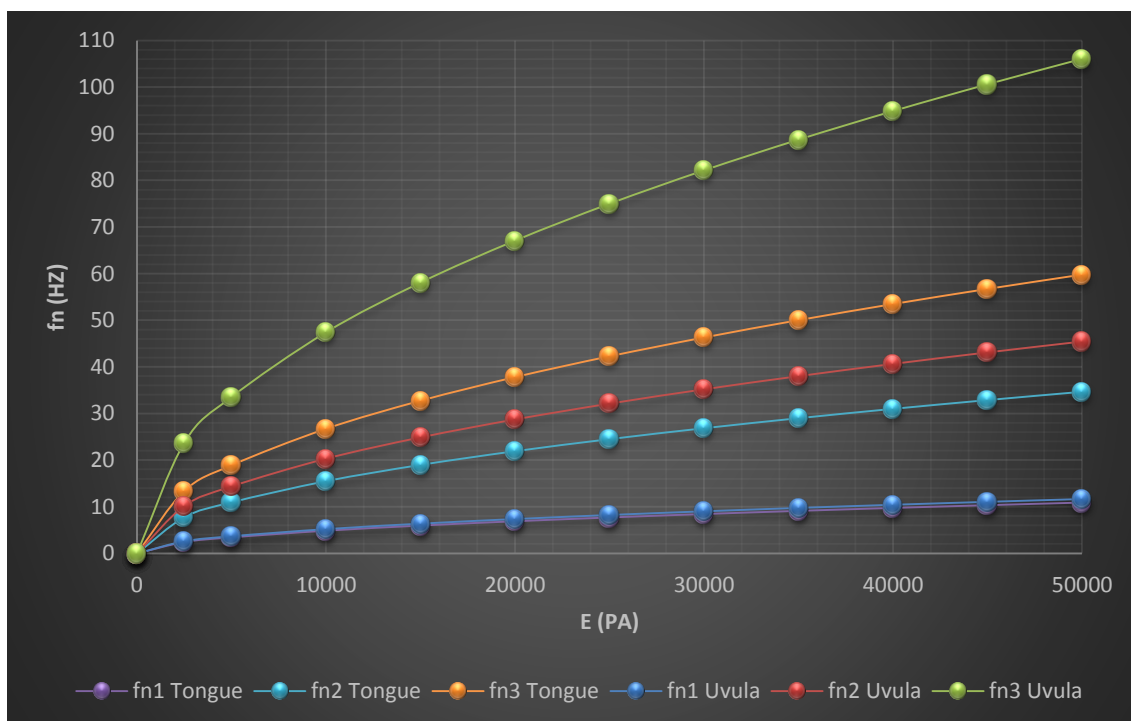


**Combined figure for unhealthy uvula and tongue models; patient 4**

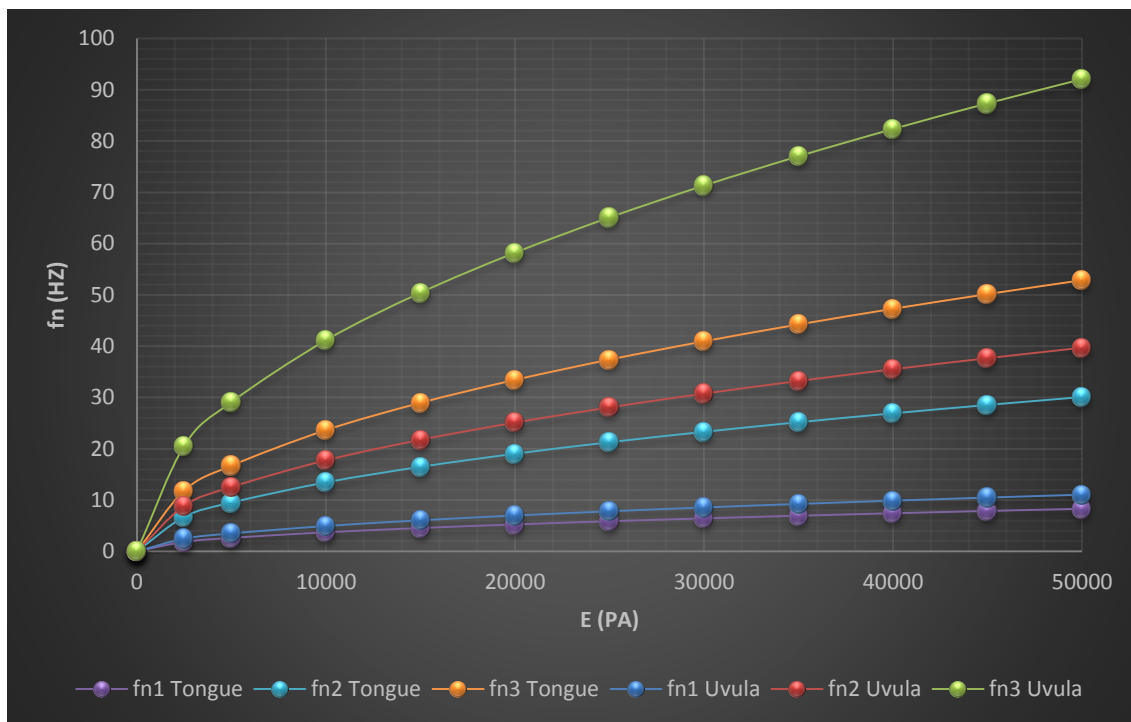




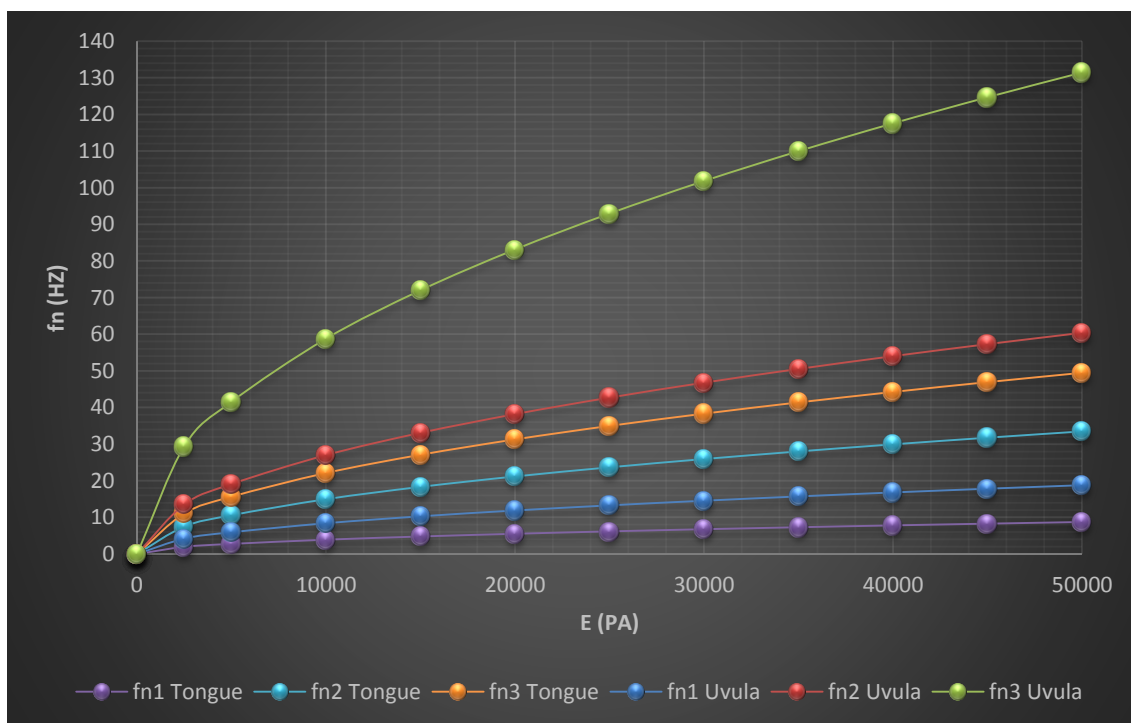
**Combined figure for unhealthy uvula and tongue models; patient 5**



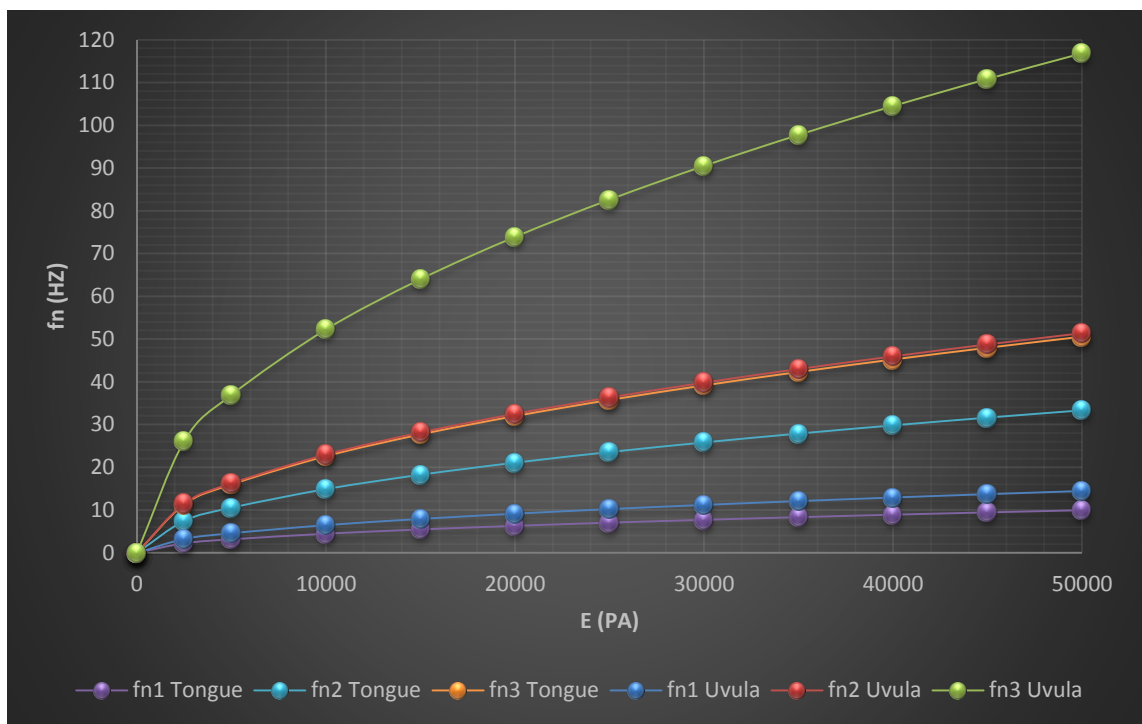
**Combined figure for unhealthy uvula and tongue models; patient 6**



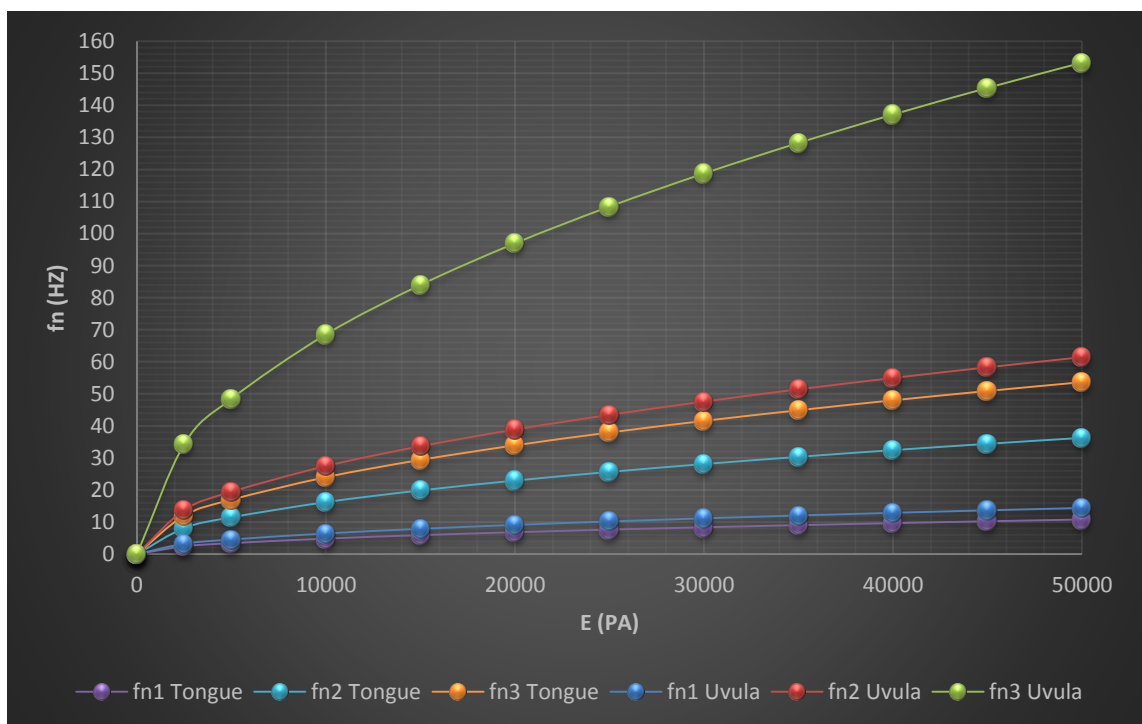
**Combined figure for unhealthy uvula and tongue models; patient 7**



**Combined figure for unhealthy uvula and tongue models; patient 8**



**Combined figure for unhealthy uvula and tongue models; patient 9**



**Combined figure for unhealthy uvula and tongue models; patient 10**

## **Appendix E**

### **Conferences and Publications**

#### **Conferences Attended**

1. New Zealand Medical Sciences Congress (MedSciNZ), Queenstown, 2012. Oral presentation titled: Understanding Upper Airway Collapse in Obstructive Sleep Apnea Patients Using CFD Modelling
2. New Zealand Medical Sciences Congress (MedSciNZ), Queenstown, 2013. Oral presentation titled: Dynamic Characteristics of Human Upper Airway
3. New Zealand Medical Sciences Congress (MedSciNZ), Queenstown, 2014. Oral presentation titled: Biomechanical Assessment of Obstructive Sleep Apnea before and after Bariatric Surgery
4. New Zealand Medical Sciences Congress (MedSciNZ), Queenstown, 2015. Oral presentation titled: Human Upper Airway Collapse in OSA Patients
5. Summer Biomechanics, Bioengineering & Biotransport Conference (SB3C), June 17-20, 2015, Snowbird, Utah, USA. Poster presentation titled: Bariatric Surgery Improvements for OSA Patients
6. International Mechanical Engineering Congress & Exposition (IMECE), November 13-19, 2015, Houston, Texas, USA. Oral presentation for a conference paper titled: Upper Airway Dynamic Characteristics-Comparative Study between Healthy Subjects and OSA Patients

#### **Publications**

1. Al-Jumaily, A. M., Ashaat, S., et al, 2013, "Uvula Dynamic Characteristics", Proceedings of the ASME 2013 Summer Bioengineering Conference (SBC), June 26-29, 2013, Sunriver, Oregon, USA.
2. Al-Jumaily, A. M., Ashaat, S., et al., 2015, "Upper Airway Dynamic Characteristics-Comparative Study between Healthy Subjects and OSA Patients", Proceedings of the ASME 2015 International Mechanical Engineering Congress & Exposition (IMECE), November 13-19, 2015, Houston, Texas, USA.
3. Al-Jumaily, A. M., Ashaat, S., et al, 2015, "Biomechanical Assessment of Obstructive Sleep Apnea Pre and Post Bariatric Surgery", Journal of Sleep Medicine (currently under review).